

STMP0-043

SAN/1111-8/2

**CENTRAL RECEIVER SOLAR THERMAL POWER SYSTEM
PILOT PLANT PRELIMINARY DESIGN REPORT**

DOE FILE COPY

Volume 3. Collector Subsystem

April 29, 1977

Work Performed under Contract No. EY-76-C-03-1111

**Boeing Engineering and Construction Company
Seattle, Washington**



U.S. Department of Energy



Solar Energy

NOTICE

This report was prepared as an account of work sponsored by the United States Government. Neither the United States nor the United States Department of Energy, nor any of their employees, nor any of their contractors, subcontractors, or their employees, makes any warranty, express or implied, or assumes any legal liability or responsibility for the accuracy, completeness or usefulness of any information, apparatus, product or process disclosed, or represents that its use would not infringe privately owned rights.

This report has been reproduced directly from the best available copy.

Available from the National Technical Information Service, U. S. Department of Commerce, Springfield, Virginia 22161.

Price: Paper Copy \$9.25
Microfiche \$3.00

VOL III

Central Receiver
Solar Thermal Power System
Pilot Plant Preliminary Design Report

COLLECTOR SUBSYSTEM

April 29, 1977

Prepared for
United States
Energy Research and Development Administration

Under
Contract EY-76-C-03-1111

by

Boeing Engineering and Construction
a Division of The Boeing Company
Seattle, Washington

FOREWORD

This document is the collector subsystem Preliminary Design Report (PDR) for the Central Receiver Solar Thermal Power System Pilot Plant to be issued under Contract EY-76-C-03-1111. The objective of this contract was to develop a preliminary design (PD) of the collector subsystem for a 10 MW_e solar thermal power plant (Pilot Plant). Research experiments were conducted on components, materials, and large scale hardware to support the PD effort. Work under this contract was initiated on June 24, 1975, and is scheduled for completion on June 30, 1978. This report complies with Contract Data Requirement No. 2

TABLE OF CONTENTS

	<u>PAGE</u>
1.0 INTRODUCTION	1
2.0 KEY DATA AND INFORMATION	13
3.0 COLLECTOR SUBSYSTEM PRELIMINARY DESIGN	15
3.1 Design Requirements/Specifications	15
3.2 Interface Requirements	20
3.3 Collector Subsystem Configuration	21
3.3.1 Heliostat Field Geometry and Performance	21
3.3.1.1 Ground Rules	21
3.3.1.2 Analysis Methodology	25
3.3.1.3 Heliostat Field Layout and Performance	29
3.3.2 Protective Enclosure Assembly	32
3.3.2.1 Configuration	32
3.3.2.2 Materials	35
3.3.2.3 Structural Design	
3.3.3 Reflective Assembly	54
3.3.3.1 Configuration	54
3.3.3.2 Materials	54
3.3.3.3 Structural Design	67
3.3.4 Drive and Control Assembly	71
3.3.4.1 Control Overview	71
3.3.4.1.1 Plant Controller	74
3.3.4.1.2 Operational Description	76
3.3.4.1.3 Field Controller	78
3.3.4.2 Drive Assembly	99
3.3.4.2.1 Tracking Rate Analysis	99
3.3.4.2.2 Gimbal/Actuator	100
3.3.4.3 Research Experiment Results	102
3.3.4.4 Error Budget	104
3.3.5 Alignment/Calibration	107
3.3.5.1 Research Experiment Results	107
3.3.5.2 Preliminary Design Configuration of Alignment System	107

TABLE OF CONTENTS

	<u>PAGE</u>
3.3.5.3 Alignment/Calibration Procedure	107
3.3.5.4 Alignment and Calibration Module	109
3.3.6 Power Distribution and Control Cabling	112
3.3.6.1 Power Distribution System	112
3.3.6.2 Signal Cabling System	115
3.3.7 Lightning Protection	117
3.3.8 Heliostat Thermal Design	120
3.3.8.1 Thermal Design Requirements	120
3.3.8.2 Analysis Model	124
3.3.8.3 Heliostat Thermal Performance	124
3.3.8.4 Results of Research Experiments	126
4.0 MANUFACTURING	133
4.1 Manufacturing Process Description	134
4.2 Quality Assurance	137
4.3 Transportation	137
4.4 Materials	138
5.0 INSTALLATION, CHECKOUT AND MAINTENANCE	139
5.1 Installation Plan	139
5.1.1 Foundation	141
5.1.2 Protective Enclosure/Reflective Assemblies	142
5.1.3 Drive and Control Assembly	143
5.1.4 Alignment/Calibration Assembly	144
5.2 Maintenance Plan	146
5.2.1 Dome Cleaning	146
5.2.2 Reflector Cleaning	147
5.2.3 Dome/Reflector Replacement/Repair	147
5.2.4 Air Supply System	148
5.2.5 Electronics	148
5.3 Support Equipment	149
6.0 RELIABILITY	150
6.1 Reliability Considerations	150
6.1.1 Loss of Control System Functions	150

TABLE OF CONTENTS

PAGE

6.1.2	Power Distribution System	151
6.1.3	Loss of Utility Power	151
6.1.4	Power and Control Cabling	151
6.1.5	Dome Pressurization	151
6.2	MTBF Estimates	152
6.3	Infant Mortality	159
6.4	Availability Assessment	159
6.4.1	Potential Improvement Areas	160
6.5	Continuing Reliability Program	160
7.0	SAFETY	162
7.1	Design Safety Features	162
7.1.1	Heliostat	166
7.1.2	Field Controller	166
7.1.3	Collector Subsystem Power	167
7.2	Operational Procedures	167
7.2.1	Stow	167
7.2.2	Standby	168
7.2.3	Receiver Track	168
7.2.4	Align	169
7.2.5	Manual	169
8.0	ELECTRICAL AND MECHANICAL SUPPORT EQUIPMENT	170
9.0	OPERATION AND MAINTENANCE	174
9.1	Dome Cleaning	175
9.2	Reflector Cleaning	176
9.3	Dome/Reflector Replacement and/or Repair	176
9.4	Air Supply System	176
9.5	Electronics	177
9.6	Support Equipment	178
10.0	TEST PROGRAM	179
10.1	Design Verification Plan	179
10.1.1	Test Program Approach	180
10.1.2	Component Testing	181
10.1.3	Assembly Testing	181

TABLE OF CONTENTS

	<u>PAGE</u>
10.1.4 Integration Testing	184
10.2 Plant Startup & Checkout	189
10.3 Two-year Pilot Plant Test Program	190
10.3.1 Reflector Scans	190
10.3.2 Alignment Checks	191
10.3.3 Environmental Tests	191
10.3.4 Maintenance	192
11.0 REFERENCES	193
12.0 BIBLIOGRAPHY	195

1.0 INTRODUCTION

Boeing Engineering and Construction, under contract with ERDA, submits herein a preliminary design (PD) of the collector (heliostat) subsystem for a 10 MW_e Solar Pilot Plant. The Boeing collector subsystem concept, operating with a central receiver installation, is shown in Figure 1.0-1. In this concept, circular membrane reflectors formed with aluminized polyester film, direct sunlight to the central receiver. Transparent air-supported Tedlar enclosures protect the lightweight reflectors from the environment. Reflectors are individually aimed with a 2-axis gimbal, driven by digital-controlled stepper motors. Minicomputers, located at the central control facility, provide signals to the stepper motors. Field geometry, performance, and cost analyses have resulted in specification of 1650 heliostats, to provide 42 MW_{th} to a cylindrical receiver at solar noon on the equinox. Overall efficiency of the heliostat field is 54.5% at the design point.

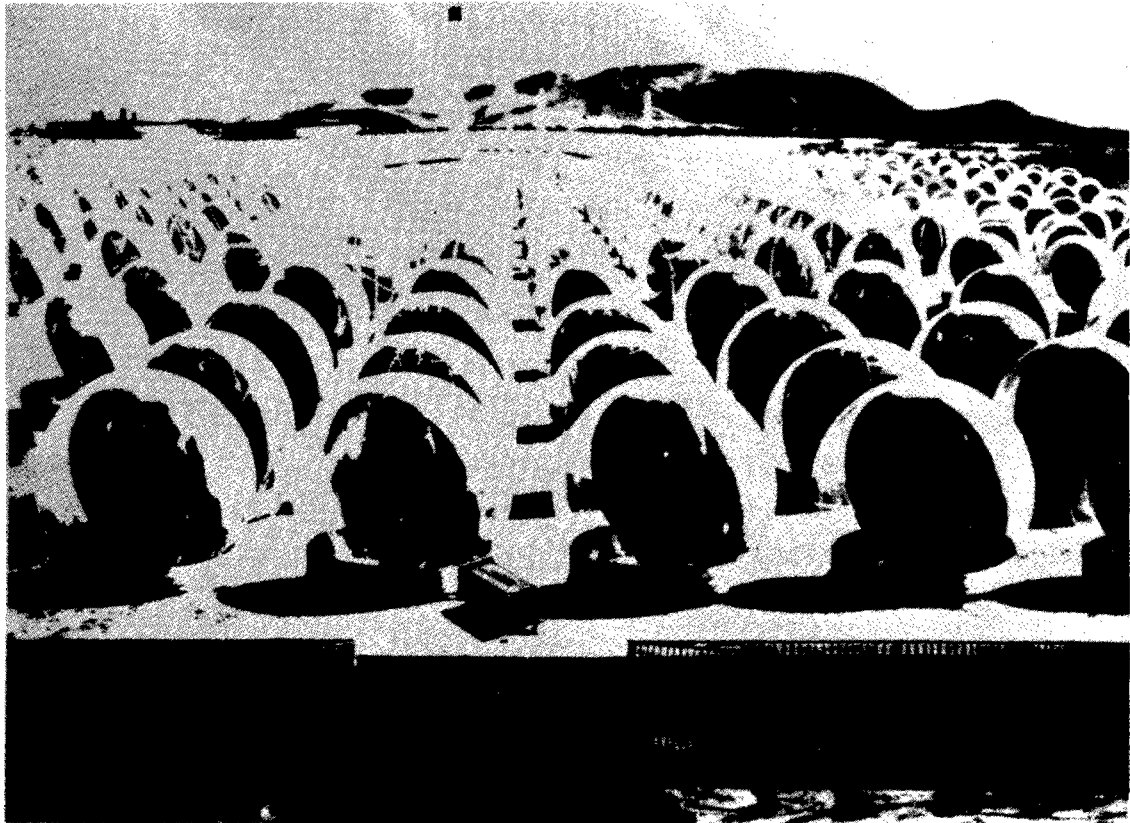
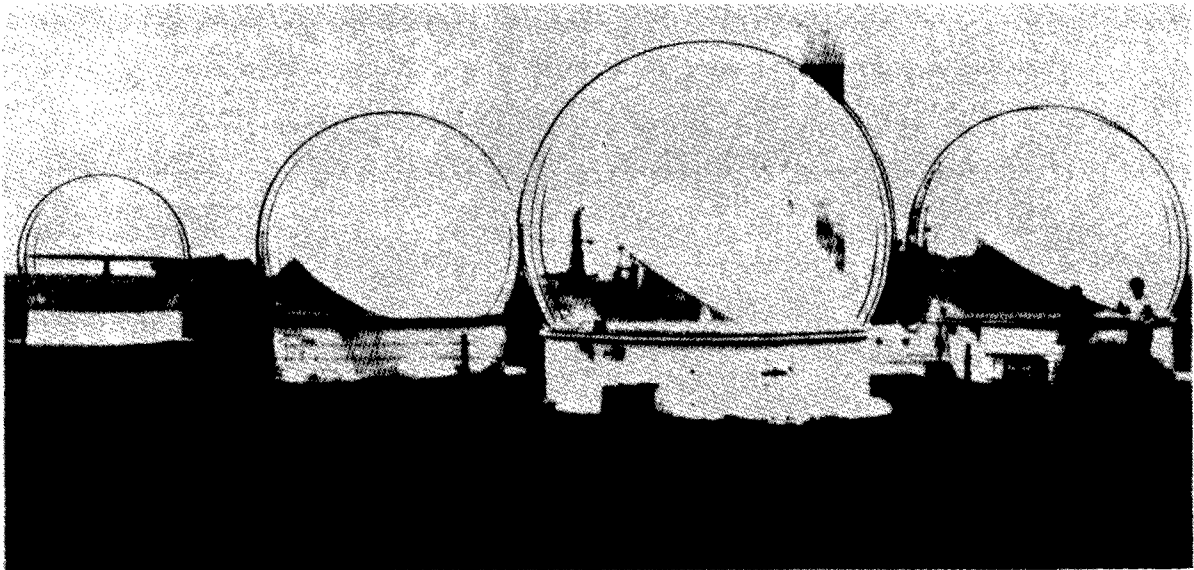


Figure 1.0-1. "Artists Concept" – Boeing Collector Subsystem

Large Scale Hardware, Figure 1.0-2, was developed and tested in the research experiment part of this Phase I effort. Test results provided the data for, and verification of, the preliminary design presented herein.



*Figure 1.0-2
Three Heliostat Array*

Major features of the collector subsystem PD are shown in Figure 1.0-3, with the exception of alignment and scanner hardware located on the central receiver tower. An array of 1650 heliostats is operated utilizing power and digital control signals, transmitted via buried cables from central control. For safety and reliability a redundant power distribution system is provided to all items down to the heliostat level. Control signal cabling is a "daisy chain" serial data bus which can be driven from each end in the event of cable failure. Four field controllers operate the field with 16 data bus circuits. In addition to redundant power cabling, a diesel-powered generator is included in the PD to provide emergency power for 24 hours in the event of utility power loss. Electrical power is transmitted to the field at 480V (3 phase), and reduced

to 120V (single phase) by a transformer located centrally in each array. Estimated power requirements for the collector subsystem are 128 kW during full operation, and 46.6 kW during shutdown. As shown in Figure 1.0-3, a bare copper wire will be installed in cable trenches 0.46m (18 in) above other cables, for the purpose of electrical grounding. This wire will provide an adequate ground for all heliostat hardware in the event of a lightning strike.

Site preparation for the collector subsystem PD includes removal of vegetation, grading, application of 0.10 m (4 in) of crushed rock, and installation of a 4.27 m (14 ft) high cyclone security fence which is slatted to about 50 percent porosity. The latter item provides partial wind protection to protective enclosures at the field periphery.

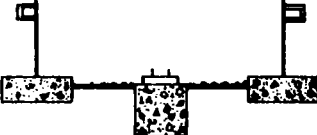
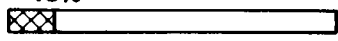
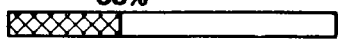
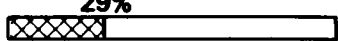
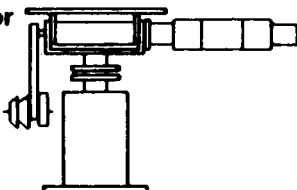
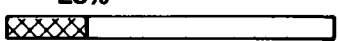
Heliostat foundations consist of a circular concrete ring to support the protective enclosure, and a cylindrical concrete footing for the reflector. Ground surface within the heliostat is covered with both a vapor-barrier membrane and 10.2 cm (4 in) of gravel. Power and control cabling is terminated in protection chasses mounted on the base wall.

Field controllers for the collector subsystem are located at the central control facility. Five controllers are provided in the PD; four for basic operation, and a spare which automatically takes over in the event of a failure of any of the four. Field controllers are operated with fail-safe power, similarly to heliostat electronics.

A weight breakdown for major components of the collector subsystem is given in Table 1.0-1. The heliostat weight, excluding foundation, is 257 kg (568 lbs). Foundation weight, (concrete + steel) is 8509 kg (18,721 lbs).

The PD protective enclosure assembly, Figure 1.0-3, includes a transparent dome, foundation, base wall and air supply system. The dome is an air-supported sphere, 8.54 meter (28 ft.) diameter, cut off at a base angle of 50° from the spherical center, to interface with a base wall of 6.54 meter (21.45 ft) in diameter. The dome is fabricated by heat sealing gores of 0.02 cm (8 mil) thick Tedlar.

Table 1.0-1. Weight Breakdown

Component or activity	Weight kg (lb)/heliostat	Weight kg (lb) research experiment heliostat
<p>Foundation</p> 	<p>Concrete: 7,833 (17,233) Steel rebar: 105 (203) Steel wall: 583 (1,285)</p> <p style="text-align: right;">97%</p> 	<p>7,915 (17,415) 394 (866)</p>
<p>Pedestal</p> 	<p>Steel: 32.5 (72)</p> <p style="text-align: right;">13% (568)</p> 	<p>29.5 (65)</p>
<p>Reflector</p> 	<p>Aluminum: 73 (161) Mylar: 4 (8.8) Foam/adhesives: 8 (17.7)</p> <p style="text-align: right;">33%</p> 	<p>14 (31) 2.3 (5) 1.4 (3)</p>
<p>Protective enclosure</p> 	<p>Tedlar: 52.5 (116) Rope: 2.2 (4.9) Scallops: 12 (27) Pressurization: 6.8 (15)</p> <p style="text-align: right;">29%</p> 	<p>9 (20) 1.4 (3)</p>
<p>Gimbal/actuator</p> 	<p>Alum/steel/ motors/enc: 27 (60) Counterweights: 39 (86)</p> <p style="text-align: right;">25%</p> 	<p>20 (44)</p>
<p style="text-align: center;">Totals</p>	<p>Foundation: 8,509 (18,721) Others: 257 (568)</p>	

Structural design of the dome to withstand a peak 40 m/s (90 mph) wind (at 10 m reference height), dictated pressurization to 0.067 N/CM² (0.098 psi). A single-stage single-speed centrifugal blower has been selected for dome pressurization, to accommodate a predicted leakage rate of 0.28 M³/min (10 cfm). Air filtration is accomplished with a disposable fiberglass filter, designed to trap 99.9 percent of 5 micron and larger particles. The blower/filter package is attached to the outside of the base wall for ease of maintenance.

A steel, cylindrical base wall, 1.24 m (49 in.) high, interfaces the Tedlar dome to a concrete-ring foundation. Segmented clamp strips are used to attach the dome to the base wall, and welded brackets are used to secure the base wall to steel plates in the foundation. The foundation design includes a 0.15 m (0.5 ft.) diameter steel pipe and concrete footing, for reflector support. Ground cover within the heliostat base includes a moisture barrier membrane, covered by sufficient crushed rock or gravel to afford sunlight and physical protection. Ingress and egress to the heliostat is provided by an access door in the base wall.

Power, control and the grounded axial cabling for lightning protection are brought into the heliostat from underground. A power breaker box, heliostat control electronics, and the manual control connector are attached to the base wall adjacent to the air supply inlet. The bare copper ground-grid cabling is attached to the reflector pedestal for minimization of electrical transients in the event of a lightning strike.

The PD reflective assembly consists of a 7.85 m (25.75 ft) diameter ring of aluminum tubing, supported by three tubular arms that interface with a gimbal attachment plate. An aluminized polyester film (Mylar XM648A) is tensioned and bonded to a rigid polyurethane foam pad on one surface of the circular ring. The foam pad is applied in a separate manufacturing operation to provide a flat surface for the membrane reflector. The 0.05 mm (2 mils) thick Mylar film is aluminized on one surface, and operated as a first-surface reflector. Recognizing that polyester films are sensitive to ultraviolet radiation, a diffusely-reflecting protective film is applied to the back side of the Mylar. Selection of an unprotected aluminum surface for the Mylar, made possible by the protected environment in the dome, provided the maximum

reflectance for least cost.

On the basis of successful experience with research experiment hardware, the reflector configuration remains the same as the PD baseline, with the exception of an increase in size. Maximum size was dictated by protective enclosure size, with provision for enclosure deflection and manufacturing tolerances. Optical tests confirmed that the reflector produces an image of satisfactory quality, a gravity focusing effect slightly less than the magnitude predicted, and retention of specular reflectance over a 16-month time period. Research experiment reflectors were fabricated with a predicted uniform biaxial membrane tension of 6.89 MN/m^2 (1000 psi). On the basis of manufacturing experience and expected improvement in collector subsystem performance, membrane tension has been reduced to 5.17 MN/m^2 (750 psi) in the PD reflector. Additionally, developmental tests are planned to confirm that the manufacturing process produces the proper membrane tension.

The control system is comprised of the interfacing Plant Controller (GFE), field controllers (FC), heliostat controllers (HSC) and the interconnecting data communication links (See Figure 1.0-4). The Plant Controller (PC) provides time-of-day and ephemeris data, issues mode commands and receives status data via a serial data link connecting the PC and all FC's. The PC also stores FC programs and data for loading via the data link. The FC's compute individual heliostat pointing angles from time-of-day, solar ephemeris, field geometry, and mode information. Each FC controls up to 512 HC's, which are linked via a half-duplex serial party-line data bus. The FC-HSC message content consists of heliostat address, position, power control commands, and HC status responses. The HSC's generate the proper motor step signals to position the heliostats to the commanded angle. They also process data from shaft position encoders on the gimbal assembly to provide incrementally closed-loop position monitoring. Use of an absolute encoder for continuous position feedback is also under consideration.

The same type data bus is used for each of the party lines. Two-wire shielded "twinax" cable carries a biphasic Manchester format signal. All bus connections

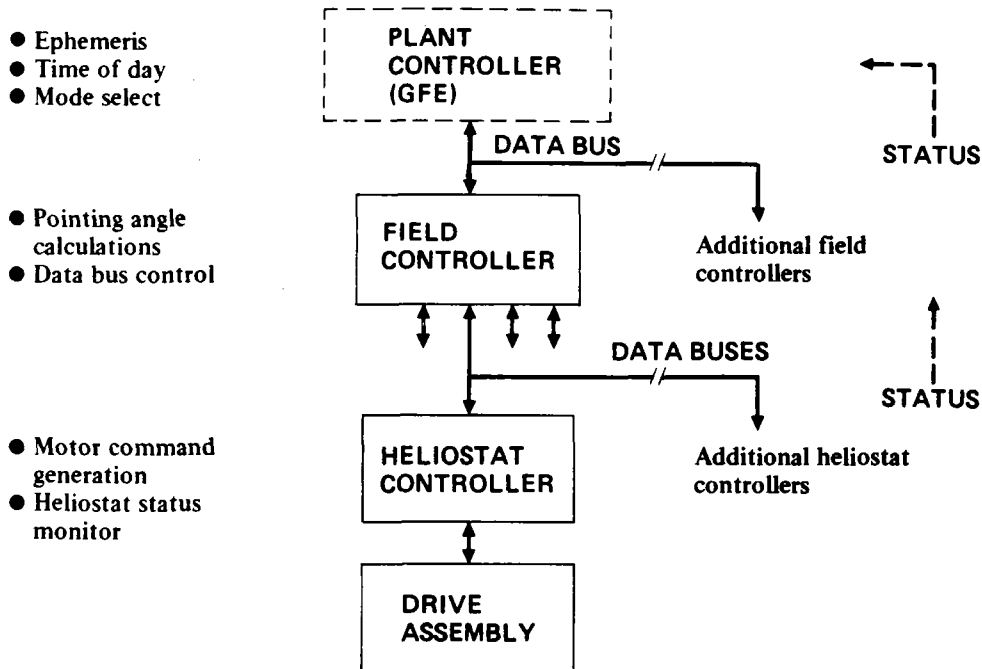


Figure 1.0-4. Control Assembly Major Elements

are transformer coupled to insure maximum failure protection and to provide immunity to signal ground differences, and common mode noise. Each terminal device on the bus has its own modem. Any number of devices from 2 to 128 may share the bus. Lightning arrestors are installed to provide lightning protection for control electronics. Reliability of the data bus twinax is assured by looping it back to the FC, so that in the event of a cable-break, it can be driven from both ends.

The FC-HSC links operate in a polled mode; i.e., the FC continually sequences HSC addresses one at a time along with a command message, and then waits a fixed amount of time for a response. The HSC's upon recognizing its address, immediately responds with status data. Message error checking consists of parity and a Manchester format check. Each transmitted message is preceded by a synchronization signal, comprised of unique pulse widths. This allows a synchronous operation for messages traveling in either direction.

The control subsystem provides the necessary commands to the heliostat drive motors to maintain the reflected solar image on target. The control subsystem also monitors heliostat status and is designed to ensure safe operation in the event of control system failures. The communication links are continuously exercised so that timely detection of a subsystem failure occurs. All commands require a response from the commanded element to verify proper receipt of the command. If communication is lost, the HSC automatically positions the reflector to a safe stow position.

Heliostat pointing angle computations are based on field geometry and knowledge of the path traversed by the sun on any given day of the year. This approach eliminates acquisition delays and loss of tracking due to clouds.

In operation, mode commands are transmitted to the FC's from the plant controller. The mode may apply to all heliostats controlled by a given FC or may be assigned to a particular heliostat. The FC's maintain the mode of each heliostat and compute target angles as required for the commanded heliostat mode. The FC's compute the sun's position relative to each heliostat and determine the heliostat pointing angle (azimuth & elevation) required to direct the reflected image onto the target. Each pointing angle is updated every five seconds and output to each HSC. Field controller redundancy is provided for by a fifth computer with automatic switchover capability. The HSC's determine the difference between current pointing angles and the new commanded pointing angles, and then output the required number of steps in each axis. The steps are uniformly spaced over a predetermined time interval to provide linear position interpolation between command updates.

The proposed design takes advantage of current technology to provide a safe, high-performance, low-cost control system. The use of microprocessors in the HSC's greatly reduces the FC workload, allowing four FC's to control all heliostats. The microprocessors also provide flexibility in message-formatting and heliostat control. The programs can be easily modified, if necessary, for specific requirements.

The data bus is based on a proven design currently in use by Boeing. The design was selected over a concept involving "dedicated-lines" to each heliostat,

based on cost savings. The data bus design permits the FC's to be centrally located in the plant control building with negligible cabling penalty. This location eliminates the need for special environmental protection and provides ease of maintenance.

Safety is a primary consideration in the collector subsystem preliminary design. The objective of the safety effort was to identify, eliminate or minimize hazards to the pilot plant operations/maintenance personnel, the general public and equipment. This was accomplished by performing a preliminary hazard analysis, and incorporating safety considerations into the operations and maintenance procedures. The principle safety concern for the collector subsystems is control of reflected light from heliostats, specifically converging light beams. Accordingly, considerable effort was applied to developing operational procedures, redundant control and power circuits, and alternate procedures initiated by warning signals, to prevent reflected light hazards.

The collector subsystem reliability has been a consideration throughout the preliminary design phase. While a primary driving force is low initial cost; by increasing reliability in key areas, the life cycle costs can potentially be lowered while increasing availability.

The design intent has been to provide redundant systems in areas where a failure would have a drastic effect on either safety or plant availability. Secondary considerations were ease or cost of maintenance, and ability to withstand the Pilot Plant environment.

As part of this effort, a PD baseline was developed during the first five months of this program. Subsequently, three heliostats and a drive and control assembly were fabricated and tested to provide design data and verification of the PD. In addition, an extensive evaluation program was conducted on the key plastic materials used in the protective enclosure and reflector. Performance and environmental exposure tests on large-scale heliostats were conducted over an 8-month period at a Boeing desert test site in northeast Oregon. Environmental exposure tests on the same heliostats are presently planned to continue

through March, 1978. Plastic materials evaluation tests included measurement of mechanical and optical properties, creep, chemical exposure, cleanability, accelerated simulated sunlight, and actual desert sunshine exposure tests. The latter test were performed at two different locations in the Southwest (Albuquerque, N. M., and China Lake, CA).

Results of the research experiment test program and design analyses have provided the basis for the final PD presented herein. Specifically, fabrication and test of the research experiment hardware has verified that:

- . Tedlar protective enclosures and lightweight aluminized Mylar reflectors can be fabricated inexpensively with conventional manufacturing processes.
- . Digital-controlled reflector orientation based on initial alignment by laser/geodolite, and incremental position feedback from optical encoders, will provide image aiming accuracy which meets performance specifications (2 milliradians on a 1 σ basis).
- . Protection of the reflector from wind, with an air-supported enclosure provides the following system operation advantages:
 - elimination of need to traverse from stow to standby during daytime hours, which can eliminate reflection of light to adjacent terrain;
 - operation of collector subsystem at any wind velocity up to the 40 m/s (90 mph) maximum;
 - minimization of parasitic power required for reflector orientation.
- . Preliminary reliability/maintainability analyses indicate that availability of the collector subsystem will meet or exceed the 0.97 requirement;

- cleaning of protective enclosures on intervals as long as 6 mos, in winter, and less than 6 mos, in summer,
- Replacement or cleaning of air supply filters at intervals no less than 9 mos.
- Replacement of domes one time over a 15-24 year time frame
- Replacement or maintenance of air-supply blower motors one time.

In general, the collector subsystem PD is substantiated by favorable manufacturing and installation experience, and with design-confirming test results on research experiment hardware. Throughout the program, only moderate design configuration changes were made for the purposes of reducing cost or improving performance. The reflector was changed from a triangular to a circular stretched membrane, which significantly increased reflector area within the protective enclosure. Concurrently, a short, vertical cylindrical wall was added between the protective enclosure base and the concrete foundation, to provide space for the circular reflector when oriented near vertical. In conjunction with DuPont, an improved composition of Tedlar was developed with improved stability of optical transmittance, and extended mechanical property lifetime. The size of the protective enclosure was increased from 7.01 m (23 ft) to 8.54 m (28 ft) diameter, along with a corresponding increase in reflector size from 6.48 m (21.25 ft) to 7.85 m (25.75 ft) diameter. The size increase, which significantly reduces collector subsystem cost, was permitted by the availability of thermally laminated Tedlar in a thickness of 0.020 cm (8 mil).

ITEM	DATA OR INFORMATION		LOCATION IN DOCUMENT		FACTOR OR DESIGN MARGIN	
	PILOT PLANT	SRE	PILOT PLANT	SRE	PILOT PLANT	SRE
1. Number of Heliostats	1650		3.3.1		3.3.1	
2. Collector Field Geometry & System			3.3.1		3.3.1	
3. Stair Step Energy Balance			3.3.1		3.3.1	
4. Nominal Characteristics of Collector Subsystem and Minimum and Maximum Operational Ranges			3.3.1		3.3.1	
5. Collector Subsystem Efficiency	54.5%		3.3.1		3.3.1	
6. Auxiliary Power Requirement (for all modes)	128kW max. 46.6 kW min.		3.3.6			
7. Field Layout			3.3.1			
8. Field Oversizing to allow for dirt on mirrors, reliability, etc.			3.3.1		3.3.1	
9. Beam pointing accuracy and error budget vs environmental effects	2 mrad.	0.1° RSS 0.17° Max.	3.3.4.4	3.3.4.4	3.3.4.4	3.3.4.4
10. Heliostat Beam quality and error budget vs environmental effects			3.3.3 3.3.4.4	3.3.3 3.3.4.4	3.3.3 3.3.4.4	3.3.3 3.3.4.4
11. Heliostat weight breakdown			1.0	3.3.2 3.3.3	1.0	3.3.2 3.3.3
12. Heliostat parts count			1.0	3.3.2 3.3.3 3.3.4		
13. Foundation and field wiring			3.3.6			
14. Identify non-standard parts			4.4			
15. Identify single-source parts			4.4			
16. Identify long-lead items			4.4			
17. Identify parts having high infant mortality rates			6.0			
18. Power required for track, slew, and emergency shutdown	128kW max.		3.3.6			

ITEM	DATA OR INFORMATION		LOCATION IN DOCUMENT		FACTOR OR DESIGN MARGIN	
	PILOT PLANT	SRE	PILOT PLANT	SRE	PILOT PLANT	SRE
	19. Heliostat operating modes			3.3.4		
20. Control system details and characteristics			3.3.4	3.3.4		
21. Operation and survival versus environmental conditions			3.3.2.3 3.3.3.3	3.3.2.3 3.3.3.3	3.3.2.3 3.3.3.3	3.3.2.3 3.3.3.3
22. Heliostat focusing and alignment procedure			3.3.5			
23. Maintenance required			9.0			
24. Mirror cleaning method			5.0			
25. Define mirror requirements			3.1	3.1		
26. Discuss mirror assembly details			3.3.3.1			
27. Provide data on degradation rates of mirrors, seals, paint, motors, drains, etc.			3.3.2.2 3.3.3.2	3.3.2.2 3.3.3.2		
28. Discuss method for safe control of reflected light			7.0			
29. Discuss fail-safe features			7.0 3.3.4			
30. Discuss reliability			6.0 6.0			

14

3.0 COLLECTOR SUBSYSTEM PRELIMINARY DESIGN

3.1 DESIGN REQUIREMENTS/SPECIFICATIONS

Performance requirements and specifications for the collector subsystem preliminary design are summarized in Table 3.1-1, and will be provided in detail in Reference 3.1-1. Requirements which are generally applicable are listed under the item, "Collector Subsystem." All other requirements are listed under the respective subassembly items "Reflective Assembly," "Protective Enclosure Assembly," and "Drive and Control Assembly." Per ERDA/Sandia request, information is provided in the table to indicate any excess capabilities of the PD over and above the requirements/specifications.

TABLE 3.1-1
SUMMARY OF PERFORMANCE REQUIREMENTS
AND SPECIFICATIONS FOR COLLECTOR SUBSYSTEM PRELIMINARY DESIGN

Item	Performance Requirement	Specification	Design Compliance
Collector Subsystem	Ambient Temperature Environment	-30 to 50°C Survival -20 + 50°C Operating	Yes
	Earthquake Environment Maintenance	Seismic Zone 3, 0.25 g's ground acceleration Use of normal skills and minimum specialized equipment and tools.	Exceeds
	Transportability	Subject to all pertinent federal and state regulations.	Yes
	Electrical Transients and Lightning	Protected against external and internal transients, on the basis of cost/risk optimization	grounded-grid, and arrestors on control cables
	Interchangeability	Major components to be interchangeable.	Yes
	Safety	Comply with pertinent OSHA rules and ERDA pilot plant regulations.	Yes
	Design Conditions	Insolation 0.95 kW/m ² Dry bulb temp. 28°C Wet bulb temp. 23°C Wind speed 3.5 m/sec @ 10 m elevation	Yes
		Receiver incident power @ solar Noon Equinox 42 mW _t Receiver flux distribution See Section 3.3.1	Yes Yes

Table 3.1-1 (Cond.)

Item	Performance Requirement	Specification	Design Compliance																			
Reflective Assembly	Nameplates	Attach nameplates to major assemblies	Yes																			
	Specular Solar Reflectance	Greater than 85% within 0.3° scattering angle.	88.6% (Normal Incidence)																			
	Stowage Position	Vertical position for maintenance and control of reflected light	Yes																			
	Stowage Initiation	Stowage to be initiated at TBD M/S Wind Velocity	No known limiting velocity.																			
Protective Enclosure Assembly	Maintainability	Ease of replacement of reflector	Yes																			
	Specular Solar Transmittance	Greater than 86% within 0.3° scattering angle.	87.0%																			
	Power Input	30 watts	20 watts																			
	Survival Wind	40 M/Sec @ 10 m	Yes																			
	Wind Velocity Frequency	<table border="1"> <thead> <tr> <th>Speed, m/sec</th> <th>Freq., %</th> </tr> </thead> <tbody> <tr><td>0-2</td><td>29</td></tr> <tr><td>2-4</td><td>21</td></tr> <tr><td>4-6</td><td>19</td></tr> <tr><td>6-8</td><td>14</td></tr> <tr><td>8-10</td><td>8</td></tr> <tr><td>10-12</td><td>5</td></tr> <tr><td>12-14</td><td>3</td></tr> <tr><td>over 14</td><td><1</td></tr> </tbody> </table>		Speed, m/sec	Freq., %	0-2	29	2-4	21	4-6	19	6-8	14	8-10	8	10-12	5	12-14	3	over 14	<1	Yes
		Speed, m/sec	Freq., %																			
		0-2	29																			
		2-4	21																			
		4-6	19																			
		6-8	14																			
		8-10	8																			
10-12	5																					
12-14	3																					
over 14	<1																					
Peak Operational Wind	Peak Gust Speeds of TBD	No known limiting velocity																				
Wind Rise Rate	0.01 m/sec ²	No known limiting rise rate																				
Wind Profile	Exponential with height to 0.15 power	Yes																				
Dust Devils	17 m/sec	No known limiting velocity																				
Rainfall	<table border="1"> <tbody> <tr><td>Average annual</td><td>75 cm</td></tr> <tr><td>Max 24 hr</td><td>7.5 cm</td></tr> </tbody> </table>	Average annual	75 cm	Max 24 hr	7.5 cm	No known limiting rainfall																
Average annual	75 cm																					
Max 24 hr	7.5 cm																					

Table 3.1-1(Cond.)

Item	Performance Requirement	Specification	Design Compliance	
Drive & Control Assembly	Snow Load	250 Pa (5 psf)	Yes	
	Ice Accumulation	5 cm (2 in.)	Yes	
	Hail	2.5 cm @ 23 m/sec	To be tested	
	Air Quality		1) Prevent condensation on internal surfaces	Yes
			2) Minimize particulate deposition on reflector, less than 5% reflectance decrease in 10 years.	Yes
	Rigidity		Provide adequate clearance from reflective assembly under all environmental conditions.	Yes
	Maintainability		1) Ease of cleaning	Yes
			2) Ease of repair of leaks	
			3) Ease of replacement of parts in air supply apparatus.	
	Safety		Fail safe operation during power outage and electrical transients	Yes for Field
	Power Input		50 watts/heliostat operating	Yes
			10 watts/heliostat (non-operating)	Yes
Orientation Accuracy		2 milliradians (1 σ basis)	Yes	
Emergency Shutdown		Reduce incident radiation on receiver to less than 3% of initial value within 40 secs.	Yes	
Track		Orient heliostats to reflect sunlight to receiver, upon command from central control simulator.	Yes	

Table 3.1-1 (Cont.)

Item	Performance Requirement	Specification	Design Compliance
	Shutdown	Orient heliostats to vertical stowage position upon command from central control simulator.	Yes
	Standby	Provide continuous tracking adjacent to receiver.	Yes
	Manual Control	Provide manual control station at heliostats.	Yes
	Limit Controls	Provide limit control switches on drive gimbal.	Yes
	Alignment	Provide alignment check upon command from central control.	Yes
	Maintainability	Ease of replacement and maintenance of components	Yes

3.2 INTERFACE REQUIREMENTS

For preliminary design purposes it was necessary to define interfaces between the collector subsystem and other portions of the pilot plant. Details of these interfaces are described in pertinent sections of the document. Major interfaces included:

<u>Interface</u>	<u>Requirement</u>
Receiver	McDonnell - Douglas cylindrical receiver
Central Control	Mode commands (group or individual) Time-of-day information Ephemeris data Field controller programming/data load Optical scanner commands Power on/off commands Data request identifier
Utility Power	480V, 3 phase, 128.6 kW (peak)
Building	Location for field controllers in central control facility Location for emergency generator and associated hardware Provision for spares and support equipment storage Maintenance/repair shop
Alignment/scanner apparatus	Provision for attachment of hardware to tower 230/115 V single phase power at tower interface point Data transmission cabling at tower interface point

3.3 COLLECTOR SUBSYSTEM CONFIGURATION

3.3.1 Heliostat Field Geometry and Performance

The following section defines the configuration of the pilot plant heliostat field. The analytic methods used to design the field, as well as the ground rules of the analysis precede a discussion of the resultant field configuration and performance.

3.3.1.1 Ground Rules

General Ground Rules

The pilot plant is located at Barstow, California (latitude of 34.9°N). The design point time is solar noon, on the equinox (solar declination of 0°). The direct insolation is assumed to be 950 watts per square meter.

Heliostat Ground Rules

The optical portion of the heliostat consists of a circular reflector housed in a transparent, spherical protective enclosure. The diameter of the reflector is 7.86 m (25.78 ft). The enclosure has a diameter of 8.54 meters (28.0 ft).

It is assumed that the amount of deflection experienced by the reflective membrane varies with the elevation angle of the reflector. For a membrane tensioned at $5.17 \times 10^6 \text{ N/m}^2$ (750.0 psi), the focal length of the reflector can be expressed, in meters, as $376.5/\sin \psi$, where ψ is the elevation angle of the reflector ($\psi = 0^{\circ}$ for vertical reflector).

The reflectivity of the membrane is a function of the incidence angle of the incoming light and is graphed in Figure 3.3.1-1.

The transmissivity of the protective enclosure material is also a function of the light's incidence angle. It is presented in Figure 3.3.1-2.

The reflector has two axis control. The pointing error in the azimuth and

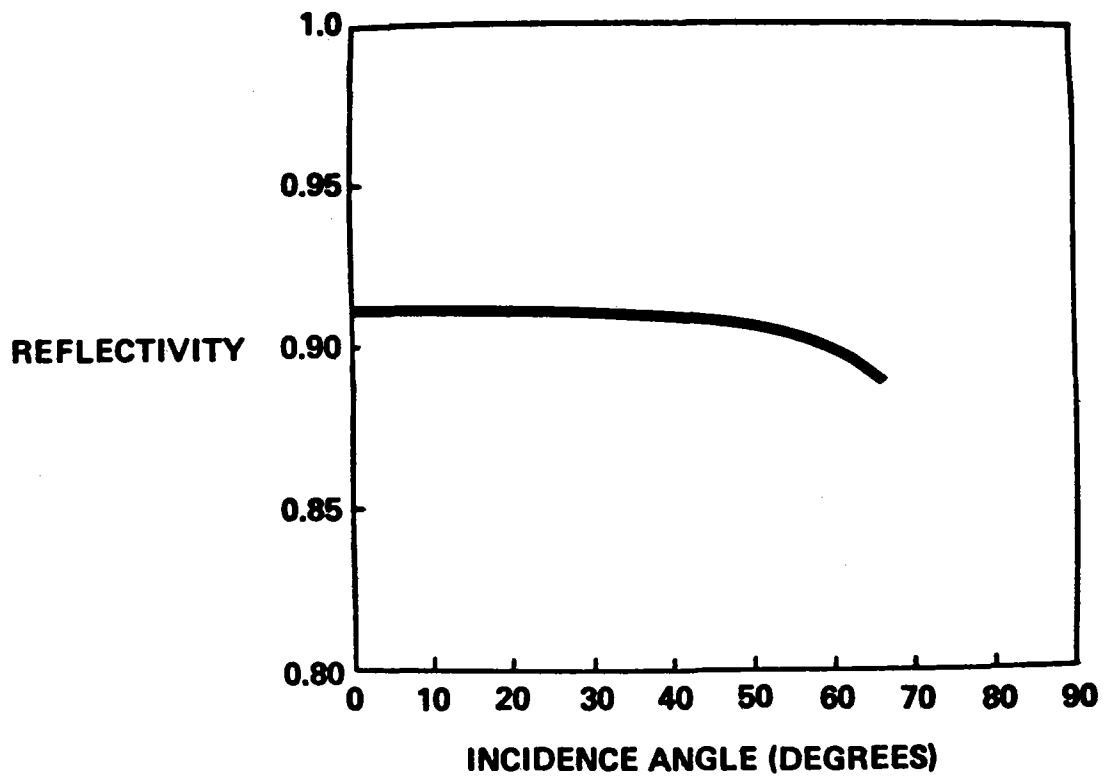


Figure 3.3 1-1 . Reflectivity vs Incidence Angle

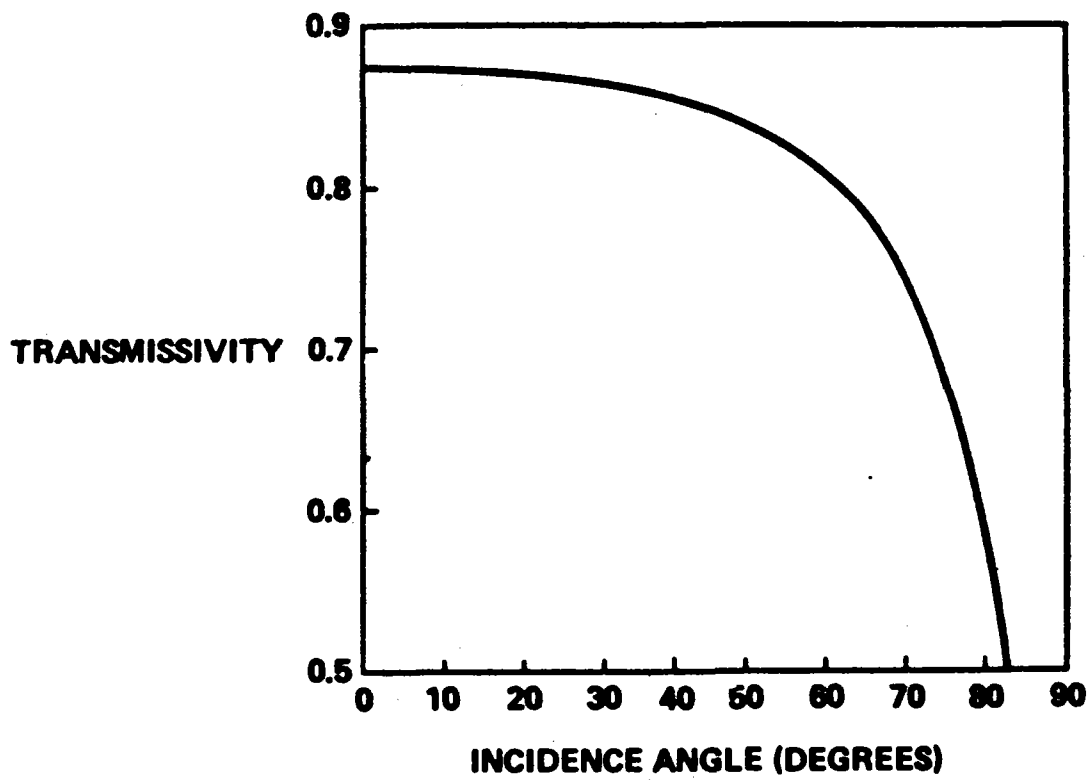


Figure 3.3.1-2 . Transmissivity versus Incidence Angle

elevation axes are each modeled as normally distributed with a mean of 0 radians and a standard deviation of 2 milliradians.

Receiver Ground Rules

The heliostats reflect the sunlight onto a cylindrical surface receiver. It is mounted atop a tower, such that it is 80 m (262.4 ft) to the center of the cylinder. The cylinder has a radius of 3.5 m (11.48 ft) and a height of 12.5 m (41.00 ft).

The heliostats are aimed at three different heights on the receiver, so as to distribute the heat flux. The absorptivity of the receiver drops off as the incident light strikes it more obtusely, as seen in Figure 3.3.1-3.

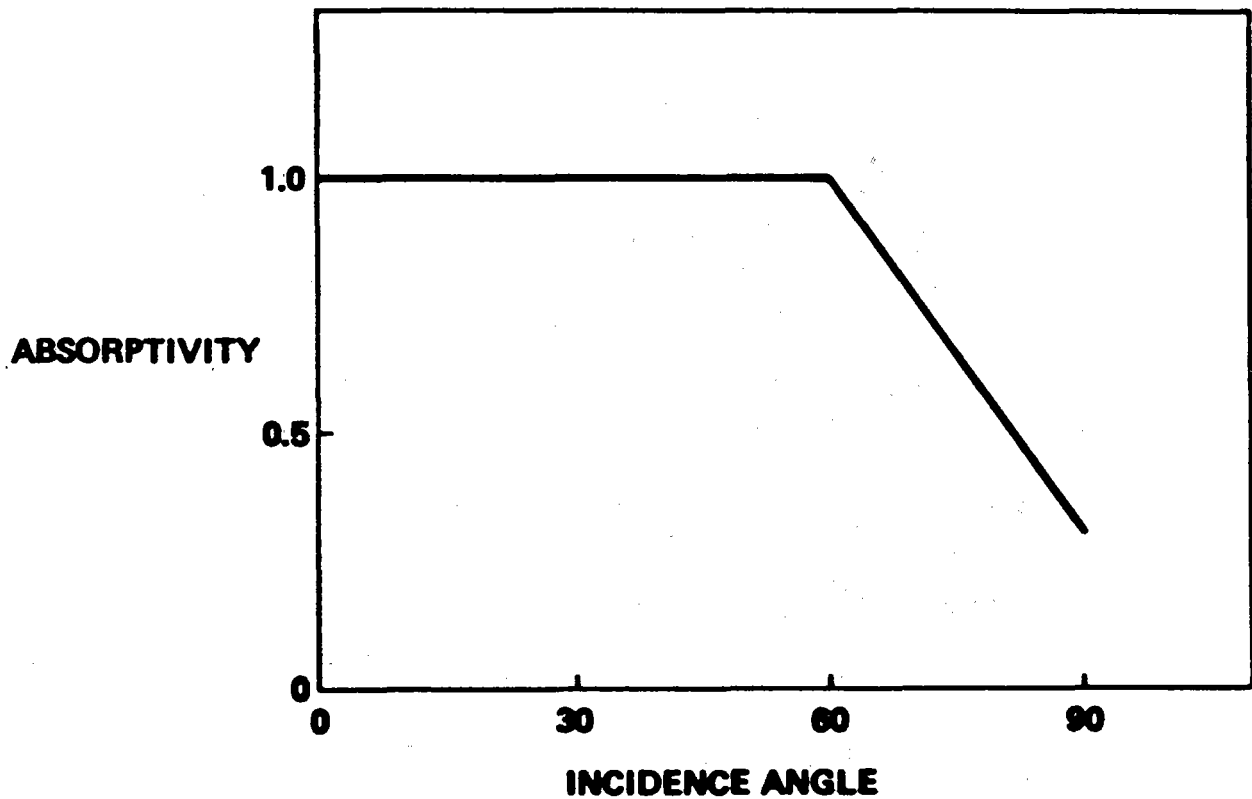


Figure 3.3.1-3. Absorptivity vs Incidence Angle

The thermal requirement of the receiver is approximately 42 MW_{th} at the design point. A specified circumferential distribution of this flux is also required. If we number the receiver panels as in Figure 3.3.1-4, then the required flux is as follows:

<u>Panel</u>	<u>Required Flux (MW_{th})</u>
1,24	2.71
2,23	2.64
3,22	2.56
4,21	2.44
5,20	2.31
6,19	1.97
7,18	1.63
8,17	1.38
9,16	1.13
10,15	.94
11,14	.75
12,13	.69

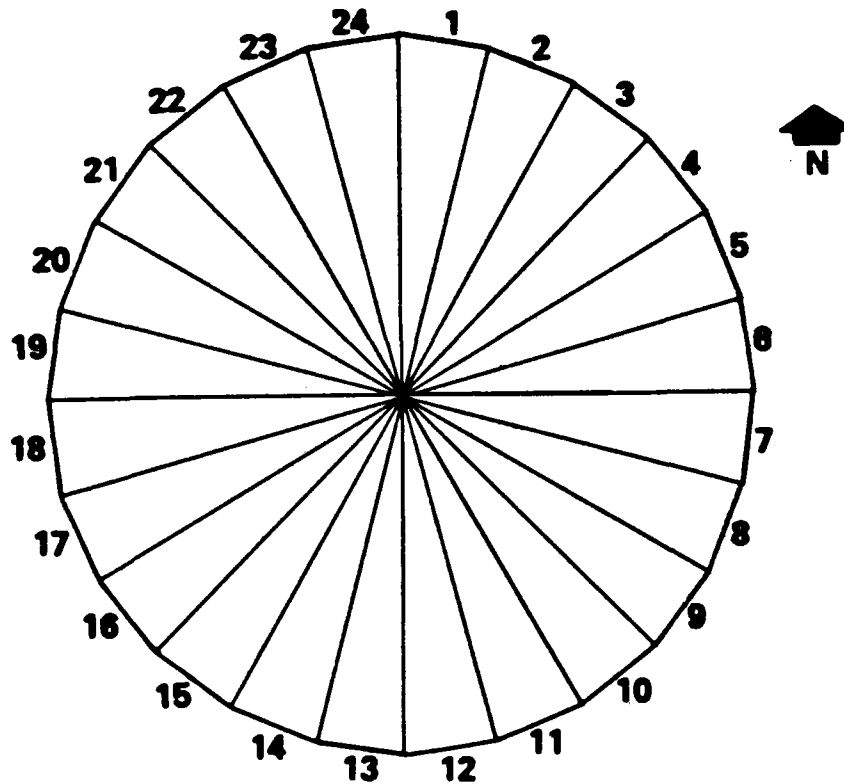


Figure 3.3.1-4. Receiver Panels

3.3.1.2 Analysis Methodology

Heliostat Array Simulation Computer Model

The Heliostat Array Simulation Computer Model (HASCAM) is the optical ray trace program used to analyze the performance of the heliostat field.* The major calculating subroutines are indicated in the flow chart Figure 3.3.1-5.

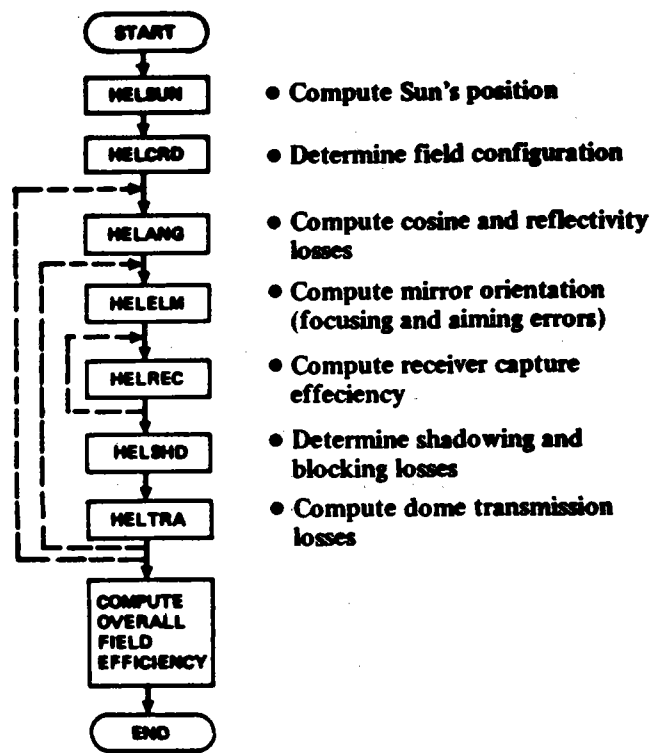


Figure 3.3.1.-5. Heliostat Array Simulation Computer Program

The program begins by calculating the position of the sun, based on latitude, day, and time inputs. Then the size and spacing input are used to develop the configuration of the field. The field is analytically sectioned and a representa-

*See reference 3.3.3.3-4.

tive heliostat is chosen for each section. The performance of this heliostat is then computed, taking into account all relevant component performance characteristics, such as mirror reflectivity, enclosure transmissivity, and pointing accuracy, and the geometric relationships of the heliostats and the receiver. These calculations result in the determination of the average heliostat efficiency for each section of the field, as well as the number of heliostats in that section.

Heliostat Field Design

The first step in designing the heliostat field is to execute HASCAM with the inputs of subsystem performance and geometry set to the appropriate values. This will generate an efficiency and total heliostat area for each section of the field. These can be combined with a value for direct insolation to yield an energy contribution for each field section.

Sections of the field are now chosen in decreasing order of efficiency until the thermal requirement of the receiver is met. If necessary, portions of a section may also be used. It must also be noted that the field is to be east-west symmetric to insure equal efficiency in the morning and afternoon.

Finally, minor modifications of the field are made to clear an area about the tower and to allow for tower shadowing. Tower shadowing effects were included in the analysis but found to be negligibly small.

Parametric Studies

Parametric studies were conducted to determine the best choice of reflector size, pointing accuracy, and focussing strategy. Heliostat fields were designed with reflector radii sized from 3.0 m (9.84 ft.) to 6.0 m (19.68 ft.).

The results are presented in Figures 3.3.1-6 and 3.3.1-7. The combination of costs for heliostats on a per unit and per area basis indicated that the reflectors should be sized at 3.93 m (12.89 ft) radius, the upper limit due to structural constraints (see Section 3.3.2.3).

- Cylindrical surface receiver
- Pointing accuracy: 1 mrad
- Insolation: 825 W/m^2
- Thermal requirement: $42 \text{ MW}_{\text{th}}$, 2:00 p.m., winter solstice

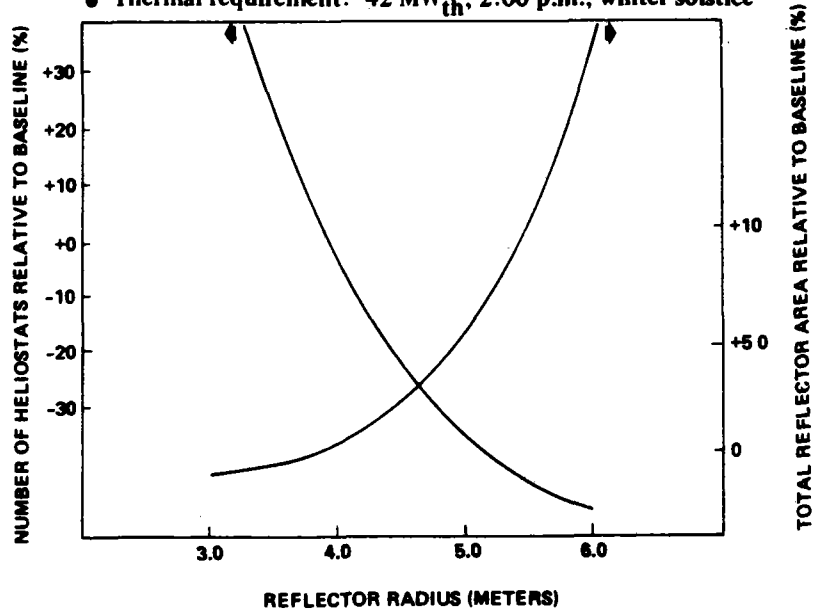


Figure 3.3.1-6. Heliostat Sizing Study

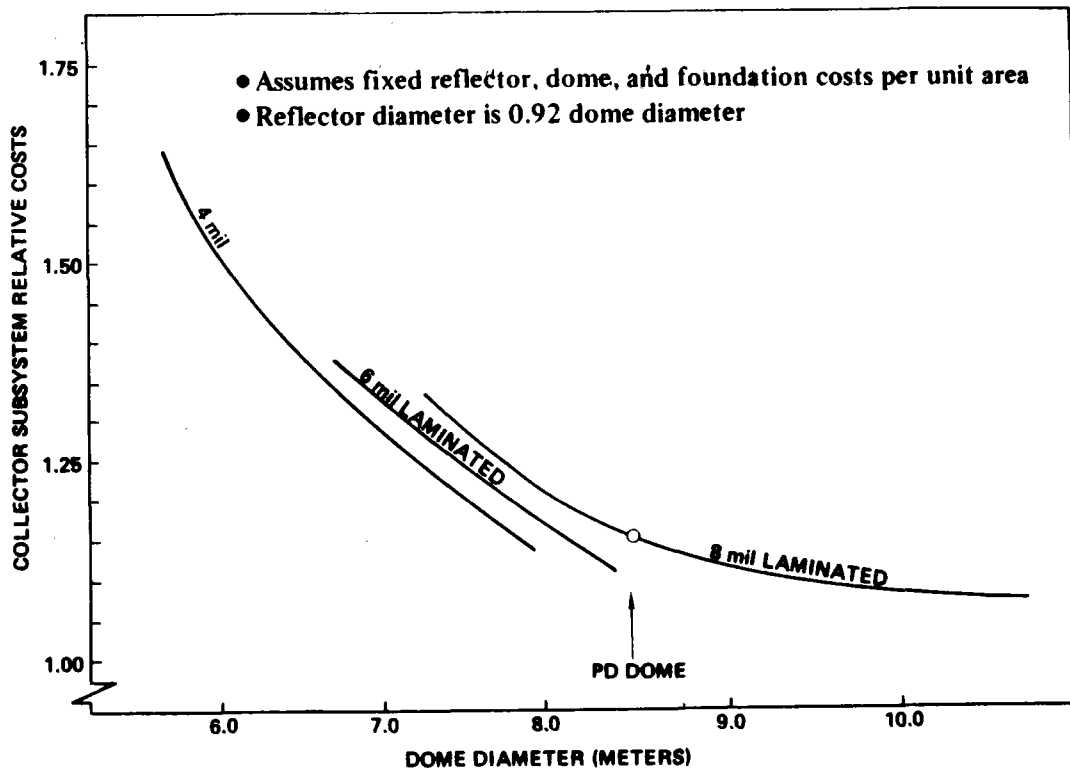


Figure 3.3.1. -7. Heliostat Costs

Varying the standard deviation of the aiming error yielded the results in Figure 3.3.1-8. Again, individual heliostat costs were traded against number of heliostats to arrive at 2 milliradians as the cost-optimum design point.

- Cylindrical surface receiver
- Reflector radius: 3.43m
- Insolation: 825 W/m^2
- Thermal requirement: 42 MW_{th} , 2:00 p.m., winter solstice

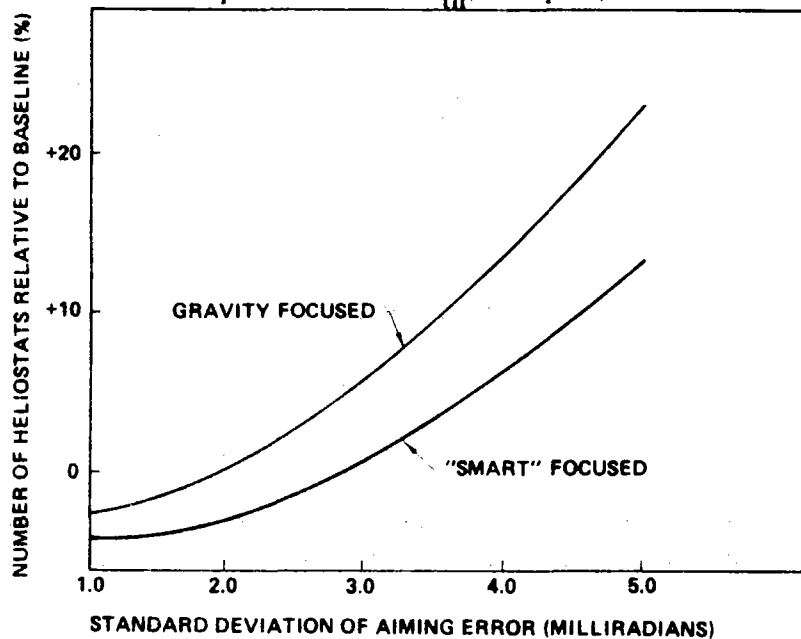


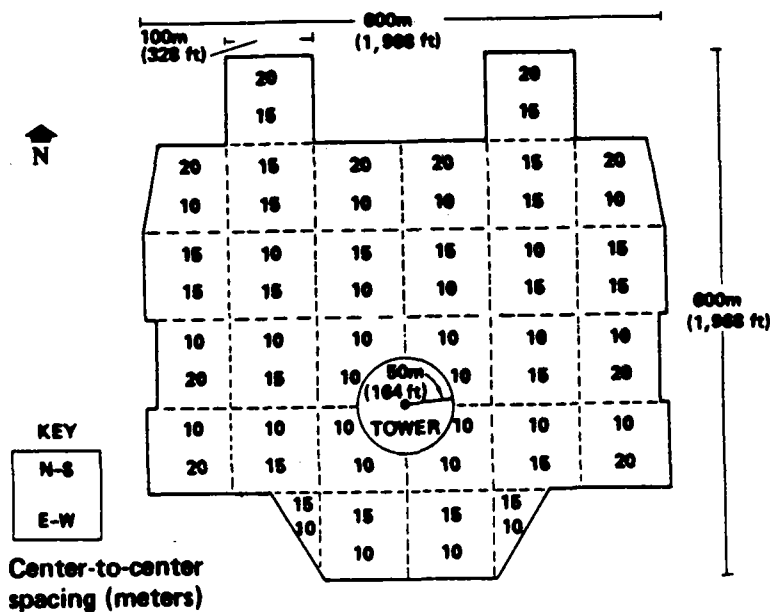
Figure 3.3.1-8. Heliostat Pointing Accuracy Study

The possibility of constructing heliostats which would vary their focal length according to their position in the field and the time of day was considered. Analysis showed about a 3% savings in the required number of "smart focussed" heliostats over a field of "gravity focussed" reflectors, was not enough to offset the additional cost per heliostat.

3.3.1.3 Heliostat Field Layout and Performance

Heliostat Field Layout

Three center-to-center heliostat spacings were considered in both the east-west and north-south direction. Taking all combinations of these spacings produces nine different spacing patterns. The Heliostat Array Simulation Computer Model was run for nine fields, each one corresponding to one of the spacing patterns. The final field was designed by combining field sections from each of these nine fields so as to minimize the total number of heliostats. Trades were made between packing inner heliostats more densely, and thereby lowering their efficiency, and adding heliostats in the less efficient outer areas of the field. The resultant field layout is shown in Figure 3.3.1-9. There are 1650 heliostats in this field.



System Efficiencies

If we define the efficiency of the heliostat field as the energy captured by the receiver, divided by the insolation times the total reflector area, then we arrive at 54.5% as the design point field efficiency. The various components of the field efficiency are broken out in Figure 3.3.1-10.

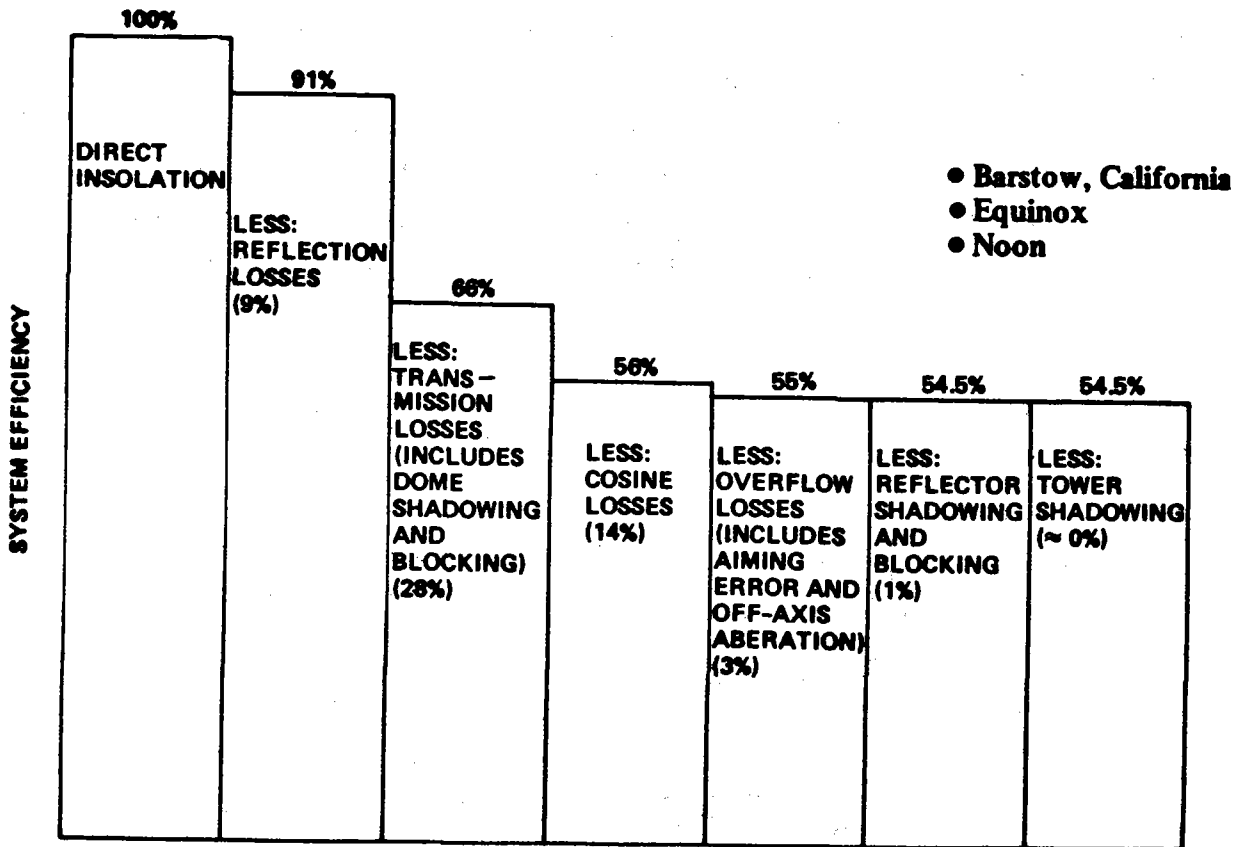


Figure 3.3.1-10. Heliostat field Field Efficiency

The field efficiencies and thermal power to the receiver (assuming insolation of 950 W/m^2) at off-design points are as follows:

	<u>Efficiency</u>	<u>Thermal Power On Receiver</u>
Noon, Summer Solstice -	56.4%	42.7 MW_t
Noon, Winter Solstice -	45.9%	34.8 MW_t
2 pm, Winter Solstice -	46.7%	35.4 MW_t

Design Allowance

For preliminary design purposes, no specific allowance was made for performance degradation due to long-term environmental effects, dirt accumulation, or reliability. Detail design analyses will, however, include degradation allowances derived from research experiment heliostats. Environmental exposure of research experiment heliostats is presently planned to continue through March 31, 1978, providing 19-month exposure data.

It should be noted that, although a specific degradation allowance was not included in the PD, excess collector subsystem capacity does exist for a large fraction of the year because of the design point established by Sandia (solar noon, equinox).

3.3.2 Protective Enclosure Assembly

Preliminary design of the protective enclosure assembly involved configuration studies, materials studies, structural analyses and evaluation of research experiment results. Results of these studies are discussed below.

3.3.2.1 Configuration

The protective enclosure assembly includes a transparent dome, base wall, foundation, and an air supply system.

Dome

The dome design selected for Pilot Plant PD is an air-supported transparent sphere as shown in Figure 3.3.2.1-1. The diameter is 8.54 m (28 ft.) and the base is truncated at an angle of 50° from the spherical center to interface with a base wall of 6.54 m (21.45 ft.) in diameter. The dome is fabricated by heat sealing gores of 0.02 cm (8 mil) thick Tedlar. Three subassemblies of gores are joined together to complete the dome: a lower section with 22 gores; an upper section with 11 gores; and a polar cap with 4 pie-shaped sections.

Base

The heliostat-base design shown in Figure 3.3.2.1-2 includes a cylindrical steel sidewall, reflector support post, foundation, and air supply. The wall is 1.2 m (49 in.) high, 6.5 m (21.45 ft.) in diameter, and is formed from two cylindrical sections; a lower section 0.15 cm (0.06 in.) thick, and an upper section 0.48 cm (0.189 in.) thick. The upper section includes a rectangular channel stiffener, and fasteners for enclosure retainers, as shown in Detail I of Figure 3.3.2.1-2. Wall perforations include a 0.61 m (2 ft.) square access door, blower port, and a connector for manual control. A portable airlock described in Section 4.0, is required for entering the protective enclosure. A similar airlock was successfully used in research experiments.

The sidewall is interfaced with a concrete-ring foundation, using brackets which are welded to steel plates in the foundation at 12 different locations. The 7351 Kg (16,173 lb.) concrete foundation, combined with the weight of steel in the wall 583 Kg (1285 lbs), provides sufficient mass to react the 43,100 N (9690 lbs) vertical force expected during peak wind loads. To minimize air leakage from the protective enclosure, a flexible caulking compound is applied at the steel wall/concrete interface and at other wall perforations.

The Tedlar dome is attached to the sidewall using 22 segmented clamping strips as shown in Detail I of Figure 3.3.2.1-2. The lower edge of each clamping strip is a circular arc, incorporated to provide uniform stress loading of dome gore sections. Using this attachment concept, upward tensile forces are reacted by the roped edge bearing against the clamping strip. A thin foam-rubber layer is applied to both the sidewall and clamping strips to protect the Tedlar from mechanical abrasion. Results of research experiments verified that this dome attachment design will be very satisfactory for the Pilot Plant P.D. No materials or structural problems were encountered over 8 months of testing. The only basic design change for the PD is replacement of "thru-bolting", eliminating holes in the Tedlar base.

Reflector support is provided by a 15.24 cm (6 in.) diameter steel pipe which is supported with a 0.38 m (15 in.) diameter by 1.83 m (72 in.) deep concrete foundation. The 0.11m^2 (1.23ft^2) foundation base area is more than adequate for supporting an anticipated bearing load of $0.07 \frac{\text{MN}}{\text{m}^2}$ (1465 lbs.) including foundation weight.

Air Supply

Pressurization of the dome to 0.067 N/cm^2 (0.098 psi) ($2.71\text{ in. H}_2\text{O}$) is accomplished with a small centrifugal blower mounted on the outside of the wall, within a filter plenum (Figure 3.3.2.1-2). Both the filter plenum and blower are attached to the wall with mechanical fasteners. Blower replacement can be accomplished without an auxiliary air supply. Tests on research experiment heliostats showed that, with reasonable caulking, leak rate was about $0.14\text{ m}^3/\text{min}$ (5 cfm). Considering the additional crack-length on larger PD protective enclosures, a leak rate of $0.28\text{ m}^3/\text{min}$ (10 cfm) has been selected for design purposes. Centrifugal blower

pressure/flow characteristics, when operating near stagnation flow, will permit moderate variations in leak rate while maintaining near-constant pressure.

Power requirements for properly-sized blower motors are estimated at 20 watts. The air filter selected for the PD is a disposable fiberglass element, 30.48 cm sq. (12 in. sq) by 10.16 cm (4 in.) thick. The filter plenum protects the element from precipitation and permits easy replacement. A filter efficiency of 99.9 percent for 5 micron particles and larger, has been selected for the PD.

3.3.2.2 Materials

Selection of dome material involved screening of various candidate materials based on their transmittance, strength, weatherability and cost. Tedlar was selected early in the program as the preferred material based on mechanical and optical properties, cost, and weatherability. Subsequently, research experiments verified that from a technical standpoint Tedlar is a very satisfactory material for the Pilot Plant domes. Experiments were conducted to select the optimum composition of Tedlar from three varieties: "standard", "UV screen"; and "no additive." Results of research experiments on these specimens (discussed below) showed that the "no-additive" composition (DuPont designation 400 XRS 158TB) exhibited superior UV resistance and specular solar transmittance, and has comparable strength characteristics. Accordingly, it was utilized for research experiment domes, and is specified for Pilot Plant domes. Since the "as produced" film has insufficient specular solar transmittance, it must be roll-polished utilizing a smooth polyester film (DuPont 200XM648A or comparable substitute).

Concurrent with the utilization of Tedlar for research experiment domes, a search for alternative lower-cost film materials has continued throughout the program. Requirements were transmitted to major U.S. film manufacturers ; and seven candidate films were obtained and evaluated. Evaluation included measurement of solar specular transmittance and mechanical properties. At the present time, Kynar (manufactured by Pennwalt Corp.) is the most promising alternative dome material.

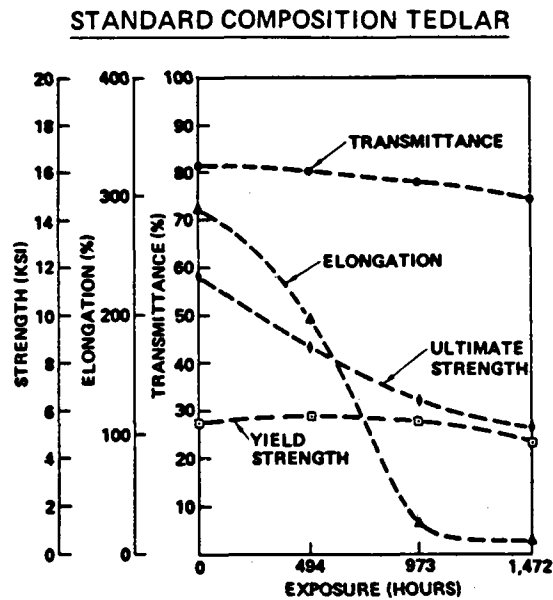
Tedlar thickness specified for the PD domes is 0.02 cm (8 mil). Research experiment domes were built with 0.01 cm (4 mil) Tedlar (the maximum thickness produced by DuPont); and 0.015 cm (6 mil) had been specified for the PD baseline on the basis that DuPont would produce it for Pilot Plant quantities. Subsequent to defining the PD baseline a process became available for thermally laminating two 0.01 cm thick layers into 0.02 cm (8 mil) material. The reduction in collector subsystem cost with increasing dome size, as discussed in Section 3.3.1, was the principal reason for selecting the thickest available material and the largest allowable dome diameter dictated by wind loads.

To evaluate the laminated material, a roll of the baseline 0.01 cm (4 mil) material was divided and thermally laminated. Tests on the 0.02 cm (8 mil) material have shown comparable strength to unlaminated 0.01 cm (4 mil) material, solar specular transmittance which exceeds minimum specifications, and satisfactory heat-sealed joints on 4.88 m (16 ft) long specimens. The design yield strength is 33.0 MN/m² (4800 psi), and the ultimate strength averages 61.3 MN/m² (8900 psi). Yield strength of heat sealed joints remained the same as the basic material, and ultimate strength averaged 25 percent greater than yield. Solar specular transmittance at normal incidence, and a 0.5° scattering cone angle, is specified at 87.4 percent for PD purposes. This value was determined from limited sampling of the experimental roll. Past experience shows that a transmittance variation in the order of ± 1 percent can be expected due to material variations and instrumentation errors.

Lifetime of the Tedlar dome is a key factor in determining collector subsystem life cycle cost. Solar specular transmittance and mechanical properties are key parameters for determining lifetime. Accordingly, research experiments emphasized conducting environmental exposure tests, and evaluating available environmental exposure data on Tedlar to estimate service lifetime. Tests included: exposure of material at two locations in the southwest; an accelerated simulated-sunlight test; exposure of large-scale domes at a desert test site in eastern Oregon; and exposure of specimens at the Desert Sunshine Test Facility near Phoenix. Available long-term environmental exposure data on Tedlar is limited to data furnished by DuPont for a test conducted at Hialeah, Florida, over a 10-year time period.

Results of tests show that reduction in elongation will eventually limit life-time. Figures 3.3.2.2-1 and 3.3.2.2.-2 show mechanical and optical property changes which occurred in a 1472 hr. accelerated simulated sunlight test using a xenon-lamp source, for two Tedlar compositions, standard production, and the non-additive composition specified for the P.D. Comparison of data in the two figures shows the superior performance of the PD composition Tedlar, which was the primary basis for its selection. Both compositions showed a reduction in elongation to an unacceptable level before the maximum exposure was reached, the PD composition Tedlar reaching the level approximately 500 test exposure hrs. later in time.

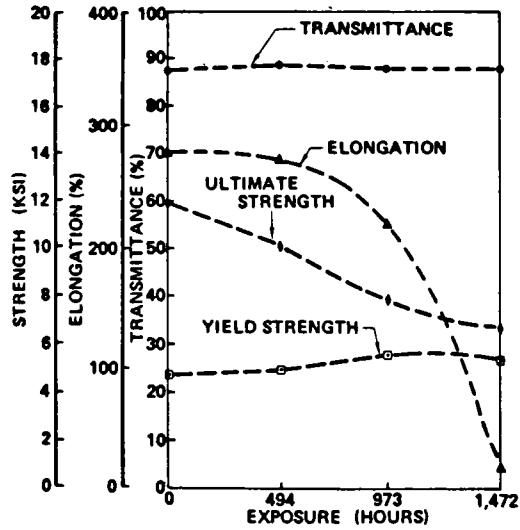
To relate the test hours in simulated sunlight tests to real-time hours, percent-change in elongation data from "standard" composition Tedlar, exposed in Florida over a 10-year period was correlated to "standard" Tedlar exposed in the accelerated test. Real-time Florida data exists for intervals of 1/2, 2, 5 and 10 years as shown by the data points in Figure 3.3.2.2-3. No degradation occurred in 5 years, however, the 10 year data point showed a 50 percent reduction. For time scale correlation, the 10 yr. point was superimposed on the percent-change-in-elongation curve established for "standard" Tedlar in accelerated testing. Elongation data from the PD Tedlar is included in the figure for comparison purposes.



● EXPOSED AT 10X AIR MASS-2 WITH XENON SOURCE

Figure 3.3.2.2-1. Accelerated Simulated Sunlight Test Results

PD COMPOSITION TEDLAR



● EXPOSED AT 10X AIR MASS-2 WITH XENON SOURCE

Figure 3.3.2.2-2. Accelerated Simulated Sunlight Test Results

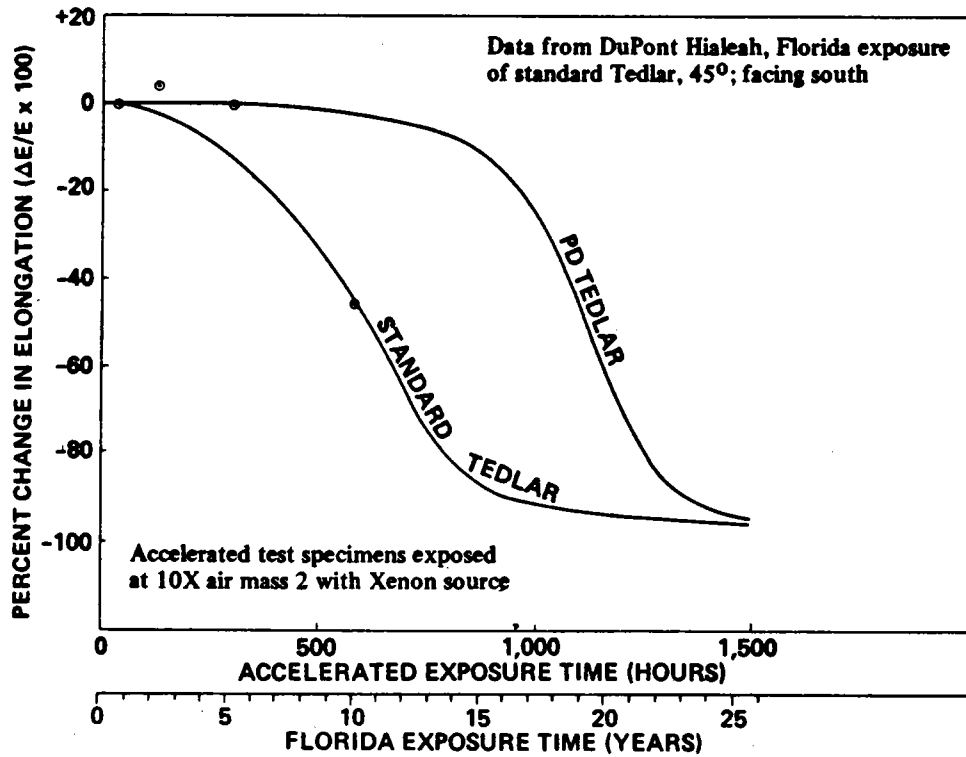


Figure 3.3.2.2-3. Tedlar Elongation Lifetime

Figure 3.3.2.2-4 shows the absolute value of elongation vs projected exposure time derived from Figure 3.3.2.2-3. The two curves represent situations where Tedlar receives only a "one-sun" exposure (best case south field), and 60 percent greater than "one-sun" exposure (worst case north field where both direct-incidence and reflected light pass through the same section of the dome). Elongation starts at about 280 percent, and degrades to the 25 percent minimum acceptable limit in 15 to 24 years, depending on field location. On this basis, domes will have to be replaced once during the plant lifetime, and replacement can be scheduled over a 9-year period if desired.

The projected degradation in ultimate strength with exposure time is shown in Figure 3.3.2.2-5. As indicated, ultimate strength is expected to drop to about 45.5 MN/m^2 (6600 psi) in the design life, 65 percent above the minimum acceptable value.

Throughout the research experiments, PD Tedlar was exposed at various locations for up to 13 months, as indicated earlier. In general, no significant changes have been observed in either strength (ultimate and yield) or elongation, confirming characteristics expected from DuPont and accelerated simulated sunlight tests. Figure 3.3.2.2-6 shows mechanical properties after 6 months and 13 months at Albuquerque and China Lake, compared to a control specimen.

Specular transmittance of PD Tedlar has also been obtained for desert exposures up to 13 months. A summary of solar specular transmittance data (0.5° scattering cone angle) on coupons exposed at three locations, is shown in Figure 3.3.2.2-7. Data are shown for both "as-received" material, and "after cleaning" with water and soft brush. Shaded areas on "as received" bars represent the variation in transmittance due to dirt/dust accumulation. Results of coupon tests confirmed that no significant change in transmittance occurs over a 13 mo. period after specimens are cleaned.

Transmittance/reflectance measurements on research experiment heliostats have shown no measurable degradation over a $3\frac{1}{2}$ month period at Boardman, Oregon.

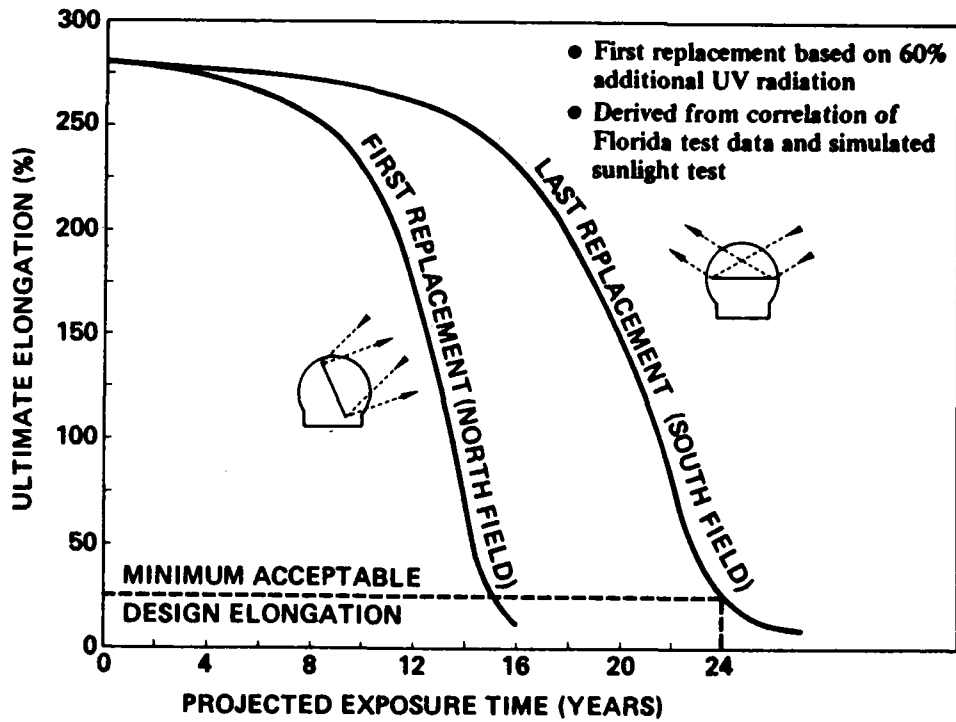


Figure 3.3.2.2-4. Projected Dome Lifetime Based on Elongation

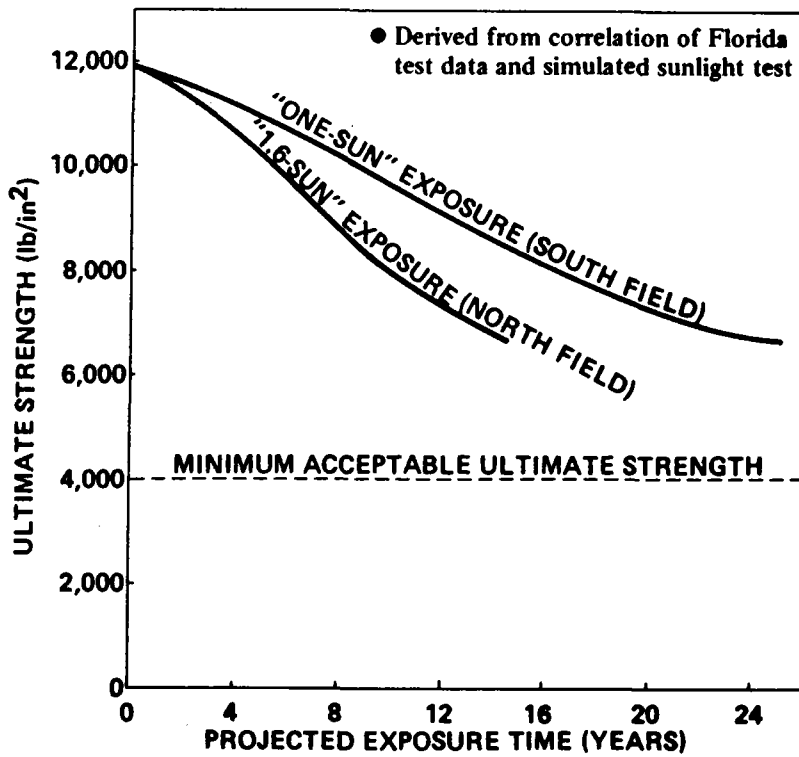


Figure 3.3.2.2-5. Projected Change in Ultimate Strength With Time

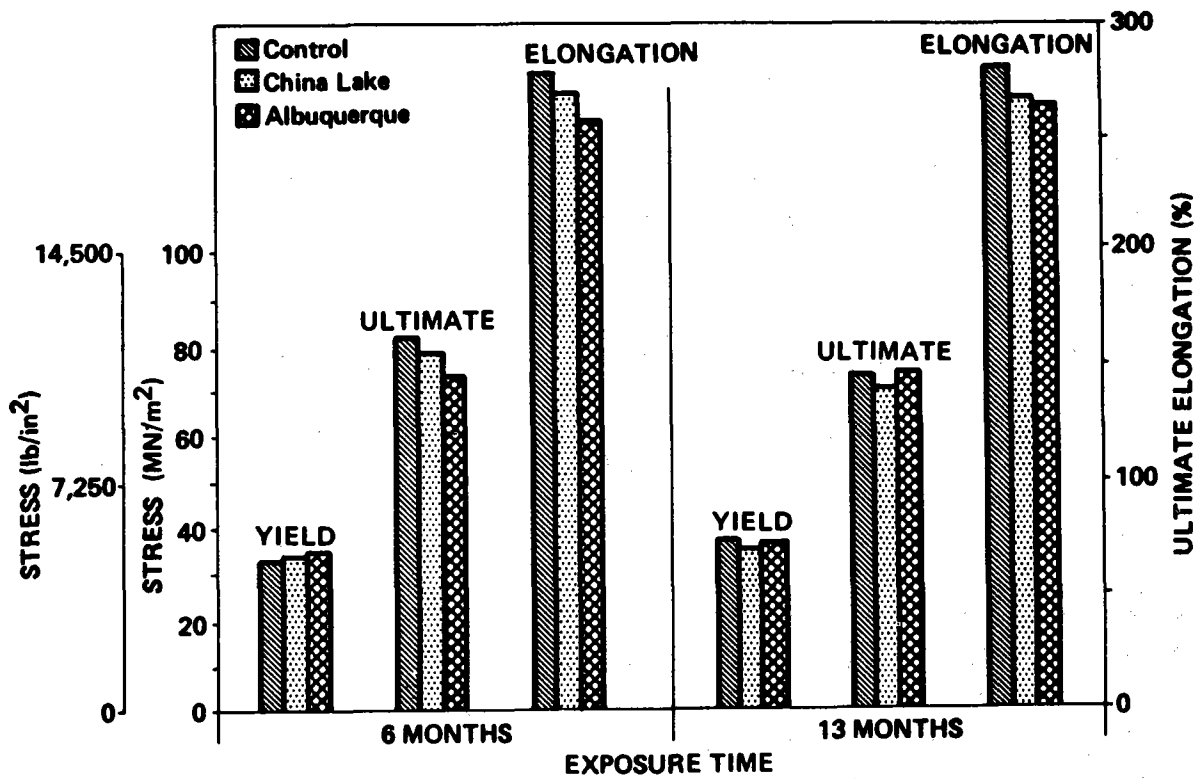


Figure 3.3.2.2-6. Mechanical Properties of Weathered Tedlar

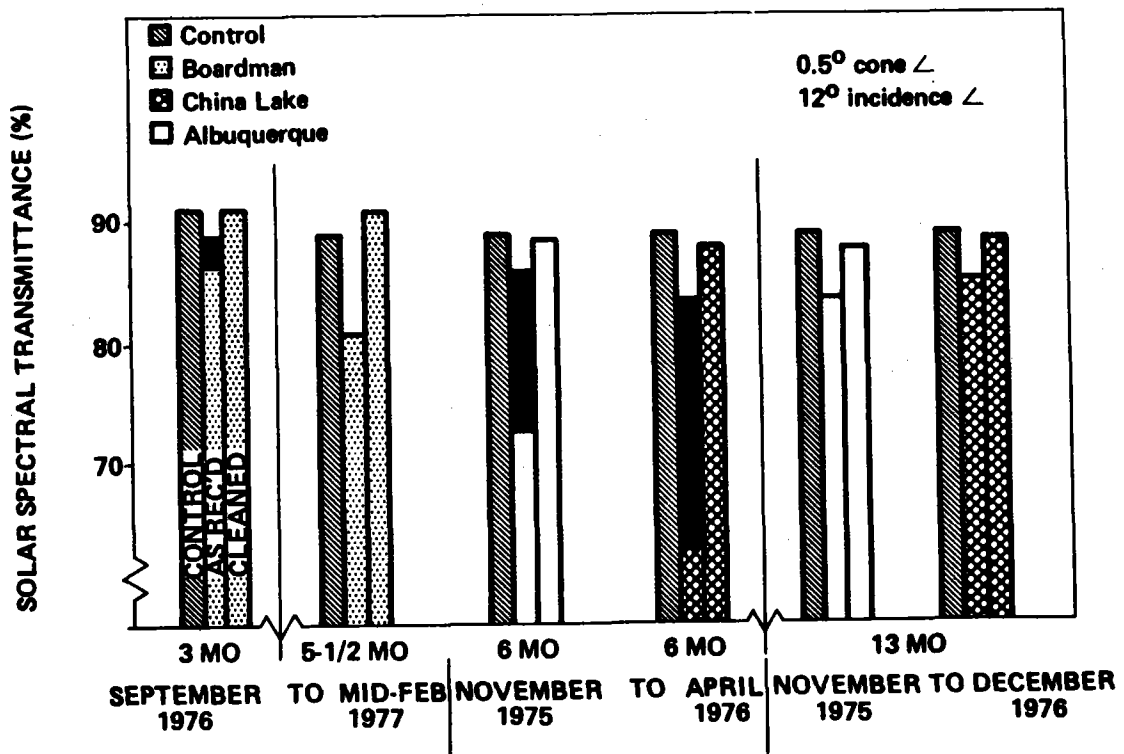


Figure 3.3.2.2-7. Transmittance of Weathered Tedlar

Typical data, obtained with an Eppley normal-incidence pyrheliometer, are shown in Figure 3.3.2.2-8. An interesting conclusion from the data is that occasional precipitation had apparently kept the dome sufficiently clean to not degrade transmittance. Since no measurable degradation occurred, it can be concluded that neither reflectance nor transmittance changed.

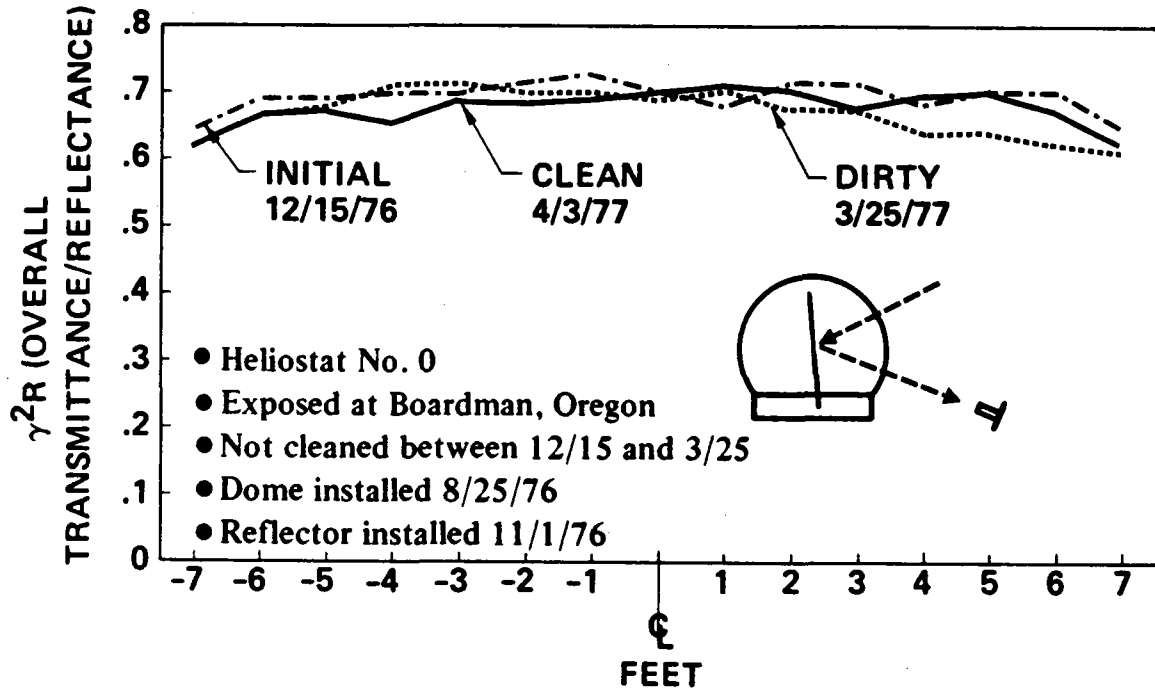


Figure 3.3.2.2-8. Transmittance/Reflectance of Heliostat

3.3.2.2 Structural Design

The preliminary design for the transparent enclosure consists of a spherical membrane supported by internal air pressure. The spherical shape is truncated at the base, where the membrane is attached to a steel skirt. The principal design parameters for the enclosure are:

Diameter	8.53m (28.0 ft)
Base Angle	50°
Material	Tedlar
Thickness	0.20 mm (8 mil)
Internal Pressure	0.067 n/cm ² (0.098 psi)

The rationale for selecting the above design is described in the following subsections:

Design Loads

The principal loads acting on the transparent enclosure are caused by the environment (wind, snow, ice, and earthquake) and by the internal static air pressure used to support the membrane dome. Structural design is also influenced by temperature because the enclosure material tensile properties are temperature dependent.

Undisturbed wind above smooth terrain is known to assume a logarithmic velocity profile, according to atmospheric boundary layer theory. Design wind profiles are commonly specified by power laws which give results similar to a logarithmic description. These take the form

$$V_Z = V_{REF} \left(\frac{Z}{H_{REF}} \right)^\alpha$$

where V_Z = wind velocity at height Z above ground
 V_{REF} = wind velocity at reference height H_{REF}
 α = exponent affecting shape of profile

Power laws are used to calculate wind velocity not only over smooth ground, but also over terrain which includes obstructions, by adjusting the value of the exponent α according to the degree of surface roughness. Reference 3.3.2.2-1 which was used to establish the preliminary design baseline, gives a reference height, H_{REF} , of 30 feet, and an exponent α equal to 0.20 for terrain characterized by "rolling on level country broken by numerous obstructions of various sizes, e.g., suburbs where lots are 1/2 acre or more." Reference 3.3.2.3-2 subsequently required that heliostats be designed for wind according to a power law with H_{REF} equal to 10 meters, and α equal to 0.15. This value is used to establish the present design. The reference velocity used to establish the preliminary design baseline, Reference 3.3.2.3-3, was the annual extreme fastest-

mile wind speed 30 feet above the ground for a 50-year mean recurrence interval, as published in Reference 3.3.2.3-4. Because local variations from the published data at specific locations are uncertain, and to obtain longer life probability, the 100-year mean recurrence interval values were used to size the present design. Figure 3.3.2.3-1 shows the distribution of this design wind velocity for the United States. The value at Barstow, California is 32.2 meters per second (72 mph). Reference 3.3.2.3-2 further requires that the heliostat survive without damage a maximum wind velocity, including gusts, of 40 meters per second (90 mph).

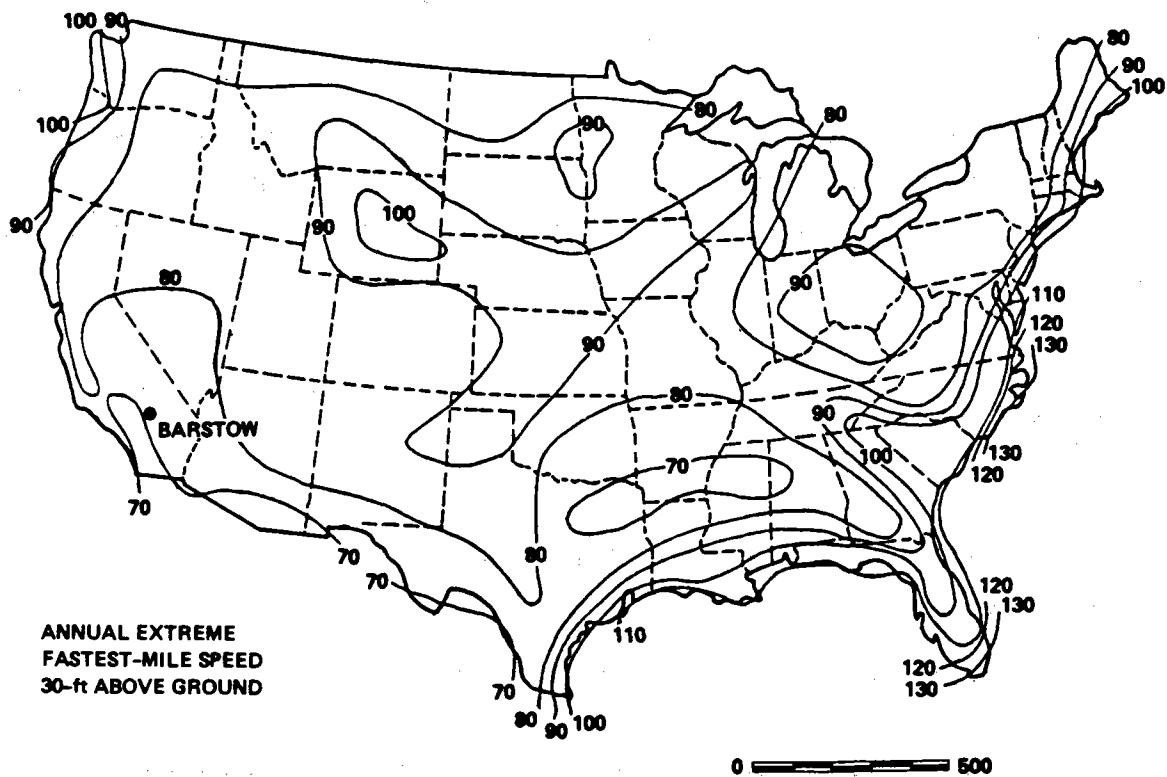


Figure 3.3.2.3-1. Basic Wind Speed in Miles Per Hour (100-Year Mean Recurrence Interval)

Wind pressure distribution on the surface of a spherical dome is shown in Figure 3.3.2.3-2. Knowing the pressure distribution and the velocity profile, the lift and drag forces acting on the dome may be calculated.

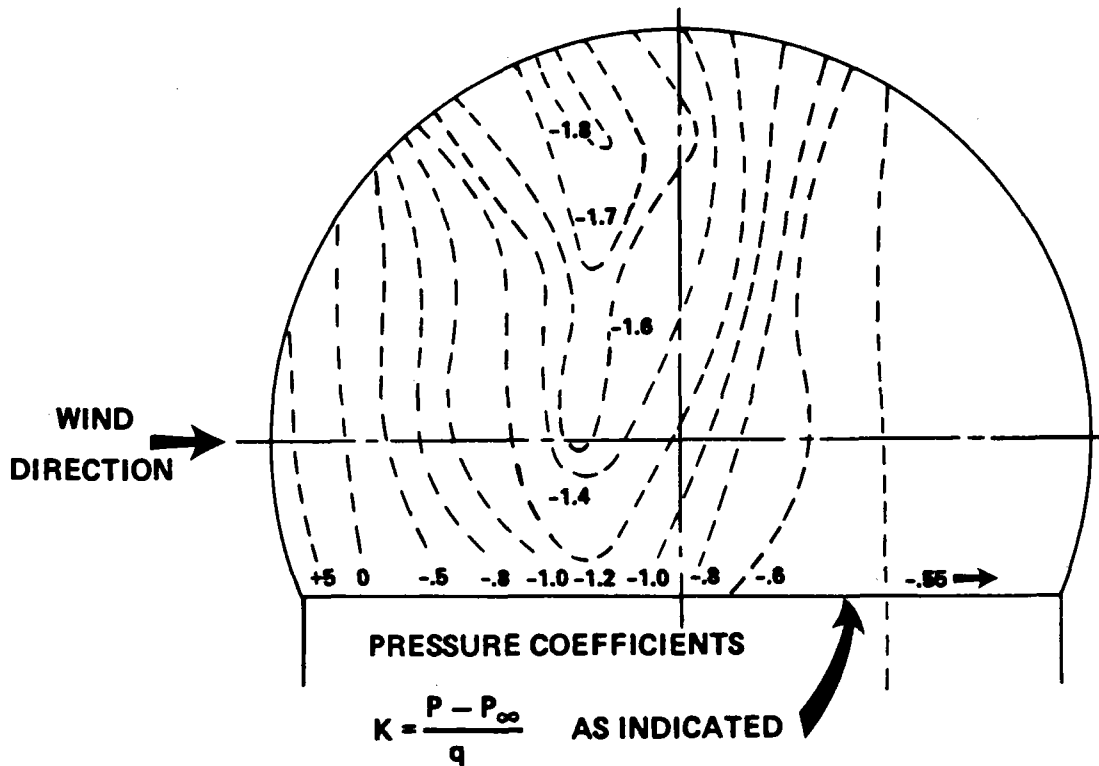


Figure 3.3.2.3-2. Pressure Contours on Dome

References 3.3.2.3-5 gives the following equations for lift and drag, respectively:

$$L = K_L q R^2$$

$$D = K_D q R^2$$

where K_L = lift coefficient

K_D = drag coefficient

q = wind dynamic pressure

R = dome radius

The coefficients K_L and K_D obtained by integrating the pressure distribution over the surface of the dome are shown in Figure 3.3.2.3-3. The dynamic pressure, q , is calculated by using the standard atmosphere air density at the elevation of the pilot plant site: Barstow, California. Air density has been corrected for temperature in calculating wind pressures at high ambient temperatures. Because the above equations give lift and drag forces acting on a dome in a

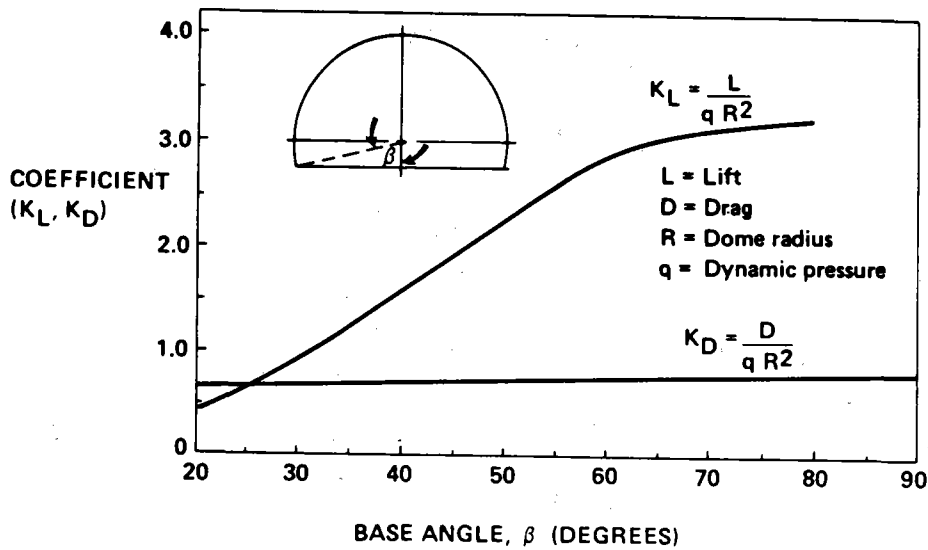


Figure 3.3.2.3-3. Effect of Base Angle on Force Coefficients

uniform velocity field, it was necessary to calculate an "effective" wind velocity based on the non-uniform design wind profile. This was done by calculating the average dynamic pressure acting on the dome from the wind velocity profile, as weighted by the incremental frontal area of the dome over its height, and then finding the effective velocity from the dynamic pressure.

This calculation leads to the following equations for "effective" dynamic pressure and wind velocity, respectively:

$$q_{\text{eff}} = 0.76 q_H$$

$$V_{\text{eff}} = 0.87 V_H$$

where q_H and V_H are the dynamic pressure and velocity, at the top of the dome.

The aerodynamic lift and drag acting on the dome for the peak survival wind of 40 meters per second (90 mph) are:

$$L = 25,875 \text{ Newtons (5817 lbs)}$$

$$D = 9408 \text{ Newtons (2115 lbs)}$$

The upward force due to internal pressurization must be added to the aerodynamic lift to obtain the total upward force that the dome base connection must withstand. Internal pressure is established to be that which will react the maximum aerodynamic stagnation pressure, in order to prevent indentation

of the dome in the peak survival wind. The force due to internal pressurization is calculated to be:

$$F_p = q_{EFF} A_{BASE} = 22,680 \text{ Newtons (5099 lbs)}$$

then the total vertical force acting on the dome is:

$$F_{TOT} = F_p + L = 48,554 \text{ Newtons (10,916 lbs)}$$

In addition to wind loads, the transparent enclosure will support a coating of ice over its upper surface having a maximum thickness of 7.6 cm (3.0 in) or a snow depth of approximately 0.9m(3ft) in a cosine distribution without exceeding the vertical force due to internal pressurization. Deflection under this loading is approximately the same as that calculated for maximum wind loading, Reference 3.3.2.3-5.

Finally, the dome will withstand the lateral force due to a Zone 4 earthquake, corresponding to the pilot plant site, as defined in Reference 3.3.2.3-6. According to this reference, lateral seismic load is calculated by the equation

$$V = ZIKCSW$$

Where V = total lateral force at base of structure

Z = 1.0 for Zone 4

I = Occupancy importance factor

K = Numerical coefficient depending on type of construction

C = function of structure's fundamental frequency

S = Site-structure resonance factor

W = Weight of structure

Using the most conservative combination of these parameters the maximum possible lateral acceleration is 0.53 g's. This value, based on more recent data, is less than the 0.86g value used in the preliminary design baseline, Reference 3.3.2.3-3.

Configuration, Material, Size

The transparent enclosure is supported entirely by internal air pressure. Internal static pressure is kept high enough to maintain the enclosure in tension, and thus in shape. This is accomplished by making the internal pressure equal to or greater than the wind stagnation pressure.

The base angle of 60° selected for the preliminary design baseline was established to limit the wind deflection of the dome and obtain a reasonable clearance envelope inside the enclosure for the reflective assembly. Quantitative test data on wind deflections of spherical air supported domes was not available, and a conservative deflection analysis was deliberately selected. Recent results of collector subsystem research experiments reported in Reference 3.3.2.3-7 support the much less conservative deflection analysis given in Reference 3.3.2.3-5. Dome deflections according to this analysis are shown in Figure 3.3.2.3-4. Maximum deflection for the peak survival wind condition is 4.67 cm (1.84 in) occurring slightly below the dome mid-height. A test point shown on the figure was scaled from the largest wind deflection observed as the Boardman test site assuming that deflection varies linearly with diameter and as the square of the velocity. On the basis of the good correlation between test and analysis the base angle for the present design has been reduced to 50° . This reduces the size and cost of the steel skirt.

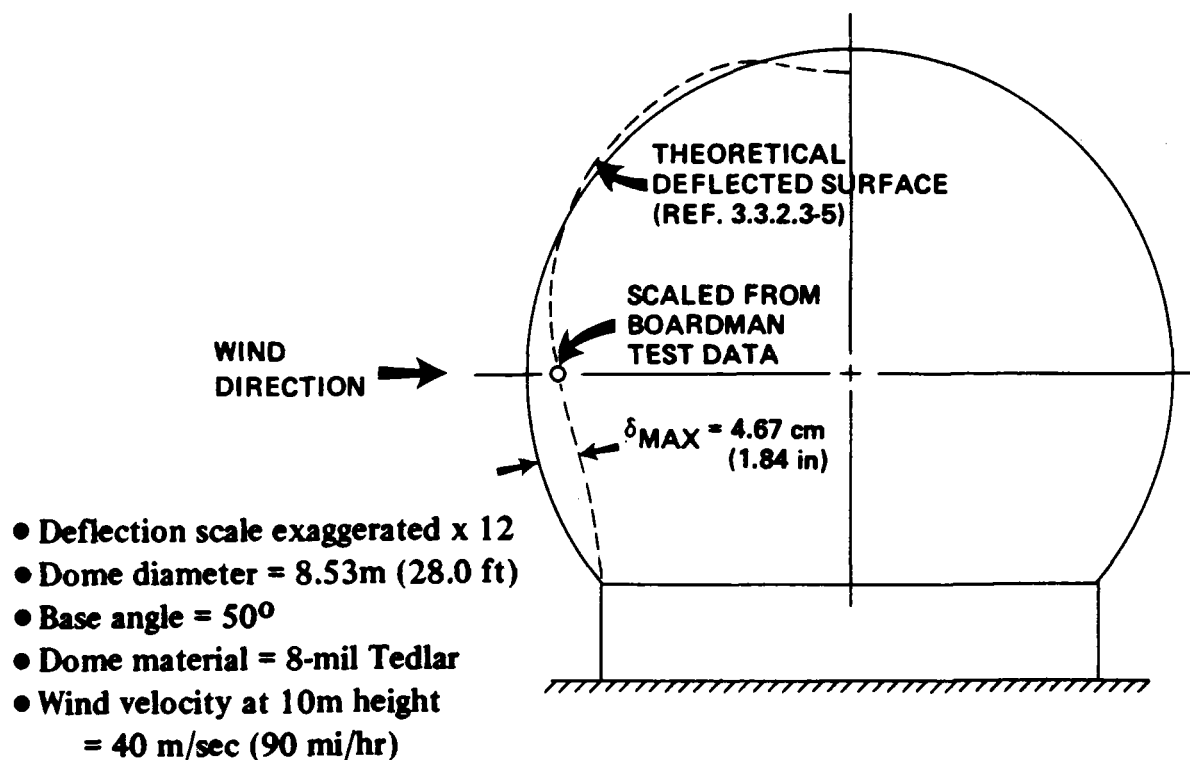


Figure 3.3.2.3-4. Dome Deflections at Peak Survival Wind Velocity, Collector Subsystem

Enclosure diameter is controlled by the wind velocity and the allowable stress of the membrane material. The maximum stress in the membrane, as given in Reference 3.3.2.3-5 is:
$$S = 2.1 q \left(\frac{R}{t} \right)$$

where: q is the dynamic pressure due to the wind velocity
 R is the enclosure radius
 t is the membrane thickness

The above equation includes the effect of internal pressure, which is assumed equal to the maximum dynamic pressure to maintain the shape of the enclosure. The maximum stress given by the equation is a peak stress that may occur locally at any point in the membrane depending on the direction of the wind.

The average yield stress of the Tedlar material selected for the transparent enclosure as measured in materials testing, and reported in Reference 3.3.2.3-8, is 33.1 MN/m^2 (4800 psi). The design allowable stress is taken as 83% of this value, i.e., 27.6 MN/m^2 (4000 psi). Tedlar has been found to have good elongation characteristics, with ultimate strength approximately twice the yield stress. Vendor information indicates that yield stress for Tedlar will not change with exposure until embrittlement is reached. A typical stress strain curve from recent tests of 0.20 mm (8 mil) Tedlar is shown in Figure 3.3.2.3-5 for comparison with the stated material yield stress and allowable design stress values. Data in Reference 3.3.4.3-9 was used to calculate the reduction in Tedlar tensile properties with increasing temperature. The reduced properties were used to evaluate enclosure performance at high ambient temperatures.

The present dome diameter of 8.53 m (28.0 ft) was obtained from analysis data presented in Figure 3.3.2.3-6, which shows enclosure diameter versus effective wind velocity for 0.20 mm (8 mil) Tedlar. Maximum enclosure diameters at various stress levels are indicated by the three solid-line curves in the figure, while effective wind velocities versus diameter for various reference wind conditions are indicated by the three dashed-line curves. Using as a basic design wind the annual extreme fastest-mile wind for a 100-year mean recurrence interval, and the design allowable stress, reduced for the maximum ambient temperature of 49°C (120°F), the design diameter given by the intersection of these two curves is 8.53 (28.0 ft). The figure also indicates that the yield stress at maximum ambient temperature will not be exceeded by the 100-yr. wind with a 1.1 gust velocity factor (recommended by ANSI, Reference 3.3.2.3-1, for ordinary structures

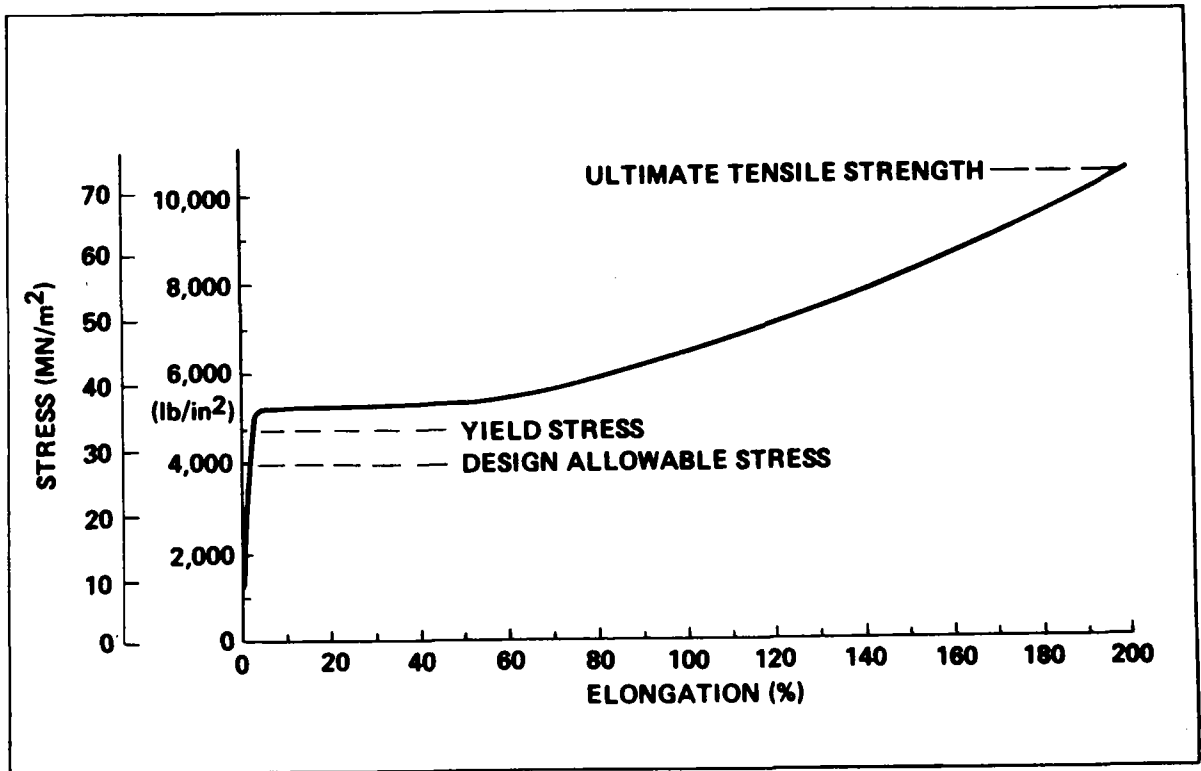


Figure 3.3.2.3-5. Typical Tensile Properties for 8-mil Tedlar

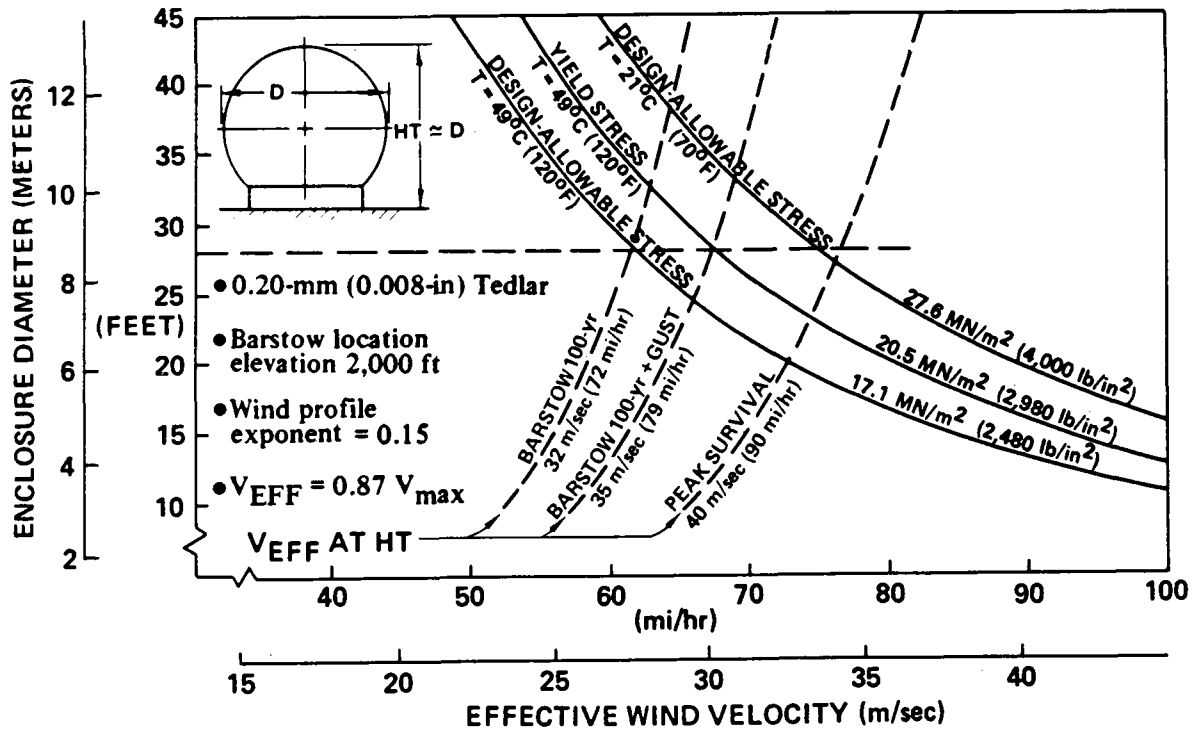


Figure 3.3.2.3-6. Enclosure Diameter Versus Effective Wind Velocity

of 18.6 m² (200 ft²) or more. The room temperature design allowable stress is exceeded only slightly by the peak survival wind condition. The subject of enclosure survival at combinations of high wind and high temperature is considered further in the following paragraph.

Figure 3.3.2.3-7 shows the maximum wind velocity that the 8.53 m (28.0 ft) dome can withstand as a function of ambient temperature. At an ambient temperature of 49°C (120°F) the design allowable stress is not exceeded for the 100-year wind with a 1.1 gust factor (Reference 3.3.2.3-1). The allowable yield stress is exceeded for the peak survival wind velocity at ambient temperatures greater than 28°C (83°F); however, the stress is less than 50% of the ultimate tensile strength for any reasonable temperature. Referring again to Figure 3.3.2.3-5 it is seen that typical 0.20 mm (8-mil) Tedlar yield stresses are somewhat higher than the allowable value indicated on Figure 3.3.2.3-7. It is expected that if the peak survival wind is experienced at ambient temperatures above about 35°C (95°F) some permanent deformation of the dome material will occur locally. This is not expected to cause any functional impairment.

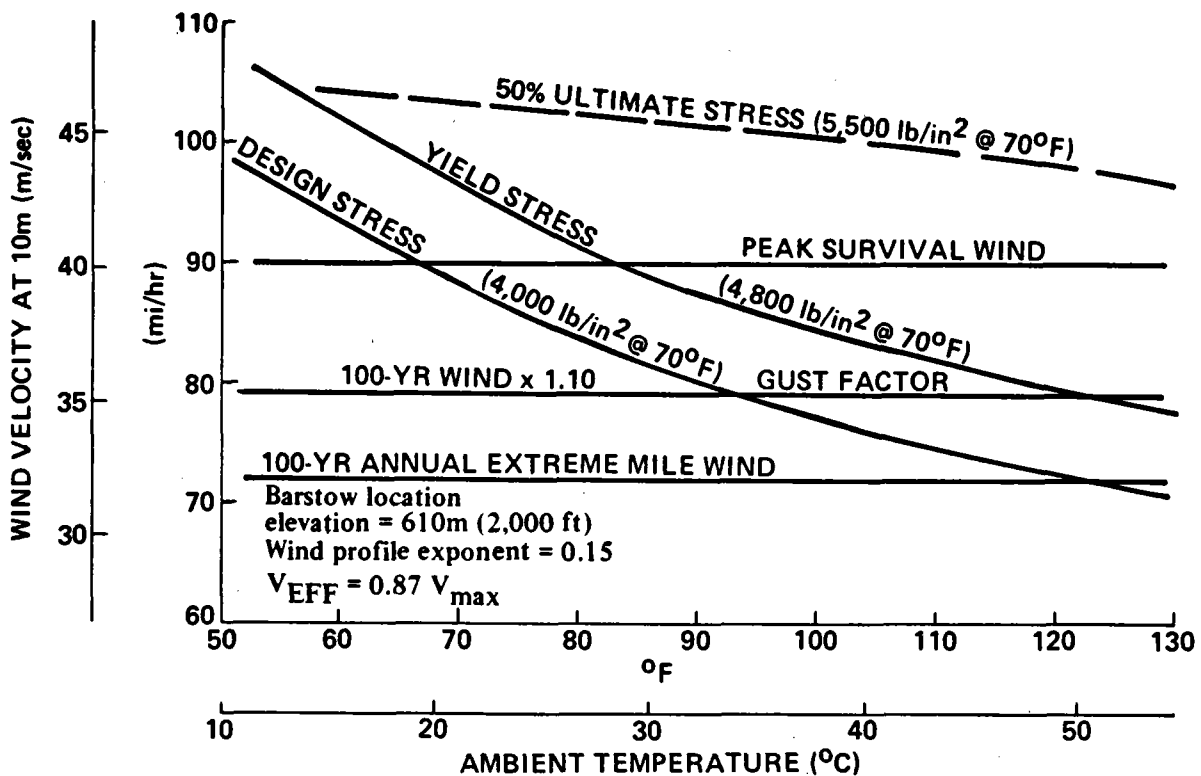


Figure 3.3.2.3-7. Maximum Wind Velocity Versus Temperature for 8.53-m (28.0-ft) Dome

A wind tunnel test program was undertaken to determine the effects on enclosure design of sheltering due to density of heliostats in the field and the addition of a peripheral fence. The results of this study are presented in nomograph form in Figure 3.3.2.3-8 for 0.20 mm (8-mil) Tedlar and the peak survival wind velocity of 40 m/sec. (90 mph) for standard atmosphere at 610 m (2000 ft) elevation. The four curves in the lower part of the figure represent four configurations studied: enclosure with and without cylindrical skirt; field with and without peripheral fence. The other independent variables are the enclosure density given by the ratio of enclosure area to ground area on the lower left edge of the graph, and the allowable membrane stress along the top edge of the graph. Enter the graph with the minimum enclosure density of 0.19 (15 m by 20 m spacing) and follow the line indicated horizontally to the curve for enclosures with skirt and with fence, thence upward to the central horizontal line and diagonally to the design allowable stress, 27.6 MN/m² (4000 psi), at the top edge of the graph. The allowable diameter given by the intersection of this line with the sloping scale in the upper portion of the graph is 8.7 m (28.5 ft). This result substantiates the present enclosure design as established in the preceding analysis and design discussions.

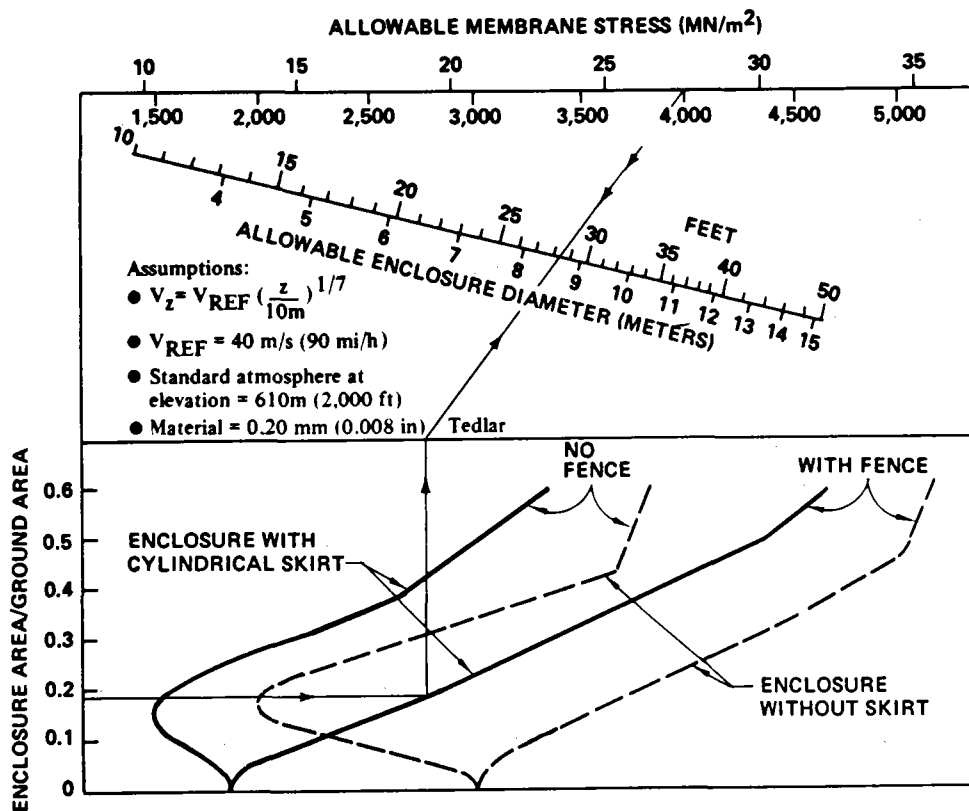


Figure 3.3.2.3-8. Allowable Enclosure Diameter From Wind-Tunnel Test Results

Total vertical and drag forces calculated for the maximum survival wind are 48.55 KN (10916 lbs) and 9.41 KN (2115 lbs), respectively. These forces are resisted with adequate margin of safety by the steel skirt and concrete ring foundation. The steel skirt is adequately stiffened by a ring at its top to withstand non uniform radial and tangential loads around its circumference caused by aerodynamic pressure distributions on the dome. Stresses in the foundation are low, and minimal reinforcing is required to distribute skirt tie-down load into the concrete. Soil bearing pressure due to the foundation weight is only 5.8 KN/m^2 (120 psf), and no soil stabilization requirement is anticipated.

An earthquake analysis of the enclosure using the Uniform Building Code approach (Reference 3.3.2.3-6) has been made. Using the most conservative values for all coefficients gives an equivalent lateral force of 0.53 g's for Zone 4* earthquake design. Applying this acceleration to the mass of the enclosure plus the mass of the enclosed air results in a lateral force of 2.23 KN (501 lbs), and causes a radial deflection approximately 25% of that caused by the peak survival wind. Film stresses for the earthquake loading will be considerably less than that for the design maximum wind condition because the larger, non uniform aerodynamic pressure distribution will not be present.

Quantitative data on hailstone penetration is not presently available. However, air-supported cylindrical 0.05 mm (2mil) Tedlar covers on solar water stills at Hialeah, Florida have reportedly survived 56 m/sec. (125 mph) winds and egg-size hailstones (Reference 3.3.2.3-10). Hail is not expected to be a problem.

*Recognizing that program requirements/specifications require designing to withstand Zone 3 earthquakes, Zone 4 was used because of data in Reference 3.3.2.3-6.

3.3.3 Reflective Assembly

Preliminary design of the reflective assembly involved configuration studies, materials evaluation, structural design, and utilized results of research experiments. Results of these studies are discussed in this section.

3.3.3.1 Configuration

Configuration studies on the reflective assembly were aimed at selecting the most cost-effective shape and support technique for the membrane reflector, consistent with meeting optical performance requirements. The reflective assembly selected for the pilot plant PD as a result of PD baseline studies and successful experience in research experiments, is shown in Figure 3.3.3.1-1. It consists of a 7.85 m (25.75 ft) diameter ring of aluminum tubing with a circular reflective surface of 0.05 mm (2 mil) thick aluminized Mylar bonded to a flat, rigid urethane foam surface, cast onto the ring. The ring is supported at three points by tubular aluminum arms welded to the ring and bolted to a gimbal interface plate. PD structural analyses have resulted in selection of 12.7 cm (5 in) diameter aluminum tubing, having 0.20 cm (0.078 in) wall thickness for the reflector structure. Key features of the structural design are; the three point support system for the planar reflective surface; light weight (161 lbs. of aluminum), a planar foam pad to interface the Mylar reflective surface with the circular support ring, and 3 spacers installed at the gimbal interface region to assure that the reflective surface is in parallel to the gimbal plate surface. The foam pad reduces required manufacturing tolerances on the aluminum structure, and improves optical performance.

3.3.3.2 Materials

It is essential that the reflective film have a highly specular (smooth) surface, low cost, and sufficient strength to carry a load $4.82-6.9 \text{ MN/m}^2$ (700-1000 psi) without significant creeping. Various film candidates were screened early in the program on the basis of these parameters. Aluminized Mylar (DuPont XM648A) was selected for research experiment reflectors, and is specified for PD reflectors on the basis of favorable experience in research experiments. Materials studies,

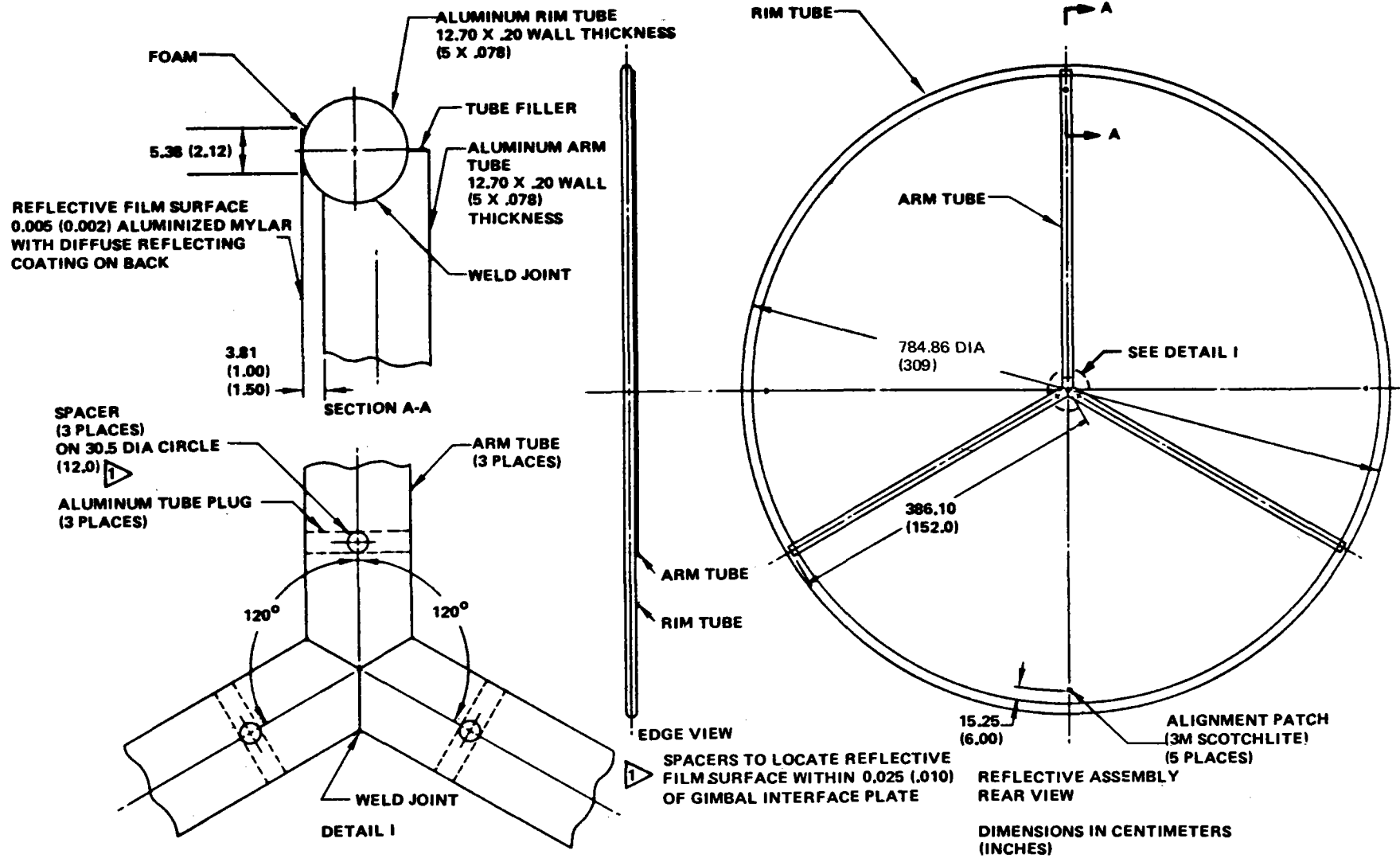


Figure 3.3.3.1-1. Reflector PD Configuration

which continued throughout the research experiment effort, revealed that Melinex 0 is an alternative film which is satisfactory from a reflectance, strength, and cost standpoint.

Research experiment reflective films were fabricated with a nominal bi-directional sheet tension of 6.9 MN/m^2 (1000 psi). This tension was proven quite adequate for removing wrinkles in the Mylar, producing a high quality optical surface and avoiding Mylar and adhesive creep. Based on research experiment experience, and the anticipated improved collector subsystem performance, PD reflector tension has been reduced to 5.17 MN/m^2 (750 psi).

An unprotected aluminum coating, functioning as a first-surface reflector, was utilized on XM648A Mylar in research experiment reflectors. This selection was made on the basis of cost, solar reflectance, and long-term stability when operating in a protected environment. Data from earlier Boeing tests, in which aluminized mirrors were measured after a 9-year period, showed that no significant change in reflectance occurred in the wavelength region longer than about 300 nanometers. (Figure 3.3.3.1-2). Those specimen had a solar reflectance of about 89.6% in 1966, and values of 89.5, 89.4, and 89.5% in September 1975, after storage in an environment of nearly constant temperature, relative humidity 30-50%, and in the dark.

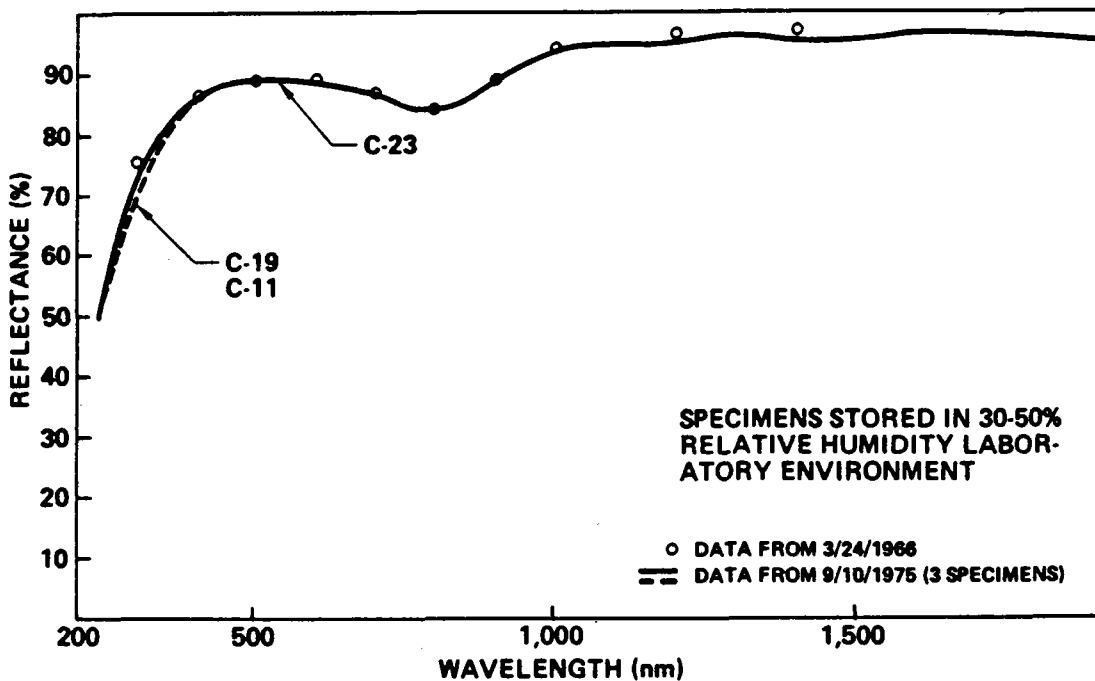


Figure 3.3.3.1-2. Long-Term Aging of Unprotected Aluminum Reflector

Considering the importance of long-term reflective coating stability in pilot plant operation, research experiments included exposure of aluminized Mylar specimens under conditions representative of the pilot plant heliostat environment. Tests included: an accelerated simulated sunlight test (Xenon lamp); exposure on a tower at Albuquerque; and exposure on front and back surfaces of a reflector within a dome at Boardman, Oregon. Elongation, tensile strength, and specular reflectance were monitored throughout testing. Results of accelerated simulated sunlight tests conducted in a 30-50 percent relative humidity laboratory environment, are shown in Figure 3.3.3.1-3. The aluminized Mylar specimen received 500 hours of actual exposure time, which, using the same correlation basis as Figure 3.3.2.2-3, is equivalent to about 9 years real time exposure in Florida. Ultimate and yield strength remained essentially constant, elongation decreased slightly, and solar specular reflectance decreased 1.5 percent. Data trends from both this test and the 9 year laboratory exposure indicate that a 30 yr. lifetime should be possible for the reflective film. Results also confirm that the aluminum coating acts as an ultra-violet shield for the Mylar.

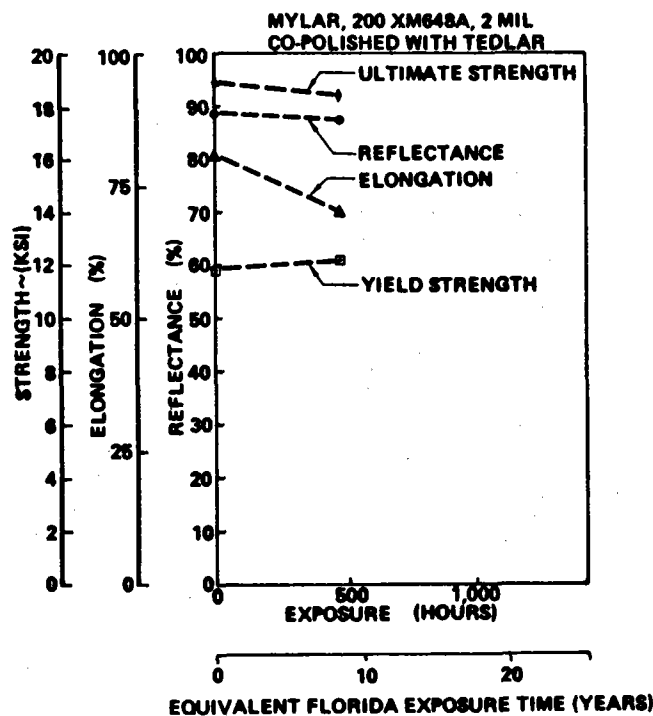


Figure 3.3.3.1-3. Accelerated Simulated Sunlight Test Results

Results of Albuquerque weathering tests on mechanical properties of aluminized Mylar are summarized in Figure 3.3.3.1-4. Data show no significant changes in yield and ultimate strength for the frontside exposed specimen, after 16 months exposure behind Tedlar. The backside exposed specimen experienced a significant reduction in ultimate strength and elongation. On the basis of this test, an ultra-violet protective film has been specified for the backside of pilot plant PD reflectors. For safety purposes, this film will have diffuse-reflecting characteristics.

Reflectance data on aluminized Mylar exposed at Boardman, Oregon and Albuquerque, are summarized in Figure 3.3.3.1-5. At Boardman, specimens were taped to a reflector within a dome, and at Albuquerque specimens were enclosed in a vented

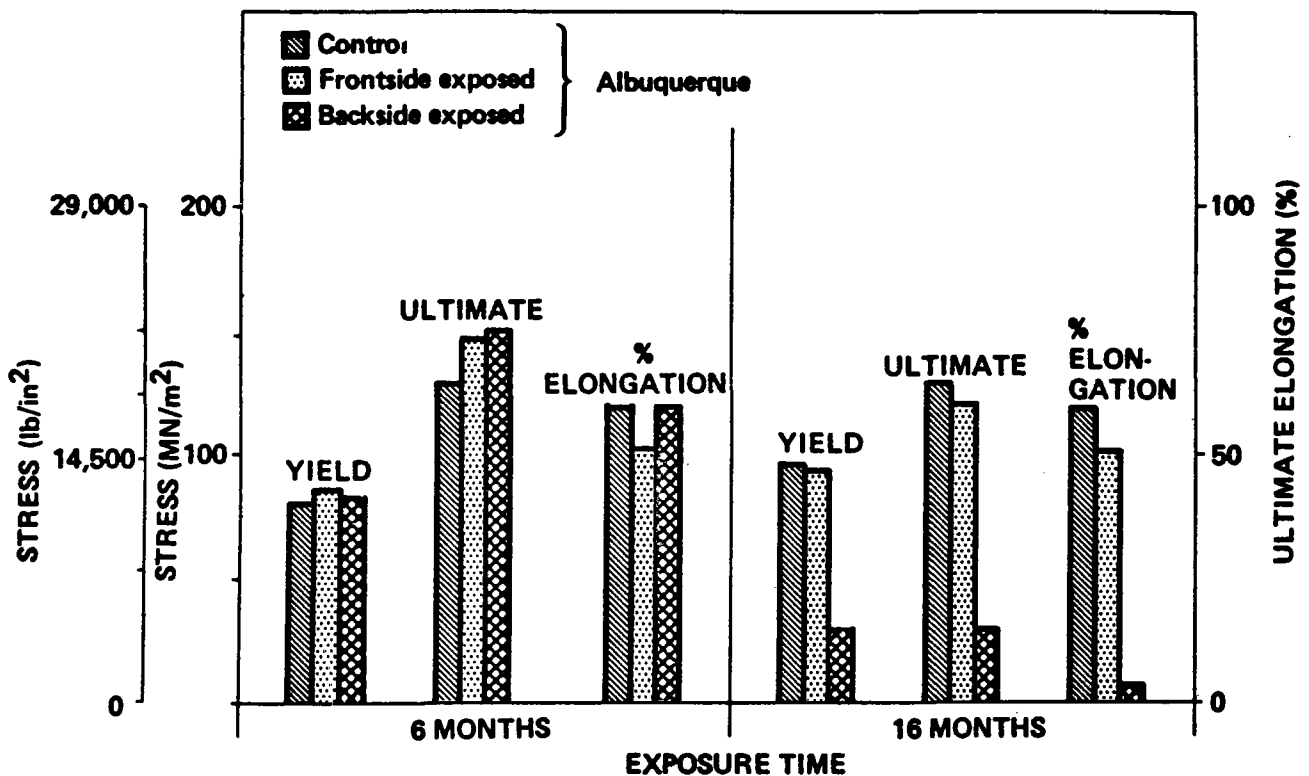


Figure 3.3.3.1-4. Mechanical Properties of Weathered Aluminized Mylar

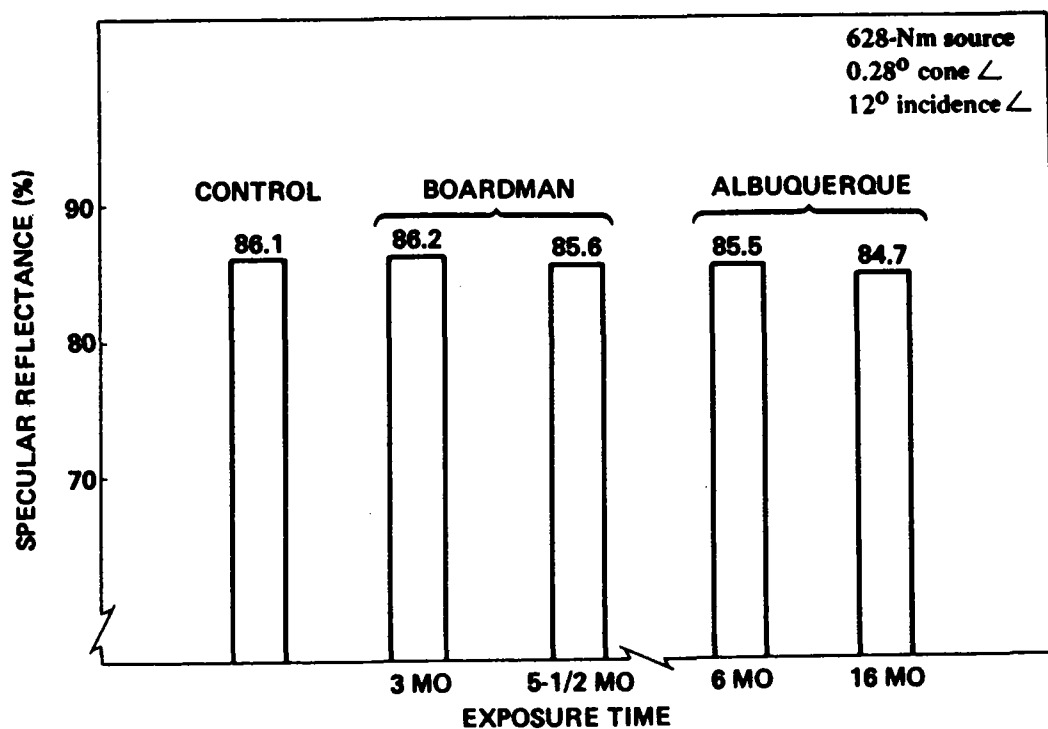


Figure 3.3.3.1-5. Reflectance of Weathered Aluminized Mylar

Tedlar envelope facing south. Six month samples were enclosed in ultra-violet screening Tedlar, and 16 mo. samples within PD composition Tedlar. Maximum reduction in reflectance observed was 1.4 percent after 16 months. The cause of the relatively small reflectance changes at Boardman and Albuquerque is not known. Ambient air humidity is a likely reason, since 60 to 90 percent relative humidity occurs frequently at both locations. Laboratory exposures, mentioned previously, involved lower relative humidity and smaller reflectance changes with time. Preliminary evaluation of Barstow relative humidity has indicated significantly lower values than Boardman and Albuquerque.

Previous studies (Reference 3.3.3-1) have shown that the short wavelength reflectance of freshly vacuum deposited aluminum degrades with time, as shown in Figure 3.3.3.1-6. This degradation is, however, limited to the wavelength region shorter than about 200 nanometers, and stabilizes with time as the protective aluminum oxide film builds up. Considering the long-term stability of aluminum observed in laboratory tests (a moderate humidity environment similar to Barstow,) and the expected long-term stabilization effect of oxide film buildup, an unprotected aluminum film has been specified for the pilot plant reflectors.

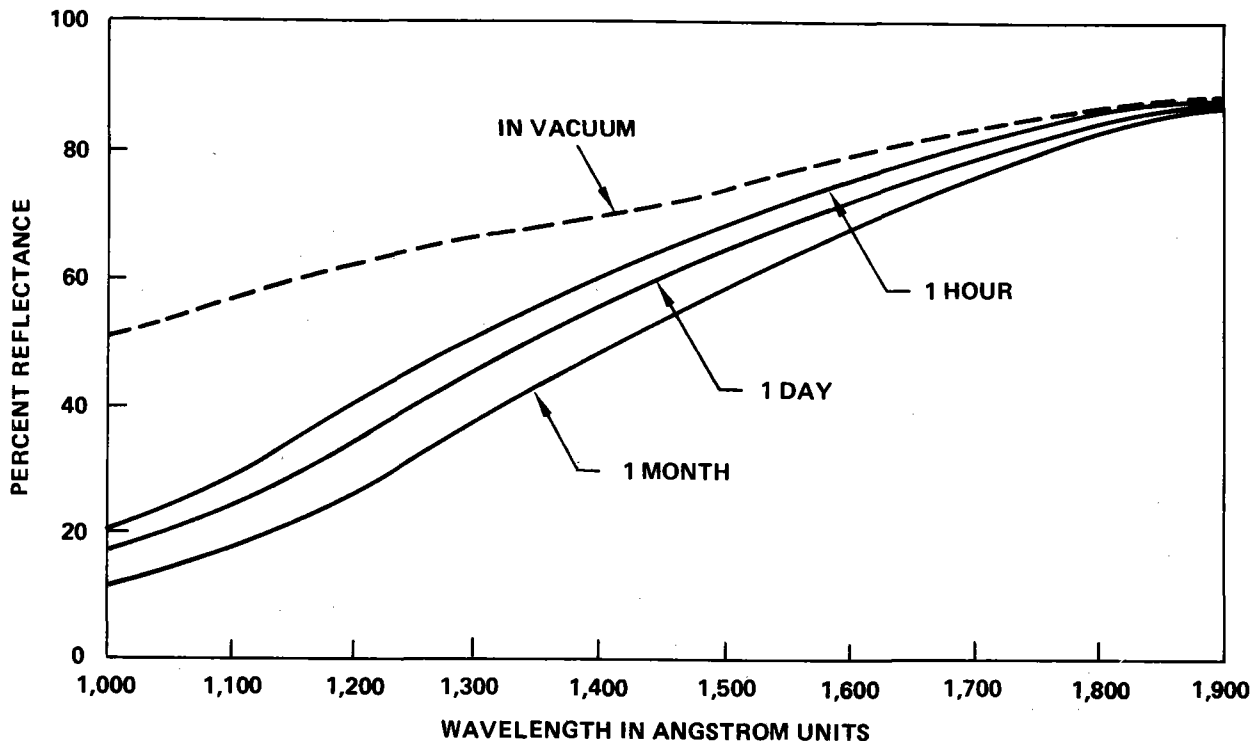


Figure 3.3.3.1-6. Reflectance of Freshly Deposited Aluminum Films After Exposure to Air

Verification of optical performance of reflectors has been obtained utilizing the test setup shown schematically in Figure 3.3.3.1-7, and the optical scanner shown in Figure 3.3.3.1-8. The three research experiment heliostats are located approximately 76.2 m (250 ft) southeast from the tower base, on 8.54 m (28 ft) centers on an east/west north/south grid. The optical scanner consists of a 3.66 m (12 ft) radius arm which has calibrated silicon photovoltaic cells spaced at 15.3 cm (6 in) intervals. A TRW DR-2 radiometer is also located on the scanner arm near center, for calibration purposes. Image scans were taken by rotating the arm one revolution in about one minute, and reading out cells at approximately 10^0 intervals with a computerized data acquisition system.

Optical performance of reflectors has been determined on the basis of image quality and overall efficiency. Image quality relates to determining size and shape, and the degree of focusing achieved. Overall efficiency defines fraction of total normal incidence solar radiation falling on the projected reflector area, which is reflected to the scanner. Typical image intensity

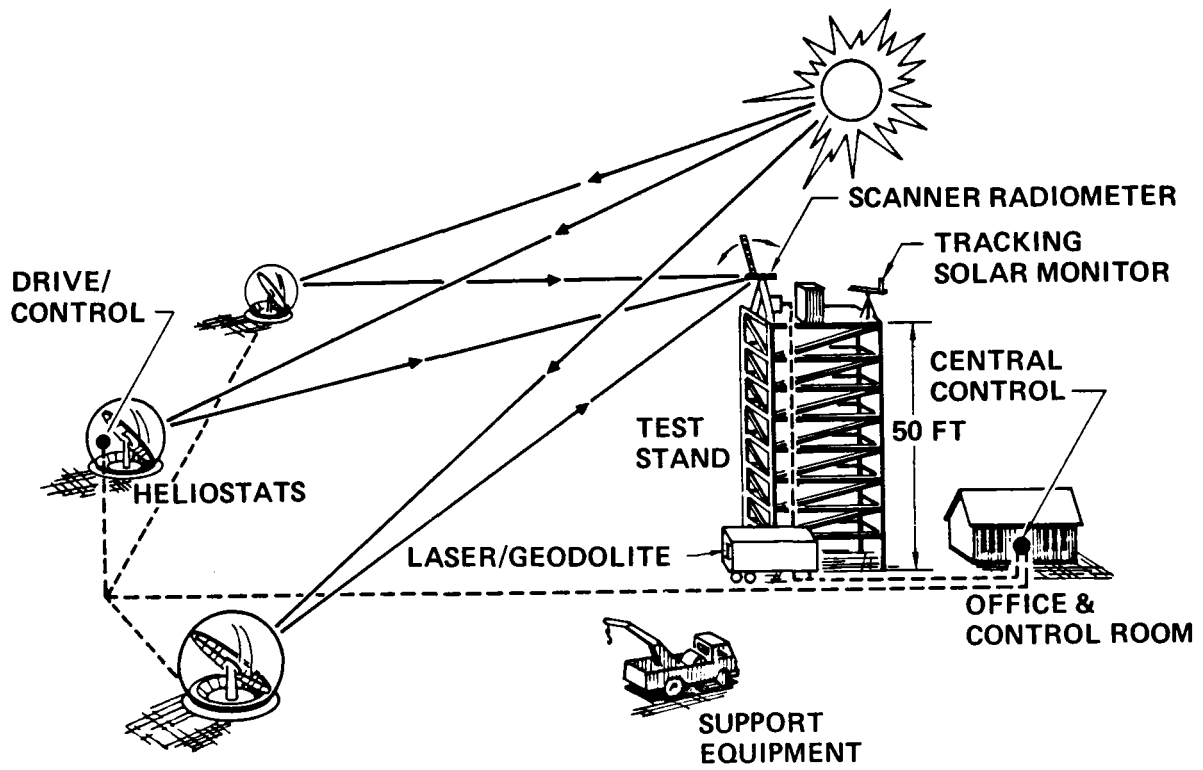


Figure 3.3.3.1-7. Research Experiment Array Test Setup

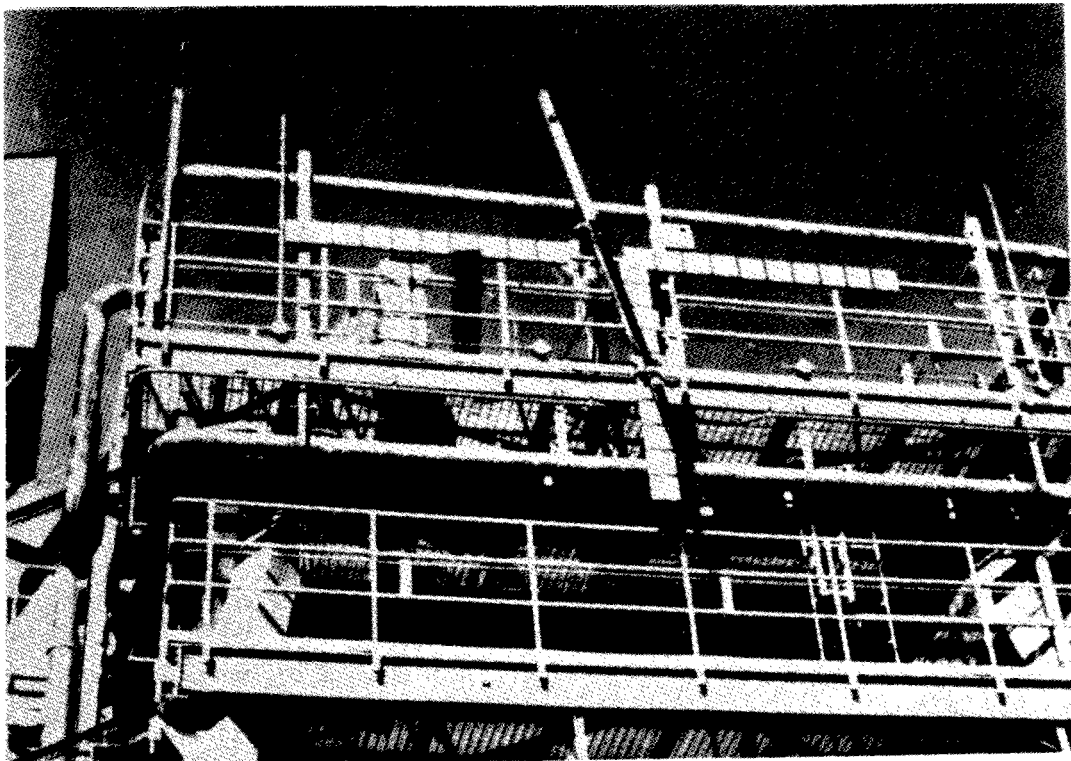


Figure 3.3.3.1-8. "Optical Scanner"

distributions for individual heliostats measured with the optical scanner, are shown in Figures 3.3.3.1-9 and 3.3.3.1-10. A similar scan for all three heliostats is shown in Figure 3.3.3.1-11. Since these scans were made at off normal angles elliptical images are observed. Small variations in iso-flux lines are attributed to reflector surface aberrations and solar intensity variations during the scan.

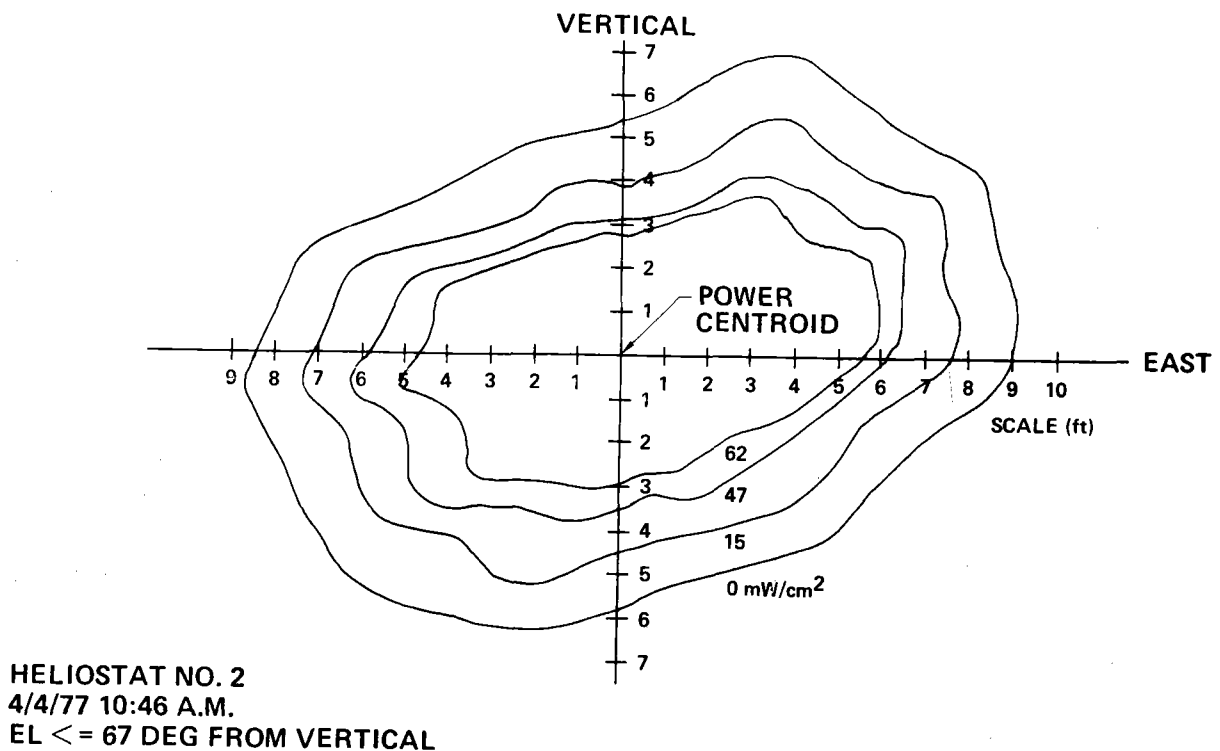
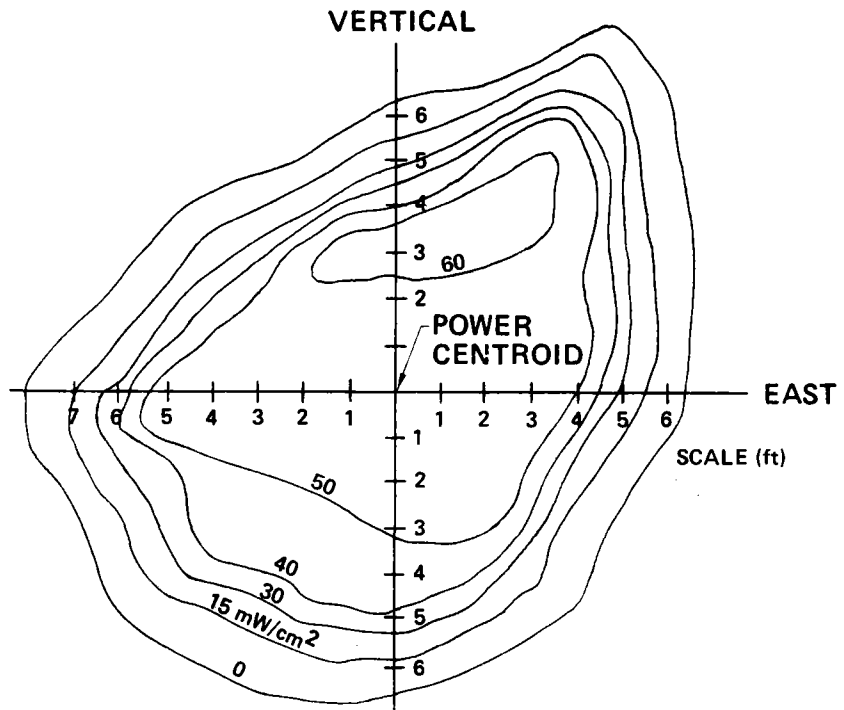


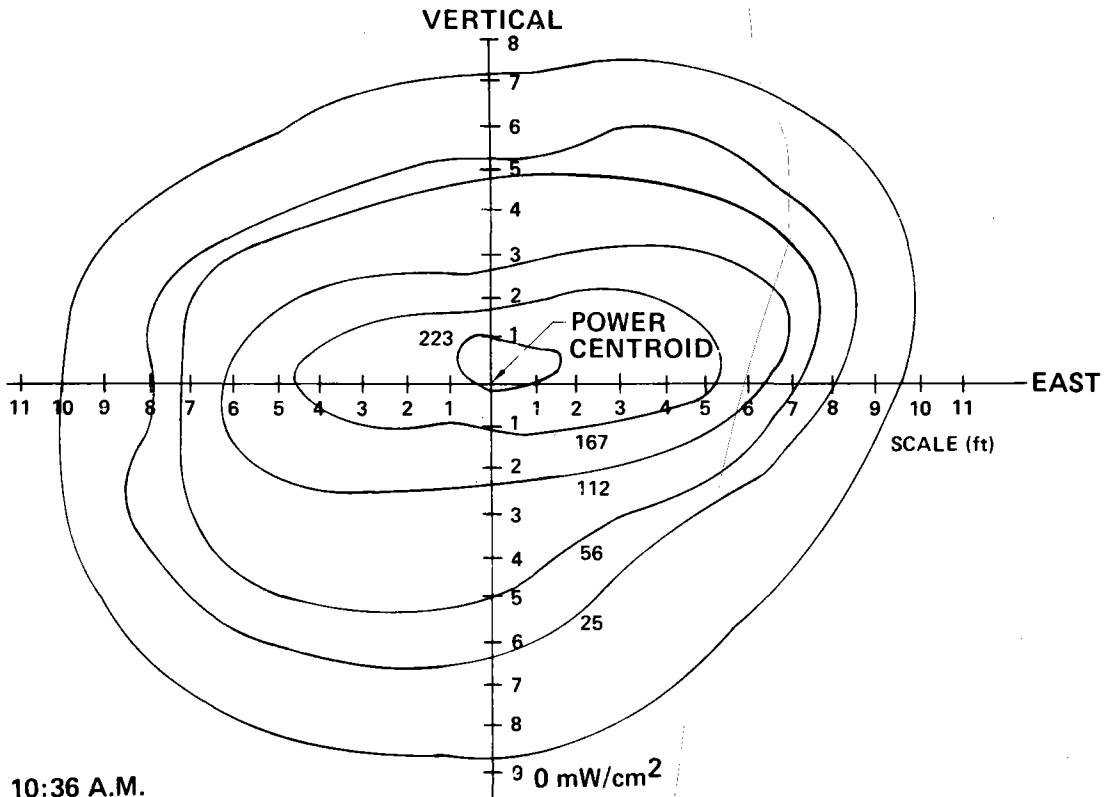
Figure 3.3.3.1-9 . Single Heliostat Optical Image

A plot of the intensity distribution across the major axis of the Figure 3.3.3.1-9 image, is shown in Figure 3.3.3.1-12. Also shown in the figure is the theoretical distribution expected from a non-focusing reflector with perfect specular reflection. The theoretical distribution was maximized to coincide with the limit imposed by the theoretical materials limit. Results show that



HELIOSTAT NO. 0
 2/11/77 12:30 P.M.
 E.L. $\leq 36.5^\circ$ FROM VERTICAL

Figure 3.3.3.1-10. Single-Heliostat Optical Image



4/2/77 10:36 A.M.

Figure 3.3.3.1-11. Three-Heliostat Composite Image

focusing does occur as indicated by the increased intensity throughout the central region of the image, and the reduction in diameter. On the basis of diameter at the 50% intensity point, the image is 0.27 m (0.9 ft) smaller than that expected from a planar reflector (dashed curve), but about 0.3 m (1 ft) larger than predicted for paraboloidal focusing at 6.89 MN/m^2 (1000 psi) membrane tension. This result suggests that the research experiment reflector may have had more membrane tension than planned. Accordingly, it is recommended that developmental tests on Pilot Plant reflectors include membrane-tension verification.

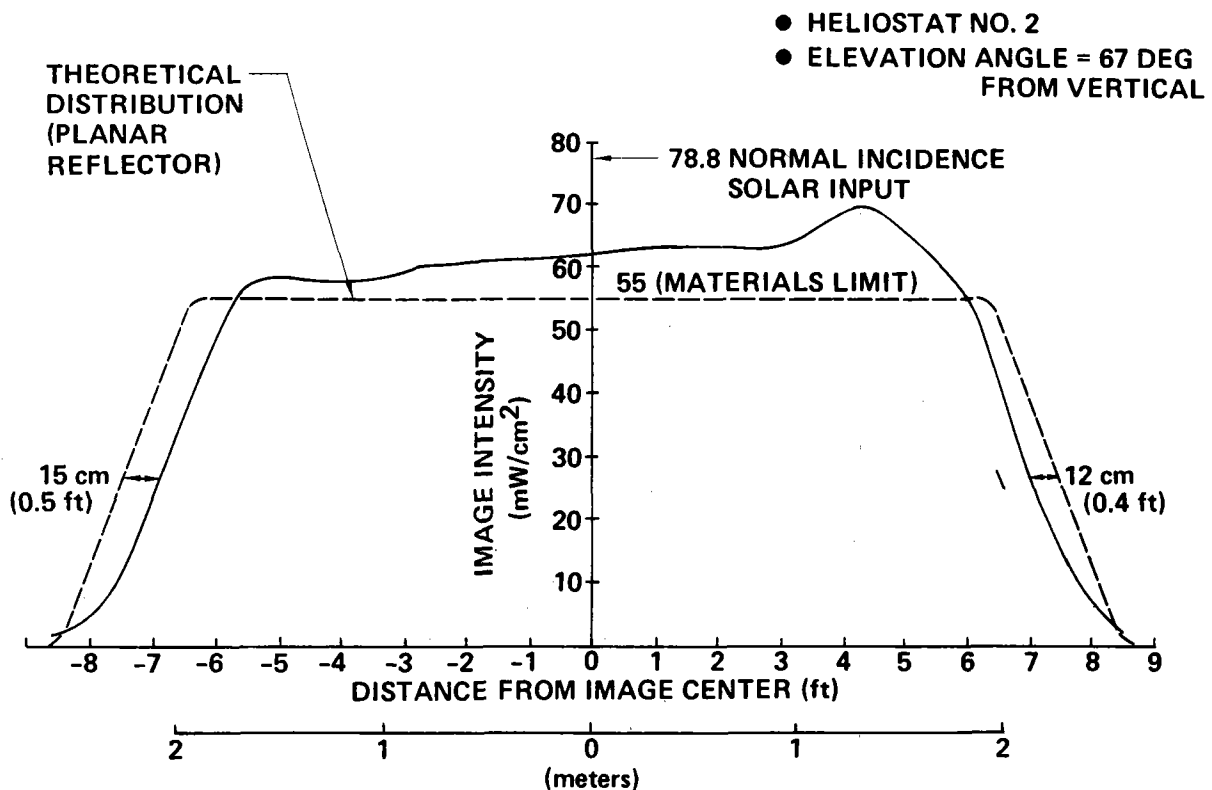


Figure 3.3.3.1-12. Image Intensity Profile

The relationship of optical images from research experiment reflectors, to a cylindrical receiver, is shown in Figure 3.3.3.1-13. A typical image was extrapolated to the maximum north-field range, scaled to the larger reflector size, and corrected for the planned reduction in membrane tension. As shown, the worst

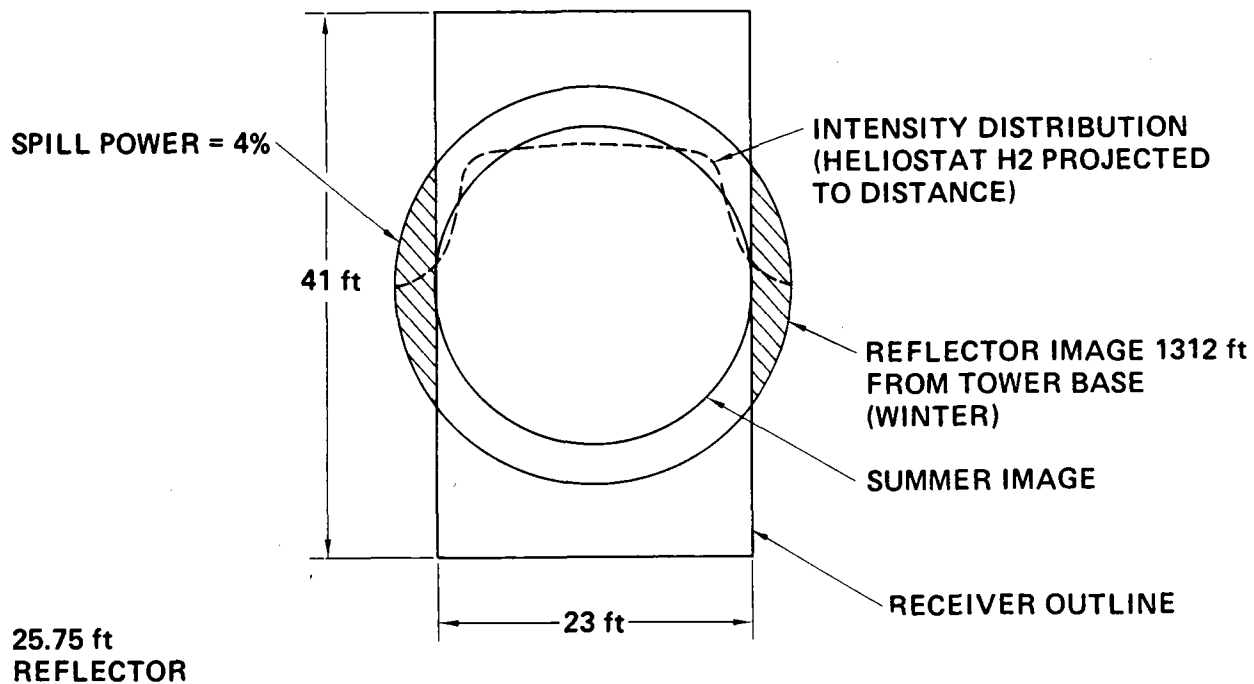


Figure 3.3.3.1-13. Reflector Image on McDonnell-Douglas Receiver

case focusing condition (north field at winter solstice) produces only an approximate 4 percent energy spill. The same reflector at summer solstice produces no spill.

A summary of heliostat efficiency data is given in Table 3.3.3.1-1. Measurements were made on both individual and the group of three heliostats, under various conditions over a 4½ month time period. Results showed a nominal average efficiency of 69 to 72 percent for heliostats with cleaned domes, with some data scatter as indicated in the Table. Heliostat No. 1 was measured in an uncleaned condition after 5 months, and found to have a nominal average efficiency of 65 percent. In general, results show no degradation in efficiency throughout the test, and are in good agreement with efficiency predicted from materials optical properties. The nominal average efficiency of three heliostat composite images was found to be 68 percent, for two cleaned domes and one uncleaned.

As indicated in Table 3.3.3-1, the efficiency of Heliostat No. 2 was measured when a 1-3 Hz vibration was being manually induced in the reflector membrane. Results showed no reduction in efficiency, indicating that reflected energy was not scattered beyond the scanner area. This test was conducted to verify that efficiency is not reduced during gusting high wind conditions (> 25 mph) when small reflector membrane vibration can occur due to dome acoustic coupling.

Table 3.3.3.1-1. Heliostat Efficiency Data

Test condition	Heliostat no.	Date	Time	Efficiency (percent)	Average efficiency
Dome clean	H0	11/19/76	1430	70	72 +1 -2
		3/30/77	1605	73	
		4/4/77	1009	72	
	H2	4/2/77	1309	64	69 \pm 5
		4/2/77	1359	65	
		4/3/77	1655	71	
		4/3/77	1552	73	
		4/3/77	1558	74*	
Uncleaned for 3 months	H0	2/11/77	1235	66	70 \pm 4
	H2	2/11/77	1100	70	
		2/10/77	1150	74	
Uncleaned for 5 months	H1	3/30/77	1240	62	65 +7 -3
		3/30/77	1514	63	
		4/02/77	1117	63	
		4/03/77	1503	72	

* Manual induced vibration of reflector membrane

3.3.3.3 Structural Design

Reflector size is controlled by the size of the protective enclosure less clearance for wind deflection and manufacturing tolerances. The Pilot Plant preliminary design enclosure diameter of 8.54m(28.0 ft) and clearance of 34.3 cm (13.5 inch) results in a reflector diameter of 7.85 m (25.75 ft.).

Design Loads

The reflective assembly is protected from direct contact with most of the severe elements of the environment (wind, snow and ice) by the protective enclosure. There will be, however, some indirect effect of wind on the reflector through buffeting of the dome. There is, in addition to these loads, the possibility that the reflective assembly will be subjected to a Zone 4 earthquake environment at Barstow, California. Other design loads are due to gravity, temperature, tensioning of the membrane, and drive of the reflector.

Membrane Stress

As described in the Collector Subsystem Preliminary Design Baseline Report, Reference 3.3.3.3-1, the reflective membrane is passively tensioned by pre-stretching to a uniform biaxial tension of 5.17 MN/m^2 (750 psi), and bonding to a circular ring. Mylar material of 0.05 mm (0.002 in) thickness is used for the reflector membrane.

Variations in temperature and humidity will cause changes in membrane stress. Differential expansion of the Mylar and the aluminum frame over an extreme temperature range of 60°C (140°F) will result in a change of plus or minus 30 percent from the nominal membrane stress of 5.17 MN/m^2 (750 psi). The effect of humidity on membrane stress is less pronounced than that of temperature. It will usually tend to reduce the effect of temperature because relative humidity tends to decrease as temperature increases.

Since the membrane pre-stress is low compared to the material yield stress of 82.7 MN/m^2 (12,000 psi), long term creep effects will not cause significant loss

of membrane tension. Creep tests performed and reported in Reference 3.3.2.3-8 substantiate this statement.

Gravity Deflection

Maximum gravity deflection of the 7.85 m (25.75 ft) diameter circular membrane stretched horizontally to 5.17 MN/m^2 (750 psi) is 1.00 cm (0.40 in). A more convenient way of expressing this deflection in relation to performance is the reflector focal length corresponding to the parabolic deflection mode that the membrane assumes. Figure 3.3.3.3-1 shows focal lengths for a uniformly-stretched circular Mylar membrane as a function of membrane stress and angle of tilt of the reflector plane from vertical. Focal length is independent of membrane thickness and diameter. Focal lengths as indicated in the figure were included in performance optimization studies which resulted in selection of the 5.17 MN/m^2 (750 psi) membrane prestress. The axis of the deflected parabolic surface remains essentially normal to the plane of the reflector support frame regardless of the angle of tilt. Therefore, gravity deflections will not significantly affect pointing accuracy.

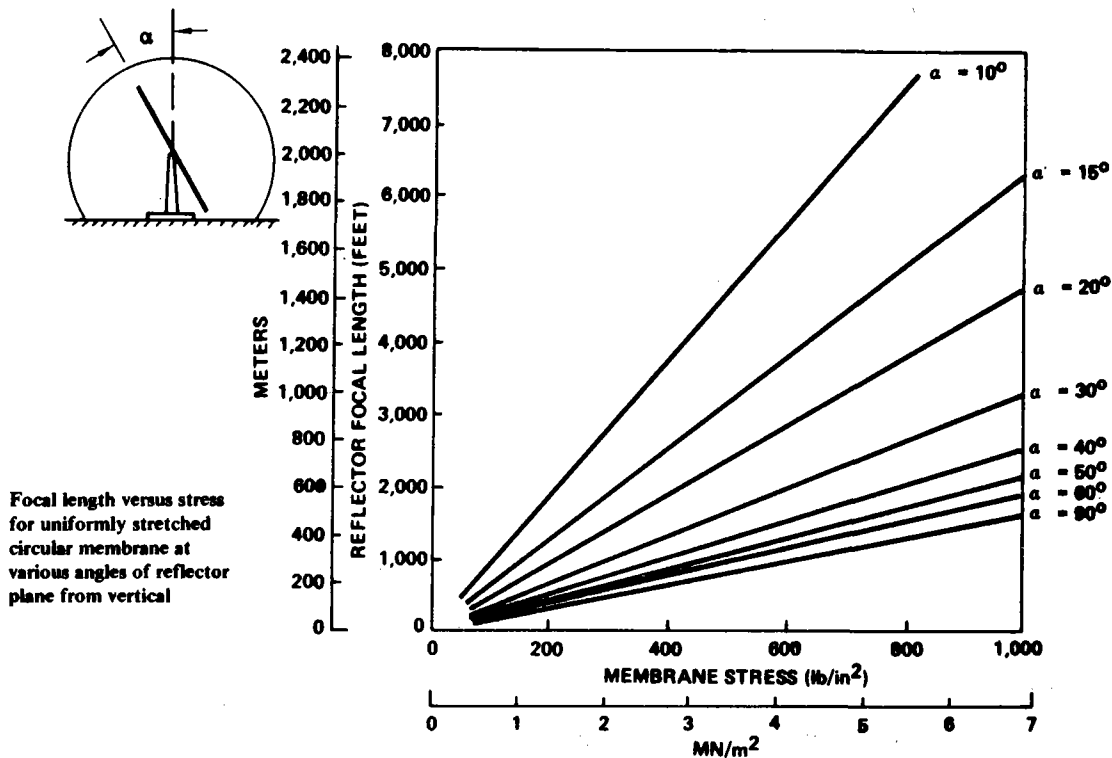


Figure 3.3.3.3-1. Membrane Deflection Due to Gravity, Circular Reflector

Variations in membrane stress caused by temperature changes will cause corresponding changes in reflector focal length. Therefore, in the detail design phase, operating temperature/time histories for the pilot plant will be determined and initial membrane pre-stress will be adjusted to maintain membrane stress variations within the range for most efficient plant operation.

The reflector support structure consisting of the circular ring and three support arms is tubular aluminum, 12.7 cm (5.0 in) o.d. x 0.183 cm (.072 in) thick. The structure is designed by stiffness, and stress levels are very low. Maximum out-of-plane deflection of the circular ring between supports due to gravity when horizontal is 0.42 cm (0.164 in). This causes a maximum angular deviation of a small portion of the reflector surface from the nominal reflector plane of 0.05° , which will have negligible effect on reflector performance. The vertical deflection at the ends of the support arms causes a rigid-body downward translation of the ring of 1.52 cm (0.60 in). Adequate clearance (3.8 cm) between the reflector plane and the central mounting hub is provided to accommodate the vertical deflection of the ring plus the sag of the membrane without interference.

Earthquake Analysis

An approximate seismic analysis of the reflector assembly has been conducted using the design earthquake response spectra shown in Figure 3.3.3.3-2, as taken from Reference 3.3.3.3-2. A peak ground acceleration was assumed equal to that measured in the 1940 El Centro earthquake, 0.35 g's, as reported in Reference 3.3.3.3-3. The fundamental frequency of the reflector assembly supported by a 15.2 cm (6 in.) diameter schedule 40 pipe was calculated to be 4.42 Hz. The peak response of this dynamic system to the above seismic environment, assuming 2% of critical damping, is then 1.60 cm (0.63 in), and 1.26 g's. Adding this displacement to the maximum seismic deflection of the enclosure (Section 3.3.2.3-2) gives a required clearance of 2.72 cm (1.07 in), which is much less than that provided in the design for wind loading. Peak bending stress in the reflector pedestal support due to earthquake loading is 62.9 MN/m^2 (9131 psi) within the design allowable.

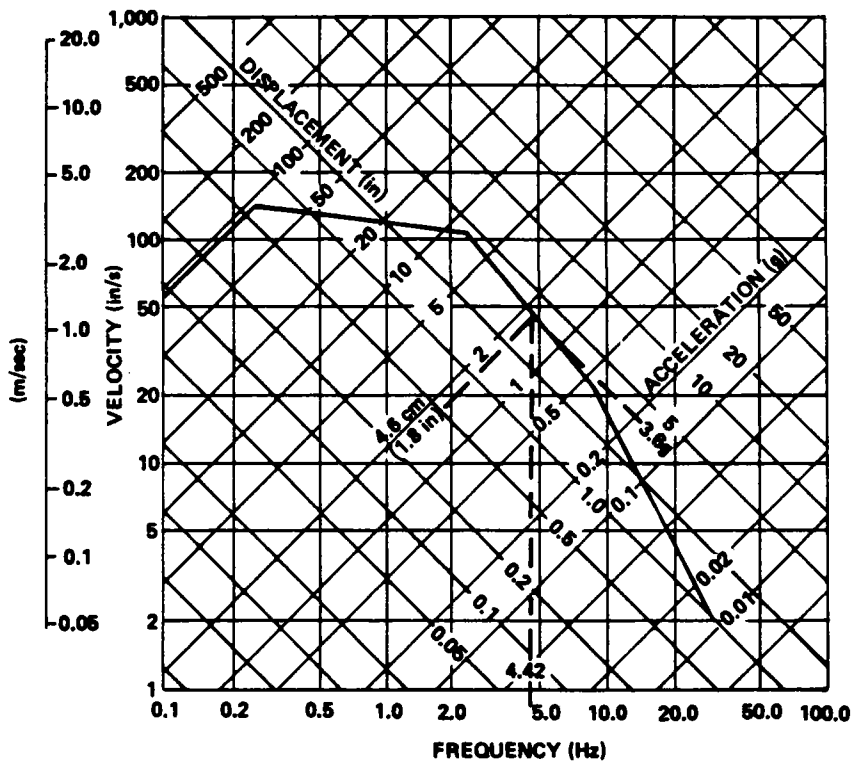


Figure 3.3.3-2. Horizontal Design Response Spectrum for 2% Critical Damping Scaled to 1g Horizontal Ground Acceleration

Thermal Stress Analysis

Thermal gradients are small enough that thermal stresses in the aluminum reflector support structure are insignificant. Furthermore, an analysis reported in Reference 3.3.3.3-1 found that thermal stresses due to differential expansion of the aluminum support ring and cast polyurethane foam ring, to which the reflector film is bonded, are insignificant because of the very low modulus of the foam. An extreme temperature change of 38°C (100°F) from fabrication temperature would increase the bond shear stress between the foam and the aluminum by only 0.69 KN/m² (0.1 psi). Thermal deflections of the reflector support structure for typical maximum operating thermal gradients were also analyzed to evaluate the effect on pointing accuracy and image quality. Deflections were found to be negligibly small.

3.3.4 Drive and Control Assembly

The drive and control assembly consists of the heliostat drive motors and gimbal assembly, motor control circuitry, position encoders, interface electronics, power supplies, computers, and communication links required to control the heliostat positions.

3.3.4.1 Control Overview

Collector control, as defined in the preliminary design, is structured as a three level system with intelligence divided between each level, as shown in Figure 3.3.4.1-1.

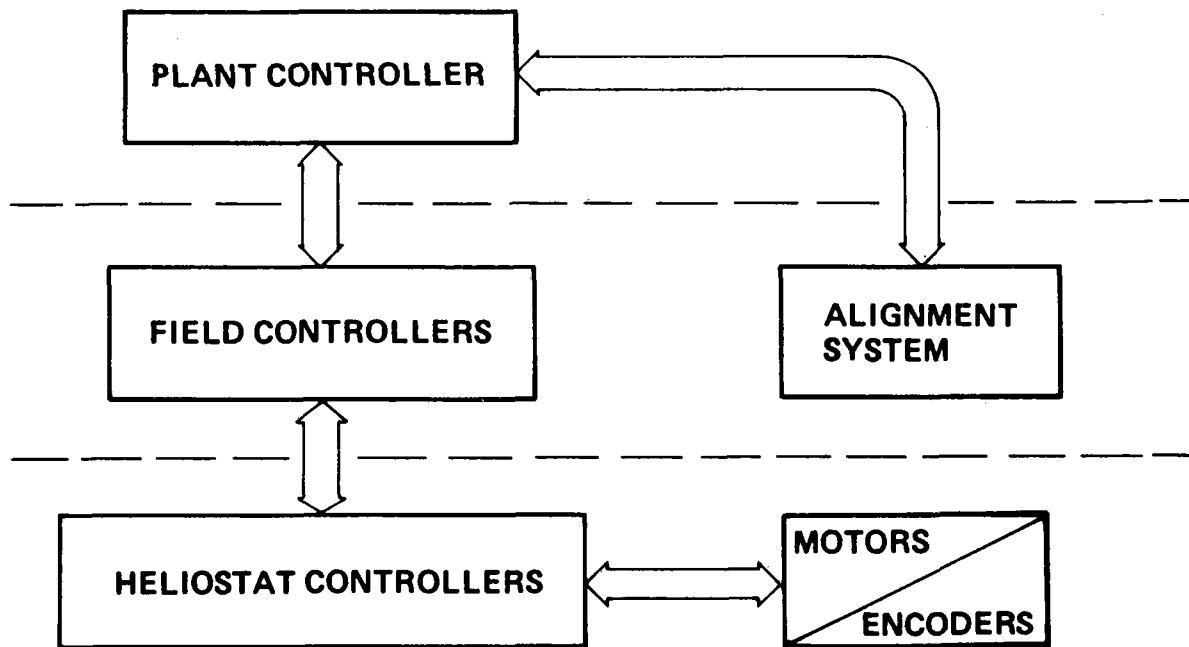


Figure 3.3.4.1-1. Collector Control Levels

Plant Controller - The plant controller issues heliostat mode content commands (either individual or group) in response to operator instructions, and automatically provides time-of-day (once a minute) and ephemeris data once each day.

Field Controller - Each field controller assimilates time-of-day, ephemeris data and mode commands, compute pointing angles, initiates commands to and stores data from heliostat controllers via data busses.

Heliostat Controller - Each heliostat controller computes motor step interpolation in response to field controller commands, issues motor step commands, and receives shaft position encoder data, compares actual to commanded gimbal shaft angle, and corrects motor step output accordingly. Gimbal motion is provided by 200 steps per revolution conventional stepping motors. Gimbal azimuth and elevation angles are provided by incremental shaft position encoders with 0.36° resolution.

Communication between the control assemblies is provided by serial data links or buses. The data buses operate in a polled mode. For example, the field controller for each data bus maintains bus control. This device initiates a message addressed to a particular heliostat controller. When that heliostat controller identifies its address and receives the message, it issues a response back to the field controller.

Each field controller operates four such data buses., with up to 128 heliostat controllers, and manual control units on each data bus. Data bus message formatting is entirely software controlled, providing a high degree of flexibility in message field utilization. The data link between the plant controller and the field controllers functions in a similar manner.

Failure response hierarchy is the reverse of the control hierarchy. If any device loses communication with the device controlling it, it initiates safe shutdown action to avoid thermal damage to equipment or surroundings. Three portable/manual controls are provided for maintenance and/or emergency operation. The manual field controller provides reduced control and status display capability of one field controller group of up to 128 heliostat controllers via the data bus. The manual heliostat controller provides for manual control and status display of any one heliostat via the data bus. When returned to field controller control, the heliostat returns to service without any subsequent re-referencing etc. If heliostat controller electronics fail, motor connectors can be plugged into the manual motor controller so that the mirror can be safely moved to a stow position.

The proposed configuration was selected from several candidates. Also considered were a higher speed field controller issuing individual motor steps to each heliostat, a sophisticated direct memory access interface controller issuing individual heliostat motor steps, and a high speed heliostat controller interfaced directly with the plant controller. These alternates were discarded for the reasons listed in Table 3.3.4.1-1. The selected configuration was studied in detail and refined to reduce cost and optimize performance. The advantages of the selected configuration are summarized briefly in Table 3.3.4.1-2. Subsystem descriptions and selection rationale are detailed in the remainder of this section.

Table 3.3.4.1-1. Other Control Systems Configurations Studied

Description	Discarded because:
<ul style="list-style-type: none"> ● High-speed field controller <ul style="list-style-type: none"> ● No microprocessor (μp) in heliostat controller (HSC) ● One command issued for each motor step ● Medium-speed field controller <ul style="list-style-type: none"> ● Buffered direct memory access interface ● No μP in HSC ● No field controller <ul style="list-style-type: none"> ● High-speed μP(s) in HSC ● All computation in HSC 	<ul style="list-style-type: none"> ● Loss of absolute beam control if communication link fails ● Inefficient communication ● Not flexible ● Higher cost ● Not flexible ● More field controllers required ● No cost advantage ● Inefficient communication ● Plant controller excessively burdened ● Adequate μP not available ● Higher cost ● Some configurations have safety problems

Table 3.3.4.1-2. Selected Configuration Advantages

<ul style="list-style-type: none"> ● Operational advantages <ul style="list-style-type: none"> ● System requirements met ● Continuous tracking capability in all-weather conditions ● Complete manual control capability ● Data provided for total system visibility ● Flexible data bus message structure ● Hardware design supports system growth if required ● Field controller centrally located
<ul style="list-style-type: none"> ● Safety advantages <ul style="list-style-type: none"> ● Automatic recovery from field controller failure ● Timely recovery from power failure ● Automatic safe shutdown on individual heliostat if communication is lost ● Fail operational protection against data bus break ● Continuous communication check
<ul style="list-style-type: none"> ● Cost trade studies show lowest cost and risk for 10-MW_e

3.3.4.1.1 Plant Controller

The portion of the plant controller which is dedicated to collector subsystem control is considered to be customer furnished. Plant controller requirements and interfaces have been defined that envisions this function to be performed by a dedicated computer-based assembly with an interactive cathode ray tube (CRT) terminal/man-machine interface similar to the console shown in Figure 3.3.4.1.1-1.



Figure 3.3.4.1.1-1. Monitor and Control Console

This equipment will be required to:

- (1) Exercise total overall control of the entire heliostat field as instructed by the plant operator.
- (2) Provide a convenient, simple method for commanding the heliostat field, analogous to existing power plant operation, i.e., plant startup, operating and shut down should be fully automatic with operator override capability. The operator has only to input the desired mode of operation and energy level (for the track mode). Specifics regarding which heliostat must be pointed in what direction will be pre-programmed in the computer memory.

- (3) Provide accurate and timely heliostat status information to the plant operator as required to conveniently operate the plant. Other visual displays such as schematic, block diagram etc. will also be desirable.
- (4) Monitor heliostat field status and automatically institute pre-programmed corrective action to insure safe operation at all times.
- (5) Provide collector alignment system data interface and exchange, command/reply sequencing as required for alignment operations.
- (6) Store heliostat operations data and if required produce hard copy print-outs.

Boeing has designed and installed SCADA (Supervisory Control and Data Acquisition) systems for Bonneville Power Assn. and the U. S. Bureau of Reclamation (Parker/Davis Dam Complex) which are analogous to the plant controller described above.

The specific control and data display configuration best suited for heliostat control can include a mix of dedicated and multifunction annunciators, lights, push-buttons, keyboards, digital readouts and a cathode ray tube(s). Considerable study and customer coordination must be completed before a final configuration can be established.

Because of the large numbers of heliostats involved, it is believed any practical display should include a CRT. CRT data presentation is software and operator controlled. Status information will be organized in groups called pages, (see Figure 3.3.4.1.1-2). One (or more if required) page could show all heliostats which are out of service, the reason and the projected return service date. Another page could show in real time, heliostat failures and failure status. Emergency situations can be highlighted with blinking displays, color changes, and audible warnings. Operator instructions can be called up manually or aid the operator in coping with unusual situations. All bookkeeping, report preparation etc., can be handled by such a system.

Fail operational capability can be insured by designing redundancy into the system wherever required.

SCHEDULED OUTAGES LIST		PAGE 3 OF 4
DATE	TIME	EQUIPMENT AND PURPOSE
11 08 76	NOTE	GRAVEYARDSHIFT PLEASE REPORT 0000-0500 OUTAGES TO DIS FRANKLIN TOMPKINS ON CALL AS OF MIDNIGHT
11 08 76		HALLA HALLA, SHORT ON CALL
		ANY HOLD ORDER REQUESTED BY DCC SHALL BE TAGGED FOR AND ISSUED TO THE NEG BY P. WE ARE NOT CONCERNED WITH THE NAME OF THE WORKMAN OR THE HOLD OUT TIME
		NOTIFY REGION OR CONTROL NIGHT OR DAY IF CONTACT STALLS. EVEN IF IT RESTARTS AUTOMATICALLY

Figure 3.3.4.1.1-2. Actual Cathode Ray Tube Display (One page of data shown)

3.3.4.1.2 Operational Description

In response to operator commands, the control system computes heliostat pointing angles for the desired operating mode and generates the drive motor step commands necessary to achieve the computed angles. Five basic operating modes are provided: SHUTDOWN, STANDBY, TRACK, ALIGN and MANUAL. In the shutdown mode, the heliostat is driven to a predetermined position for overnight stowage. In STANDBY and TRACK, the heliostat is driven such that the reflected solar image continually tracks a designated target point. The STANDBY and TRACK modes are similar. When in the TRACK mode, the heliostat tracks a designated point on the receiver. In STANDBY, the target is offset laterally a fixed distance from the TRACK target. The ALIGN mode operates in conjunction with an alignment system to calibrate heliostat positions and pointing angles.

During normal operation, master or individual heliostat mode commands are sent from the plant controller to the field controllers. In addition, the plant controller provides time-of-day updates on the order of once per minute and

solar ephemeris data once per day. Using this information, the field controllers compute the sun's angular position with respect to each heliostat. The solar angles are then combined with the appropriate target angles for the commanded mode to derive heliostat pointing angles. The pointing angles are computed every five seconds and output to the heliostat controllers via serial data bus. Each heliostat controller compares its current position to its new commanded position and outputs uniformly spaced motor step commands over the next 5 seconds to achieve the desired position.

The control system continually monitors operational status. The communication system is designed so that when a device is polled or interrogated, it issues a reply to the interrogating device. The reply verifies receipt of the message and allows the interrogated device to report data including any failures. Each device on a data bus is polled at regular intervals to allow timely reporting of status. Heliostat failures or data bus failures are reported to the plant controller where they are brought to the attention of the operator either by visual or audible alarms, or both. A back-up field controller monitors field controller operation by communicating through shared memory with each field controller. If a field controller failure is detected the back-up field controller automatically takes over. The back-up field controller includes an electronic data bus switch which allows it to take over communication control of the data buses associated with the failed field controller. In addition, each heliostat controller maintains a timer which monitors the time interval between messages from the field controller. If communication with the field controller is lost, the heliostat controller automatically proceeds to the SHUTDOWN mode to prevent any possible damage to plant equipment or surroundings.

The control system includes three separate devices for manual control of the heliostats. A manual field controller allows pseudo-field controller operation of all heliostats on a data bus. The manual field controller is essentially a portable field controller with an operator interface in place of the plant controller interface. It attaches to a data bus in place of the field controller. The manual field controller will be used to support in-plant system testing on site control system checkout and as required for maintenance and troubleshooting.

A second device, called a manual heliostat controller, operates in conjunction with the normal field controller to allow manual control of individual heliostats from the field by attaching to the data bus. The field controller polls the manual heliostat controller. If the manual heliostat controller is in use, it issues a response containing the address of the heliostat to be controlled and the commands desired. The field controller places the selected heliostat in the manual mode, issues the proper commands, and informs the plant controller of the mode change. When a new heliostat is selected or the manual heliostat controller is disconnected, the heliostat is automatically restored to the current bus operating mode.

A third device, called a manual motor controller, is provided to move the mirror if a heliostat controller fails. Motor connectors are plugged directly into the box. The manual motor controller contains its own power supply and motor drive circuitry, and allows direct stepping of the drive motors.

3.3.4.1.3 Field Controller

3.3.4.1.3.1 Configuration

The control configuration is shown in Figure 3.3.4.1.3.1-1. Four field controllers are employed, with each field controller handling up to 512 heliostats. A back-up unit is provided to take over in the event of a field controller failure. Serial data buses provide the communication links between field controllers and heliostat controllers. A similar data bus links field controllers and heliostat controllers. A similar data bus links field controllers to the plant controller. Four heliostat controller data buses are used per field controller to reduce the number of address bits required in the message and to avoid excessive loading of the data bus. The daisy-chain nature of the data bus allows the field controllers to be centrally located in the plant operations building for maximum accessibility and reliability without significantly increased cabling costs. The field controllers are housed in two equipment racks which provide power distribution and cooling.

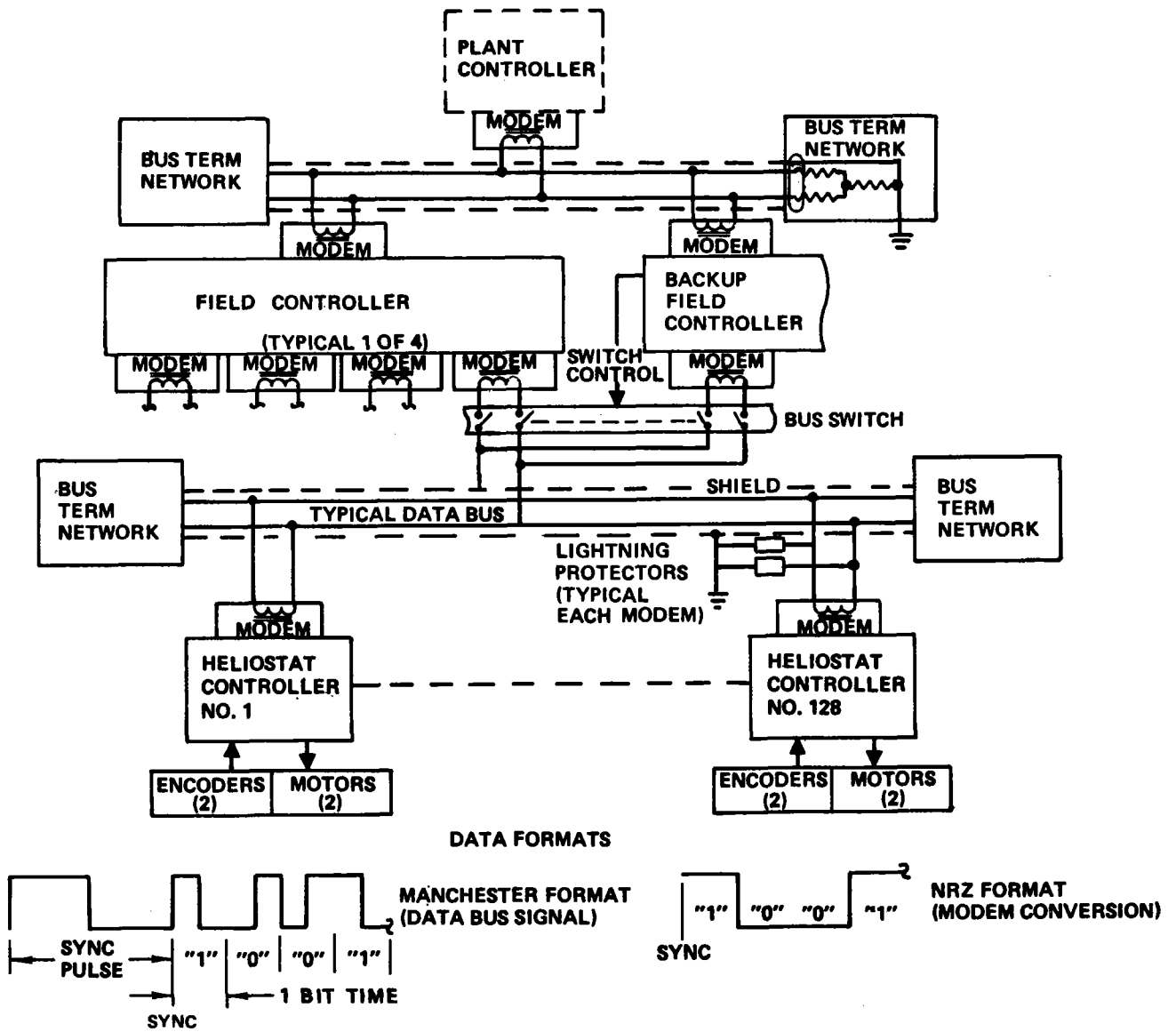


Figure 3.3.4.1.3.1-1. Control System Block Diagram Microprocessor-Based Heliostat Controllers

3.3.4.1.3.2 Central Control Interface

The field controllers are loaded and receive mode commands and data from the plant controller. Two data links are provided to accomplish this task. Each field controller contains a dedicated teletype interface to the plant controller. The teletype interface is used during startup to load a high speed data bus driver and loader into the field controller memory. Once this has been accomplished, the balance of the field controller program and data is loaded via the serial data bus. This bus operates in a polled mode under control of the plant controller. The bus is idle until the plant controller issues a message to a selected field controller. The message includes the field controller address and one of several types of data or mode commands as listed in Figure 3.3.4.1.3.2-1. Receipt of the message at the addressed field controller causes the field controller to input the message, interpret it, and format and issue a response. The nature of the response is determined by the plant controller message. The plant controller

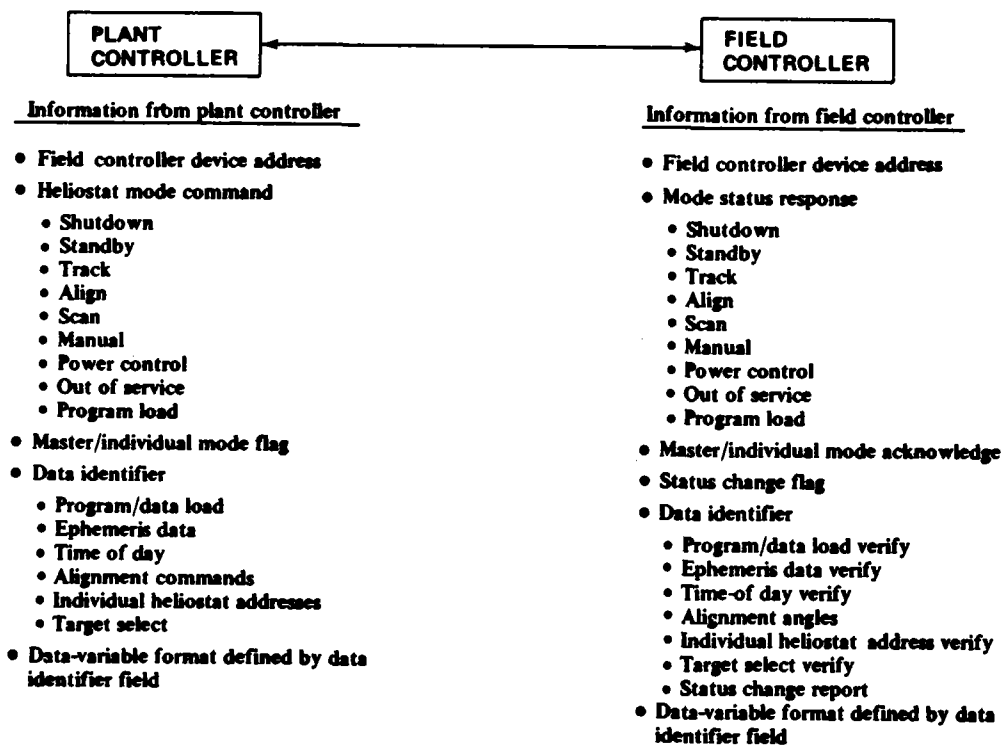


Figure 3.3.4.1.3.2-1. Plant Controller/Field Controller Interface and Information Flow

utilizes the response to verify field controller receipt of commands or data and to monitor heliostat status on a group or individual basis.

The plant controller also provides the link between the field controllers and the alignment system. Single step commands from the alignment system are relayed through the plant controller to the field controller which then issues the proper command to the selected heliostat. Upon completion of alignment, the field controller transmits the alignment angles to the plant controller where they are saved for future use in loading the field controllers.

Communication between the plant controller and the field controllers is on a demand basis with one exception. Time-of-day information is provided to each field controller automatically once per minute. This information is used to synchronize field controller clocks to the plant controller. Between updates, time-of-day is integrated by the field controller for use in pointing angle calculations.

3.3.4.1.3.3 Software

The major modules comprising field controller software are shown in Figure 3.3.4.1.3.3.-1. The main function of the software is to compute heliostat reflector pointing angles as a function of field geometry, heliostat mode, designated target, and time-of-day. The pointing angles are converted to motor steps from reference and output to the heliostat controllers. These command updates are output to each heliostat once per 5 seconds, nominally.

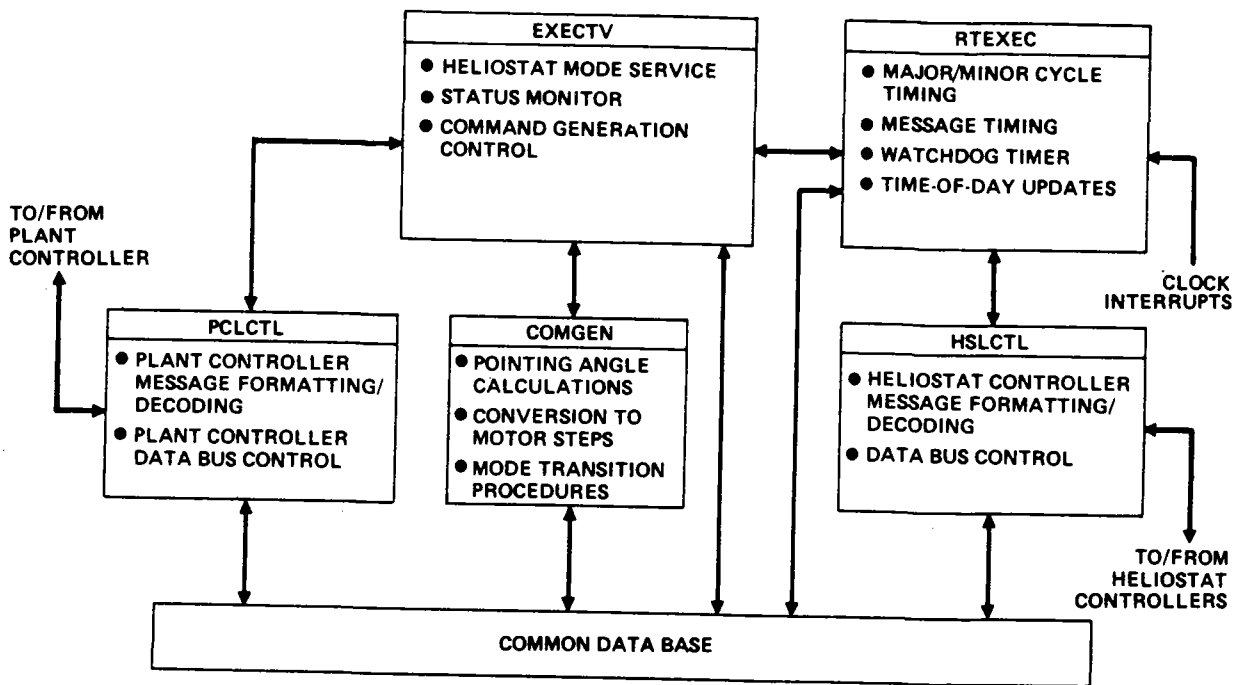


Figure 3.3.4.1.3.3-1. Field Controller Software Block Diagram

Field controller software execution is controlled by the RTEXEC module. This module is driven by a real time clock interrupt derived from the power supply line frequency. RTEXEC updates time-of-day every five seconds for use in computing command angles. It also initiates the heliostat polling sequence at five second intervals and maintains a watchdog timer to determine if a heliostat has not responded in the allotted time or if field controller software execution is stalled.

The HSLCTL module controls formatting and output of heliostat messages and inputs heliostat responses. It is interrupt-driven after the output/input cycle is initiated. It sets up the data bus interface controller to output the first command and then releases processor time for background command calculations. When the heliostat controller response is received, an interrupt to HSLCTL is generated which causes data to be read into memory and initiation of the next heliostat command output. This process continues until all command updates have been serviced.

The EXECTV module executes in a background mode during each five second cycle. This module examines the mode and status of each heliostat and schedules execution of the COMGEN module to compute heliostat pointing angles for the next cycle. Any heliostat failures are tagged for output to the plant controller during the next plant controller message cycle. Mode change requests received from the plant controller are also tagged for processing by the COMGEN module.

The COMGEN module employs time look-ahead to compute motor step increments for each heliostat for the next major cycle. It uses future time-of-day based on time-of-day from the RTEEXEC module to compute pointing angles in the form of motor steps at the end of the next major cycle. The sun's position relative to each heliostat is computed from the time-of-day, heliostat location, and solar ephemeris data obtained from the plant controller at the start of the day. The sun's position is combined with the location of the desired target point relative to the heliostat, to compute heliostat elevation and azimuth angles. These angles are compared to pre-defined zero-step reference angles and converted to motor steps from reference in each axis.

During transitions between heliostat operating modes, the COMGEN module ramps the target points along a selected profile to avoid safety hazards. All target point transitions on or off the receiver are handled by first slewing to the STANDBY mode, which is a lateral offset from the designated track point. Transitions between STANDBY and TRACK are made by lateral interpolation of the target point at a rate compatible with the heliostat tracking capability. Transitions between STANDBY and SHUTDOWN are more complex, but are accomplished in a similar fashion by slewing the target point along a safe path.

The PCLCTL module controls communication with the plant controller. This module is entered when a message is received from the plant controller. The message is read into memory and decoded by PCLCTL. Mode changes are tagged for service by the EXECTV module and data requested by the plant controller is formatted for output. The data bus interface controller is loaded with the plant controller response message which is then output to the plant controller.

The field controller software modules utilize a large common data base to reduce data access times. The data base includes heliostat positions, target locations, modes, status, pointing angles, motor step commands, formatted heliostat controller messages, heliostat status, and reference and alignment angles. The data base is initialized by the plant controller when the field controller program is loaded and is maintained thereafter by the field controller. Certain data is available to the plant controller upon request.

The field controller software will be written in assembly language to maximize software efficiency. Software development and checkout will be supported by an existing Varian computer facility at Boeing Engineering and Construction.

3.3.4.1.3.4 Computer

The computer selected for the field controllers is the Varian V77-210. The V77-200 is a low cost, high performance single-board processor which includes hardware multiply/divide, real-time clock, teletype/CRT controller, direct memory access (DMA), and automatic program loader. The processor features a 16-bit word length and includes byte and double word addressing modes. The basic field controller configuration is illustrated in Figure 3.3.4.1.3.4-1. The V77-210 is an integrated computer system which includes a V77-200 processor card, a 19-inch wide by 14 inch high card frame chassis, backplanes which mount to the chassis, an integral power supply, bus terminators, and an operator console which mounts on the front of the chassis.

The semiconductor memory features a 660 nanosecond cycle time and is inserted in the cardframe chassis. The memory is supported by the data save and power fail/restart option which supplies memory standby power for power outages of up to 1.5 hours. This option also includes the logic to detect power failure and alert the processor so that volatile registers may be saved for orderly power-up.

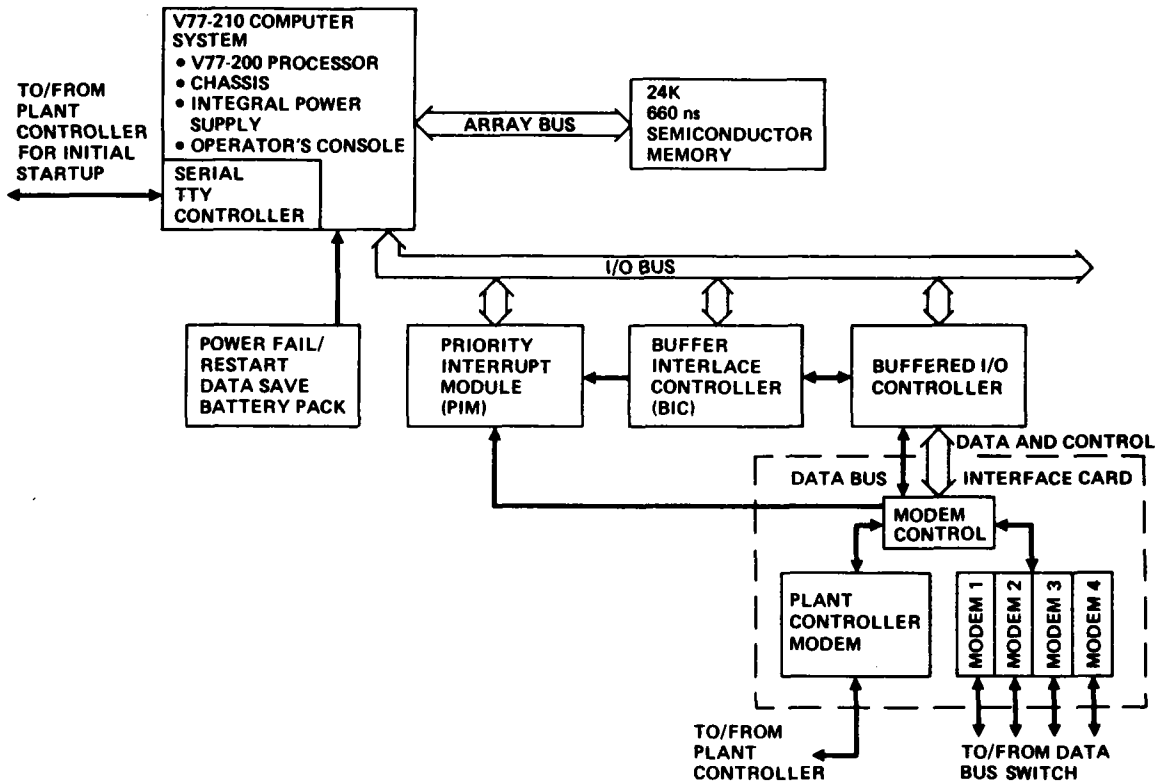


Figure 3.3.4.1.3.4-1. Varian V77-200 Basic Field Controller Configuration

The priority interrupt module (PIM), buffer interface controller (BIC), and buffered I/O controller are standard Varian cards which are used to support the Boeing-build data bus interface card. The PIM accepts up to 8 interrupt lines and generates the proper interrupt vector for the processor upon receipt of an interrupt from a peripheral. The BIC provides DMA block transfer capability

between memory and the buffered I/O controller, allowing processing to continue while the I/O controller card buffers 16-bit words to or from the data bus interface controller and provides the necessary I/O bus timing and control logic. External control and sense lines on the buffered I/O controller are tied to the data bus interface controller to provide modern control.

The back-up field controller configuration is shown in Figure 3.3.4.1.3.4-2. A V77-400 processor was selected because of the extended addressing requirement for the 48K memory. The memory is sited to maintain status data on all heliostats. The processor is similar to the V77-200 processor in the field controller. A system power supply and data-save battery pack are included to support the increased memory. The memory controller performs a memory mapping function to allow direct addressing of up to 32K memory at a time. The PIM, BIC, and buffered I/O controller are identical to those used in the field controllers. A heliostat controller bus switch module is included which allows the back-up unit to take over the four heliostat controller data busses used by any given field controller. The data bus interface controller card is the same as that used in the field controllers.

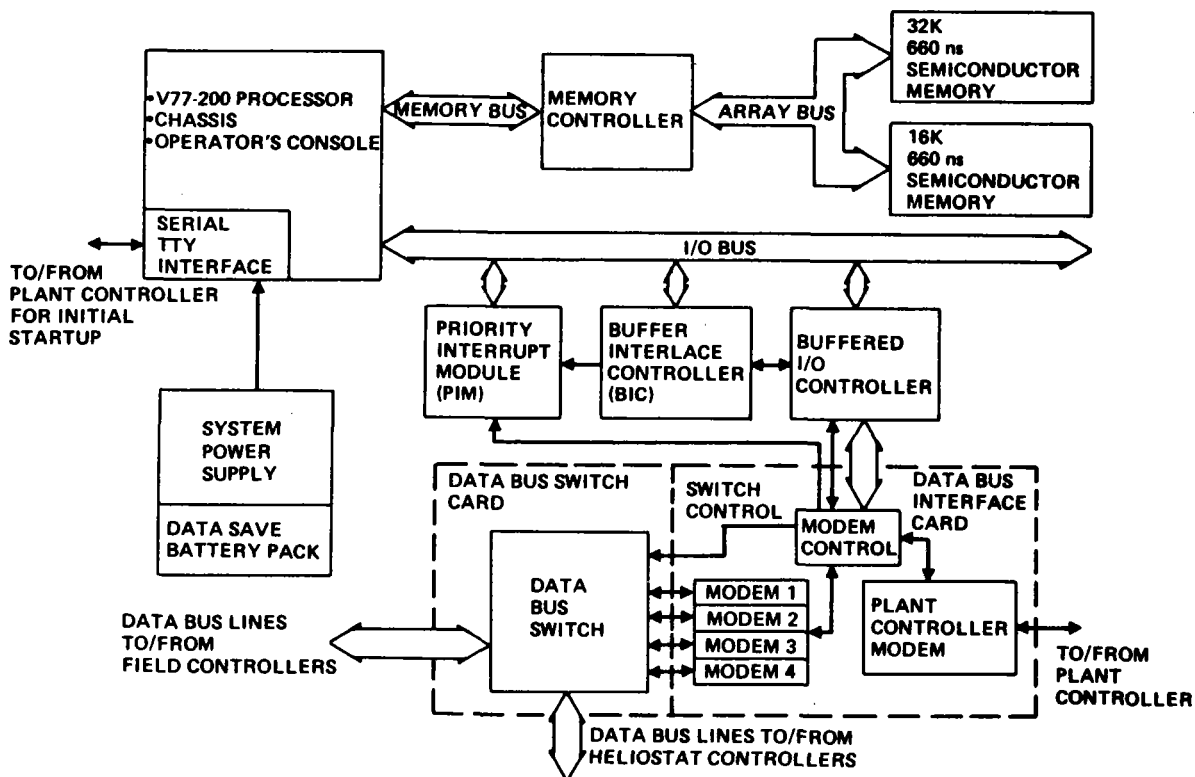


Figure 3.3.4.1.3.4-2. Varian V77-400 Backup Field Controller Configuration

The field controller equipment is housed in two equipment cabinets as shown in Figure 3.3.4.1.3.4-3. The Varian minicomputer was scheduled for the field controller application on the basis of cost/performance trade studies. The DEC PDP11/03 was compared with the Varian computer. Timing estimates were performed for each candidate, and costs were obtained for representative configurations. The PDP11/03 was configured with core memory which required no standby power. The Varian system offered only volatile semiconductor memory, so a battery backup was included to prevent loss of memory contents during power interruptions. The results of the study are summarized in Table 3.3.4.1.3.4-1. The Varian system controlling up to 512 heliostats was selected as the most cost effective configuration. The Varian system had the additional advantage of offering low cost, high performance I/O options to maximize the efficiency of the communication system. Additionally, software development costs are lower for the Varian since Boeing Engineering and Construction has a software development laboratory utilizing a Varian V75 computer which is compatible with the V77 series instruction set. This facility will be used for software development and preliminary checkout prior to delivery of the field controller development test equipment.

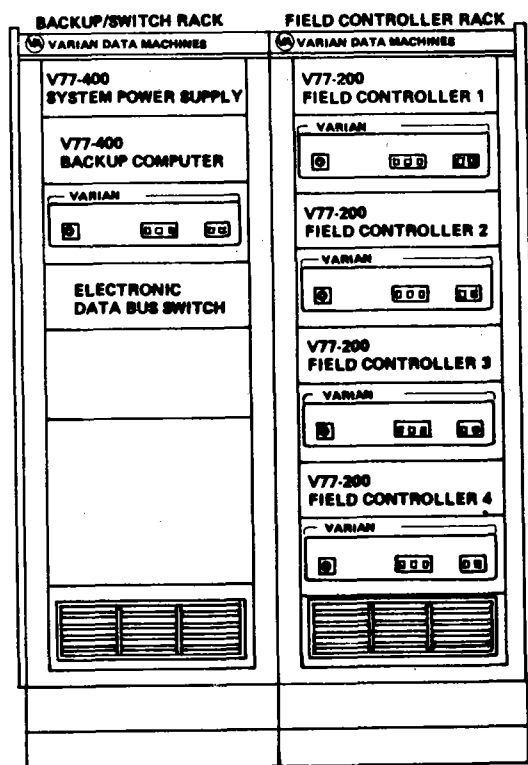


Figure 3.3.4.1.3.4-3. Field Controller Equipment Installation

Table 3.3.4.1.3.4-1. Field Controller Computer Comparison

<u>Number of Heliostats per Field Controller</u>	<u>CANDIDATE COMPUTERS</u>			
	<u>DEC PDP 11/03</u>		<u>VARIAN V77-200</u>	
	<u>Normalized Computer Loading</u>	<u>Normalized Cost Per Heliostat</u>	<u>Normalized Computer Loading</u>	<u>Normalized Cost Per Heliostat</u>
64	.41	4.85	.07	5.92
128	.78	2.46	.26	3.0
256	1.48	1.46	.52	1.62
512	Exceeds PDP 11/03 Capability		1.0	1.0
			(Proposed Configuration)	

3.3.4.1.3.5 Data Bus Switch

All of the heliostat data bus lines are routed through an electronic data bus switch module. This module is controlled by the back-up field controller. The switch module allows each data bus to be electrically connected to either the normal field controller or the back-up field controller. All heliostat data bus lines associated with a given field controller are switched simultaneously, and only one such group may be switched to the back-up unit at a time. Thus, five data bus switch states are possible: none switched to back-up, or one of field controllers 1, 2, 3, or 4 switched to back-up.

The data bus switch is housed in the back-up field controller rack where terminations are provided for the bus lines going to the field and to field controllers in the adjacent equipment rack.

3.3.4.1.3.6 Data Transmission/Information Flow

A serial data bus network is used for communication between the field controller and the heliostats. Each field controller utilizes four individual heliostat control buses, with up to 128 heliostats on each bus. Data bus control is provided by the field controller. Each heliostat on the bus has a unique device address which is determined by switches on the heliostat controller. Messages transmitted over the bus are 48 bits long plus parity. The messages include the heliostat or master mode address, heliostat mode, data, and heliostat returned status. Master mode addresses are recognized by all heliostats for such functions as motor power control and clock synchronization. Use of these addresses allows the field controller to control common functions with a single message transmission. No heliostat message response is transmitted when a master address is detected. The message information content is shown in Figure 3.3.4.1.3.6-1.

The message sequence is initiated by the field controller. The heliostat message is formatted and transmitted as a serial bit stream by the field controller. A sync code is inserted at the start of the message. Each heliostat controller in service on the data bus detects the sync code and inputs the message. The address field is then examined by all heliostat controllers. If the address does not match that assigned to the device and is not a master mode reserved address, the message is ignored. If the address matches, the message parity is examined. If no parity error is detected, the message is decoded and data saved. Requested

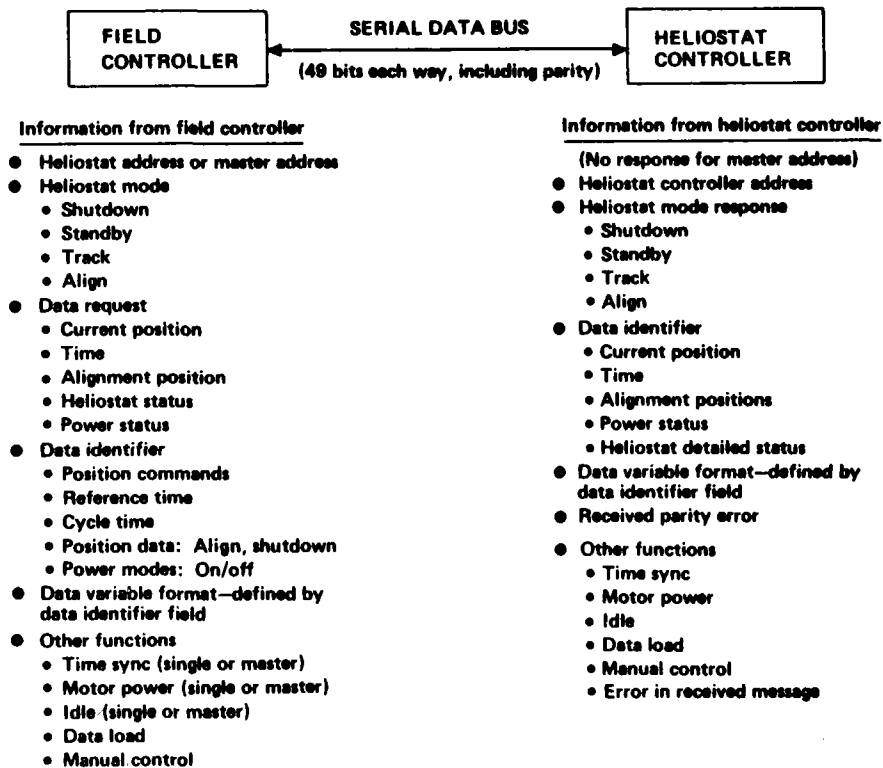


Figure 3.3.4.1.3.6-1. Field Controller/Heliostat Controller Interface and Information Flow

return data is fetched and combined with heliostat status data and address to form the return message. If a parity error was detected in the received message, an error condition mode is entered in the return message and the received message is not processed. The return message is then transmitted to the field controller. The field controller examines the return message, and if an error is indicated, reissues the message. If no error is indicated, the message is processed and the next heliostat command assembled and transmitted.

The field controller accesses all heliostats on one bus, then switches to the next bus and repeats the cycle. The field controller polls each heliostat controller once per major cycle even if no command update is required. This allows the heliostat controller to report status thus updating operational status of the heliostat controller. The field controller maintains a timer which is initialized at the start of message transmission. If a heliostat response is not received in a specified time, the field controller will flag the error and proceed to the next heliostat. Similarly, the heliostat controller monitors the time between

messages. If this time becomes excessive, the heliostat controller assumes communication has failed and initiates emergency shutdown slewing. A RESET mode command must be issued by the field controller to restore heliostat control.

3.3.4.1.3.7 Interface Electronics & Data Bus Description

The outputting of field controller computer data onto a data bus and the receipt of plant controller or heliostat controller data from a data bus is accomplished by the field controller interface card. A modem circuit transformer coupled to the data bus detects, filters and converts incoming data to TTL voltage levels then routes it to a sync detector circuit where the unique Manchester sync code is detected. From there the data goes through a Manchester to NRZ converter and parity generator circuits, then on to a forty-eight bit data register where it is held until the field controller computer accepts it in sixteen bit parallel words. Data to be transmitted essentially goes through a reverse process. Handshake signals between the field controller computer I/O controller and the interface circuitry control the data transfer and timing.

Five modems are included in each field controller's data bus interface card: four are used for heliostat control and one is used for plant controller communication. A multiplexer circuit selects the modem to be used according to control signals from the I/O controller.

The serial data buses which interconnect the field controllers with their respective heliostats and the plant controller is a two-wire shielded Belden 8227, or equivalent, Twinax cable. This is a balanced line having a characteristic impedance of 100 ohms and with the Manchester code format (Fig. 3.3.4.1.3.1-1) provides transmission of data over distances up to 6,000 ft. Transformer coupling to the bus by modem circuitry at each terminal insures maximum terminal failure protection and provides immunity to signal ground differences. The bus cable is buried where possible, and lightning arrestors are placed at all exposed points.

3.3.4.1.3.8 Power Requirements

The field controllers operate on 115 vac, 60 hz single phase power. Line voltages

ranging from 104 volts to 128 volts are acceptable for operation. Line frequency deviations of -13 to +13 hz are acceptable for computer operation. However, the computer real-time clock is triggered by the line frequency, requiring $\pm 1\%$ regulation in line frequency.

The maximum current required by the four field controllers and back-up unit is 35 amps at 115 VAC. Normal operating current is estimated to be 20 amps, resulting in a nominal field controller power consumption of 2300 watts. The field controllers may be turned off when not in use, or left in standby operation with reduced power consumption.

3.3.4.1.4 Heliostat Controller

3.3.4.1.4.1 Configuration

The heliostat controller is physically located inside the dome. It consists of one large conformal coated printed circuit board containing all the electronics and +5VDC power supply, an aluminum hat section under which the printed circuit board is mounted and a ± 10 VDC power supply mounted on top of the aluminum hat section. J-BOX mounted on the dome support wall terminates and provides lightning protection for the data bus. Figure 3.3.4.1.4.1-1 shows details of the heliostat controller and data bus and power junction boxes.

The heliostat controller receives command and control messages from the field controller and sends status responses via the serial data bus, transmits stepping motor pulses to the azimuth and elevation motors, receives and processes digital data from elevation and azimuth encoders, accepts and processes status information from limit switches, and is capable of switching motor power on and off.

The logic components were selected to operate in the temperature environment within the dome. The selected design maximizes flexibility and minimizes power consumption. Connectors are the quick disconnect type to minimize replacement time and are suitably potted to prevent moisture and dust contamination.

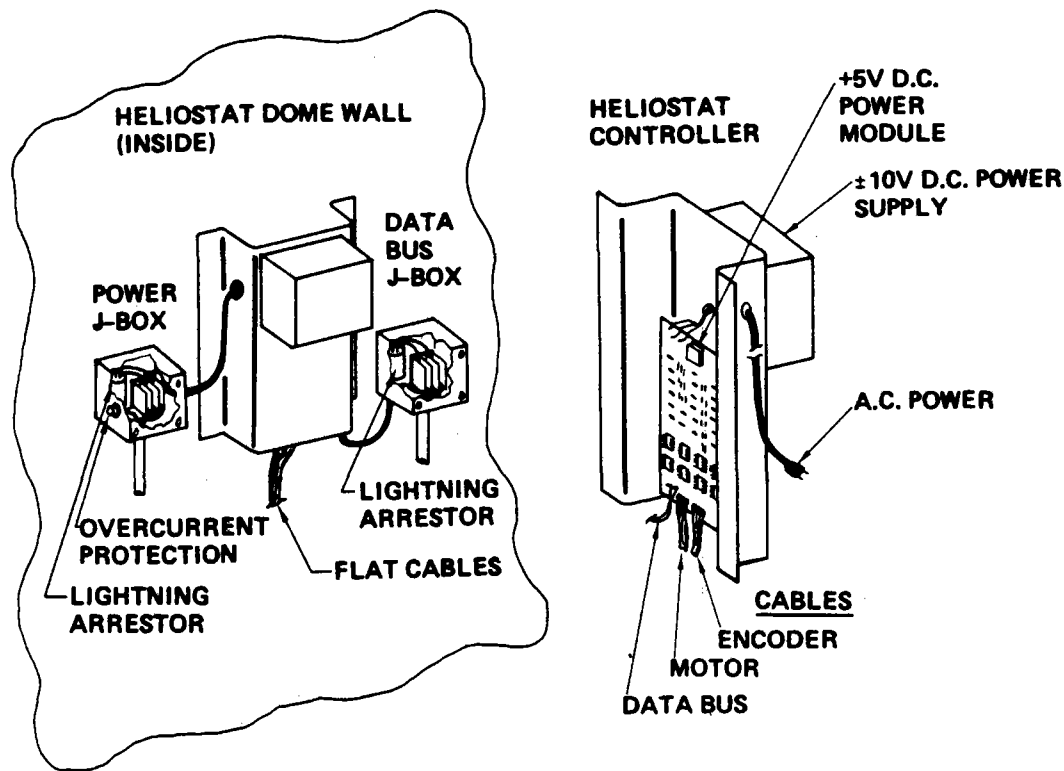


Figure 3.3.4.1.4.1-1. HelioStat Controller and A.C. Power and Data Bus Junction Boxes

A block diagram of the heliostat controller logic circuitry is shown in Figure 3.3.4.1.4.1-2. The data bus is terminated in a junction box designed to allow removal of the heliostat controller without affecting the party-line data bus. The junction box also has terminals to accept control from the manual heliostat controller test equipment (refer to paragraph 3.3.4.1.5). Lightning protection equipment is provided in the junction box. Signals are accepted from the data bus and driven onto the data bus by a high performance data modem. Data processing with the heliostat control circuitry is performed by two microprocessors. The first microprocessor performs incoming message handling and response message formatting including synchronization pattern checking, parity generation and checking, watchdog timing, address decoding, and data buffering to the second microprocessor. The second microprocessor accepts field controller pointing angle data in the form of motor steps, calculates slew rates, drives the heliostat drive motors to proper position, accepts and processes incremental azimuth and elevation encoder data, formats heliostat position data for transmission to the

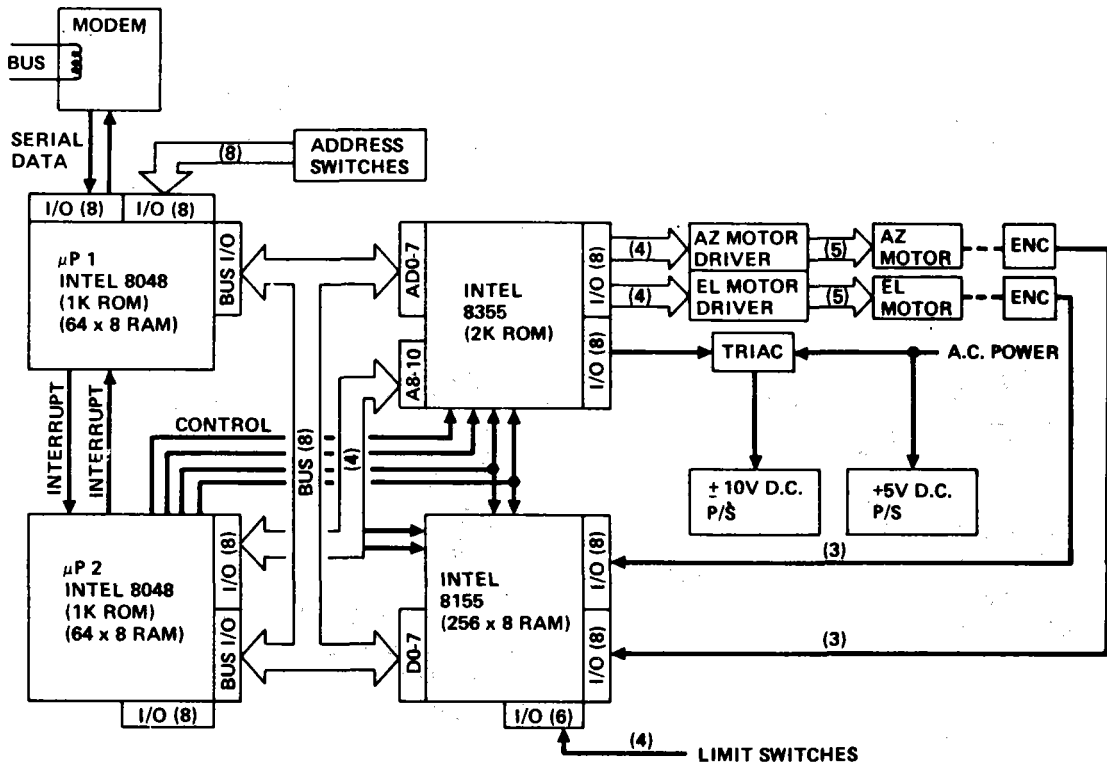


Figure 3.3.4.1.4.1-2. Microprocessor Heliostat Controller Block Diagram

field controller, and accepts limit alarm data. The heliostat control logic allows the motor drive power to be turned on or off under command from the field controller. Each heliostat controller has its own unique address which can be set through eight switches. The motor drive circuitry uses power transistors to switch the current to each motor winding.

The Intel 8048 microprocessor was selected for several reasons. The 8048 utilizes a single low cost 5 volt power supply. Clock circuitry is built into the chip, requiring only the addition of an external crystal to provide a precise time base. The processor is sufficiently fast (2.5 microsecond cycle time) to meet the stringent timing demands of the data bus processing task. Extensive I/O capability is provided on the processor and expansion chips, satisfying both I/O and memory requirements at low cost and low parts count. The 8048 also includes a programmable interval timer to simplify the time cycle management task. An additional programmable timer is provided on the 8155 RAM and I/O expander chip to facilitate watchdog timing functions. Intel also provides an erasable programmable version of the 8048 to facilitate system development. The 8048 will be certified to a very wide temperature range with a very low failure rate.

3.3.4.1.4.2 Operational Programs

The heliostat controller software performs the functions of data link control, message processing, motor control, encoder feedback processing, motor power control, and heliostat status monitoring and reporting. The major software modules are shown in Figure 3.3.4.1.4.2-1. The data bus control software detects incoming messages from the field controller, checks and converts the data link Manchester code to NRZ, checks message parity, and relays the message to the heliostat control processor. The heliostat control processor examines the message and generates the appropriate response which is relayed back to the data link control processor where message parity is generated and the message is converted to Manchester code and output serially to the field controller.

The heliostat control software accepts heliostat pointing angles, converted to motor steps, from the field controller. Depending on the mode commanded by the field controller, the software will single step the heliostat drive motors,

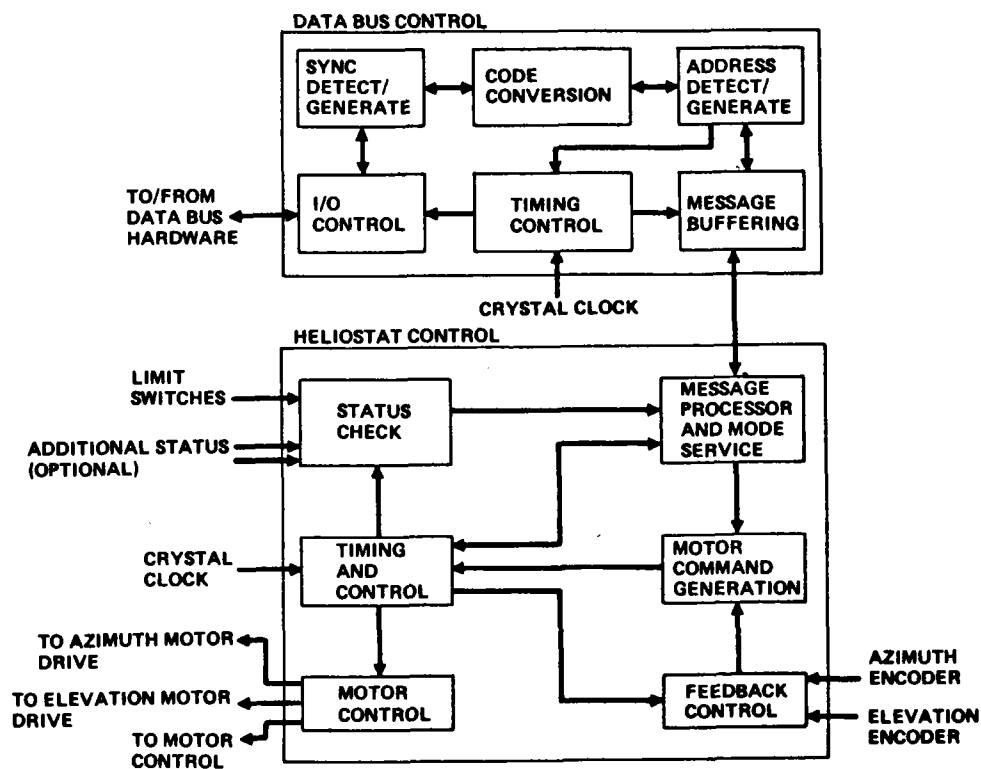


Figure 3.3.4.1.4.2-1. Heliostat Controller Software Block Diagram

slew them at a fixed rate to the commanded positions, or compare the commanded angle to the present position and compute command output intervals to achieve the commanded position in a specified time interval. This capability provides smooth tracking between pointing angle updates by the field controller. Closed loop control is provided by shaft position encoder feedback. The software automatically compensates for position errors. In addition, the software monitors heliostat performance and informs the field controller if excessive errors or failures occur.

The software implements plant safety requirements by providing controlled slewing of the heliostat to a safe position if field controller communication is lost due to field controller or data bus failure. A software timer keeps track of the interval between receipt of field controller messages. If no message is received in the allotted time, the heliostat will be slewed to an emergency standby position to allow time for the back-up field controller to take over. If communication is not restored during a specified interval, the heliostat is slewed to the shutdown position and motor power shut off to minimize power consumption.

3.3.4.1.4.3 Interface Electronics

The interface electronics consists of a modem, motor drive electronics, shaft encoder electronics, and power control logic. The modem signals are transformer coupled and impedance matched such that 128 modems may be operational on one single party-line data bus. The modem transmitter has sufficient power to drive the line, the power being consumed only when the modem is transmitting. The power control circuitry consists of a diac and triac to switch 115V AC on and off the $\pm 10V$ DC supply.

3.3.4.1.4.4 Motor Drive Circuitry

Each motor is driven by four power transistors with two transistors biased on at the same time and two biased off. The transistors are driven by standard logic drivers that interface to the microprocessor. Each power transistor has its own heat sink for power dissipation.

3.3.4.1 4.5 Encoder Interface

The interface to each (azimuth and elevation) incremental shaft encoder consists of five wires: two wires carry square waves that are 90° out of phase, which represent rotation angles; and one wire carries a reference signal. The two remaining wires provide power and return. The microprocessor determines the number of pulses required to move the motors from the reference to a point on one of the squarewaves. The second square wave is used to determine the direction of gimbal rotation. The microprocessor monitors the incremental encoder position and verifies absolute position at each positive square wave transition. Any missed steps are corrected by the microprocessor.

3.3.4.1.4 6 Power Requirements

The heliostat controller derives 115V AC power from the heliostat dome facility power. A + 5 VDC logic power supply module provides 4.5 watts of power for the modem, microprocessor devices, triac control, motor power transistor bias and encoders. Motor power of 10 watts per motor is obtained from a dual ± 10 VDC supply. The total combined power required for the electronic control circuitry and motor drive is 50 watts. Less than 4.5 watts are consumed by the heliostat controller when motor power is commanded off.

3.3.4.1.5 Manual Control Equipment

Three items of manual control equipment provide three-level manual control of the collector subsystem operational electronics. Thereby maintenance personnel are provided with the capability to verify operation, diagnose failures, and command heliostat(s) to a safe attitude in the event of a failure of any part of the electronic system. Figure 3.3.4.1.5-1 illustrates the basic manual control equipment configuration.

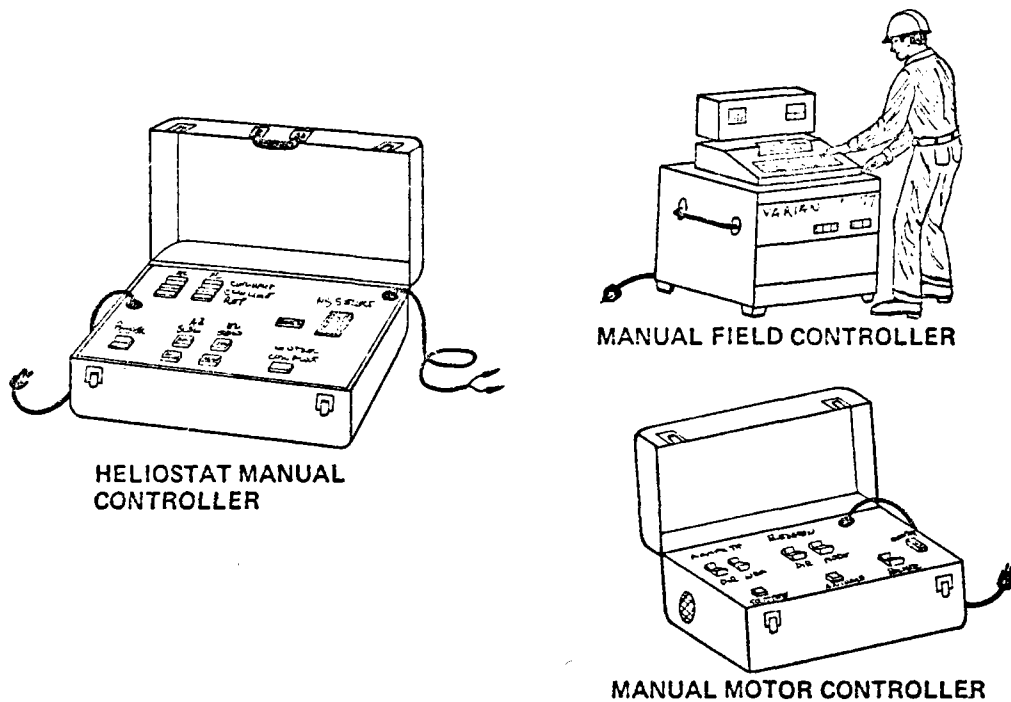


Figure 3.3.4.1.5-1. "Manual Central Equipment"

3.3.4.1.5.1 Manual Field Controller

The manual field controller replaces and functions as an operation field controller with the exception that the plant controller/field controller communications link is broken and replaced by a manual I/O terminal with mag tape storage for loading and data logging. This item is portable and is used to control any number of heliostat controllers on a given heliostat controller data link in either normal operation or test modes.

3.3.4.1.5.2 Manual Heliostat Controller

This is a suitcase size unit which connects to a field controller/heliostat controller data bus at a heliostat location and is used to manually position

a heliostat via the data bus and operating field controller. The bus connection is accomplished by plugging manual controller leads into bus access jacks which are located outside each heliostat dome. A modem circuit within the manual controller provides the proper bus interface so that normal system operation continues undisturbed. Field controller software allows more than one unit to be used at the same time on the same data bus and also prevents conflicting command processing. This unit provides maintenance personnel with local manual control of a heliostat and its electronic circuitry. Also, because the field controller remains in the control loop to process the manual position commands, it also continues to track the heliostat position and thereby can return it to service with minimum down time.

3.3.4.1.5.3 Manual Motor Controller

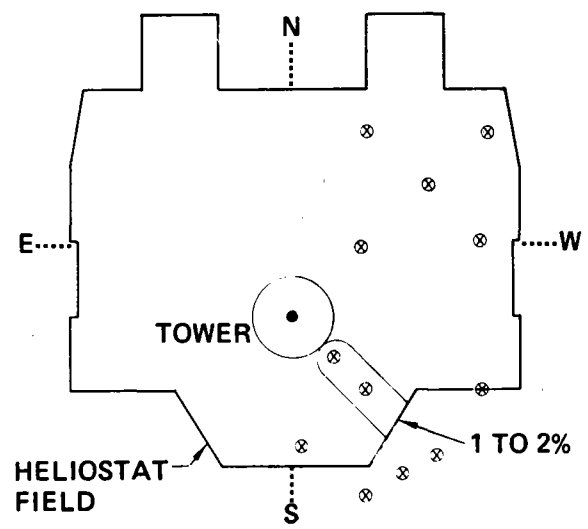
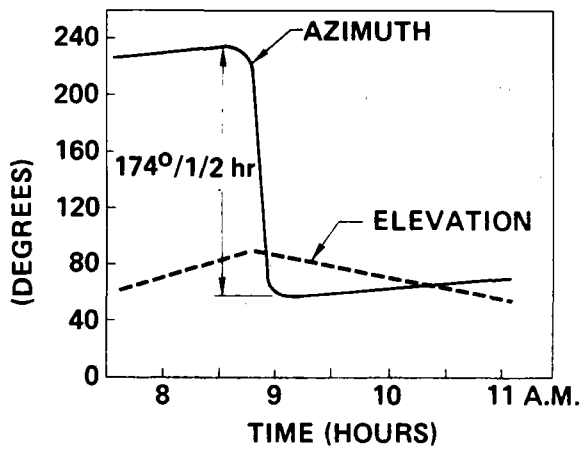
This is a suitcase size unit to which a heliostat's azimuth and elevation stepping motor leads are connected for direct manual control of heliostat position if the heliostat controller electronics are not operational. The heliostat controller motor control circuit connector is removed at the heliostat controller and then plugged into a like connector on the manual controller, disabling normal operation and giving total independent control of the stepping motors to maintenance personnel. A circuit interlock within the heliostat controller disables its response transmission and thereby notifies the field controller of an out-of-service heliostat.

3.3.4.2 Drive Assembly

3.3.4.2.1 Tracking Rate Analysis

One critical aspect of heliostat performance is the ability of the drive and control unit to step at a rate fast enough to keep the reflected image on the receiver. An analysis was conducted to determine the range of necessary tracking rates. Heliostats were chosen from throughout the field (indicated in Figure 3.3.4.2-1), and their required tracking rates were calculated as a function of time for several days of the year. The analysis showed that heliostats in the south field required the highest tracking rates. A worst-case heliostat motion profile for a south-field heliostat is presented in Figure 3.3.4.2-1. As the mirror approaches horizontal, its azimuth track rate increases. As shown in Figure 1, at any given time there is a band of heliostats requiring high azimuth

track rates. It was estimated that an azimuth rate of $0.45^{\circ}/\text{sec}$ would be required to remain on-target 100% of the time. Alternatively, a maximum azimuth tracking rate of about $0.14^{\circ}/\text{sec}$ results in 1-2% of the heliostats being off-target by various amounts at any given time. Considering torque requirements, control system cost, and minimal reduction in performance (1-2%), $0.14^{\circ}/\text{sec}$ maximum azimuth rate, is the best compromise.



Tracking Options

- 100% on target ($0.45^{\circ}/\text{sec}$ required)
- 1 to 2% off target ($0.14^{\circ}/\text{sec}$ required)

Figure 3.3.4.2-1. Gimbal Rotation Rates

3.3.4.2.2. Gimbal/Actuator

The drive assembly (gimbal and actuators) specified for the pilot plant PD is similar to that utilized in research experiment heliostats. Comparing the PD gimbal to the research experiment gimbal design, several minor changes have been made as shown in Figure 3.3.4.2-2. These include inclusion of: larger diameter shafts; higher torque stepper motors, gears, and actuator couplers; three point interface with reflector support pedestal; larger counterweight; reflector

support pedestal; reflector interface fasteners which permit spacing adjustment; and refinement of interface-plate orthogonality tolerances.

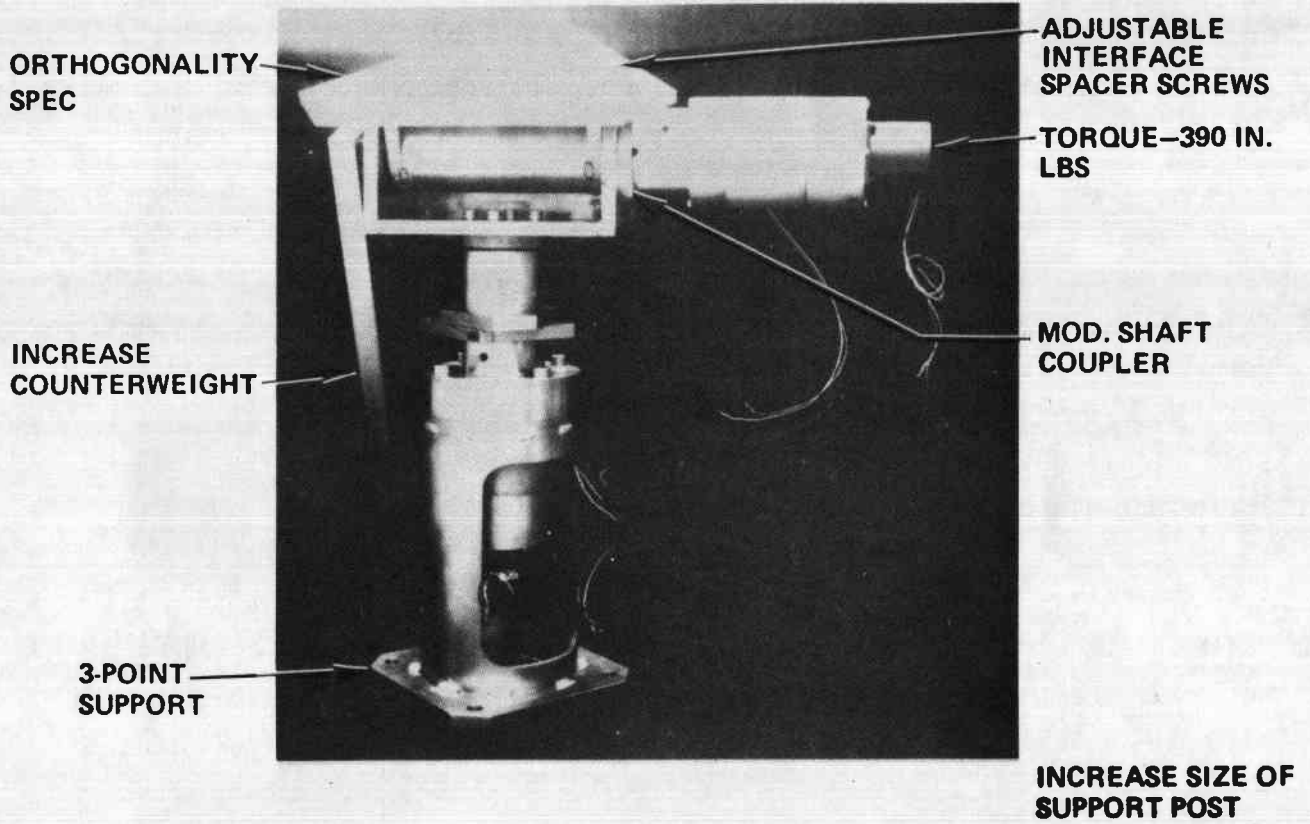


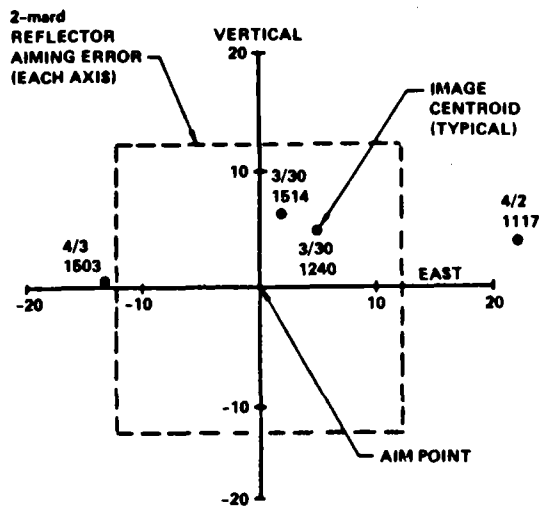
Figure 3.3.4.2-2. Gimbal/Actuator Configuration

3.3.4.3 Research Experiment Results

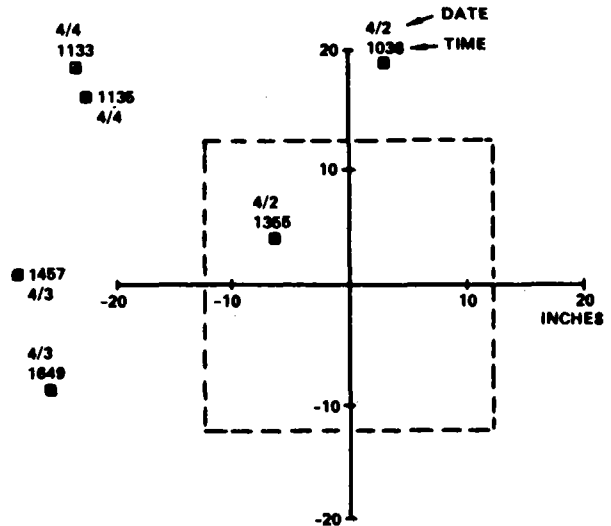
The primary objectives of research experiment tests on the control system included; functional demonstration of operational modes, semi-unattended operation in track-mode for extended time period, and measurement of aiming accuracy. All modes of operation were successfully demonstrated including track, standby, align, shutdown, and manual modes. Semi-unattended operation in track mode has continued for approximately 55 days, using shop personnel for daily system operation. The prolonged operation has resulted in several electronic component failures, and failure of one of the PDP 11/03 computer memory banks. In each case the items were repaired and operation continued. Tests have also successfully demonstrated the ability of the computer to shut down operation of one heliostat, as a result of out-of-tolerance aiming, while maintaining other heliostats in track.

Aiming accuracy measurements with the optical scanner have verified 2 milliradian accuracy for one heliostat on a short term basis. Data for this heliostat are shown in Figure 3.3.4.3-1, which relates image centroids to the aim point at the scanner center. Aiming accuracy data for three-heliostat composite images is also shown in the figure. Generally, the aiming accuracy goal was not achieved. Accordingly, an investigation was conducted to determine the cause(s).

Two significant aiming error sources were identified as shown in Figure 3.3.4.3-2: gimbal axes orthogonality; and reflector/gimbal planar conformance. The effect of these mechanical errors on the planned error budget is also shown in the figure. Gimbal orthogonality error was observed by placing a precision level on the reflector interface plate, and rotating the azimuth axis. The error was evidently caused by gimbal parts, which has been rectified for the PD gimbal design. Reflector/gimbal planar conformance error was observed by rotating the reflector when horizontal, and monitoring wobble with the alignment laser telescope. This error has been attributed to the tolerance allotted to interface plate shims. For the PD, tolerance on the shims has been reduced, and adjustable screws have been incorporated in the interface plate for field-leveling of the reflector surface if required.



HELIOSTAT NO. 1 IMAGE CENTROIDS



THREE-HELIOSTAT-IMAGE CENTROIDS

Figure 3.3.4.3-1. Aiming Accuracy

Research experiment error budget (degrees)

	Planned	Estimated achieved	Image centroids	PD
Field controller	0.012	0.02		0.02
Gimbal	0.042	0.080		0.05
Alignment	0.037	0.037		0.037
Reflector	0.057	0.190		0.095
Protective enclosure	0.057	0		0
(RSS)	0.10	0.21	0.21	0.115
(max)	0.17	0.33	0.28	0.20

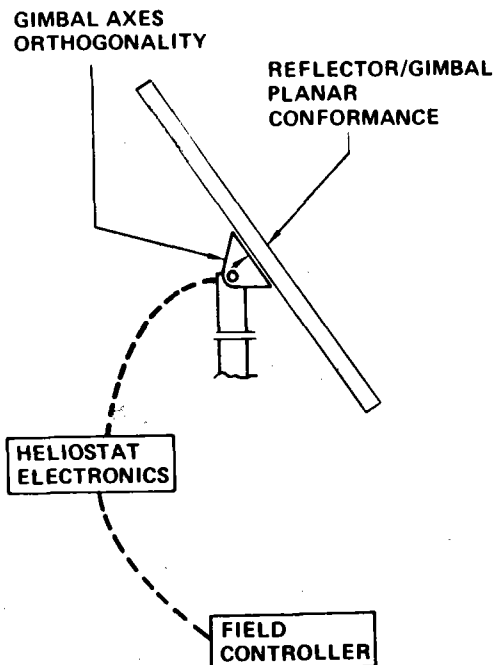


Figure 3.3.4.3-2. Research Experiment Aiming Accuracy Assessment

As shown in Figure 3.3.4.3-2 the maximum and RSS aiming errors observed with image centroids (0.28 and 0.21 degrees, respectively) are in good agreement with estimated-achieved values based on component measurements.

3.3.4.4 Error Budget

Results of research experiments, and analyses of the control system for the pilot plant, have resulted in the PD error budget shown in Figure 3.3.4.3-2. The errors are based on a reflector pointing accuracy requirement of $\pm 0.115^\circ$ (± 2 milliradians), 1σ . The error contributors are subdivided into the various system components.

Drive system errors consist of stepper motor static and dynamic positioning errors, transmission backlash and drive train compliance, gimbal orthogonality and placement errors, and shaft position encoder errors. Analysis of the reflector dynamic response indicates a maximum error on the order of one motor step may be achieved with proper balancing of the reflector. The dynamic response error is the result of the rise time and overshoot motion of the drive system. The static motor stepping accuracy is specified as 3% of one step, or 0.0007° . This is the accuracy to which the motor can be statically positioned to a specified step. The motor step resolution contributes an error of $\pm 1/2$ motor step, worst case, if the desired position is in the middle of a motor step. The effects of motor step resolution for perfect synchronization are shown in Figure 3.3.4.4-1.

Drive transmission errors are attributed to backlash compliance, and friction in the gear reduction drive. The gear drive design essentially preloads the gears to compensate for wear and thus maintains high performance over a long period of service.

The gimbal system introduces errors primarily due to manufacturing tolerances. Pointing errors are introduced if the gimbals are not perfectly orthogonal, and if the reflector surface and gimbal axes of rotation do not coincide. The error attributed to the gimbal system is based on data obtained from the research experiments.

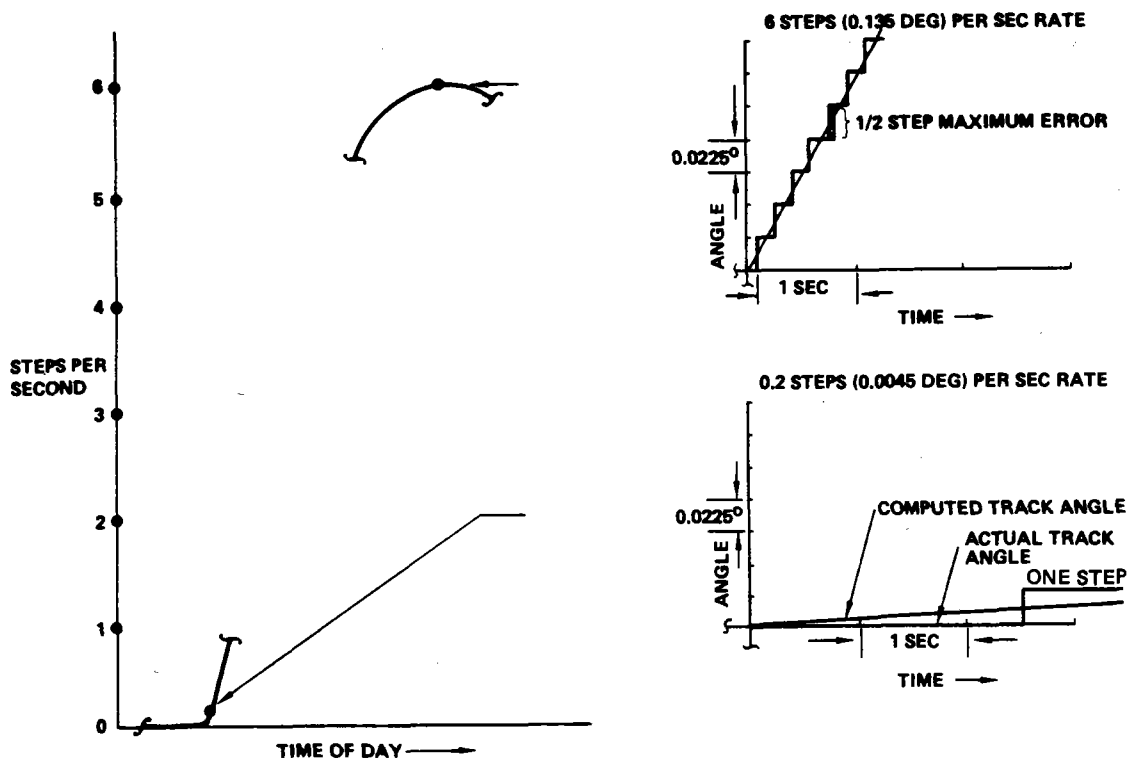


Figure 3.3.4.4-1. S.E. Field Azimuth Rate (Example)

Encoder errors are the result of manufacturing tolerances in the encoder mask, and tolerances in the optical detection circuitry. These tolerances contribute a small uncertainty in the absolute position information derived from the encoder. Offset errors in the encoder and its alignment are accounted for in the automatic alignment system and do not contribute to reflector pointing errors.

The control system introduces errors in the heliostat pointing angles as a result of pointing angle calculations, imperfect knowledge of the sun's position, deviations from perfect step synchronization, and errors in heliostat locations and target angles provided by the alignment equipment. The control system is designed to maintain these errors within acceptable limits. An accurate system time-of-day clock is incorporated, and ephemeris data is maintained with sufficient accuracy to minimize errors in solar position determination. Angle computations in the field controllers utilize double precision math routines to confine truncation errors to the lower half of the double precision word. The final angles are rounded to single

precision to conserve field controller memory. Absolute position information is computed every field controller cycle to avoid cumulative errors which would be introduced by integrating position updates. The final pointing angles are converted to an integer number of motor steps and relayed digitally to the heliostat controllers. The maximum error introduced is less than 1/2 motor step.

The control system provides near-perfect time synchronization of the motor step commands. The field controllers look ahead in time to provide pointing data to the heliostat controllers so they can determine the proper command, time phasing, and step intervals for the next cycle. This approach compensates for time delays in performing calculations and communicating the results to the heliostat controllers. The synchronization error is then a function of the heliostat controller timing resolution. For a 100 Hz clock interrupt at the heliostat controller, the step timing could be off as much as 5 milliseconds. At the maximum step rate of 6 steps per second, the resulting error is 0.0007° .

The alignment error budget is based on conventional benchmark survey accuracy, laser ranging accuracy, laser sensor resolution, and laser gimbal accuracy. The alignment system provides the tower pointing angle reference for each heliostat, as well as ranging information to each heliostat. The angles and ranges, in conjunction with survey information defining the alignment system location, are used to determine the heliostat positions on the earth's surface and to define the angles between the heliostats and TRACK or STANDBY target points.

3.3.5 Alignment/Calibration

3.3.5.1 Research Experiment Results

Five alignment/calibration checks were made on full-scale research experience heliostats using the spherodolite laser measuring system. The system was positioned in a trailer enclosure approximately 76.2 m (250 ft) from the three heliostats which were aligned. The Scanner, which measured energy reflected from the heliostats, was installed approximately 12.2 m (40 ft) above the laser system. The relative positions of each element (scanner, heliostat, measurement system) closely simulates the pilot plant configuration. Typical alignment tasks, transformation calculations, and scan measurements conducted at Boardman, will be used in the pilot plant with minimal change.

Alignment confirmed that the alignment procedures used provided satisfactory data inputs to the control system. In addition an autocollimation technique was verified as a rapid means for re-checking alignment after initial alignment has been completed.

3.3.5.2 Preliminary Design Configuration of Alignment System

The spherodolite system will be mounted in a small enclosure positioned on a circular track near the top of the tower, beneath the receiver (described in Section 3.3.5.4). The spherodolite system, which consists of a laser ranging device and two angle measuring devices (azimuth and elevation angles), will be interfaced to an alignment computer for data storage and subsequent automatic alignment checks. The computer section will consist of a minicomputer, a mass storage device, and appropriate hardware and software interfaces to control the spherodolite, manipulate data, perform calculations, and communicate with the central controller. A leveling platform, which will automatically respond to tower tilt movements, will be employed to support and maintain the spherodolite system in a level attitude.

3.3.5.3 Alignment/Calibration Procedure

The alignment procedure is divided into two phases: the initial alignment

phase and the subsequent alignment check phase. The initial alignment phase is a man-assisted task which establishes all reference and alignment data necessary to perform automated subsequent alignment checks. Because of the relative position of the alignment system situated directly below the receiver zones, the first task will be to establish the relative vertical distances from the alignment system to the center of the receiver zones. These measurements are necessary to calculate the vertical transformation angle the heliostat must move from the laser alignment position to the respective receiver zone alignment position. These distances will be obtained from manufacturing drawings.

The second task relative to initial alignment is to establish a true south azimuth direction reference. This reference is required in the tracking software to orient the ephemeris data for accurate solar tracking. The southerly direction is obtained from two monuments installed by a surveyor. The true positions of the monuments and the direction of an interconnecting line-of-sight are defined from star and sun sightings or other suitable references. The south orientation is input to the azimuth angle sensor such that direct azimuth angle readings can be obtained for each heliostat.

The initial heliostat alignment is a man assisted task and is performed for each heliostat. The mode of operation and specific heliostat to be aligned is identified by the Central Controller (CC) by identification number (ID). The information is transmitted between the alignment computer (AC) (located near top of tower with laser ranging system) and the (CC) via an RS 232 modem interface which will be compatible with both systems. The AC records the heliostat ID number and defines memory space for the coordinates of the aligned target positions. The CC operator then commands the respective field controller (FC) to point the identified reflector toward the alignment system located on the upper part of the tower. The spherodolite measuring system operator then points the laser beam to the four rim targets to measure their respective distances. Calculations are made and appropriate signals are sent from the AC to the CC and FC to adjust the reflector gimbal mount to equalize all rim target distances. The spherodolite's coordinates for each rim target are then stored in the AC for subsequent re-alignment checks.

The operator then points the laser beam to the center reflector target, and records and stores its coordinates as identified by the spherodolite. At this time the AC verifies acquisition of autocollimation, calculates the elevation transformation angle and the heliostat's azimuth and elevation reference angles relative to true south and normal vertical, respectively; and transmits the data to the CC with an end statement that initial alignment is complete for that collector. The CC stores the reflector gimbal's coordinates for the alignment position. The procedure is then repeated for all heliostats.

The subsequent alignment checks are accomplished in the following manner. The CC communicates to the AC the ID number of the heliostat to be checked. The AC locates the identified heliostat's center target coordinates and directs the spherodolite to point the laser beam to those coordinates. At the same time the CC signals the FC to move the respective heliostat to its alignment position. The AC then checks for autocollimation. If autocollimation is achieved, the AC sends the CC a signal that the heliostat is aligned and to retain the same alignment coordinates. If autocollimation is not achieved, the AC signals the CC that it is going to re-align and to prepare to receive new alignment data. The AC will then re-measure the rim targets, send the appropriate signals to the CC and FC to re-position the gimble to equalize distances, replace old with new alignment coordinates for rim and center targets, and signal CC that re-alignment is complete.

3.3.5.4 Alignment and Calibration Module

Alignment of reflectors requires the use of a laser spherodolite as described earlier. The spherodolite must be positioned on the receiver tower high enough to have a clear optical path to all heliostat reflectors but below the receiver. It must have provision to traverse about the tower 360° for full field access.

Figure 3.3.5-1 describes the alignment and calibration module. An adequate stairway and catwalks must be provided for the operator and maintenance personnel. The only utility requirement is 115 V, 60 Hz, 30 A power with a 4 nema plug receptacle. Also mounted on the alignment and calibration module is the Heliostat Solar Image Scanner. The scanner shares the module because

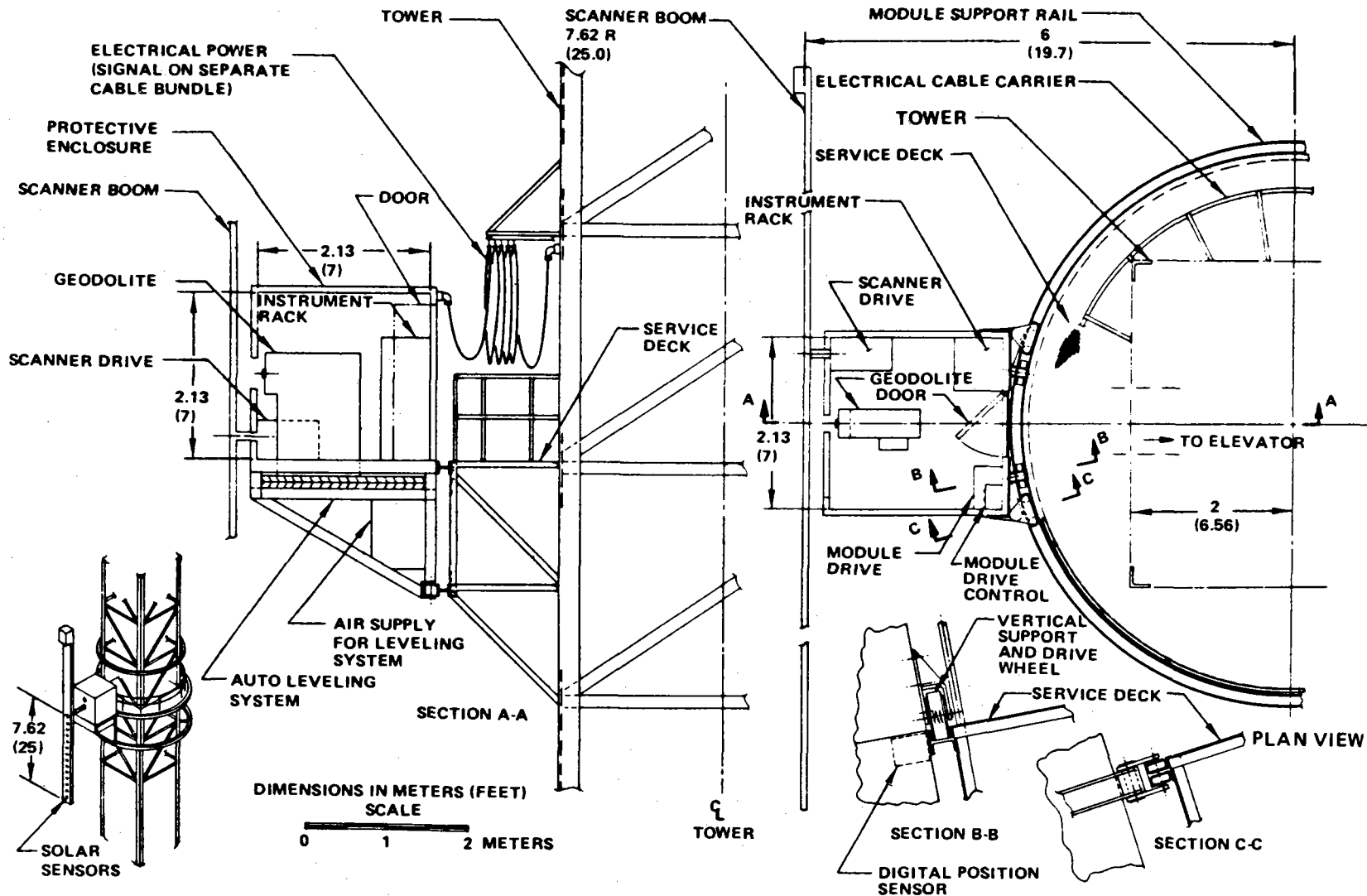


Figure 3.3.5-1. Laser Scanner Module

it has the same requirements for a clear optical path to all heliostats in the field. A description of the scanner follows.

The structure of the scanner consists of a water cooled boom attached to a rotational drive shaft. The drive shaft is mounted on bearings and is driven by a two direction DC motor. This will allow for complete scanning of the projected solar image in less than 10 seconds. Limit switches will be applied to the drive shaft to protect instrumentation cables and water hoses from over winding. Solar cells and/or radiometers will be mounted on the water cooled boom to measure the projected solar image. The water-cooling loop (closed loop system with heat exchanger) is required to provide constant operational temperature of the scanner during operation. An insulated wall will be mounted behind the scanner to absorb the passed solar energy.

The scanner rotation plane can be rotated to allow normal-incidence measurements on all heliostats. Scanner motions will be motor driven, and location and directional encoders used for position indication. The output signals from selected sensors can be integrated to calculate the total energy incident on the receiver. Receiver view information for each heliostat location will be stored in the data system memory. Equatorially mounted solar monitors will provide direct solar radiation information to compare incident solar energy to that returned to the scanner. The heliostat efficiency can be calculated by comparing the total receiver-incident energy to the local incident solar irradiance. In addition, the energy centroid of each heliostat will be computed to assess aiming accuracy.

3.3.6 Power Distribution and Control Cabling

3.3.6.1 Power Distribution System

The power distribution system provides completely redundant, fail-operational power for the entire collector assembly system. The system is diagrammed in Figure 3.3.6.1-1.

The power distribution system includes connection of power cable to the site electrical supply, assumed to be located 304 m (1000 ft) from the central control building. A 200 KW diesel generator with fuel storage will provide emergency power for operation of the heliostat field for 24 hours if required. The total field operating power requirements are:

	<u>Operating</u>	<u>(Night) Quiescent</u>
Blowers (20 W x 1650 heliostats)	33,000 W	33,000
Helio Controller(49 W x 1650 heliostats)	80,850 W	8,250
Field Controller (900 W x 5 controllers)	<u>4,500 W</u>	<u>1,875</u>
Sub-Total	118,350 W	= 43,125
System Power Losses	<u>9,650 W</u>	<u>3,516</u>
Total Power Requirement	128,000 W	= 46,640 W

The 200 KW generator is more than adequate for system start-up transients. Automatic start-up of the emergency generator provides full power to the field within approximately 15 seconds of any loss of site utility power.

A completely redundant power system throughout the heliostat field is provided from the main transfer switches, 480 V, single-phase power is provided to the transformers located at each array (4 arrays per collector field). 120V power is provided to each heliostat.

All power cabling is jacketed for direct burial in a 0.3 m (1 ft) wide by 0.61 m (2 ft) deep trench as shown in Figure 3.3.6.1-2. System redundancy

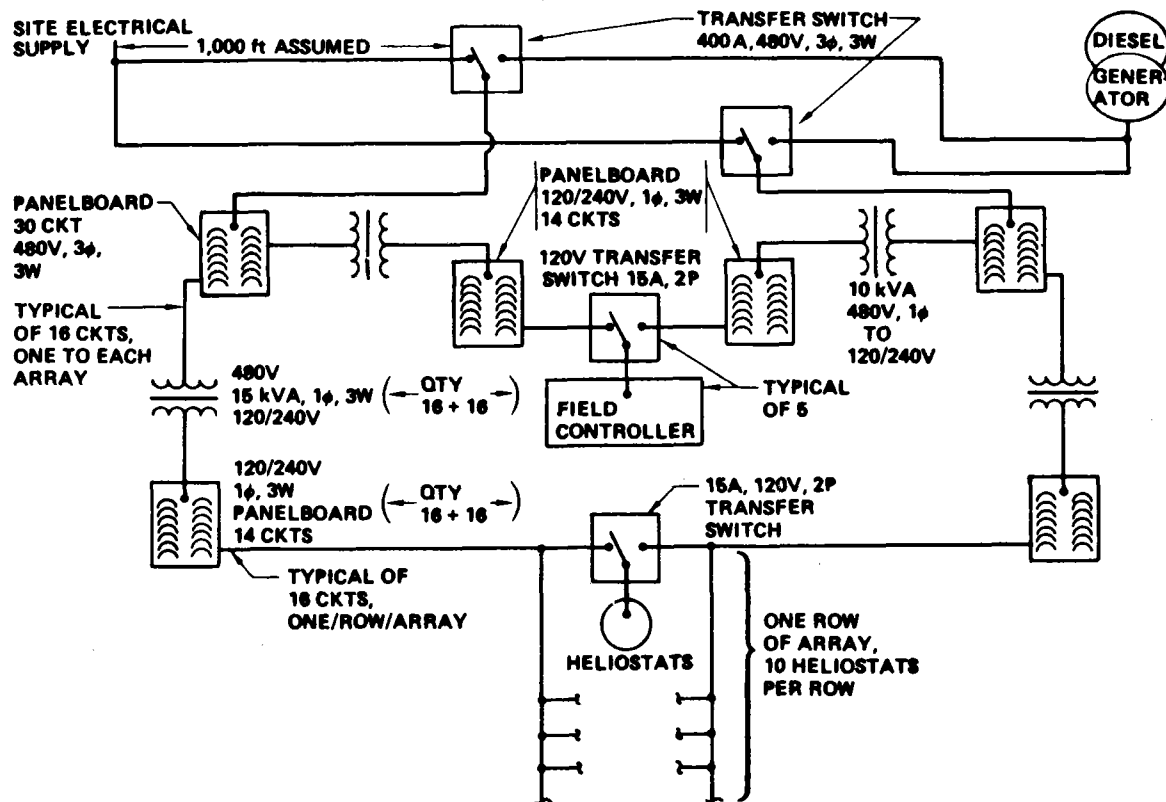


Figure 3.3.6.1-1. Power One-Line Wiring Diagram

provides a fail-operational capability for each heliostat for any single failure, except for a "backhoe type" failure within a row, which could fail no more than 10 heliostats. The redundant cabling as shown in Figures 3.3.6.1-2 and 3.3.6.1-3 feeds the adjacent array to preclude loss of a complete array in the event of a cable failure. A small, automatic power transfer relay is used at each heliostat to provide a completely redundant power source.

Power enters each heliostat through conduit stubs (see Figure 3.3.6.1-4) and terminates in a junction box with the automatic power transfer relay which switches to emergency power in the event of primary power failure anywhere in the system. Power for the heliostat controller is available from a power receptacle mounted in the junction box.

This design minimizes the amount of trenching throughout the field while providing a complete fail-operational system. The total field requires nearly 20 miles of trenching. The capability of direct burial jacketed cable to reliably survive 30 years has been demonstrated by many commercial applications

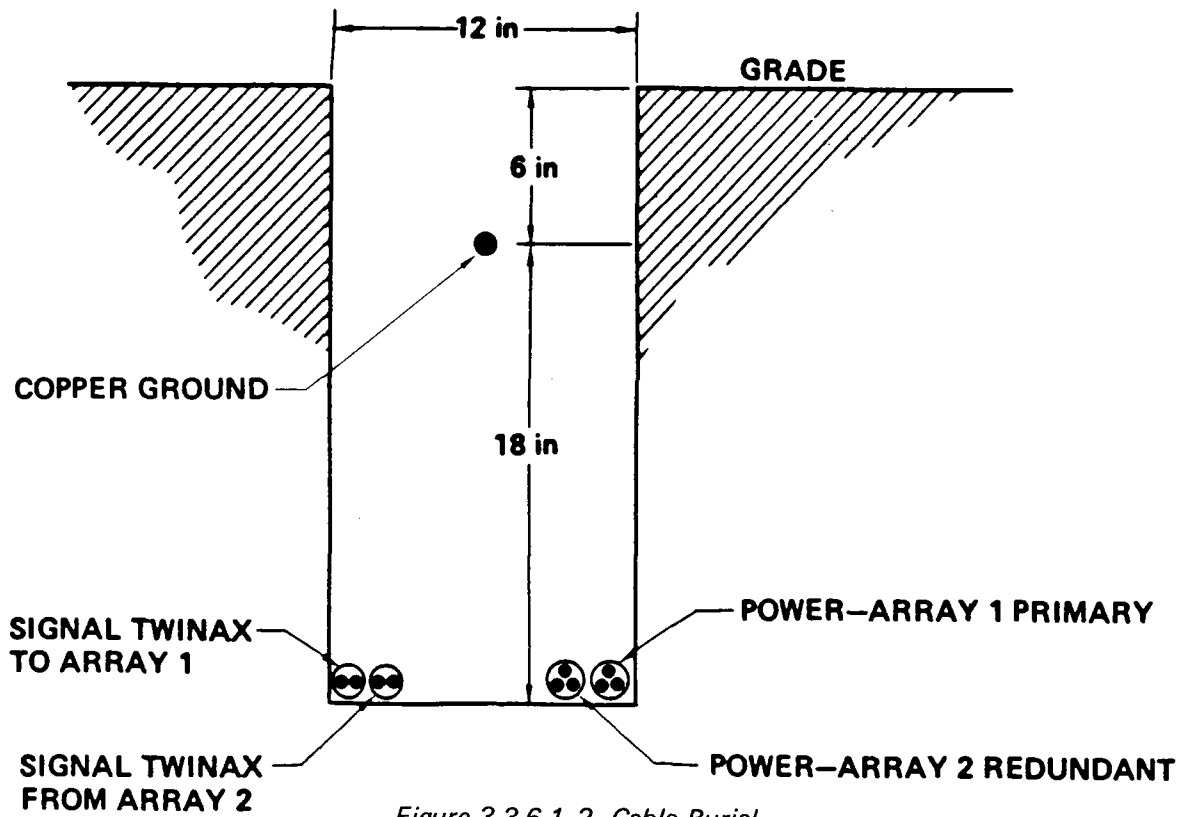


Figure 3.3.6.1-2. Cable Burial

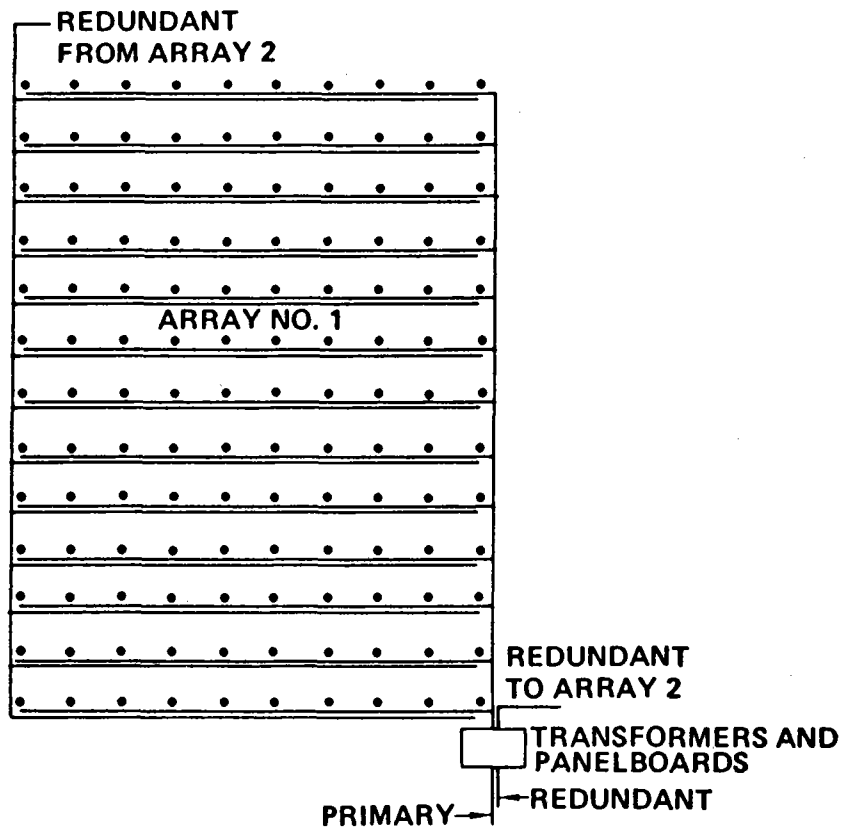


Figure 3.3.6.1-3. Array Power Circuitry

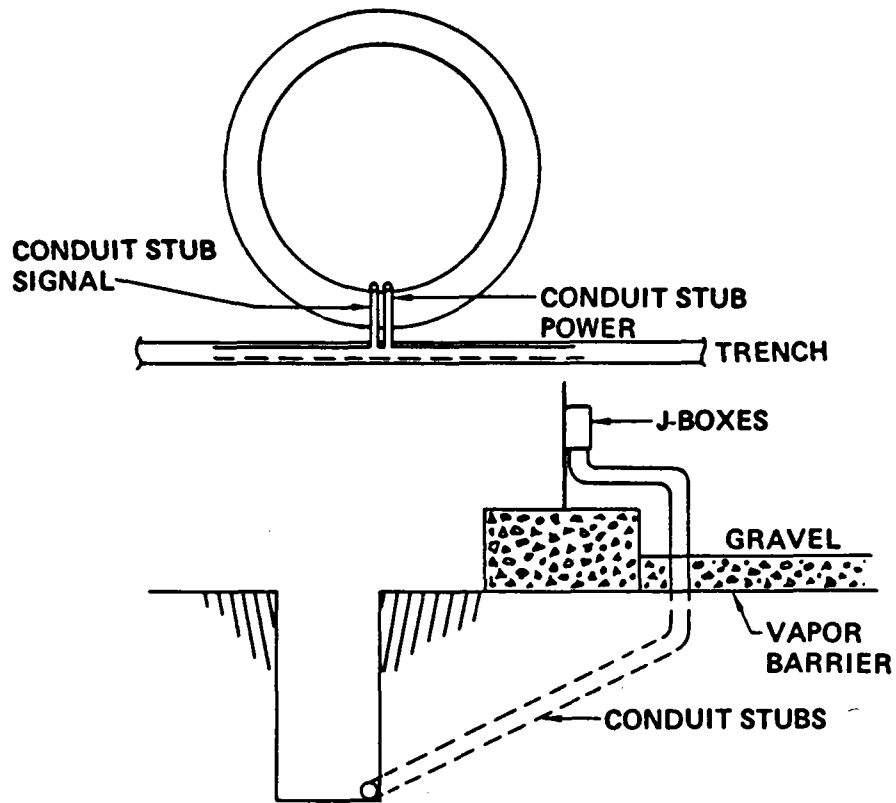


Figure 3.3.6.1-4. Heliostat Power Termination

such as telephone and utility power cables.

3.3.6.2 Signal Cabling System

Signal cabling for the collector system is specified to be a direct burial, shielded "Twinax" similar to Belden 8227.

It is installed in the trench with 0.3 m (12 in) of separation from the power cabling as shown in Figure 3.3.6.1-2. Signal cabling will be installed in a "daisy chain" fashion through each array as illustrated by Figure 3.3.6.2-1. This "Twinax" data bus link is from the Field Controller through the array and back to field controller. A modem loss of signal detector and bus switch allows the data bus to be driven from both ends in the event of a cable break anywhere within the array. There is no loss of control for any single cable failure of this type. The return half of the data bus cable loop will be installed in the trench of the adjacent array to preclude a "backhoe type"

failure between field controller and array from causing loss of control of a complete array. This signal cable enters and leaves the heliostat through a conduit stub. The signal connection is made in the data bus "J" box using crimp terminals.

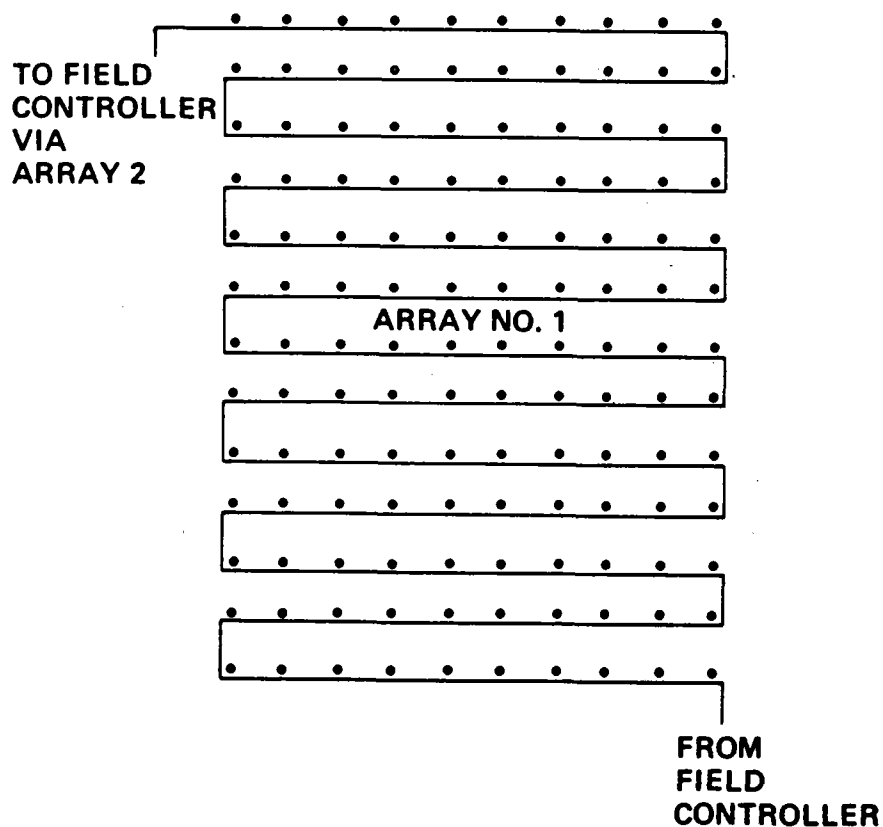


Figure 3.3.6.2-1. Array Signal Circuitry

As discussed in Section 3.3.7, number 6 copper grid is installed throughout the 20 miles of trenching in the heliostat field and clamped to the mirror pedestal and "J" boxes of each heliostat. A lightning arrester is installed in each of the power and data bus "J" boxes to prevent lightning damage from propagating throughout the field. This ground wire will be "ploughed in" after backfilling of the trench. The backfill is then roller compacted.

Due to the pilot plant soil condition, it should not be necessary to use any special sand for backfill material.

3.3.7 Lightning Protection

The collector subsystem, because of its large physical area is subject to lightning strikes and therefore requires protection for personnel and equipment. Protection is provided in the Pilot Plant PD by the proper use of shielding, bonding, grounding and application of voltage-limiting devices. Providing proper bonding between all possible lightning attachment points and ground reduces hazardous induced voltages to acceptable levels. A compromise between lightning exposure and possible damage was traded off against the cost of installing and maintaining a full-protection lightning system. The lightning protection system selected for the PD prevents operational failures at a system level which could cause safety hazards or reduce collector subsystem availability. A strike on an individual heliostat will cause only localized damage. Evaluation of lightning exposure and stroke incidence of the heliostat facilities was obtained through the use of isokeraunic maps of "thunderstorm day" incidence and "stroke factors"(Reference 3.3.7-1). The expense of a protection system, including an electrical ground electrode system, was then weighted against the probability of lightning damage. This approach is outlined below.

The frequency of lightning strikes to a structure is a function of the frequency of thunderstorms in the surrounding locality and the effective area of influence of the structure due to its height and/or its physical extent. A third factor, called stroke factor, which relates the number of thunderstorm days to the number of strokes which strike the ground per given area, is required to analyze the probability of a lightning strike to a structure.

The effective strike area of low structures is essentially equal to the physical area of the structure. An array of heliostats placed on 12.2 m (40 ft) centers would have an effective area of 148.7 m^2 (1600 sq. ft) times the number of heliostats. The proposed system will contain 16 subgroups of up to 128 heliostats each for a total of 1650 units. The effective area is therefore approximately 0.26 sq Km.

The annual incidence of thunderstorm days for South Eastern California is 10 (Reference 1). The stroke factor is a function of latitude and is approximately

0.37 for areas within the United States where a relatively large number of frontal storms exist (Ref. 3.3.7-2).

The probable number of strokes per year to an antenna structure is equal to the effective area, times the thunderstorm days, times the stroke factor. For the proposed array of heliostats this becomes:

$$\begin{aligned} N &= (0.1 \text{ square miles}) (10 \text{ thunderstorm days per year}) \\ &\quad (0.37 \text{ square miles/thunderstorm day}) \\ &= .37 \text{ strokes per year or one hit every 2.7 years.} \end{aligned}$$

This exposure relates to a lightning stroke with a typical current level of 20 kiloamperes. Distribution plots of peak currents for the first return stroke (major damaging part of a lightning strike) show this value is 50% probable (Reference 3.3.7-3). If protection is provided to 200 kiloamperes peak current (considered 0.5% probable), the probable number of strokes per year that would exceed this value would be 0.0037 per year, or one hit greater than 200 kiloamperes every 270 years. For design purposes, 200,000 ampere is generally considered a worst case lightning strike.

Grounding of the PD heliostat equipment and structures is accomplished with a network of buried copper wires. Since the power and control wiring between heliostats is buried, a good ground for the lightning protection system is obtained by burying a No. 6 bare copper ground wire 0.3 to 0.6 m (1-2 ft) above the power and control wiring. Assuming a minimum of 6.1 m (20 ft) of buried ground wire per heliostat, the total length, L, of buried wire would be 14,048m (46,080 ft) over an area of 0.26 sq Km (0.1 sq mi). Assuming a ground resistivity, ρ , of 1000 ohm-meter the resistance, R, of such a buried grid to true earth can be determined using the following equation from Reference 1:

$$R = \frac{\rho}{L} \left[\log_e 6L - 5.6 + 1.4 \sqrt{\frac{L}{A}} \right]$$

$$R = \frac{1000}{46080} \left[\log_e (6 \times 46080) - 5.6 + 1.4 \sqrt{\frac{46080}{(5280)^2 \times 0.1}} \right]$$

$$R = 0.99 \text{ ohms}$$

For adequate protection, lightning currents require a low resistance path to the buried grid system. This will be provided using ground straps and good conductive paths between the lightning-arc attachment point (for example, the top of the reflector) and the grid system. Protection of the power and control system has been provided by incorporating arrestors at various points in the wiring system as discussed in Section 3.3.4.

3.3.8 Heliostat Thermal Design

A comprehensive heat balance and thermal design verification is presented for the PD heliostat. Design requirements are established based on the Barstow thermal environment. The heliostat system is required to operate with ambient air temperatures which range from -20 to 50°C, and to survive nonoperating with ambient temperatures of -30 to 50°C while being exposed to wind, sunlight, and other environmental conditions typical of the Southwest United States. Individual components such as reflector, enclosure, gimbal drive systems, and electronics each have their own operating temperature requirements which are established based on the commonly accepted limits for candidate PD Heliostat materials and components.

PD Heliostat temperatures are described for a variety of environmental and operational conditions. These predictions show that the PD Heliostat design is thermally acceptable for the pilot plant environment.

This discussion covers four major topics. Heliostat thermal design requirements are described in 3.3.8.1. The Analysis Model developed for these studies is described in 3.3.8.2. Results and conclusions of the heliostat thermal analysis are described in 3.3.8.3. Section 3.3.8.4 describes the thermal and environmental operating experience gained during conduct of research experiments.

3.3.8.1 Thermal Design Requirements

Four design days are utilized to define the range of environmental conditions which are expected for the PD heliostat. They characterize the Barstow site, or others having similar climatic conditions and latitude. Normal winter and summer days characterize the design environment range which includes most of the heliostat operational lifetime. Worst summer hot and winter cold days define the additional range of conditions for which only occasional events can be expected but satisfactory short term performance is required. Table 3.3.8-1 describes the environmental conditions assumed for these days. This is supplemented by Figures 3.3.8-1 and 3.3.8-2.

Table 3.3.8-1. Thermal Design Conditions Summary

Thermal environment		Design day			
		Extreme hottest	Nominal conditions		Extreme coldest
			Summer	Winter	
Daily temperature range °C(°F)	Max	50 (122)	37 (98)	15 (58)	-15 (05)
	Min	34 (93)	21 (69)	0 (32)	-30 (-23)
Sky temperature °C		Ambient minus 6		Ambient minus 20	
Average wind m/sec (mi/hr)		0.5 (1.1)	1.0 (2.2)	2.0 (4.5)	4.0 (9)
Direct total insolation at noon W/m ²		1,135	1,005	1,040	930

Note: Reflector orientation

- Stowed (Near vertical reflector facing south)
- Solar tracking (Reflected beams on receiver)

Figure 3.3.8-1 describes ambient air temperatures assumed for the four design days. Nominal ambient temperature data are 30 day averages of hourly temperatures taken from the "Aerospace Data Tapes" for Inyokern, California, 1962 and 1963. The summer data is collected for 15 days, each side of August 7, and winter for 15 days each side of December 21. The hot summer day temperature profile results by equally increasing the nominal summer day profile so that it reaches a daily maximum of 50°C (122°F). The cold winter day, generated similarly from nominal winter data, reaches a daily minimum of -30° (-22°F).

Figure 3.3.8-2 describes "Direct Total Insolation" as affected by solar elevation angle and time of year. Here, rather than utilizing only direct insolation, total solar flux is used. The "Direct Total Insolation" includes all solar radiation which reaches the ground and assumes it to be direct and circumsolar flux. The data are best suited for thermal analysis on clear days, a typical condition for both the hottest summer and coldest winter days.

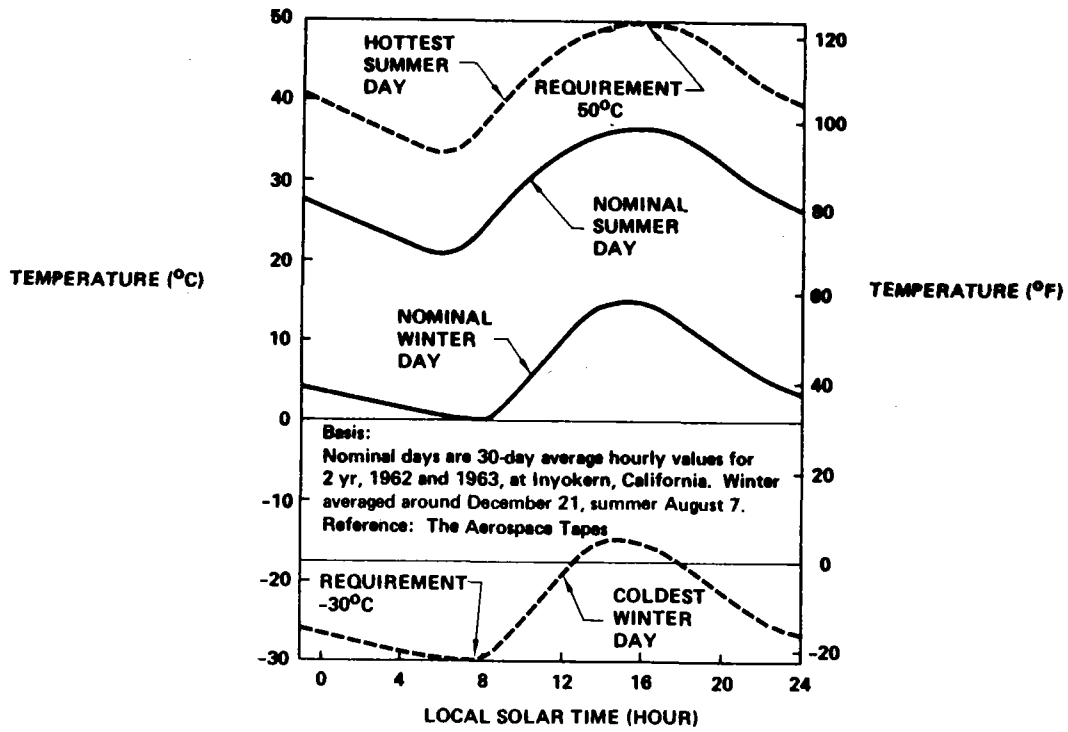


Figure 3.3.8-1. Ambient Temperatures for Design of PD Heliostat

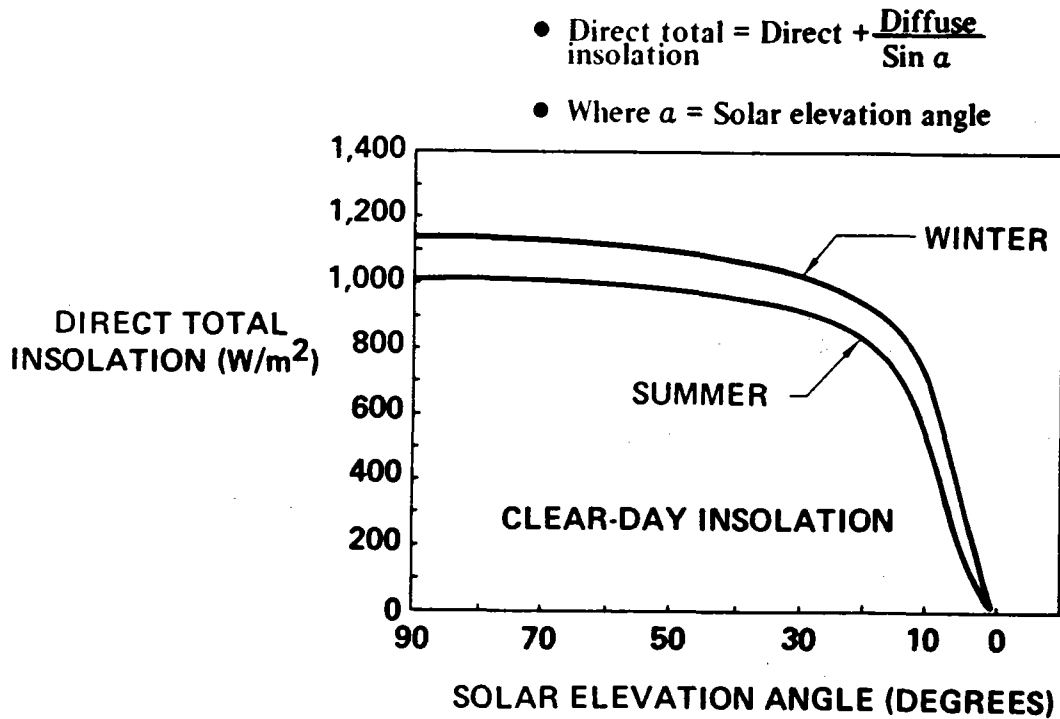


Figure 3.3.8-2. Design Insolation Values Barstow, California

The design wind velocities used here are assumed after collecting and reviewing the wind data for Inyokern which is provided on the Aerospace Data tapes. Nominal winter and summer velocities are 1 and 2 meters per second, respectively. These are halved for the hot summer day and doubled for the cold winter day.

Temperature critical components of the PD heliostat are listed on Table 3.3.8-2, along with their operating and non-operating temperature limits. These temperatures are obtained from a variety of sources. Consultation with vendors and cognizant subsystem engineers provides initial operating temperature goals. These are the limits which result in negligible impact of operating temperatures on cost, performance, and reliability. The design is initially evaluated with respect to accomplishment of these temperature goals. The enclosure, reflector, gimbal drive motors, encoders and gear drive units did not require temperature range increases over their initial goals. The heliostat electronics temperature limits had to be increased from initial values to those shown in Table 3.3.8-2 by utilizing some mil-spec type components. Also the power supplies contained within this unit are designed with high conversion efficiency. Even so, the power supplies dissipate half of the approximately 50 watt electrical input to the operating heliostat.

Table 3.3.8-2. Temperature Limits

- **System environment and temperatures:**
 - -30° to +50°C nonoperating
 - -20° to +50°C operating
 - Humidity and insolation in southwest U.S.

Components	Temperatures (°C)	
	Nonoperating	Operating
Enclosure	-35 to 55	
Reflector	-35 to 65	
Gimbal drive motor	-30 to 125	-20 to 100
Gear drive	-30 to 93	-20 to 93
Encoder	-65 to 95	-20 to 75
Heliostat electronics	-60 to 125	-60 to 100

The thermal design goals are to: provide temperature data for selection of components and design analyses; and to specify surface coatings and finishes in the heliostat which result in acceptable equipment temperatures without requiring supplemental heating or cooling. This has been accomplished in the PD heliostat.

3.3.8.2 Analysis Model

The Boeing Thermal Analyzer Computer Code has been utilized for these studies. It is a lumped parameter forward difference analyzer capable of steady state and transient simulations. The problem has been formulated by defining collector thermal interfaces throughout a 24-day of interest. Initial temperatures are assumed and temperatures determined as functions of time for several consecutive identical days. When temperatures begin to repeat on a 24-hour cycle, the process is complete and final day temperatures are reported.

The thermal analysis model includes a single heliostat with thermal boundary conditions which include; air, sky and surrounding ground level temperatures, thermal capacity of soil beneath the heliostat base, and solar heating of components. A comprehensive listing of heliostat heat transfer mechanisms and their independent variables is shown on Table 3.3.8-3. Those which are included in this analysis of the PD heliostat are noted.

Two models of reflector orientation have been used in this analysis. For normal daily operation, the reflector solar incidence angle is varied as a function of solar elevation angle. This is shown on Figure 3.3.8-3. The other case simulates reflector orientation in the stowed position. Here the reflector surface is vertical facing due south. This case has been evaluated for summer conditions which are most critical.

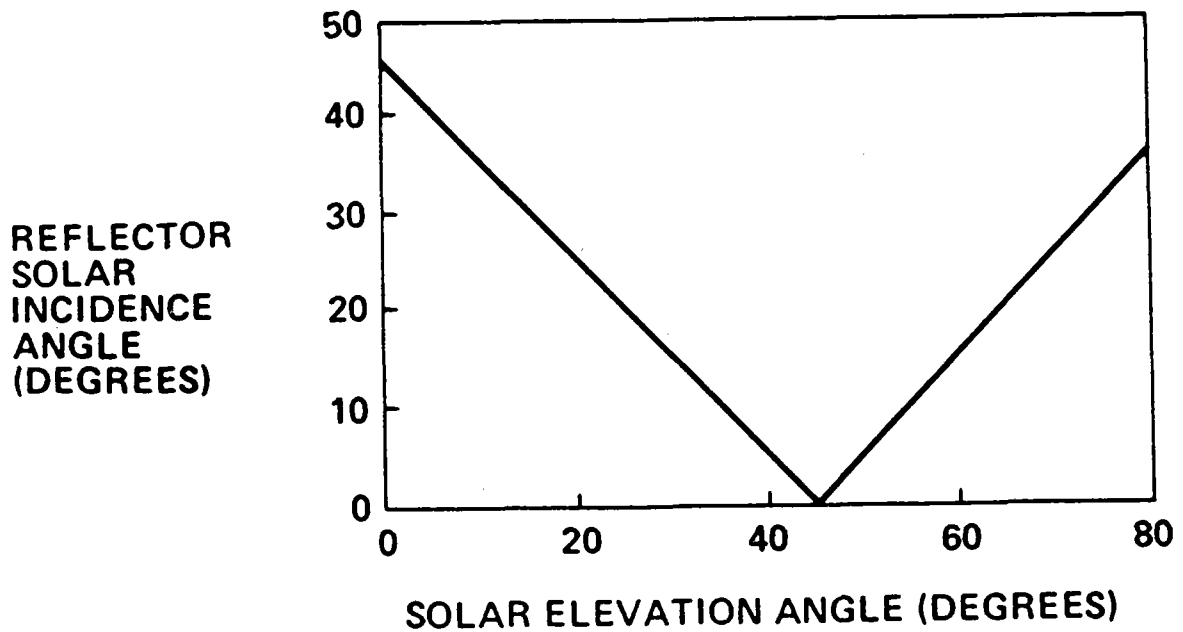
3.3.8.3 Heliostat Thermal Performance

The Heliostat Thermal Model has been exercised for a variety of operational conditions. Five cases are reported here. Operating temperatures are shown in

Table 3.3.8-3. Heat Transfer Mechanisms – PD Heliostats

External mechanisms	Independent variables
Direct solar heating Radiation to sky and surroundings Free convection Forced convection Solar heating via reflection from surroundings	Solar elevation, azimuth, intensity at ground Temperatures of sky and surroundings External geometry, air temperatures Air temperature, wind velocity, heliostat geometry Collector field layout, orientation of adjacent reflectors, solar elevation, azimuth, intensity solar reflectance of ground
<u>Internal mechanisms</u> Solar absorption reflection and shadowing Free convection Radiant exchange Electric heat dissipation Mass transport Thermal capacity	Heliostat thermal coatings, reflector orientation, solar azimuth and elevation Air and component temperatures, geometry Heliostat thermal coatings, reflector orientation Component heat loads, operational status Heliostat air supply rate, air temperatures Component mass and materials

Not included in PD heliostat thermal model



Note: Stowed reflector; surface vertical facing due south

Figure 3.3.8-3. Typical Solar Tracking Reflector

Figures 3.3.8-4 through 3.3.8-7 for each of the design day environments. These include the effect of the tracking solar reflector, per Figure 3.3.8-3. The stowed heliostat temperatures are shown for the hottest design day on Figure 3.3.8-8. Each of these cases actually represents a number of sequential identical days. In the thermal model the diurnal conditions are repeated until equal temperatures occur on successive days. This process generally requires 4 to 6 days.

The extreme temperatures of critical components have been extracted from this data and are shown on Figure 3.3.8-9. As shown, the encoder temperatures are most critical on hot days due to their 75°C limit, the lowest of all the electronic components. These temperatures need to be carefully evaluated during detail design. If encoder temperatures cannot be reduced by judicious design of the gimbal mechanism, then their temperature limit will have to be increased by using some mil-spec electronic parts. All of the gimbal components are lower than their -20°C operating limit on days with overnight temperatures which exceed -20°C. This results because all the heliostat temperatures are close together and very near the ambient temperature for a few hours before dawn. However, the temperature predictions also show that gimbal component temperatures rise rapidly after being turned on. Therefore, it is proposed to turn on gimbal drive motors and encoders a few minutes before dawn on days with these very low overnight temperatures. They will be turned on but not operated until well above their -20°C lower operating limit. This has been simulated in laboratory tests of research experiment heliostats.

3.3.8.4 Results of Research Experiments

The research experiment heliostats have been installed and operated at the Boardman Oregon test site during both summer and winter conditions. Temperatures of most components have been recorded. Figure 3.3.8-10 shows temperatures recorded during typical cold and hot days.

None of the research experiment test conditions are close enough to PD heliostat conditions to allow a direct data comparison. However, the temperature differences between heliostat components and the ambient air temperature during tests are similar in many cases to the differences predicted for the PD heliostat

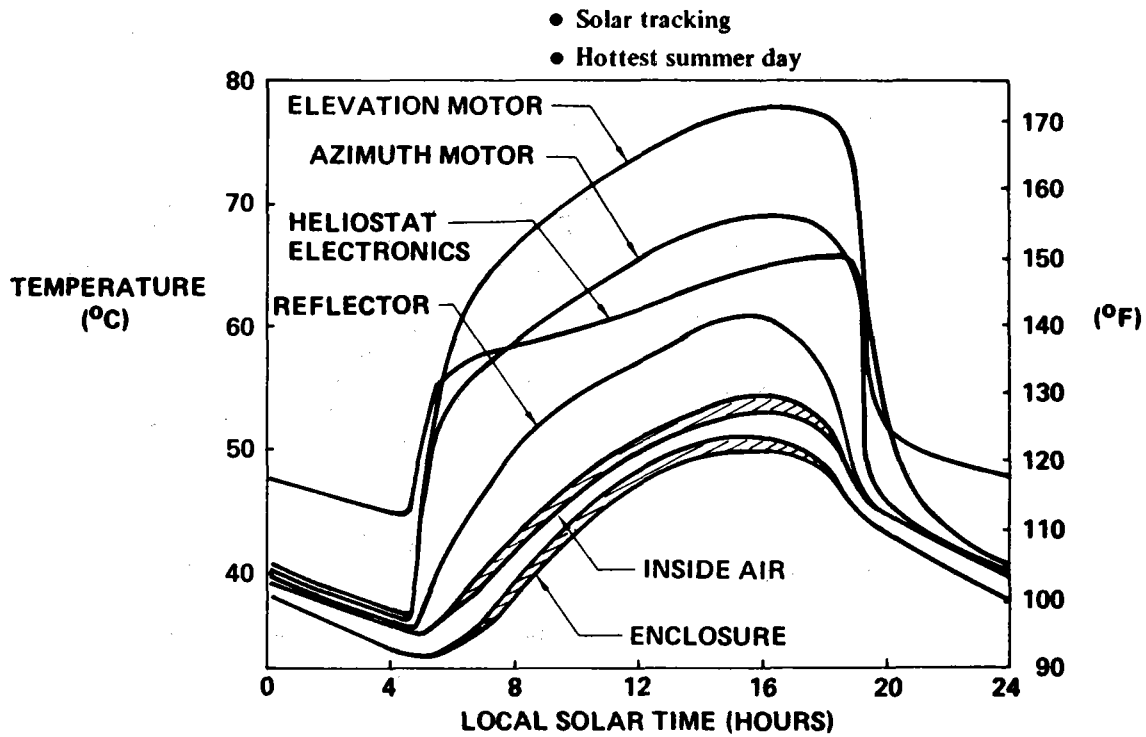


Figure 3.3.8-4. PD Heliostat Thermal Analysis

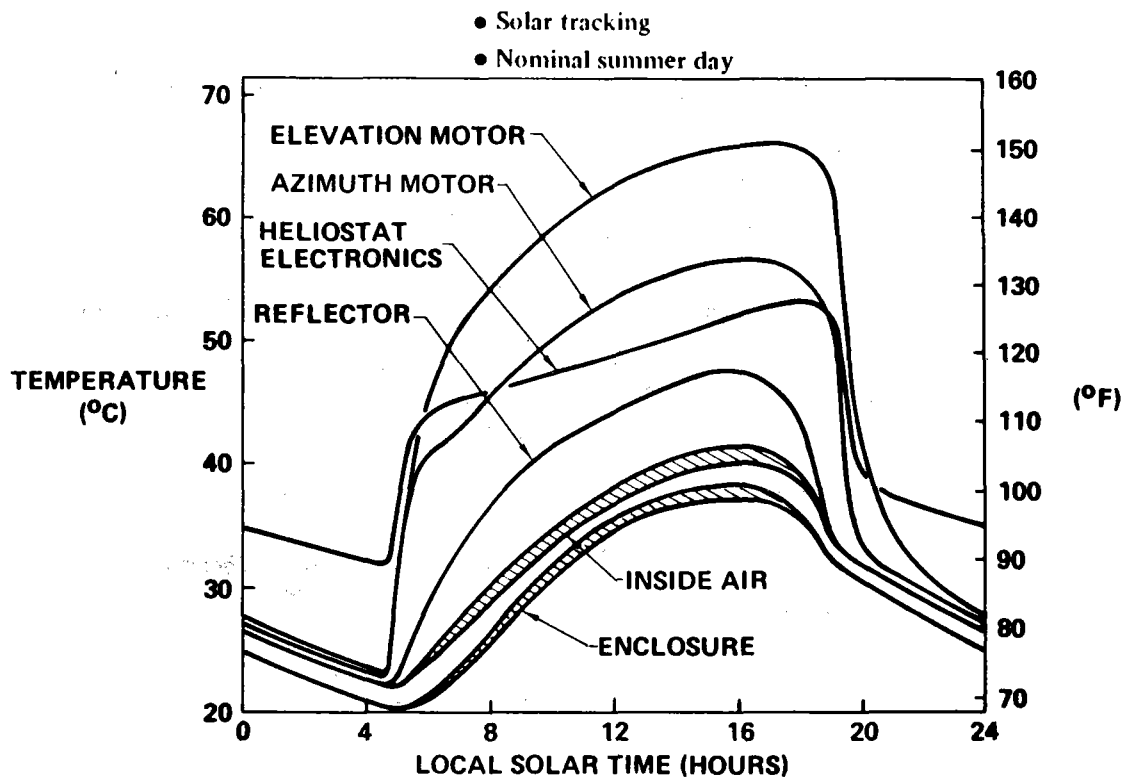


Figure 3.3.8-5. PD Heliostat Thermal Analysis

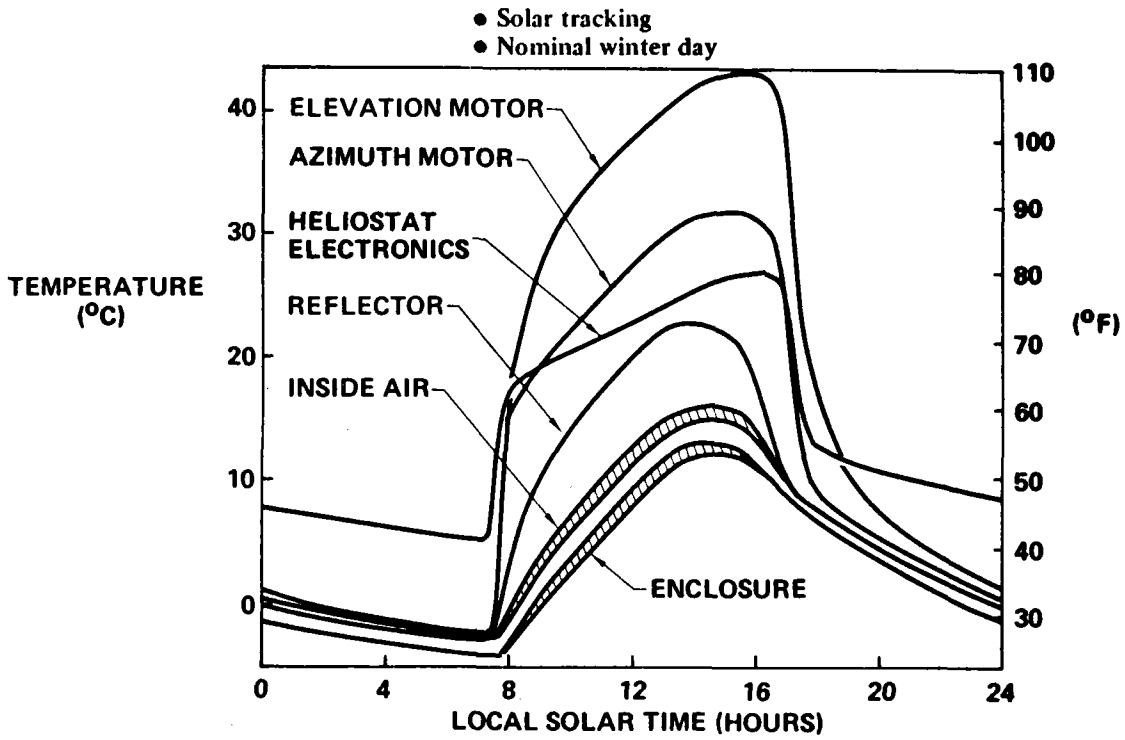


Figure 3.3.8-6. PD Heliostat Thermal Analysis

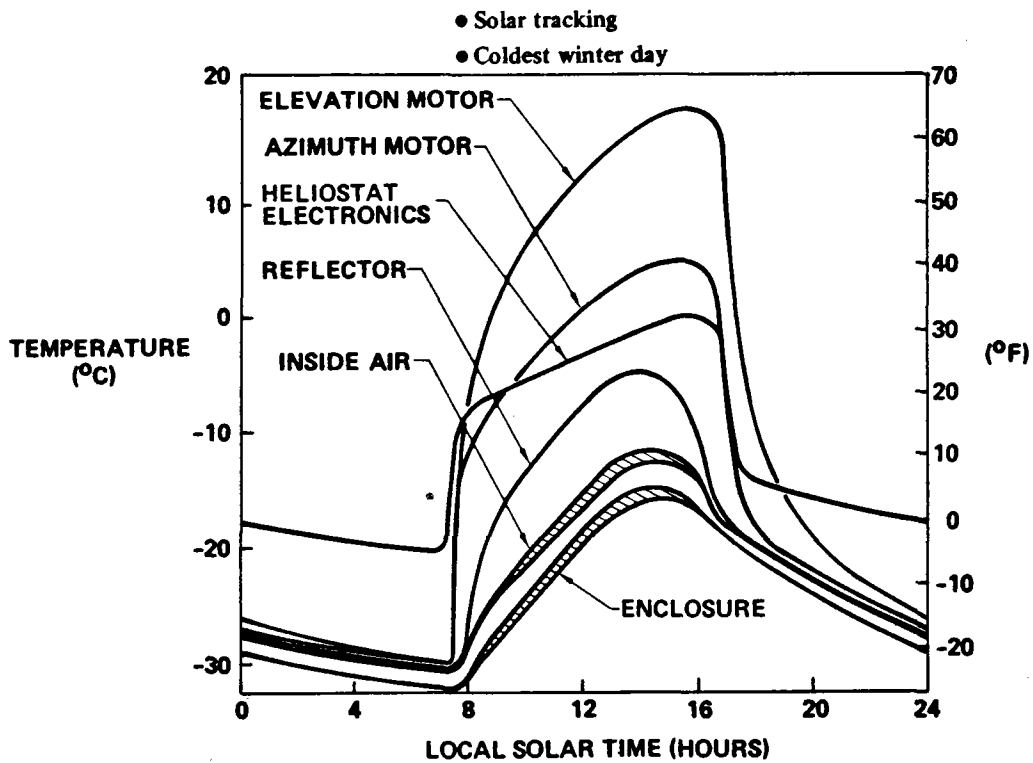


Figure 3.3.8-7. PD Heliostat Thermal Analysis

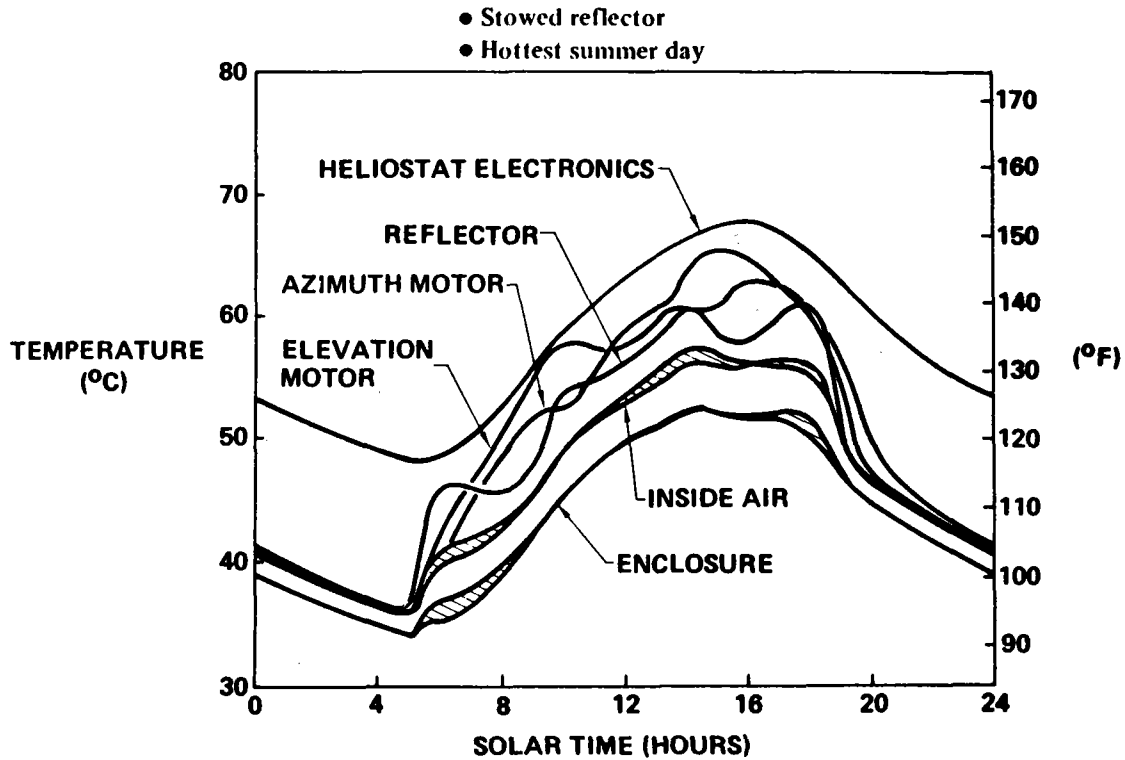


Figure 3.3.8-8. PD Heliostat Thermal Analysis

Temperatures (°C)

	Temperature limits 1		Normal operation								Stowed	
			Hottest summer day		Nominal summer day		Nominal winter day		Coldest winter day 2		Hottest summer day	
Enclosure	55	-35	51	35	38	20	3	-4	-15	-32	53	34
Reflector	65	-35	61	36	47	22	23	-2	-5	-30	61	36
Elevation drive motor	100	-20	78	36	66	23	43	-2	18	(30)	63	36
Elevation gear drive	93	-20	74	36	61	23	39	-2	14	(30)	63	36
Elevation encoder	75	-20	(78)	36	66	23	43	-2	18	(30)	63	36
Azimuth drive motor	100	-20	69	36	57	23	32	-2	5	(30)	65	36
Azimuth gear drive	93	-20	66	36	53	23	28	-2	1	(30)	65	36
Azimuth encoder	75	-20	69	36	57	23	32	-2	5	(30)	65	36
Heliostat electronics	100	-60	66	45	53	32	27	5	0	-20	68	48

- 1 Temperature limits Maximum/Minimum operating
- 2 System must be turned on early on days with temperature below -20°C
- (xx) Denotes temperature outside the desired limits

Figure 3.3.8-9. PD Heliostat Service Temperatures

	Typical cold day ¹		Typical hot day ²	
	(°C)	(°F)	(°C)	(°F)
Outside air	-2	28	25	77
Inside air	-1	30	35	95
Reflector	0	32	38	101
Enclosure	-2	28	33	91
Skirt	-2	28	32	90
Foundation	2	36	27	80
ETU power supply	—	—	60	140
ETU card rack	—	—	40	104
Drive motor	—	—	42	107
Drive motor	—	—	38	101

¹ 0805, December 16, 1976
² 1400, April 4, 1977

Figure 3.3.8-10. Typical Operating Temperatures SRE Heliostat

(between its component and ambient air temperatures). Reflector, enclosure, and internal air temperatures are about equal in proportion to the ambient air temperature for the two configurations. Electronic components in the research experiment heliostat are different from the PD heliostat. The research experiment power supplies are less efficient, resulting in relatively higher heliostat electronics temperatures. Gimbal drive motors dissipate less heat than the PD heliostat units and operate relatively cooler. Also, the research experiment electronics and gimbal drive units are left on 24 hours per day rather than reduced to standby power levels at night.

There were no occurrences of high temperature operational problems with the research experiment heliostats. Condensate, dew and frost, formed on enclosures during cold winter nights when humidity was high (50-90%) and did not interfere with testing. The humid conditions at Boardman during December provided an opportunity to observe the interior of the enclosure under conditions of 100 percent relative humidity. Even under these adverse conditions, condensation did not occur on the reflector or other internal components.

The relative humidity of the Barstow, California site has been compared with conditions experienced at Boardman, Oregon. This shows that condensation on the heliostat enclosure will not be significant at the much drier pilot plant site.

Figure 3.3.8.11 compares maximum daily humidity conditions for Boardman and Inyokern California in the month of December. The ambient temperature at Boardman approached within 1°C of the dew point (relative humidity over 90 percent) on about 1/3 of the days in December 1976. It came close enough, about 2°C, to result in condensation on the enclosure on almost every morning during December. This agrees with our observations. By comparison, the Aerospace Data Tapes for Inyokern in December of 1962 and 1963 show much drier conditions at that location. There are only three December days on the tapes during which condensation would occur on the heliostat enclosure. The relative humidity

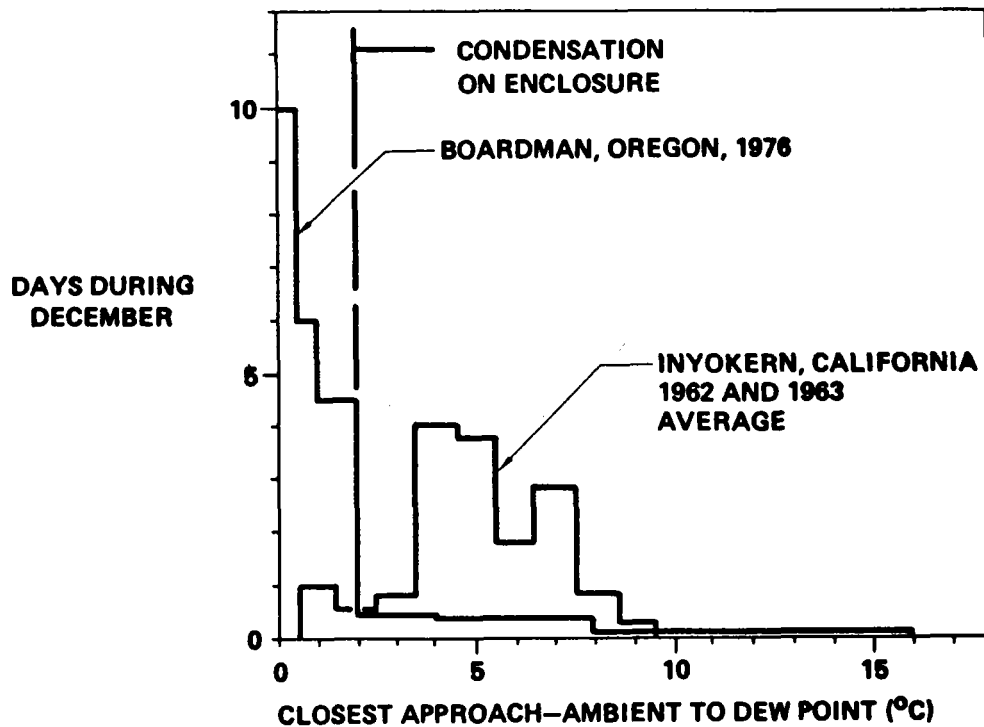


Figure 3.3.8-11. Condensate Deposition on Enclosure

does not exceed about 90 percent during the 62 days examined. A source of relative humidity data has been provided which describes the Barstow California environment. This data, taken during daylight hours, indicates that humidity conditions at Barstow are similar to the conditions at Inyokern.

The PD heliostat will experience some condensation on its enclosure during the most humid winter nights. The SRE experience at Boardman Oregon shows that no condensation occurs on the internal heliostat components and that the enclosure recovers from this exposure without measurable effect on its performance.

4.0 MANUFACTURING

Manufacturing processes and tool design have been selected based on the experience obtained in fabricating the research experiment hardware and subsequent investigations aimed at reducing the cost of fabrication. The increased size of the heliostat has caused some complication in the tooling and handling concepts, but has not required any change in the basic processing. All of these processes have been proven during the fabrication of the research experiment heliostats and subsequent tests of any design variations. A list of the fabrication processes that were used for the research experiment is given in Figure 4.0-1.

Operation	Research experiment process	Difference for pilot plant
Enclosure		
Tedlar seams	"Heat sealing Tedlar film with impulse heating"	Thicker material and longer seams
Reflector		
Aluminum structure	Formed and welded per BAC 5975, class C	Larger sections
Mylar joints	"Bonding Mylar to Mylar with polyester adhesive"	None
Inplane surface	"Restrained molding of rigid self-skinning plastic foams"	None
Tensioning and bonding reflective film	"Bonding Mylar to urethane foam with a polyurethane adhesive"	None

Figure 4.0-1. Fabrication Processes

4.1 MANUFACTURING PROCESS DESCRIPTION

The protective enclosure will be fabricated from polished Tedlar film using a 4 piece polar cap, an upper row of 11 gore sections and a main row of 22 gore sections. These will be joined by heat seals to form a spherically shaped enclosure. The fabrication procedure is shown in Figure 4.1-1. The main gores are first trimmed and the base seams made while the gore is still on the trim table. Two of these are joined by heat sealing and then a trimmed upper gore is added to form a large 3 piece gore subassembly. These are then joined to form the spherical shape. The polar cap is made by joining 4-90° circular sections. It is then heat sealed to the gore sections to complete the enclosure.

The use of 2 rows of gores and a 4 piece polar cap results in less cutting waste of the Tedlar film. The shape of the enclosure will have less out of roundness than the research experiment enclosures. Around the circumference at the maximum width of the gores the out of roundness will be 1.02%. Yielding of the material during pressurization will improve this.

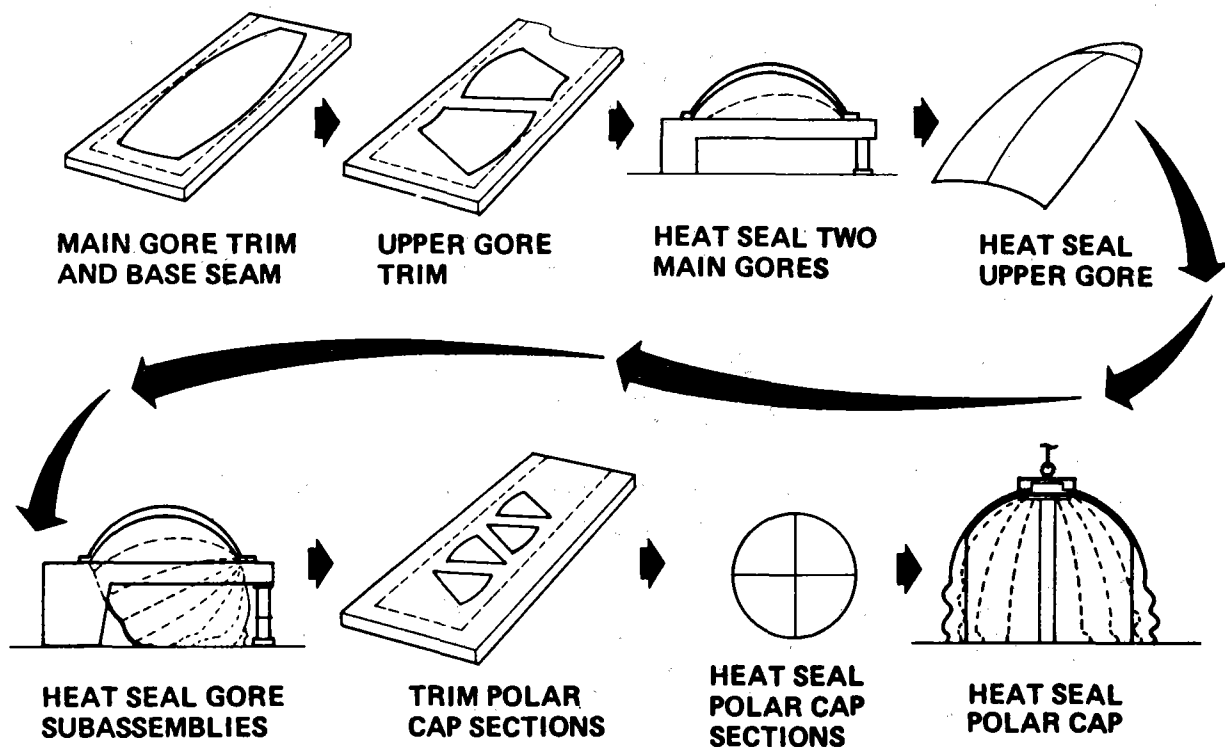


Figure 4.1-1. Protective Enclosure Fabrication Steps

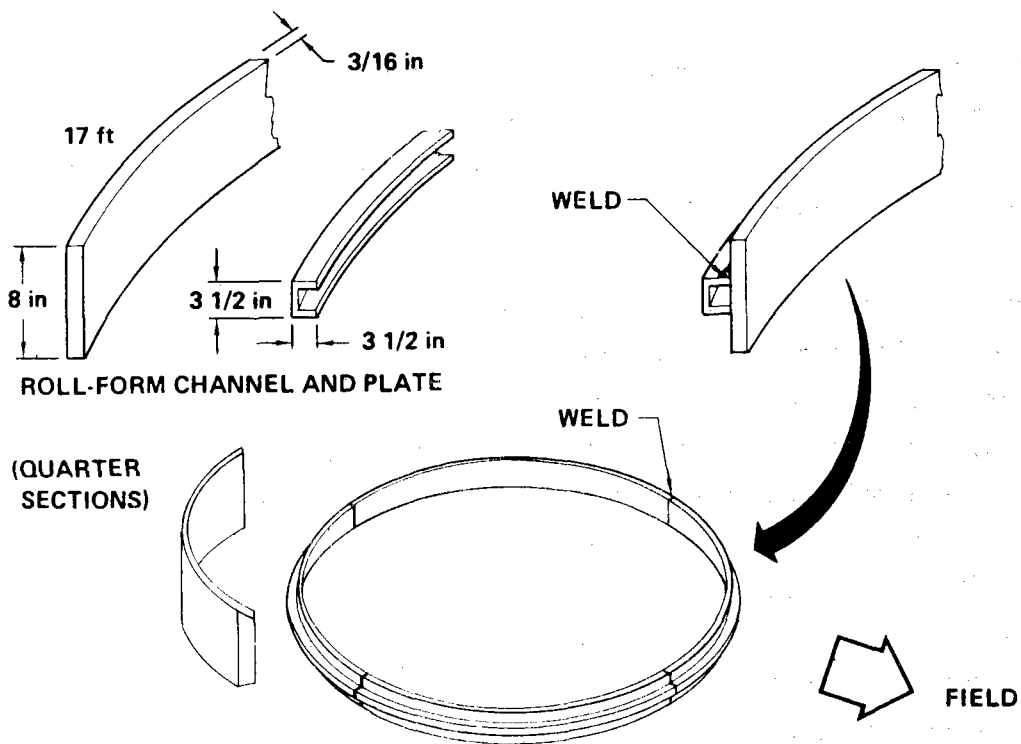


Figure 4.1-2. Fabrication Sequence for Upper Portion of Base Ring

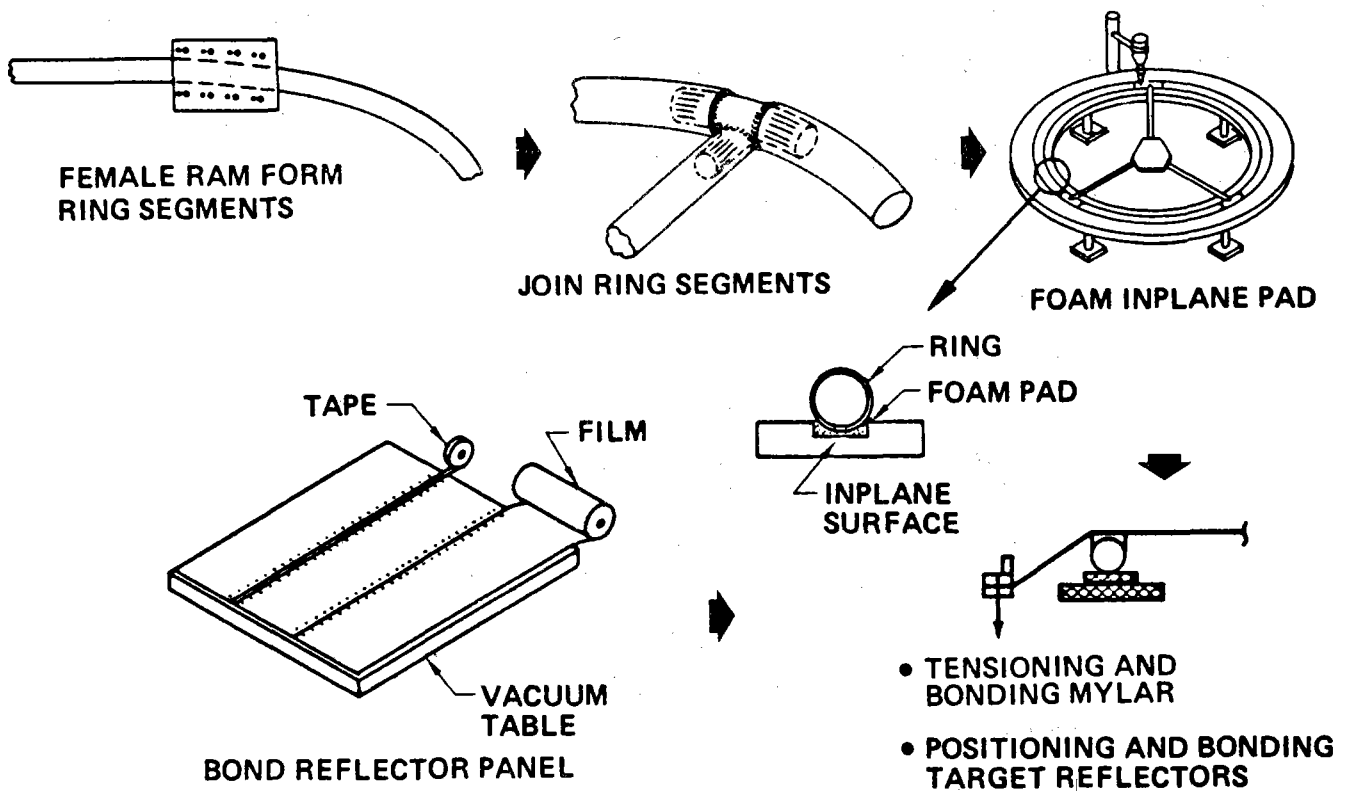


Figure 4.1-3. Reflective Assembly Fabrication Steps

The enclosure base will be made of a steel sidewall attached to a concrete base. The steel sections will be formed and rolled to contour prior to assembly on the site. The fabrication sequence for the upper portion of the base ring is shown in Figure 4.1-2.

The reflective assembly will be fabricated by tensioning an aluminized Mylar film over a flat tubular structure. The sequence of fabrication is shown in Figure 4.1-3. The entire structure will be fabricated at the remote site fabrication area in a hangar at Daggett Airport adjacent to the pilot plant field. The aluminized Mylar film will be joined by bonding with a polyester adhesive. The tubular ring segments will be formed, trimmed, joined, and a flat surface foamed in place. The aluminized film will then be placed over the foamed surface to which an adhesive has been applied. The film will then be tensioned and bonded to the foam. After trimming the excess Mylar, the reflector will be boxed and transported to the assembly site.

The fabrication area at the Daggett Airport will contain equipment and tooling to form and trim the tubing, weld the reflector, foam the flat surface, and tension and bond the film. An overall layout is shown in Figure 4.1-4. Also shown is an area for partially assembling the enclosure base ring and painting, before transfer to the installation site. The hangar will be modified as necessary to obtain adequate conditions.

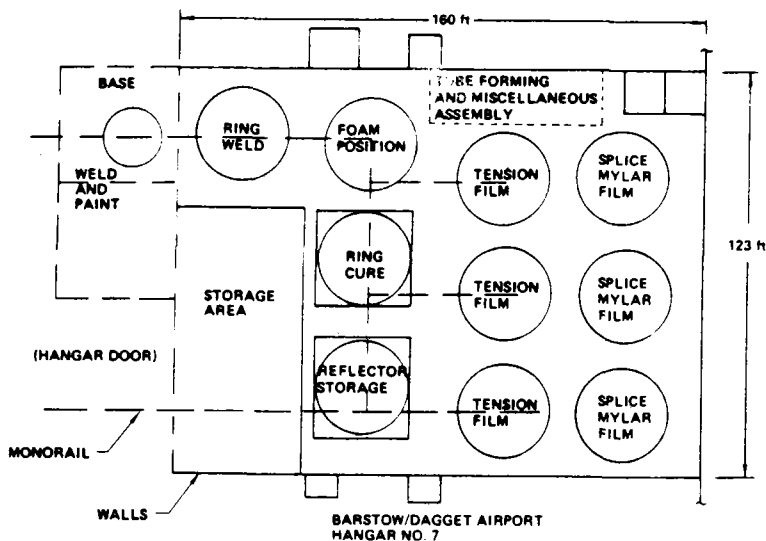


Figure 4.1-4. Remote Site Fabrication

4.2 QUALITY ASSURANCE

Quality Assurance will be provided through surveillance of the manufacturing operations. Hardware and tooling drawings and specifications will be reviewed to assure adequate quality requirements to clearly establish critical parameters such as reflector flatness, membrane tension, enclosure and base circumference and parallelism of the gimbal interface with the reflective surface. Planned inspection operations will be defined based on these requirements and will cover all fabrication, installation, check-out, and alignment. Critical dimensions of all tooling will be verified prior to first usage and first production items will be checked for conformance. Random selection of fabrication and installation operations will be made to verify compliance with drawings and specifications. Both visual inspection and material tests where required, will be made to verify purchased materials and parts conforming to requirements. All of the necessary measurement and test equipment will be calibrated and certified to the National Bureau of Standards, consistent with good industry practice.

All non-conformance will be documented on a job pickup form. Appropriate discrepancy disposition will be documented, approved by responsible supervision, and accepted by Quality Assurance.

4.3 TRANSPORTATION

Purchased items and in-house fabricated items will be shipped to the Daggett site fabrication area where they will be stored and sorted prior to delivery to the installation site. These shipments will be by commercial carrier and will be packaged only where necessary. The Tedlar enclosures will be packaged in multiple quantities in wood containers such that they receive no stacking loads. From the remote site location oversize loads will transport daily items required to support the work crews at the installation sites.

4.4 Materials

In accordance with ERDA request, the following information is provided on materials and parts:

System	Non-Standard Part	Single-Source Part	Long-Lead Item
Tedlar	X	X	X
Mylar (XM648A)	X	X	X
Gimbal			X
Actuators			X
Microprocessors			X
Diesel Generator			X
*Laser/Geodolite	X	X	X
*Digital Position Sensor for Alignment/Scanner Module		X	X
Varian V77-210 Computer			X

* Only 1 + 1 spare required for Pilot Plant

5.0 INSTALLATION, CHECKOUT AND MAINTENANCE

The installation, checkout and maintenance plans are based on procedures used to install and align the research experiment heliostats and on tests conducted with these heliostats. Maximum repetitive operations will be performed which will allow a systematic modular buildup of the collector array and associated subsystems. The installation schedule and rate is shown in Figure 5.0-1. Crew size has been held constant, and learning curve improvement allows for reduction in flow hours and increased installation rate.

5.1 INSTALLATION PLAN

Installation of the heliostats will be done by assigned work crews that will cycle from heliostat to heliostat on a pre-determined schedule as shown in Figure 5.1-1. They will consist of skilled field test engineers, technicians and support personnel. Mandatory sequences and functional flows will be used as a tool in establishing the prime flow of the installation task.

The transportation and handling functions between the Daggett fabrication facility and the installation site will be performed using general purpose vehicles, such as carry-alls, pickups, fork lifts, trucks, etc. Handling equipment will generally be leased. The Daggett fabrication facility will be utilized as a staging area to support the collector field installation. All incoming equipment, components, and materials will go through a formal receiving function at this facility. It will then be stored and when needed, assembled into work packages and delivered to the installation site in the field.

A special Mobile Erector-Cleaning Vehicle, as shown in Figure 5.1-2, will be used during installation of the reflector and enclosure. This vehicle will be designed to allow the erection of an enclosure in winds up to 10 m/sec (22 miles per hour). With it a maximum of 10% of the time will be lost

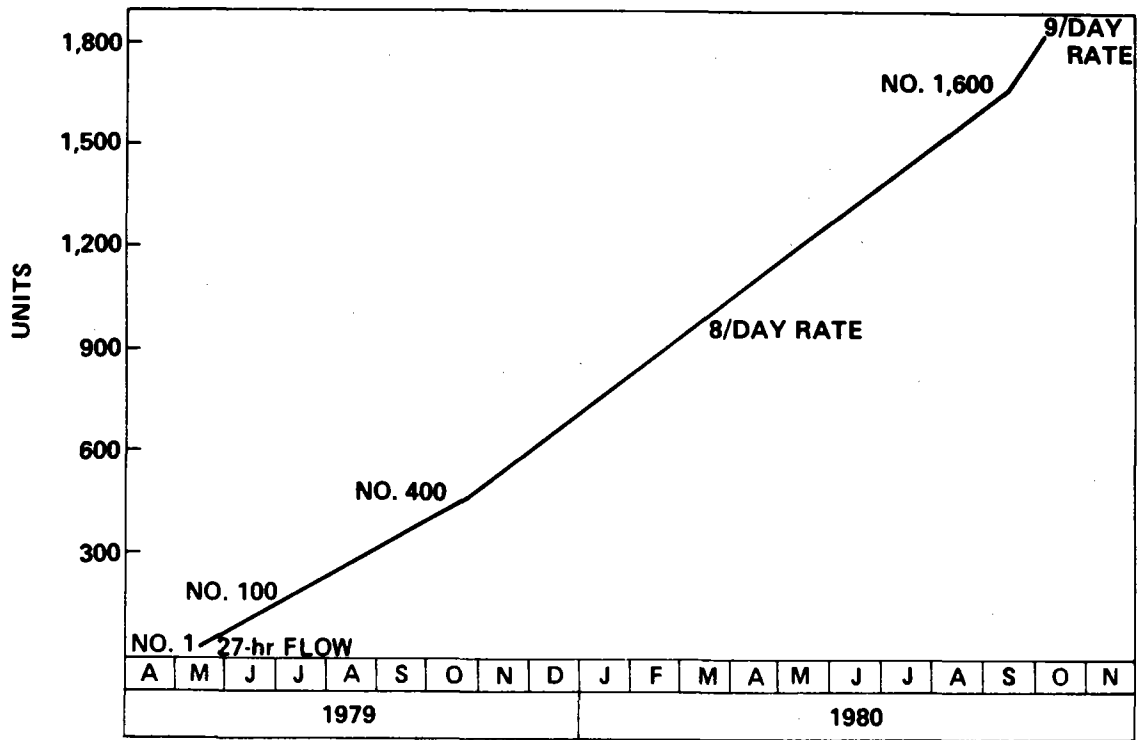


Figure 5.0-1. Heliostat Installation and Checkout and Build Rate

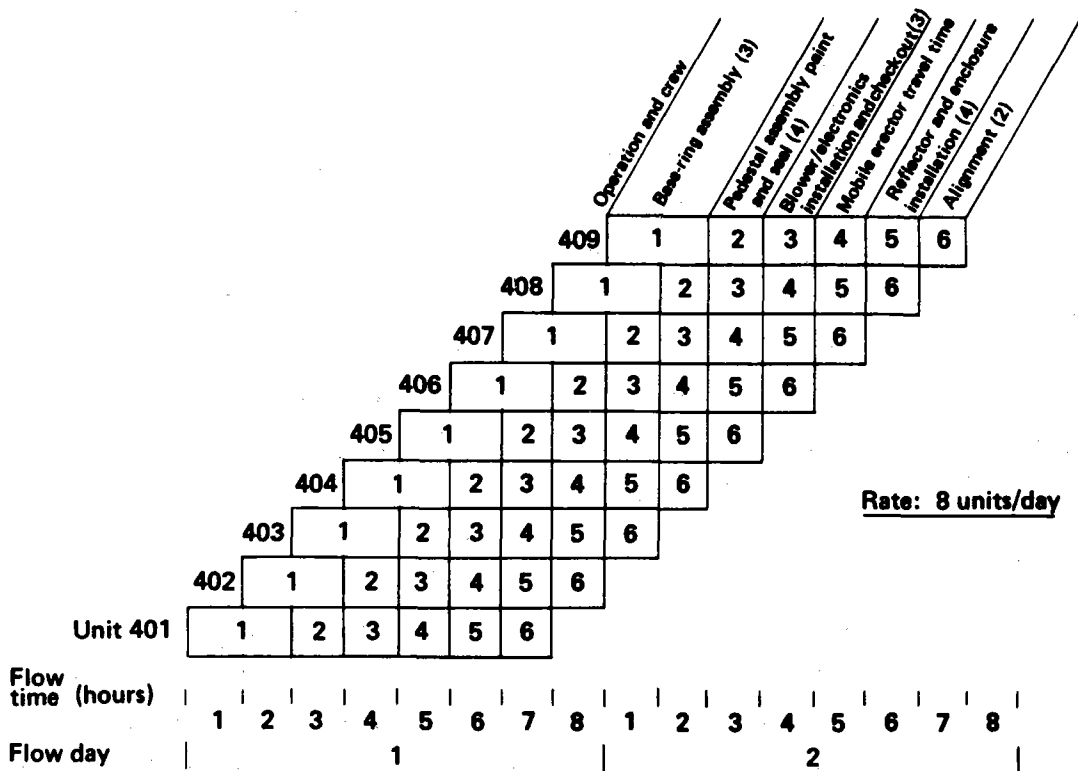


Figure 5.1-1. Crew Cycling—Installation and Checkout

due to high winds. This loss is accounted for in the basic schedule but is expected to be less by scheduling working time during preferred hours of the day.

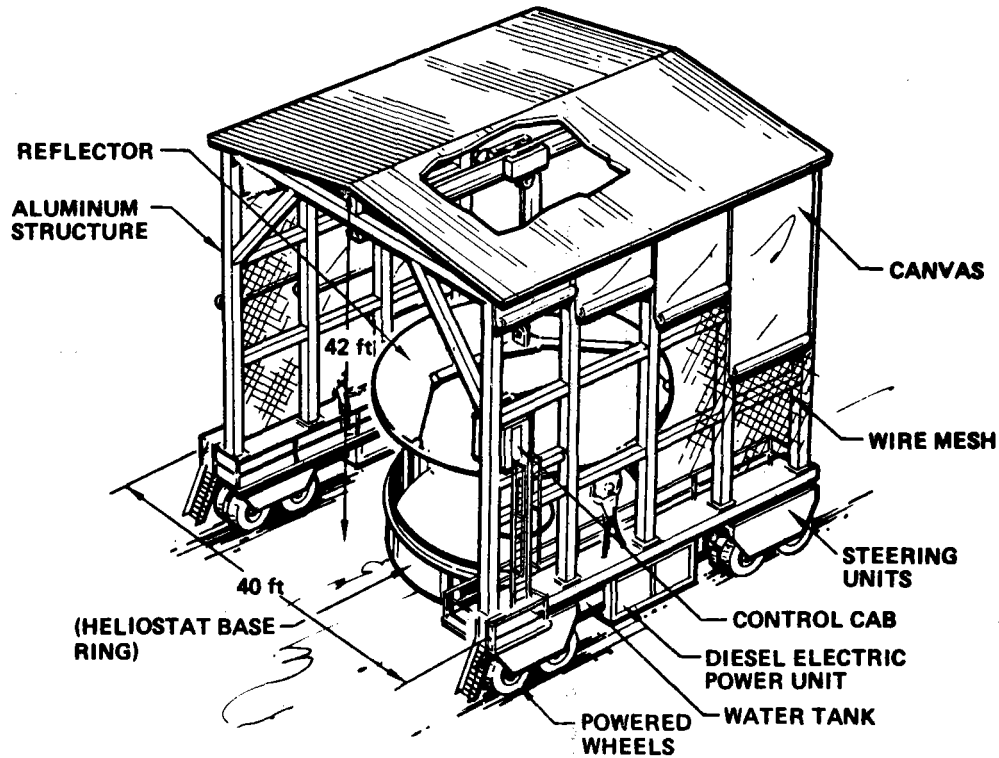


Figure 5.1-2. Mobile Erector Cleaning Facility

5.1.1 Foundation

The initial steps in installation of the collector field will be to prepare the site and layout the heliostat locations. The underground power and control wiring will be installed, the site will be gravelled, and then the concrete foundations will be poured. This work will be carried out by subcontractors equipped for this type of construction.

The steel section of the base will be assembled at the site utilizing a pre-fabricated steel ring, a pre-fabricated door and steel slabs. The sections will be welded together and bolted to the concrete foundation. All of the steel will be pre-painted. This installation and installation of the pedestal is shown in Figure 5.1.1-3.

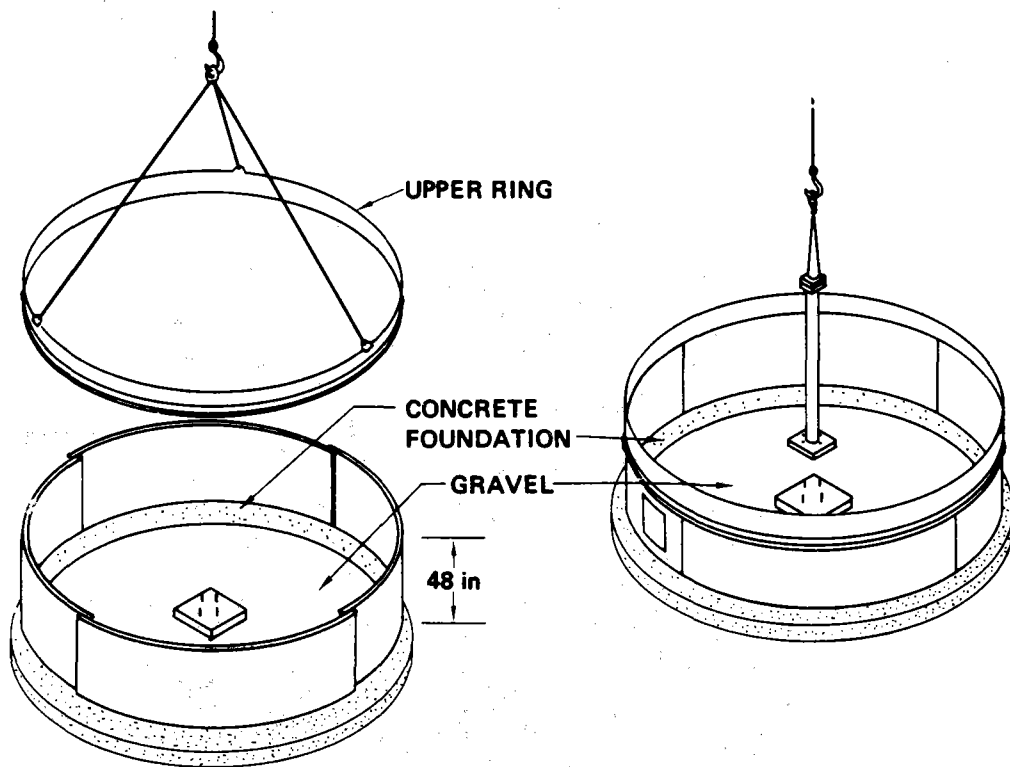


Figure 5.1.1-3. Installation of the Steel Base and Pedestal

5.1.2 Protective Enclosure/Reflective Assemblies

After the steel base and pedestal have been installed, a different crew will install the pressurization system, and the drive and control assembly. Prior to any installation effort a verification of critical interfaces (power phasing and sensing lines and pedestal mounts) will be made. Power lines to the blowers and drive motors will be tested for proper identification, connectors, and voltages. Control lines will be checked for identification, connectors, and continuity. Operation of the gimbal drive motors will be verified by exercising the manual control system and a checkout of the pressurization will be conducted. The gimbal plate will be moved to the horizontal position and a temporary protective covering will be placed over the drive and control assembly and all exposed wiring.

The sequence of events to install the reflector and enclosure is given in Figure 5.1.2-1. The reflector will be positioned horizontal and parallel to the gimbal plate by using reference marks placed on the reflector ring directly

after foaming the flat surface of the reflector. The initial inflation of the enclosure will be made by an auxiliary blower in the mobile erector. This will enable rapid inflation of the dome and eliminate the need for an air lock during the installation procedure.

- **Truck loaded with multiple site of reflectors/enclosures on site; unload reflector hardware truck to next site**
- **Move mobile erector in position; pick up reflector in horizontal position, locate to pedestal**
- **With hoist, lower reflector to pedestal interface; hook up reflector/pedestal**
- **Position reflector horizontal**
- **Uncrate, attach enclosure to hoist adapter**
- **Elongate at bottom and pass enclosure over reflector**
- **Attach enclosure to foundation curb**
- **Turn on blower, remove hoist attachments, and move shelter to next site**

Figure 5.1.2-1. Reflector/Enclosure Sequence Concept

5.1.3 Drive and Control Assembly

The drive and control assembly will have the gimbal interface plates leveled and the elevation encoder set as the final part of its fabrication. The pedestal interface will be leveled using the adjustable fasteners attaching the assembly to the pedestal. Adjustable fasteners will also be used to attach the reflector to the top plate of the gimbal. This will allow the reflective surface to be adjusted parallel to the gimbal plate and eliminate the wobble that occurred during the research experiments. The underground cabling will be installed before the concrete foundations are in place. Individual hook-ups of the wiring will occur during installation of the drive

and control assembly.

5.1.4 Alignment/Calibration Assembly

Equipment that will be installed for aligning the reflectors consists of a geodolite/scanner system mounted on the receiver tower and directional monuments in the field that will establish true south. The geodolite/scanner will be assembled on the site and installed on tracks on the receiver tower. The monuments position will be defined from star sightings or other suitable references. An alignment computer will be used as part of the geodolite/scanner system.

The initial alignment procedure will be as follows: (Reference Figure 5.1.4-1)

- . Identify operation - (Initial Alignment)
- . Identify and store heliostat identification number (central controller and alignment computer)
- . Point reflector toward tower
- . Measure rim target distances with geodolite
- . Adjust gimbal to equalize all distances
- . Store rim target coordinates in alignment computer
- . Measure and store center target coordinates in alignment computer
- . Calculate elevation transformation angle
- . Calculate reflector reference azimuth angle relative to true south
- . Transmit data from alignment computer to central controller

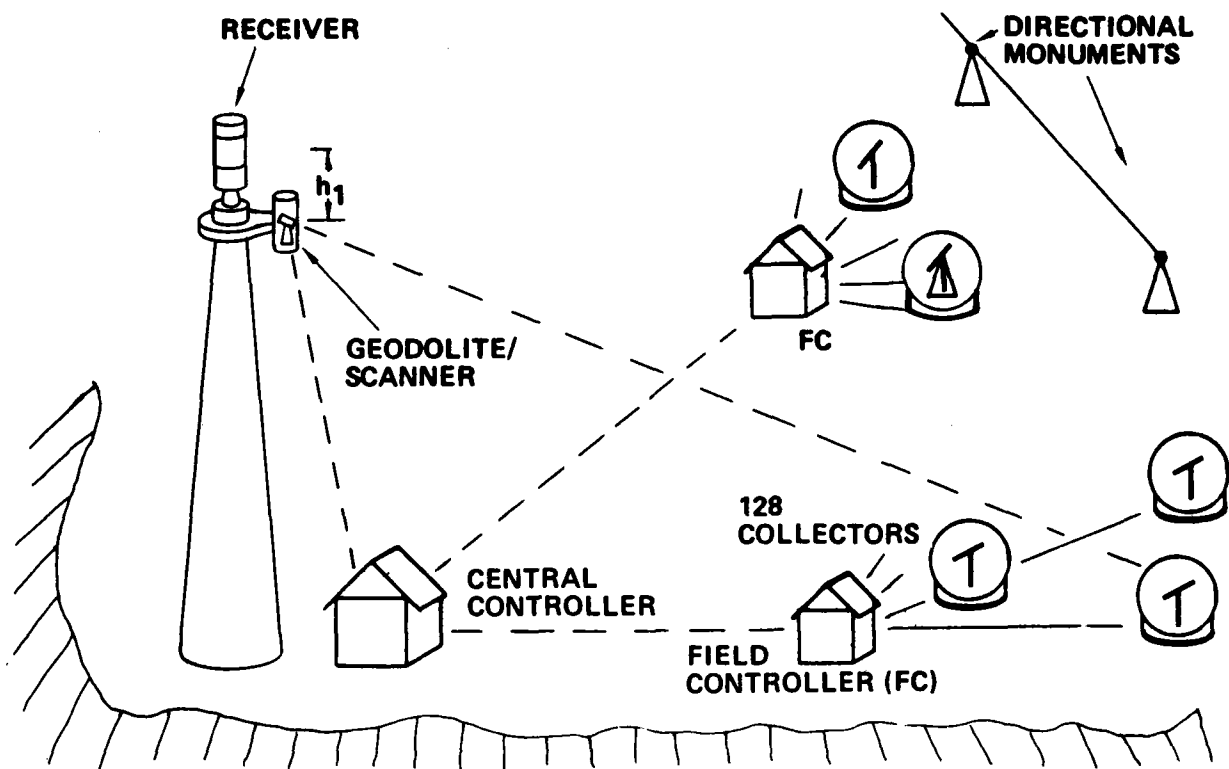


Figure 5.1.4-1. Initial Alignment

1. Alignment complete
2. Elevation transformation angle
3. Azimuth reference angle

The alignment will be verified by using the scanner to check the reflected solar image while tracking. The above steps will be repeated for each heliostat.

The procedure to be used for any subsequent alignment will be automatic and consist of the following steps.

- . Signal the alignment computer from the central controller the identification number of the heliostat to be aligned.

- . The geodolite/scanner system will move to the center target alignment position
- . The reflector will move to the alignment position
- . Check for auto-collimation by use of the geodolite

If the reflector is not aligned it will be realigned.

5.1.5 Cabling

Power and control cabling will be installed underground to all heliostats using direct buried cable. Power and control cabling to field controllers and the geodolite/scanner will be routed through plant utilities conduits. Both the power and control cables will be in the same trench along with a copper ground-grid wire used for lightning protection. The three will form a triangle with the copper wire on top. Hardware in each heliostat will be grounded to this grid.

During installation of various components, on-site preparation of the cable will consist of preparing ends for crimp lugs and then crimping lugs to the cable. Prior to connecting the cables they will be checked for identification voltages, and continuity.

5.2 MAINTENANCE PLAN

Routine maintenance will include dome cleaning, filter changing, blower replacement, and heliostat inspection. Replacement/repair maintenance will occur on an as-required basis. Parts and equipment will be available to repair or replace any or all parts in a heliostat. Skilled maintenance personnel will be available at all times.

5.2.1 Dome Cleaning

The mobile erector-cleaning vehicle used to install heliostats, will be used for this purpose. An adaptor, utilizing soft bristle brushes will be rotated around the dome while being sprayed with demineralized water. The water will be collected and reused. The modified vehicle is shown in Figure 5.2.1-1.

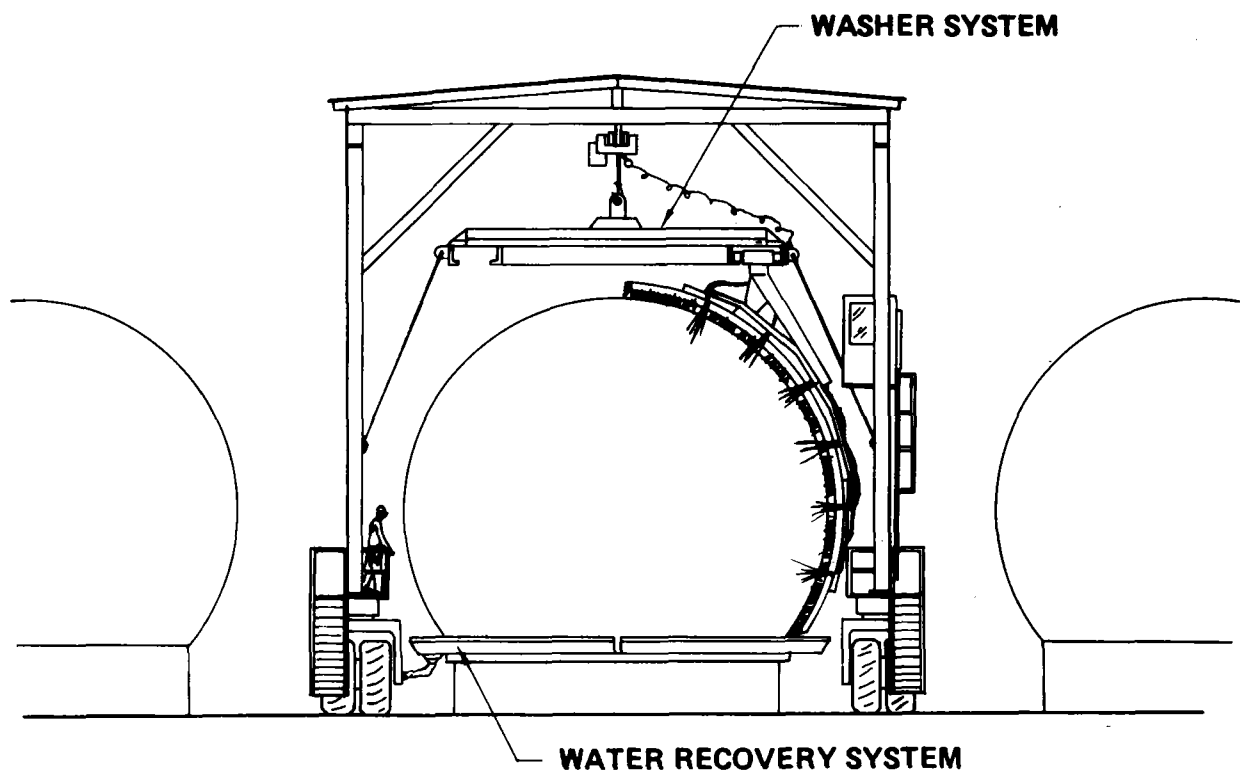


Figure 5.2.1-1. Mobile Erector Cleaning Facility

5.2.2 Reflector Cleaning

Reflector cleaning will be done primarily by an air wash. It will only be done if the reflector is inadvertently exposed to dusty or dirty conditions. For severe areas a water-alcohol rinse will be used. If the reflectance of the surface is still not adequate, the reflector will be replaced and taken to a central area for refurbishment. This type of action should only be required if the enclosure is damaged.

5.2.3 Dome/Reflector Replacement/Repair

The mobile erector-cleaning vehicle will be available to replace a dome or a reflector as used to install them. They will be replaced only if a satisfactory repair cannot be made.

Small punctures or slits in the enclosure can be repaired with adhesive backed Tedlar tape. This has been demonstrated on one of the research experiment enclosures. The acrylic adhesive used will provide some strength to the patch, but it will not sustain the loads expected in the enclosure film. This restriction, plus the limited accessibility of the upper portion of the dome, will limit the repair to small holes. Only limited repair, such as taping down a frayed edge or small holes will be attempted for the reflector. Any damage that would significantly change reflector optical performance will require replacement of the reflector.

Both the dome and reflector can be refurbished using the original fabrication tooling. Gores can be replaced in enclosures, and the reflecting film can be replaced in the reflector.

5.2.4 Air Supply System

Based on research experiment results, it is planned to replace filters on the air supply system every 9 months as a scheduled maintenance function. In addition, unscheduled replacements could occur after a severe storm or other occurrence that would tend to plug the filter.

The blowers will be replaced only as required. They have a nominal 10-year life with less than 10% expected to be replaced during that time. Upon noting an enclosure with reduced pressure, the portable air lock/maintenance trailer will be dispatched to the heliostat. This trailer will have a portable blower system to prevent damage to the enclosure and/or reflectors while replacing a faulty blower.

5.2.5 Electronics

Maintenance of the electronics system will be on an as-required basis. It will consist of replacement of components as the standard maintenance action. Faulty connections and similar problems will be corrected as required.

5.3 SUPPORT EQUIPMENT

Support equipment for installation of the heliostat field will primarily be general purpose vehicles that are leased. Special boxes will be used to transport reflectors from the remote site fabrication area to the installation site. Fork lifts and a small truck mounted crane will be used to load, unload, and position the heliostat parts prior to installation. A special mobile erector-cleaning vehicle will be used during installation of the reflector and enclosure. The same vehicle will be available for maintenance functions during the life of the collector subsystem.

Special air lock/maintenance trailers will be used for routine maintenance work. The trailers as shown in Figure 5.3-1, will consist of a portable air lock and all the maintenance tools required to replace or repair any heliostat part. The air lock will be required to permit access to the interior of the enclosure without reducing the internal pressure. The trailer will also have an auxiliary blower to supply emergency pressure.

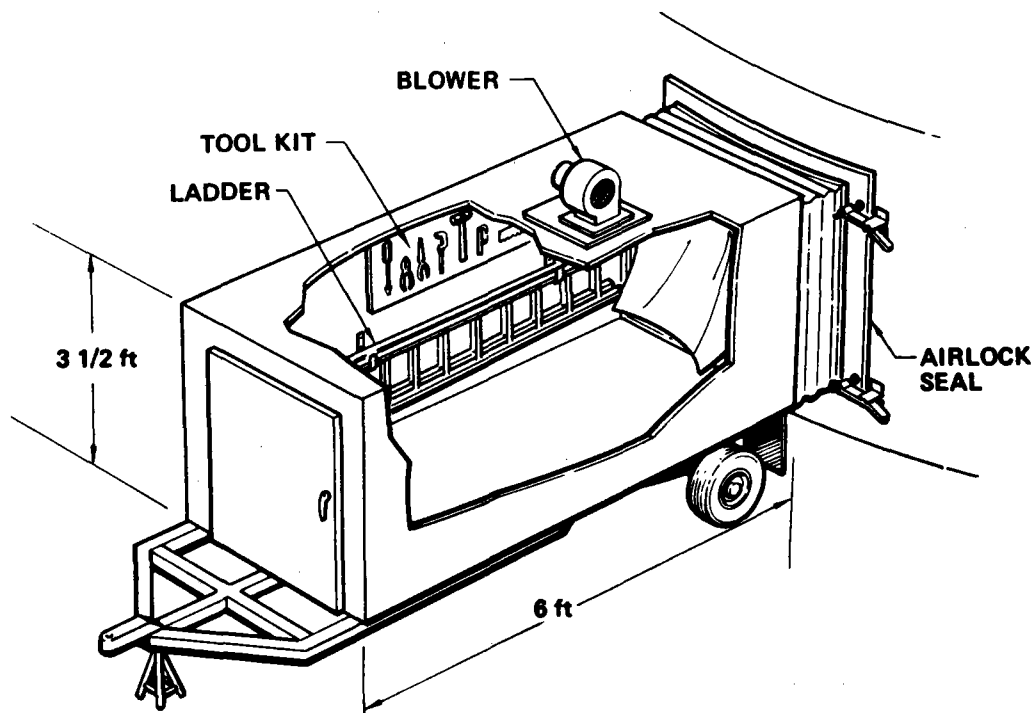


Figure 5.3-1. Airlock/Maintenance Trailer

6.0 RELIABILITY

A preliminary reliability and availability analysis has been performed on the collector subsystem PD. While a primary driving force is low initial cost, by increasing reliability in key areas life-cycle costs can be lowered while increasing availability. The analysis demonstrates that the 0.97 availability goal for the collector subsystem can be met.

The design intent has been to provide redundant systems in areas where a failure would have a drastic effect on either safety or plant availability. Secondary considerations were ease or cost of maintenance, and ability to withstand the pilot plant environment.

6.1 RELIABILITY CONSIDERATIONS

With 1650 heliostats in the field, the loss of one entails a power reduction of approximately 0.06%. Therefore, the failure of as many as one heliostat in each of the 16 control subgroups at the same time results in less than 1% power loss to the receiver and will have no significant impact on availability.

6.1.1 Loss of Control System Functions

Loss of a field controller could impact up to 512 heliostats, and accordingly would impact plant availability. Therefore, a backup field controller has been designed into the subsystem to automatically take over control of heliostats if any of the primary field controllers fails. This will allow the failed field controller to be repaired off-line, keeping the subsystem available and decreasing potential safety problems. Loss of a field controller interface card could impact up to 128 heliostats. This type of failure is also treated by switching to the backup field controller.

The individual microprocessor heliostat controllers have been designed to operate without field controller inputs for sufficient time to allow automatic change-over of field controllers. They also will maintain pointing control for safe operation during the switchover. This eliminates the necessity to go to stow or reference

positions since the reference is maintained.

6.1.2 Power Distribution System

A redundant power distribution system will be supplied from the utility or back-up generator source down to the individual heliostats. Automatic switch-over to the redundant system will be accomplished at the heliostat in the event of loss of the primary system.

6.1.3 Loss of Utility Power

A back-up diesel generator is provided to both primary and secondary power distribution circuits in the event of loss of utility power. After switchover, the field controllers will automatically reinitialize each microprocessor memory. Therefore, heliostats will not be required to return to stow for referencing.

6.1.4 Power and Control Cabling

Power and control cabling is designed for direct burial service. Discussions with cable suppliers, telephone and power companies, and Boeing experience with Minuteman buried cable system, indicate that the 30-year life requirement will be met with this type of installation. Redundant power cabling is supplied to each heliostat. Redundancy is provided in the control cables by designing each data bus to be driven from either end in the event of a break in the line.

6.1.5 Dome Pressurization

The dome pressurization is supplied by a single blower motor. Loss of a blower may cause loss of a single reflector and dome depending on wind conditions. Installation of a redundant blower was considered and judged not to be cost effective at this time for the following reasons:

- Minimal expected blower failure rate during first 10 years
- Possible detection of a malfunctioning blower prior to failure
- Redundant blower has to be mounted in series with the primary blower causing pressure loss and aging even when not powered.
- Introduction of more circuitry to effect change-over to the redundant blower.

- Trade-off costs of redundant blowers versus repair costs for the domes and reflectors. If pressure loss occurs in low wind-velocity condition, no significant damage is expected.

Present plans are to replace the blowers prior to their wear out. This will be determined by the failure rate of blowers and experience with actual damage modes.

Options still under consideration to improve the reliability include:

- Pressure monitoring system to detect malfunctioning blower.
- Central duct system with redundant blowers.
- Redundant blower modification during plant operation. Use data from 2-year test program to make decision.

6.2 MTBF ESTIMATES

Preliminary estimates of the MTBF's of system elements were made to help in assessing the availability of the collector subsystem. This was accomplished by summing the piece-part failure rates as shown in Table 6.2-1. Taking the reciprocal of the sum of the failure rates in units of failure per million operating hours results in the MTBF in hours (F/MOH). Since the failure rate data is based on a 90% confidence level, the MTBF figures indicate the interval for which 90% of similar elements can be expected to operate without failure.

The MTBF results are summarized below:

ELEMENT	MTBF (NO REDUNDANCY)	ESTIMATED AVAILABILITY (SINGLE POINT FAILURES)
Field Controller		
Interface Board	16,100 Hours	~ 1.0 with redundancy
Computer	8,000 Hours	~ 1.0 with redundancy
Heliostat Controller	31,390 Hours	Negligible effect on Power Output
Heliostat Drive System	23,400 Hours	Negligible effect on Power Output
Dome Pressurization	99,000 Hours	Negligible effect on Power Output
Electrical Power Distribution	11,000 Hours	~ 1.0 with redundancy
Cabling	30 Years	~ 1.0 with redundancy

TABLE 6.2-1 FAILURE RATE/MTBF TABLES

FIELD CONTROLLER - INTERFACE BOARD

COMPONENT	PART NUMBER	FAILURE RATE $\times 10^{-6}$ (F/MOH)	NO REQ'D	TOTAL PART FAILURE RATE $\times 10^{-6}$ (F/MOH)	DATA SOURCE
Integrated Circuit	SN 7400N	.58	39	22.62	RADC-TR-70-232
Integrated Circuit	SN 74164	1.27	24	30.48	"
Capacitor - Ceramic	CK	.22	21	4.62	MIL-HNDBK-217B
" Electrolytic	CE	.41	2	.82	"
Resistor	RN	.017	2	.034	"
"	RC	.01	16	.16	"
Variable Resistor	RT	.33	1	.16	"
Voltage Comparator	LM 111	.24	2	.48	"
Zener Diode	IN 971B	.8	4	2.4	"
Transformer	182-11380	.066	1	.066	"
Inductors-Filter	PC 53-4, -10	.063	2	.126	"
Connector - PL Card		.0024	1	.0024	"

TOTAL FAILURE RATE

61.97

MTBF

16,100 HRS.

TABLE 6.2-1 (CONTINUED)

FIELD CONTROLLER COMPUTER

COMPONENT	PART NUMBER	MTBF	SOURCE
Computer	V77- 210, 400 Varian	8000 Hrs.	Vendor, Boeing Exp. Anal. Ctr.

TABLE 6.2-1 FAILURE RATE/MTBF TABLES (Cont'd)

HELIOSTAT CONTROLLER

COMPONENT	PART NUMBER	FAILURE RATE $\times 10^{-6}$ (F/MOH)	NO REQ'D	TOTAL PART FAILURE RATE $\times 10^{-6}$ (F/MOH)	DATA SOURCE
Integrated Circuits	CD4000 AD	.145	12	1.74	Mil HNDBK-217B
Integrated Circuits	SN 5400	.145	5	.725	"
Capacitor - Ceramic	CK	.22	13	2.86	"
Capacitor - Electrolytic	CE	.41	2	.82	"
Resistor	RN	.017	1	.017	"
Resistor	RC	.01	75	.75	"
Transformer	182-11380-2	.066	1	.066	"
Inductors - Filter	P53-4, -10	.063	2	.126	"
Zener - Diode	IN 971B, IN746A	.8	4	3.2	"
Voltage Comparator	LM 111	.24	2	.48	"
Triac	T2300B	.8	1	.8	"
Diac	D32024	.8	1	.8	"
Transistor	B0278	.9	8	7.2	"
Crystal OSC	20A0111	.2	1	.2	"
Relay	1A012	.6	1	.6	"
*Switch	PIP-8	.57	1	.57	"
Micro Processor	8000 Series	.2	4	.8	Vendor
Power Supplies	-	5.0	2	10.0	Mil-HNDBK-217B
Fuse	-	.1	1	.1	RADC-TR-67-108
Total Failure Rate				31.854	
MTBF				31,390 Hours	

*Switch failure rate was derated by a factor of 10 due to extremely low cycle date.

TABLE 6.2-1 FAILURE RATE/MTBF TABLES (Cont'd)

HELIOSTAT DRIVE SYSTEM

COMPONENT	PART NUMBER	FAILURE RATE $\times 10^{-6}$ (F/MOH)	NO REQ'D	TOTAL PART FAILURE RATE $\times 10^{-6}$ (F/MOH)	DATA SOURCE
*Gimbal					
- Bearings	-	.095	4	.38	RADC-TR-75-22***
Encoder					
- Electronics	KT-23A	10.0	2	20.0	VENDOR
- Lamp		10.0	2	20.0	VENDOR
**Stepper Motor	20-3424 D200	1.0	2	2.0	Boeing
*Gear Reducer					
- Bearings	.	.095	4	.38	RADC-TR-75-2 ***
TOTAL FAILURE RATE				42.76	
MTBF				23,400 HRS	

* Bearing failure rate has been derated by a factor of 10 due to extremely low cycling

** Stepper motor failure rate was selected at lower end of the data spread due to low cycle rate

*** Rome Air Development Center

TABLE 6.2-1 FAILURE RATE/MTBF TABLES
 DOME PRESSURIZATION SYSTEM

COMPONENT	PART NUMBER	FAILURE RATE $\times 10^{-6}$ (F/MOH)	NO REQ'D	TOTAL PART FAILURE RATE $\times 10^{-6}$ (F/MOH)	DATA SOURCE
Blower Motor	ROTRON	10.0	1	10.0	VENDOR
Fuse	-	.1	1	.1	RADC-TR-67-10
TOTAL				10.1	
MTBF				99,000 HRS	

TABLE 6.2-1 FAILURE RATE/MTBF TABLES
ELECTRICAL POWER DISTRIBUTION

COMPONENT	PART NUMBER	FAILURE RATE $\times 10^{-6}$ (F/MOH)	NO REQ'D	TOTAL PART FAILURE RATE $\times 10^{-6}$ (F/MOH)	DATA SOURCE
Circuit Breaker Magnetic	-	.5	13	6.5	RADL-TR-67-108
Transformer Switch	-	.063	13	.819	MIL-HNDBK-217B
Circuit Breaker Magnetic	-	.5	165	82.5	RADC-TR-67-108
TOTAL				89.819	
MTBF				11,100 HOURS	
TOTAL (For Failures that affect more than 10 Heliostats)				7.319	
MTBF				136,000 HOURS	

6.3 INFANT MORTALITY

The collector subsystem PD was reviewed to identify items which may have high infant mortality rates. Items identified include:

- Computer
- Microprocessor
- Integrated Circuits

Normal processes for improving infant mortality include screening and burn-in. Discussions with manufacturers has resulted in the following pertinent information on infant mortality:

Varian computer parts are operated for a limited time period;

Intel microprocessor parts are put through extensive in-process tests and operational tests after assembly. Dynamic burn-in is performed on production samples at 125⁰C.

Mil Spec integrated circuits are normally tested and processed to different levels.

6.4 AVAILABILITY ASSESSMENT

The preliminary design provides redundant power and control capability that will eliminate single failure points that can cause loss of more than one heliostat at a time. Due to this provision the on-line maintenance will be very low for these systems. This will allow the availability to approach very close to 1 for the field controllers, the power distribution and cabling.

Since loss of less than 16 heliostats is not likely to cause plant shutdown, loss of individual heliostats is considered to have negligible impact on plant availability. The heliostat components have been designed for quick replacement to improve heliostat availability. All major and many minor components are completely interchangeable.

6.4.1 Potential Improvement Areas

As shown in the MTBF summary (Section 6.2) the failure rate data in Table 6.2-1 and the redundancy provisions of the collector subsystem, demonstrate a cost effective PD from an availability standpoint.

If subsequent design analyses show the need for increasing reliability, flexibility exists for improving the design. Some of these areas are listed below:

- Use Mil Spec parts in the Interface Cards-MTBF increase to 35,000 Hrs.
- Use Mil Spec parts in the Heliostat Electronics-MTBF increase to 66,000 Hrs.
- Replace encoder lamp with solid state light source. At least double the life expectancy.
- Specify MIL Spec parts in the encoder electronics - Increased MTBF
- Provide redundant blower motors or central ducting system.
Reduce down time for blower maintenance.

6.5 CONTINUING RELIABILITY PROGRAM

The reliability assessment will continue to be an important consideration in the detail design phase to assure meeting the availability goal.

The following steps will be taken to assure maximum reliability consistent with availability goal, design feasibility and costs:

- Detailed single point failure analysis to identify critical failures that can be potentially hazardous to equipment or personnel;
- Identify areas where reliability could be improved that would significantly reduce maintenance costs and down time;
- Maintain a continuing appraisal of component parts so that the most reliable parts can be selected consistent with costs;

- Provide failure analysis support to help find solutions to high cost maintenance items;
- Review change-over procedures and capabilities for back-up systems to assure minimum effect on down time and system reliability;
- Provide reliability inputs for life cycle costs trade studies.

7.0 SAFETY

Critical safety areas were considered during the preliminary design of the collector subsystem, including its interface with other portions of the pilot plant. The objective of the preliminary safety effort was to identify, eliminate, or minimize hazards to the pilot plant operation and maintenance personnel, the general public and equipment. This was accomplished by performing a preliminary hazard analysis using Reference 9.0-1 (February '77, Draft "System Safety Design Criteria - Central Receiver Power Systems") as a guide, and incorporating safety considerations into the preliminary operations and maintenance procedures. The principle safety concern for the collector subsystem is control of reflected light from heliostats. Accordingly, considerable effort was applied to control of reflected light by developing operational procedures, redundant control and power circuits and alternate procedures initiated by warning signals to prevent reflected light hazards. As discussed in detail later, the wind protected reflector concept offers a unique solution to the stray light during transition from "stow" to "standby" problem, if required.

7.1 DESIGN SAFETY FEATURES

The collector subsystem PD was rigorously reviewed for applicability and cost-effective compliance to Reference 9.0-1. A safety program plan, (Table 7.0-1, was developed to assure management visibility and consideration of all program aspects through pilot plant operations. A preliminary hazard analysis was performed to find safety problems and develop cost-effective and reliable solutions, as summarized in Table 7.0-2. The preliminary hazard analysis includes only those hazards which were found to affect the collector subsystem design. Reference 9.0-1 hazard identification table was used as a hazard source to insure that all hazardous conditions were reviewed for applicability. The most significant hazard which we had to consider in our preliminary design and operational procedures was misdirection of beam convergence (beam convergence is defined as multiple heliostats having intersecting heliostat optical axes). This hazard would occur if more than one heliostat beam converged at a location other than the "standby" position or the "receiver track" position. An individual non-

TABLE 7.0-1

SAFETY PROGRAM PLAN FOR SOLAR THERMAL POWER - COLLECTOR SUBSYSTEM

- . PERFORM SAFETY ANALYSES OF OVERALL SYSTEM DESIGN AND OPERATIONS, UPDATED CONSISTENT WITH PROGRAM DEVELOPMENT. THIS PROVIDES MANAGEMENT VISIBILITY AND ASSURES THAT ALL SAFETY CONSIDERATIONS HAVE BEEN EVALUATED AND COMPLETED PRIOR TO SYSTEM OPERATIONAL PHASE. ANALYSES CONSISTS OF:
 - . HAZARD ANALYSES - SYSTEM DESIGNS AND OPERATIONS INCLUDING NORMAL, CONTINGENCY, TEST, CHECK-OUT, AND MAINTENANCE
 - . TRADE STUDIES - SUPPORT TO ENGINEERING OR SPECIAL SAFETY TRADES WHICH INCLUDE RISK COMPARISONS
 - . DETAILED DESIGN ANALYSIS - SUPPORT TO ENGINEERING WHERE A HAZARDOUS FUNCTION/ OPERATION MAY BE A SAFETY CONCERN
 - . EVALUATE APPLICABILITY OF OSHA STANDARDS
- . SUPPORT MILESTONE REVIEWS
 - . REVIEW DESIGN AND OPERATIONAL DATA
 - . REVIEW PREVIOUS PROBLEMS AND THEIR STATUS
 - . IDENTIFY NEW SAFETY CONCERNS
 - . MONITOR SAFETY CONCERN CLOSEOUT ACTIVITY
 - . PERFORM CLOSEOUT ACTION AS ASSIGNED
- . TRACK STATUS AND RESOLUTION OF HAZARD ELIMINATION/REDUCTION MEASURES
 - . DESIGN FOR MINIMUM HAZARD
 - . INTRODUCTION OF SAFETY DEVICES
 - . USE OF WARNING DEVICES
 - . USE OF SPECIAL PROCEDURES
- . SAFETY COMPLIANCE DATA PACKAGE - COMPLETED PRIOR TO SYSTEM OPERATIONAL MODE
 - . PROVIDE SAFETY ASSESSMENT REPORT DOCUMENTING RESULTS OF HAZARD ANALYSES INCLUDING IDENTIFICATION OF HAZARDS AND RESOLUTION MEASURES/DECISIONS MADE
 - . RECORD OF WAIVERS APPROVED FOR SAFETY REASONS
 - . RECORD OF OSHA STANDARDS INCORPORATED
 - . RECORD OF TESTS AND ANALYSES PERFORMED TO SHOW VERIFICATION OF THE RELATED SAFETY REQUIREMENTS
 - . PREPARATION OR APPROVAL OF DETAILED OPERATING PROCEDURES WHICH ARE HAZARDOUS IN NATURE.

TABLE 7.0-2
PRELIMINARY HAZARD ANALYSIS OF SOLAR THERMAL POWER COLLECTOR SYSTEM

<u>Assy/Component</u>	<u>Hazard</u>	<u>Hazard Cause</u>	<u>Hazard Effect</u>	<u>Hazard Control</u>
Heliostat Drive Motors & Control Assemblies	Radiation Equipment Failure Resulting in loss of Reflecting Surfaces Pointing Capability (Azimuth/Elevation)	Loss of Power to Drive Motor Due to Open/Short Circuit (3300 Motors)	Eye Injury, Burns or Equipment Damage if Undetected.	For single point failures. Heliostat failure is reported to plant control. Light weight of mirror permits manual safeing by single maintenance person.
		Loss of power to Drive Motor due to primary commercial power failure	Eye Injury, Burns or Equipment Damage if Undetected.	Secondary (Diesel) power system.
	Electrical Energy	Exposure to Electrical Supplies and Wires/Circuits	Personnel Shock	Low voltage use in heliostat design. In high voltage situation, appropriate design practices regarding grounding insulation and other protections are used.
		Lightning	Personnel Shock and Equipment Damage	Gas discharge device and grounded copper grid as well as the use of appropriate design practices regarding insulation and grounding practices.
	Human Hazards	Sharp Edges	Personnel Injury Entanglement, Bumping by moving parts, entanglement in gears.	Moving parts, sharp objects will be guarded. Protective head gear, gloves, etc. will be worn by maintenance and operations personnel.
Protective Enclosure Assembly	Enclosure Collapse	Loss of Power to Enclosure Blower	Potential abrasion damage to enclosure and/or reflector	Secondary (Diesel) electrical power system.

Assy/Component	Hazard	Hazard Cause	Hazard Effect	Hazard Control
Reflective Assembly	Radiation	Structural Failure Gimble Assembly Slippage	Eye or other tissue damage due to mis-directed light	Protective clothing, dark glasses. Hazard occurrence probability and effect very small.
	Human Hazard	Inadvertent movement while maintenance performed	Personnel hit by moving assembly	Minor hazard, mirror assembly movement is very slow (Maximum of .135 degrees per second).
	Radiation	Intersecting beams on airplane or land vehicle	Disorientation causing possible accident	Operating parameters and constraints disallowing beams to intersect other than at or right off the tower have been designed into the control system
	Thermal . Overheating	High Temperature inside enclosures	Minor Burns to maintenance crew	Wearing of protective clothing and gloves while inside heliostat enclosures.
	. Fire	Flammability of protective enclosure	Heliostats becoming inoperative	Minor hazard, Tedlar meets flammability and toxicity requirements and is used in airplanes. Also, there is nothing else in the enclosure that could assist the spread of fire.
	. Toxicity	Overheating of plastics and other non metallics	Personnel sickness	"
. Mechanical Energy	Dome and reflector assembly falling onto other heliostats causing even further damage (chain reaction) during severe wind storm	Equipment damage	Heliostat spacing selected to minimize cascading effect.	

focusing heliostat presents no significant hazard until its beam converges with other heliostat beams. There are other significant hazards which must be considered as well in the collector subsystem design, they are lightning, commercial power loss, and fire.

Design compliance to safety requirements and the elimination of hazardous conditions was based on trade studies used to balance cost effectiveness versus hazard magnitude. Redundancy was carried as far as required to minimize hazards to an acceptable level. During these trades we concluded that the dome-protected reflector assemblies, heliostat and field controller systems, were not only cost effective, but inherently safe without costly redundancies in the individual heliostats.

7.1.1 Heliostat

The Tedlar dome-protected reflector assembly design allows safe operation of the reflector in all environments. Since the reflectors are enclosed, they can be kept light, therefore easily driven or manually moved by maintenance personnel to any position including "safe-stow". The enclosure also allows the heliostat to contain a highly reliable microprocessor driven heliostat control system. This is an excellent safety feature because it can detect bad or no data coming from the field or plant controller and immediately initiate a safe stow position of the mirror assembly. Also portable electronic boxes can be plugged into a heliostat for manual control through the heliostat control system or directly to the drive motors.

Each heliostat is periodically tested for beam pattern, intensity and alignment accuracy by a laser-aided alignment system located on the receiver tower. This individual heliostat calibration data is used to insure that the beam is safely on target and not causing a hazard by hitting the tower structure or a distant ground object.

7.1.2 Field Controller

The field controller is a mini-computer operated control system which monitors and commands up to 512 heliostats during normal operation. This enables

prompt safing of heliostats under hazardous conditions. A redundant field controller automatically takes over for a malfunctioning field controller. This feature assures a continued "safe configuration" of heliostats at maximum receiver and power subsystem outputs. Also, the PD includes a manually-operated electronics package that connects to a data bus, and can operate up to 128 heliostats. This allows additional "safing" capability during maintenance or trouble shooting operations. The field controller input and output signal and motor drive power busses are protected from lightning transients by use of discharge devices and a grounded copper-grid protects cabling and heliostat structure.

7.1.3 Collector Subsystem Power

A diesel operated generator for power backup is used as the secondary power source for the primary commercial power. Both primary and secondary power is bussed to individual heliostats through a completely redundant system including transformers, circuit breakers and junction boxes.

7.2 OPERATIONAL PROCEDURES

Operational procedures have been developed for the safe operation of the collector subsystem. The procedures have been reviewed for contingencies and exposure to hazardous conditions with emphasis on beam convergency, lightning, primary power failure, and fire. There are five operational modes to consider.

7.2.1 Stow

"Stow" is the heliostat position used for maintenance, night-time stowage or the "safe stow" that is reverted to when there is a power or control circuit malfunction. The reflective surface is near vertical in the "stow" position. The preferred azimuth angle for stow is to be selected in detail design studies. With the vertical stow position, the sun's rays reflect harmlessly onto the ground inside the outer limit of the collector field or are blocked by the 4.27 m (14 ft) fifty percent porosity fence which surrounds the collector field.

7.2.2 Standby

Heliostats are in standby when each beam passes through the space just to the left of the receiver, and at the same height as the receiver track position. When all the heliostats are in standby, their converging beams form a toroid around the receiver. This mode assures that the beams diverge after converging near the tower and, therefore, cannot converge at any other point. To go from "stow" to "standby" mode all mirrors are rotated together in azimuth so that they all are parallel and facing the sun. The mirrors are then rotated in elevation so that the reflected beams point straight up and parallel. Next, all mirrors are rotated to the proper azimuth positions for "standby" while keeping the beams pointed straight up. The last step is to rotate individual heliostats in timed sequence to "standby" position. Using this procedure the beams never converge nor do they impinge on facilities or the receiver tower.

There are additional transfer modes that are possible because of the unique dome protection. Mirrors are completely decoupled from wind forces up to maximum expected conditions. Because of this protection, the mirror assemblies can be in any position during severe environmental conditions, and the following optional procedures can be used to control all stray beams from impinging on land or air vehicles and distant ground objects.

- Perform "stow" to "standby" transition and the reverse only in dark or cloudy periods.
- After sundown pre-position mirrors in "standby" (instead of "stow") for the next day's sunrise.

7.2.3 Receiver Track

Heliostats are in receiver track mode when their beams are maintained on target on the receiver. Heliostats can be rotated from "standby" to "receiver track" and vice versa individually, in groups, or all together. This mode is made "safe" because of the ability to remove heliostat beams from the receiver in forty seconds. Also, because of the align and scanner verification procedure, heliostat beams are accurately placed on the receiver.

7.2.4 Align

The heliostats can be individually commanded to an align position for purposes of laser assisted calibration. The mirrors are aimed directly at the laser and scanner and their beams are checked for intensity, pattern and position. This assures that each mirror is safely on-target when in the "receiver-track" mode.

7.2.5 Manual

The heliostats can be controlled manually to perform in all operational modes, including maintenance, by using either the manual field controller, manual heliostat controller or a manual motor controller. The manual field controller when connected to the data bus can control up to 128 heliostats in a control group. The manual heliostat controller connects to and operates any individual heliostat. The motor controller by-passes the heliostat control circuitry and operates the drive motors directly.

With all these operational modes and procedures of the collector subsystem control assembly, hazardous conditions are prevented and the system is always in a safe controlled configuration.

8.0 ELECTRICAL AND MECHANICAL SUPPORT EQUIPMENT

Three phases of pilot plant field activity are envisioned at this time. The first phase will be Installation and Checkout. In addition to installation, the effort includes such activities as demonstration of the Heliostat Erection and Cleaning Facility, demonstration of the calibration and alignment module, control system tests, and subsystem interface tests. The second phase will be plant startup. During this phase, all subsystem interfaces will be verified, all modes of operation demonstrated and the collector subsystem accepted by ERDA. The third phase will be the Two Year Pilot Plant Test Program.

A considerable quantity of equipment will be required to support the Pilot Plant from initiation of the construction phase through 2 years of plant operation. Table 8.0-1 is a list of equipment that has been identified as necessary for field operations.

TABLE 8.0-1 PILOT PLANT ELECTRICAL AND MECHANICAL SUPPORT EQUIPMENT

Equipment	Pilot Plant Phase		
	Installation & Checkout	Plant Start Up	2 Yr. Pilot Plan Test Program
o Maintenance building for preparation of reflectors and storage of spares and support equipment. Minimum area - 460 sq. meters (5000 sq. ft.)	X	X	X
o Complete foundation dedicated to checkout heliostat components and assemblies; preferably located in or near Maintenance building.	X	X	X
o Alignment and Calibration module	X	X	X
o Heliostat Mobile Erecting and Cleaning Facility Includes: (1) Large enclosure for weather protection during heliostat installations (2) Crane for reflector and transparent dome erections (3) Platforms for use during erections (4) Auxiliary blower for initial inflations (5) Storage space for additional reflective and transparent dome assemblies (6) tools required during erection operations (7) Cleaning system for transparent domes;	X	X	X
o Maintenance/spares inventory	X	X	X
o Maintenance/spares kits	X	X	X
o Transparent enclosure repair kits	X	X	X
o Portable air locks	X	X	X
o Motor Generator Unit	X		
o Equipment Vehicles (pick-up trucks)	X	X	X

PILOT PLANT ELECTRICAL AND MECHANICAL SUPPORT EQUIPMENT
(Continued)

	<u>Equipment</u>	<u>Pilot Plant Phase</u>		
		<u>Installation & Checkout</u>	<u>Plant Start up</u>	<u>2 Yr. Pilot Plant Test Program</u>
	o Portable 2-way radio communicators (several sets)	X	X	X
	o Welding Equipment	X		
	o Power tools for Maintenance building - drills, saws, etc.	X	X	X
	o Mechanical tool kit - wrenches, etc.	X	X	X
	o Portable scaffolds and stepladders	X	X	X
	o Instrumentation			
172	o Breakout boxes for: heliostat electronics control transmission interface and central control transmission interface	X	X	
	o Digital multimeters - HP 8000A	X	X	X
	o Strip chart recorders - Hewlett Packard 7100B	X	X	X
	o +5V, +15V, +28V DC power supplies for static tests of heliostats with field controller out of loop	X	X	X
	o Electronic counters to count motor steps and encoders discretes during tracking & slew tests	X	X	X
	o Miscellaneous electronic trouble-shooting instrumentation - hand tools test leads, etc.	X	X	X
	o Oscilloscope - Techtronic 461	X	X	X
	o Signal Generator - variable 0-5 volts; stepping rate 0-100/sec	X	X	X
	o Digital Logic Analyzer - 16 bit capability	X	X	X

PILOT PLANT ELECTRICAL AND MECHANICAL SUPPORT EQUIPMENT
(Continued)

	<u>Equipment</u>	<u>Pilot Plant Phase</u>		
		<u>Installation & Checkout</u>	<u>Plant Start-up</u>	<u>2 Yr. Pilot Plant Test Program</u>
	o Vacuum tube voltemeter - Calif. Instr.	X	X	X
	o Volt - OHM meter - Simpson	X	X	X
	o Strip chart recorders - 6 channel sanborn 150	X	X	X
	o Accelerometers - 16 Total			X
	o Wind velocity monitors - 2 portable - 1 fixed; Beckman 0-100 mph		X	X
	o Deflection indicators - 12 Total			X
173	o Thermocouple wire - 2500F7 Chromel-Alumel			X
	o Pyrheliometer - Eppley - Model NIP	X	X	X
	o Equatorial Mount - Edmunds Model 85111	X	X	X
	o Pyrheliometer - Eppley Model VFN (1/2°)	X	X	X
	o Equatorial Mount - Eppley ST-1	X	X	X
	o Recording Hygro Thermographs	X	X	X
	o Data Logger for Environmental Instrumentation		X	X

9.0 OPERATION AND MAINTENANCE

An operation and maintenance study was made of the experimental research design for the 10 MWe Solar Thermal Power Collector Subsystem. This study was performed to establish preliminary estimates of 30 year maintenance manhours and to identify necessary support equipment. The study was also used to identify system areas which had unacceptably high maintenance requirements.

A summary of the major areas of O&M support and their estimated 30 year manhour requirements is shown in Table 9.0-1. Figure 9.0-1 shows estimated O&M support hours as a function of operating years.

Table 9.0-1. Operations and Maintenance Analysis

Function	Frequency	Unit time	No. of units	30-year accum total
Dome assembly				
Clean dome	4 months	1/6 hr	1,650	49,500 hr
Repair dome	Yearly	2 hr	3	540 hr
Replace dome	30 years	3 hr	1,650	14,850 hr
Replace dome and reflector	Yearly	6 hr	3	1,620 hr
Blower assembly				
Replace blower	30 years	1 hr	1,650	1,650 hr
Replace/clean filter	9 months	1/6 hr	1,650	11,000 hr
Gimbal assembly				
Replace bearings	30 years	6 hr	165	990 hr
Replace limit switches	Yearly	1 hr	3	90 hr
Drive actuator assembly				
Replace motor	30 years	1.5 hr	868	1,302 hr
Replace harmonic drive	30 years	2.0 hr	150	300 hr
Replace encoder (elect)	30 years	2 hr	8,678	17,356 hr
(lamp)	30 years	0.25 hr	8,678	2,170 hr
Replace bearings	30 years	3 hr	165	495 hr
Heliostat controller assembly	30 years	0.5 hr	13,822	6,911 hr
Computer system assembly				
Operational checks and monitoring	Daily	5 min*	1	913 hr
Replace plug-in boards	30 Years	10 min	164	27 hr
Replace soldered components	Yearly	20 hr	1	600 hr
Field interface cables and wiring				
Replace	Yearly	8 hr	-	240 hr
Data bus terminal box	30 years	1 hr	10	10 hr
Lightning arrestor	30 years	0.5 hr	2,209	1,105 hr
Facility maintenance				
Vehicles and equipment	Yearly	160 hr	-	4,800 hr
Grounds	Yearly	400 hr	-	12,000 hr
Utilities and services	Yearly	160 hr	-	4,800 hr
Total				133,269 hr

*Assumes diagnostic program permanently stored in memory

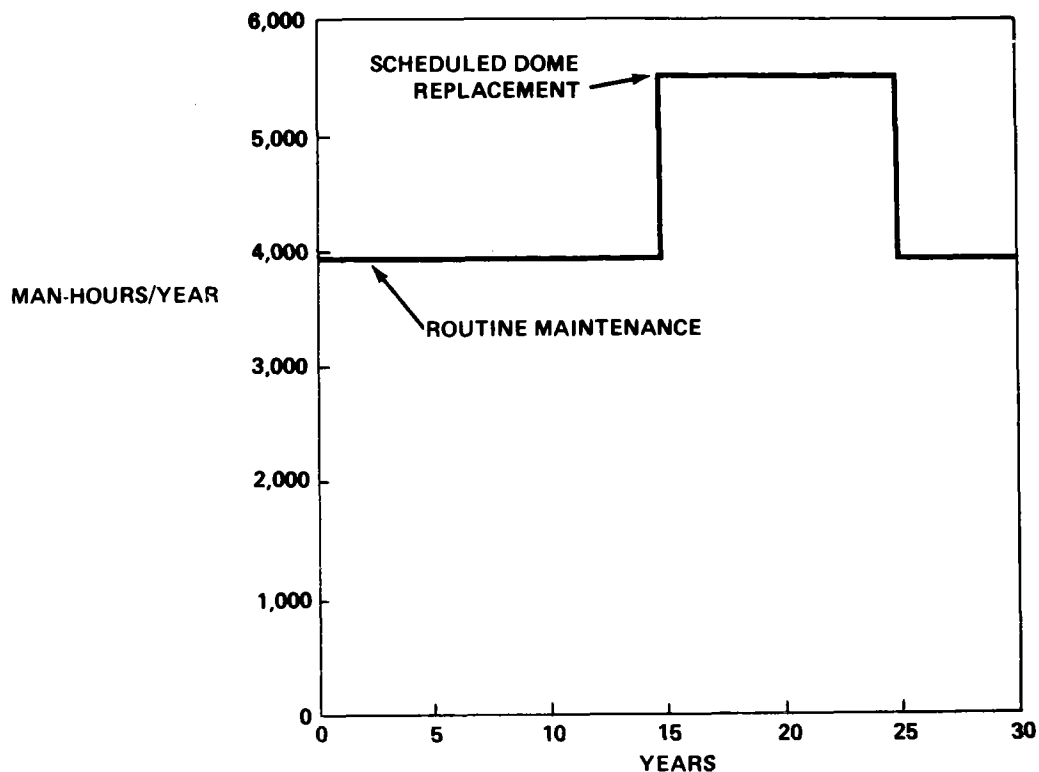


Figure 9.0-1. Operations and Maintenance Man-Hours

9.1 DOME CLEANING

Research to date indicates that over a period of time, dust will adhere to the external surface of the protective domes in sufficient quantities to reduce transmittance below acceptable levels. Conceptual studies were conducted on cleaning methods ranging from manual to fully automatic. Based on field tests of the experimental research design domes and sample coupons exposed at Albuquerque, New Mexico and China Lake, California, cleaning will be required at intervals of less than six months in summer, and possibly more than 6 months in winter.

The mobile erector-cleaning facility as shown in Figure 5.2.1-1 will be used for dome cleaning. When used for cleaning it would be equipped with hemispheric arms containing rows of nozzles and/or soft brushes, which sweep around the dome and clean the surface. Self contained tanks would provide the cleaning solution and recover the residue for later filtering and reuse. Cleaning action may be further enhanced by supplying the nozzles with pulsating pressure.

9.2 REFLECTOR CLEANING

Adequate filtering of the dome pressurizing system combined with the protective environment of the dome should preclude the necessity to periodically clean the reflector surface. Stowing the reflector in a vertical position during non-operational hours should minimize deposition of dust.

Based on research experiment experience, the reflectors will be cleaned only when the domes are replaced or have been damaged. Since the front surface mirror is vulnerable to deterioration from any physical contact, cleaning will be accomplished primarily by an air wash. A water/detergent rinse will be used for localized contaminated areas. This technique has been found to restore the reflectance of samples of aluminized mylar.

9.3 DOME/REFLECTOR REPLACEMENT AND/OR REPAIR

The mobile erector-cleaning facility is considered to be a multiple use vehicle. It will provide facilities to erect the collector subsystem field, provide a protective environment from adverse weather for major maintenance efforts, and support routine operations such as dome cleaning. It will be equipped with protective curtains that will allow work in winds up to 10 m/sec.

Field tests of the dome material and research to date indicates that the domes will have to be replaced once during a 30 year cycle. The replacement period is estimated to range from 15 to 24 years, depending on the dome's position in the collector field. This replacement period allows a scheduled replacement program which will have negligible impact on power production. Any replacement, repair or cleaning of reflectors may be accomplished simultaneously with dome replacement with little additional effort. Minor repairs of rips or tears to the domes or reflectors can be accomplished by adhesive backed patches.

9.4 AIR SUPPLY SYSTEM

The research experiment heliostats utilized a separate air pressurization blower for each protective enclosure. The dedicated blower is advantageous in assuring negligible input on availability in the events of failure of an individual blower or dome. Investigation to date indicates that the blowers will have a

Mean-Time-Between-Failure (MTBF) of approximately 11 years with a 90% confidence level. Accordingly, at least one blower replacement would be required during a 30 year life cycle.

Each air pressurization system has its own filter. Based on field test results, filter replacement for the PD has been planned at approximately nine month intervals.

In detail design, it may be possible to increase the MTBF of the blower by selecting improved materials and incorporating air bearings. The filter replacement interval may be extended through selection of higher capacity filters. The adoption of a central air distribution system might be contemplated based on test results.

9.5 ELECTRONICS

Present reliability studies on the power system electronics show a MTBF of between one and three and one half years. The field controller is expected to have the highest failure rate, but because of redundancy and a few number of controllers in the system, its failure is not expected to create a maintenance or power production problem. Ten percent of the heliostat controllers can be expected to fail in the first three and one-half years. The relatively high failure rate of the heliostat controller will have a negligible effect on power production but will impact maintenance operations due to the large number in the system.

The reliability of the power system electronics could be increased by substituting higher quality components and running a preconditioning cycle prior to field installation. Reliability cost trade studies for component selection, are planned for the detail design effort.

9.6 SUPPORT EQUIPMENT

Typical support equipment will consist of the following:

- 1) Mobile Erector - Cleaning Facility
- 2) Maintenance Vehicles
- 3) Reflector Support Stands
- 4) Dome Expander
- 5) Air Lock/Maintenance Trailer
- 6) Dome and Reflector Slings
- 7) Manual Control Unit
- 8) Electronic Test Equipment

10.0 TEST PROGRAM

This section of the document describes the testing to be performed starting with design verification through the two year test program. A complete design verification is planned including component development, assembly development and verification, assembly integration, and a 2 heliostat array test (at Kent, Wa.) prior to final tooling fabrication. Acceptance testing of the delivered collector subsystem will be performed at the Barstow site during plant startup and checkout. Two years of subsystem testing will follow. A schedule of the 3 test tasks appears in Figure 10.0-1

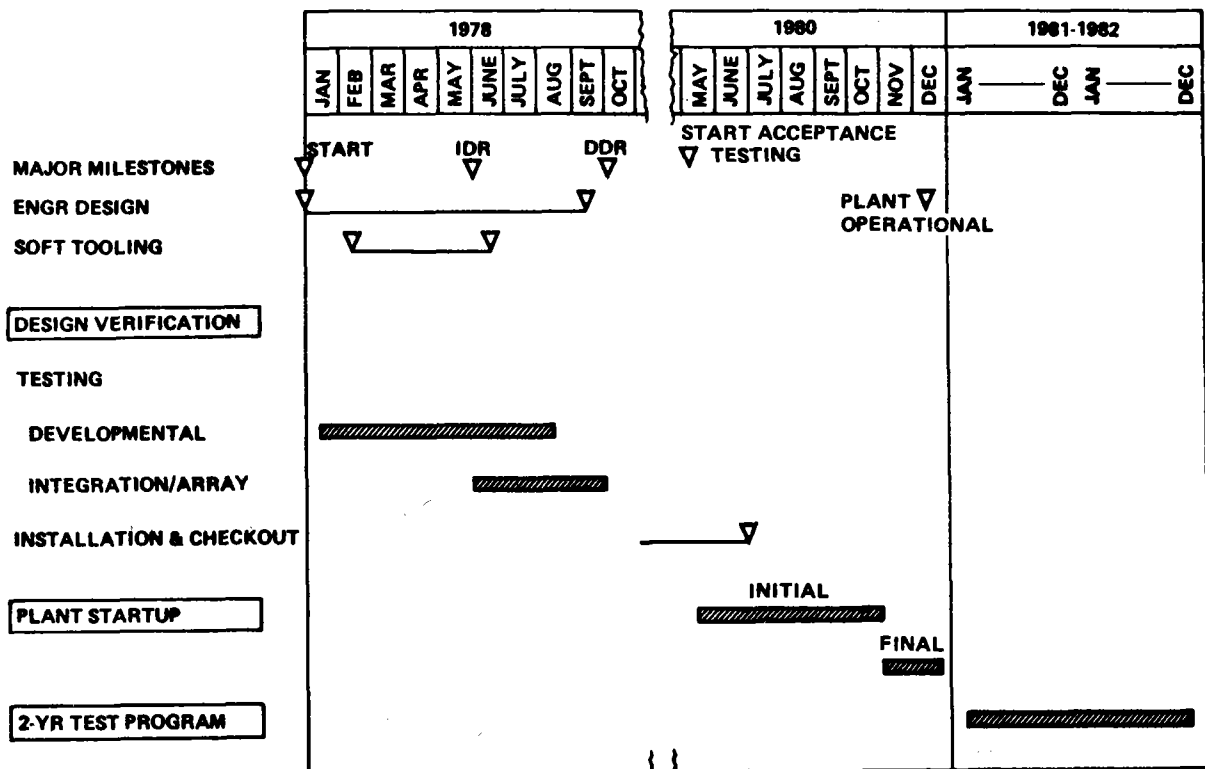


Figure 10.0-1. Collector Subsystem Test Program

10.1 DESIGN VERIFICATION PLAN

The purpose of the recommended test program is to conduct those tests required to qualify the design and to verify performance of deliverable heliostats, control system, and support equipment. The test program is formulated for early imple-

mentation to assist in early definition and resolution of design and manufacturing uncertainties. The program is designed to be compatible with the delivery schedule requirements. This is achieved through detailed test planning; minimization of development effort; maximum "off the shelf" hardware procurement; parallel testing; and utilization of test results from research experiments.

10.1.1 Test Program Approach

The four-step design verification plan, commences with minimal component testing and culminates with array tests. Figure 10.1-1 outlines logically the flow, as well as specific tests planned at the component, assembly, integration, and array levels. Two heliostats will be fabricated for qualification use only. The qualification heliostats will be configured to simulate "near field" and "far field" conditions relative to a simulated central receiver at the Boeing heliostat test site (Kent, Washington). Testing will be supplemented with analysis to lead to a fully qualified heliostat.

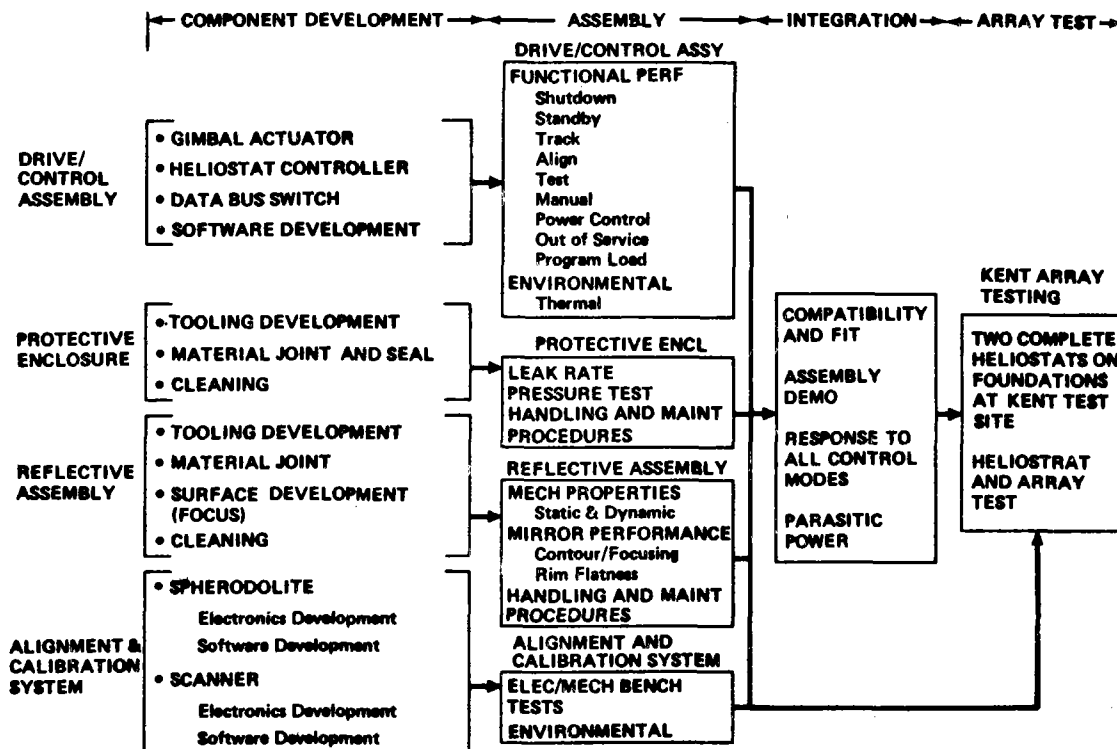


Figure 10.1-1. Design Verification Logic Diagram

10.1.2 Component Testing

Testing at the component level will consist primarily of acceptance testing of materials and parts purchased "off the shelf" from vendors. All components that are Boeing-made will be tested.

The transparent dome and reflective assembly materials planned for utilization in the proposed design were selected based upon tests and analyses conducted in the Collector Subsystem Research Experiments Program. Minimal additional materials and process testing is planned for these materials for this program.

Development and qualification testing of the gimbal actuators will be performed. Included will be static and dynamic tests to evaluate gear backlash, shaft windup and structural stiffness. Thermal testing will be included at the assembly level.

Boeing designed and fabricated electronic components will be utilized in both the drive and control system, and the alignment and calibration system. These components will require normal electrical breadboard testing to verify input and output performance and to verify interface compatibilities with other purchased components.

10.1.3 Assembly Testing

Boeing will perform tests and analyses which will demonstrate that the heliostat design is qualified to the conditions defined. Heliostat qualification testing will begin at the assembly level. Figure 10.1-2 is a matrix of the assembly tests, along with the hardware facilities required to perform these tests.

Pressure Test - A pressure test will be performed to verify the ability of the enclosure to withstand the combined stress of internal pressurization and wind loading.

Leak Test - A leak rate test will be performed to evaluate enclosure leakage.

Handling - A protective enclosure unit will be subjected to development of handling and installation techniques.

Assembly	Test type	Boeing facility	Hardware required
Protective enclosure	Pressure test	Engineering lab	1 enclosure assembly
	Leak rate test	Engineering lab	
	Maintainability	Manufacturing lab	
	Handling	Manufacturing	
	Foundation demonstration	Kent	
Reflective assembly	Dynamic testing	Structures lab	1 reflective assembly
	Static load	Structures lab	
	Rim flatness	Engineering lab	1 reflective assembly
	Contour/focusing	Engineering lab	
	Handling	Manufacturing lab	
	Maintainability	Manufacturing lab	
Drive and control assembly	Thermal-heliostat controller	Environmental lab	1 drive/control assembly
	Functional performance	Electronics lab	1 drive/control assembly
	Maintainability	Electronics lab	
Alignment and calibration system	Electrical/mechanical bench	Engineering lab	1 calibration/alignment system

Figure 10.1-2. Matrix of Assembly Tests

Maintainability - Methods for cleaning the protective enclosure will be demonstrated at this level. Methods and techniques of removing dust, dirt, and grease (such as would occur from maintenance installation activities) will be demonstrated. Methods of removing, replacing, stowing, repairing, and handling the protective enclosure will be demonstrated and documented.

Foundation Demonstration - The foundation concept is simple and conventional, and is not expected to require any testing, other than demonstration of installation technique.

Reflective Assembly

Structural - Structural testing will consist of a modal survey, static load, and deflection testing. The purpose of the modal survey will be to determine response frequencies and modes over the range of significance, which is expected to be 0 through 50 Hz. This data will provide verification of the response of the assembly to seismic events, mechanical vibration from motors, and pressure waves inside the enclosure due to variable wind loading.

The purpose of the static load test will be to verify predicted deflections of the reflective assembly structure. Deflection data will be taken primarily to evaluate how the assembly deforms during rotation through varying attitudes and the subsequent effects upon the reflector contour integrity.

Mirror Rim Flatness - A laboratory laser will be used to measure the flatness of rim in the horizontal and vertical attitudes.

Membrane Tension - Membrane tension will be determined by measuring deflection of the membrane when horizontal and comparing it to predicted deflection for 750 psi stress.

Mirror Performance - The mirror performance will be qualified during integration of the reflective assembly with the transparent enclosure. Integration testing is described in paragraph 10.1.4.

Handling - Handling of the assembly and techniques for installation, removal, and replacement of the reflective surface will be developed.

Maintainability - Methods for cleaning the reflective surface will be developed. Any special tools and equipment required for reflective surface maintenance will be verified.

Drive and Control Assembly

Electrical/Mechanical Bench Tests - Tests will be performed to verify that assembly performance and interface requirements are met, and as required in support of design and development of total assembly. Functional tests will consist of tests to assure compliance with performance specifications. As a minimum, responses for the following modes will be tested:

Shutdown

Standby

Track

Align

Manual

Power Control

Out of Service

Program Load

The drive actuator and gimbal assembly will be tested as a unit to indicate correct operation as to direction correspondence with input signals, response characteristics, and load capability.

Thermal Test - Thermal tests will be conducted to verify that the drive and control assembly can withstand the thermal cycling environment representing temperature extremes expected inside the protective enclosure. The performance of the system will be verified at specification temperature limits by performing real-time program routines.

10.1.4 Integration Testing

Subsequent to assembly testing, assemblies will be integrated into a complete heliostat. Three integrations are involved: protective enclosure-to-reflective assembly, and reflective assembly-to-drive and control assembly and protective enclosure-reflective assy-Drive & Control Assy. These integrations and the necessary tests are discussed below.

Integration of Protective Enclosure and Reflective Assembly - The following integration tests will be performed:

- 1) Verification of physical fit and clearance
- 2) Energy collection efficiency

These tests will all be conducted with a single test setup. The reflective assembly will be set up on the Boeing-Kent Heliostat Test Range inside of the protective enclosure. The target area will be scanned to determine the point-by-point irradiation. A sun-monitoring radiometer on an equatorial mount provides short-term variation correction to changes in solar intensity and a reference for determining heliostat efficiency. Iso-solar mapping provides evaluation of image shape, and focusing. Figure 10.1-3 describes the test setup.

Integration of Reflective Assembly and Drive and Control Assembly - The objective of this test is to verify operation of the drive and control system in conjunction with the reflective assembly through all modes of operation. It will be performed in a laboratory high bay without a protective enclosure (Figure 10.1-4).

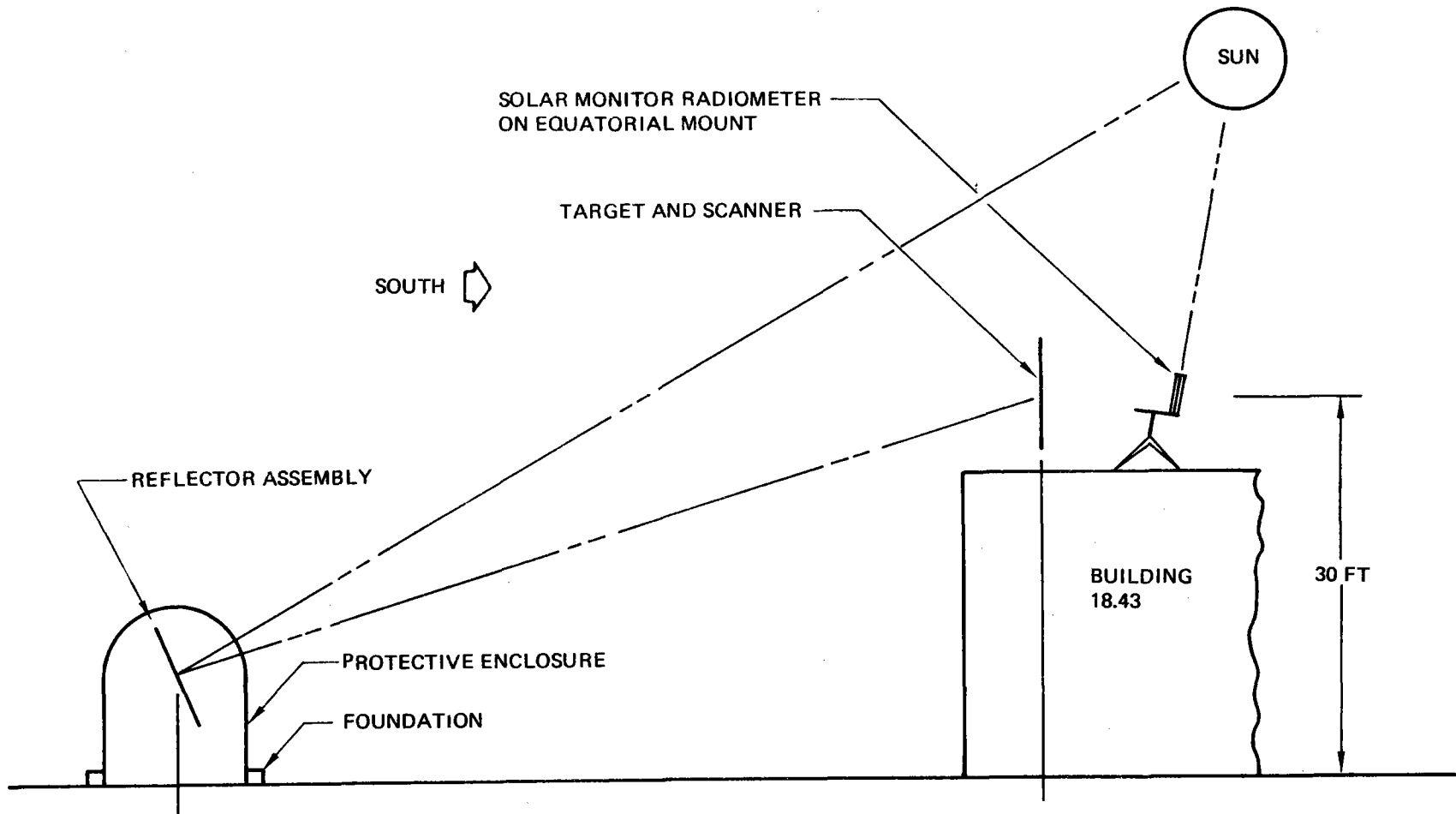


Figure 10.1-3. Heliostat Assembly Integration Test Setup

- Reflective assembly rim flatness
- Reflective assembly contour
- All drive/control modes except tracking
- Assembly fit demonstration

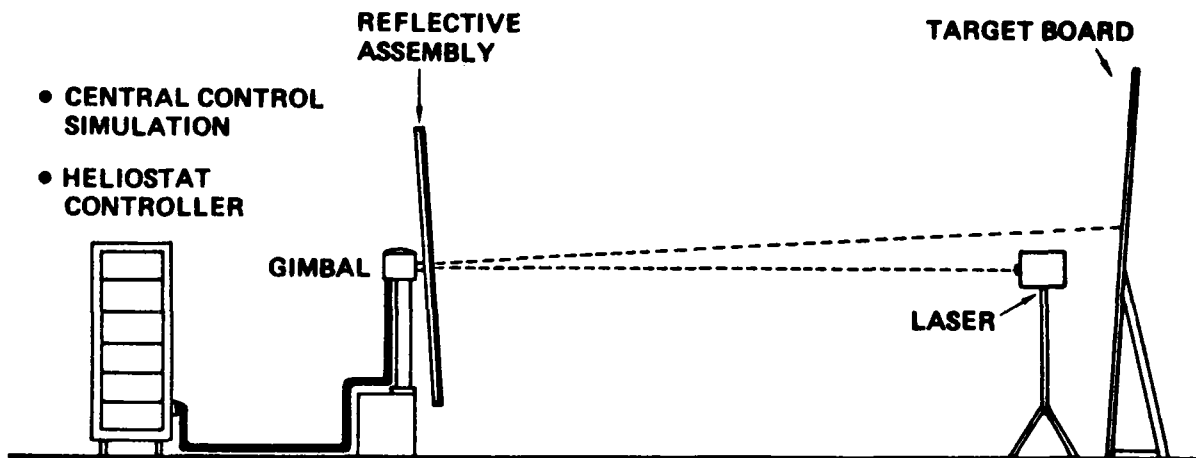


Figure 10.1-4. Drive/Control and Reflective Assembly Integration

This test prepares the integrated drive/control/reflector assembly for integration with the protective enclosure.

Integration of Drive and Control/Protective Enclosure/Reflective Assembly

This is the same setup used for the structural dynamic test described in Paragraph 10.1.3, and is the final integration. The configuration is shown in Figure 10.1-5.

10.1.5 Heliostat Array Tests

Array testing will be performed at the Boeing Space Center, Kent, Washington. All required test facilities are available at this center. The objective of this

testing is to demonstrate the overall operation of a collector subsystem, using a two-heliostat array. Figure 10.1-6 shows the detailed test setup. The first two production heliostats will be used in tests.

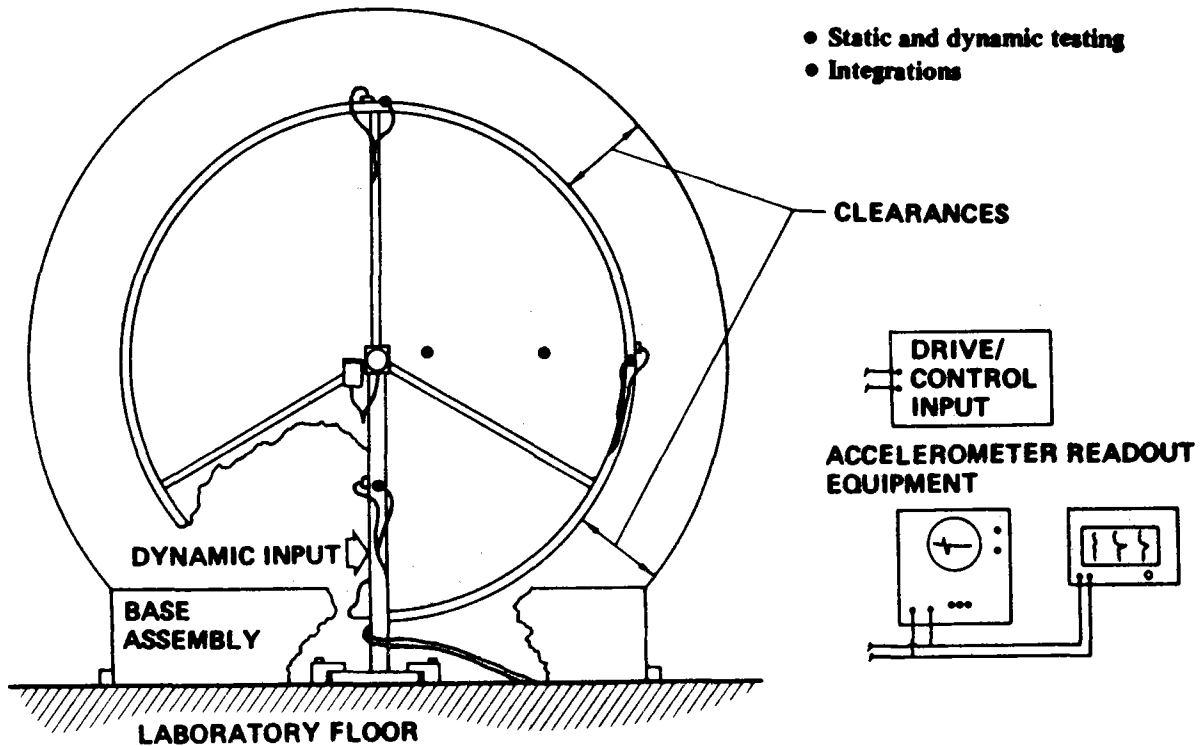


Figure 10.1-5. Drive and Control/Reflector Assembly/
Protective Enclosure Integration

The setup will consist primarily of the heliostats, alignment laser, calibration scanner, and the central control station simulator. The heliostat positioned in the field at various positions during the test program will be representative of extremes of receiver views. Demonstration of installation and alignment of the heliostat will be included. An optical scanner, located on the roof of a laboratory building, will evaluate reflected images. The optical scanner, will be similar to that used in research experiments. Also on the roof will be a solar monitor, mounted on an equatorial mount for direct tracking and measurement of the sun. The drive/control assembly will be set up in its

entirety. Heliostat efficiency will be determined. To measure this, the heliostat is positioned onto the calibration scanner. Energy received by the solar cells or radiometers representing the receiver's view of the heliostat is integrated by the computer to determine the energy received. This energy is compared with the solar energy incident on the heliostat mirror to compute efficiency. Efficiency data will be used to determine if design criteria have been met.

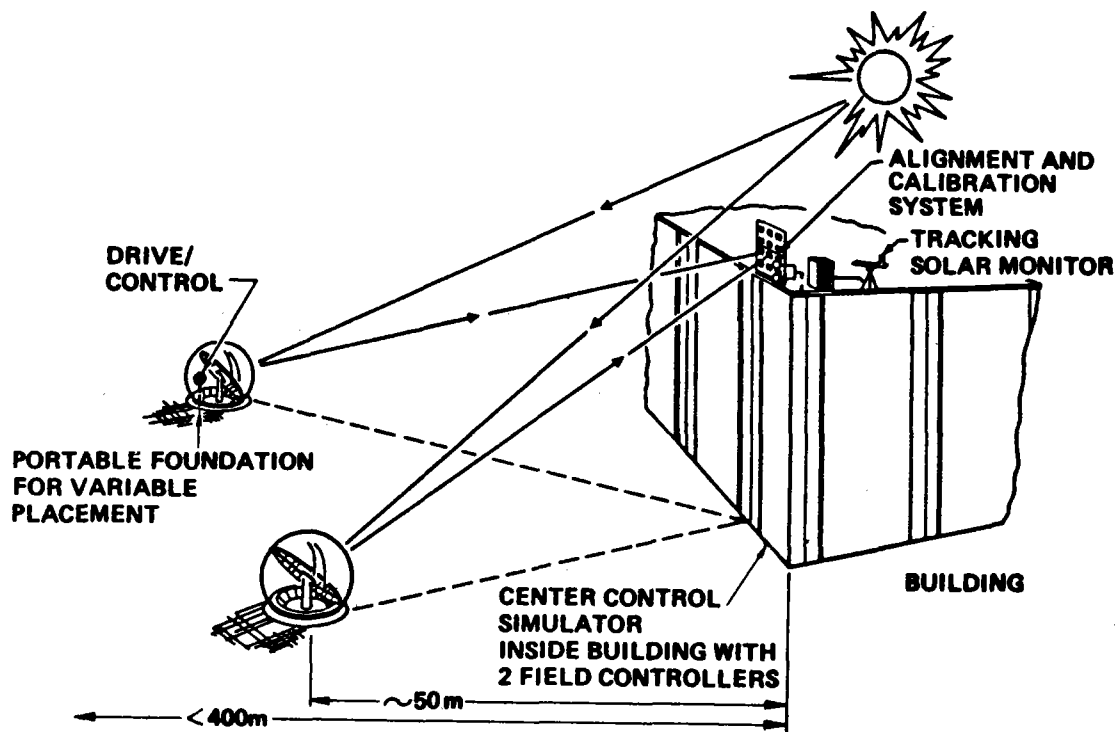


Figure 10.1-6. Array Test Site—Boeing Space Center

The drive/control assembly will be demonstrated under varying sunlight conditions. Shutdown, standby, track, align, scan, manual, power control, out of service, and program load will be demonstrated. Two heliostats will be located in the field to verify the ability of the drive/control assembly to command independent reflector assemblies. Pointing and tracking accuracy will be demonstrated under variable environmental and operating conditions.

Data and experience taken from array testing will be utilized directly in the preparation of the test procedures for acceptance test in the field.

10.2 PLANT STARTUP & CHECKOUT

Deliverable items will be subjected to acceptance testing by ERDA during plant startup and checkout. Acceptance of heliostats, the drive and control assembly and the alignment and calibration system is contingent upon passage of customer controlled tests. The recommended schedule for the acceptance testing is the time period of May 1980 through December 1980. Figure 10.2-1 is the logic diagram of the testing proposed by Boeing.

All 1650 heliostats will be tested individually to obtain initial pointing accuracies, image signatures and collection efficiencies. Individual heliostat optical data scans will be accomplished with the Alignment and Calibration Module Scanner. Subsequent to individual heliostat optical scanning, irradiation of the receiver can commence. It is assumed that this will proceed in a gradual, incremental fashion as suggested in Figure 10.2-1.

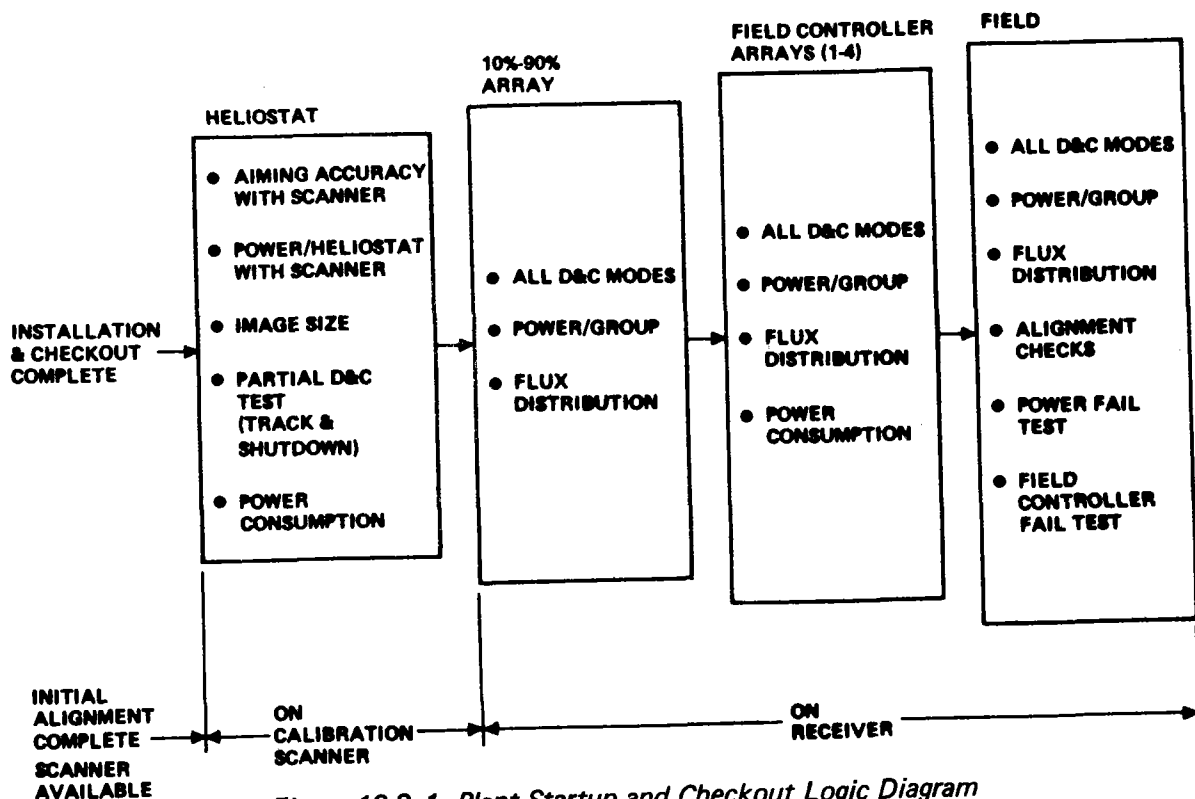


Figure 10.2-1. Plant Startup and Checkout Logic Diagram Collector Subsystem Acceptance Testing

Incident flux distributions and total power per group will be measured as the number of heliostats aimed at the tower is increased from a few to an entire array or field, depending upon the power-up procedure defined. All modes of the drive and control assembly will be demonstrated during this time.

At or near the completion of acceptance testing, alignment checks will be made on all heliostats to evaluate individual alignment changes with time, and provide necessary correction inputs.

Acceptance of the Alignment and Calibration Module will be accomplished earlier in the program, since it is required during the Installation and Checkout phase. A set of monuments of known angular and linear position relative to the receiver tower will be required for the spherodolite calibration and subsequent recalibrations. Testing of the scanner will be accomplished by comparing the individual cell outputs with a certified sun tracking pyrhelimeter.

Individual heliostat parasitic power consumption as well as power consumption at the array or field level will be measured. A random sampling of approximately 2% of the heliostats is recommended to establish statistical variations.

10.3 TWO-YEAR PILOT PLANT TEST PROGRAM

Subsequent to the plant startup and checkout, a 2-year test program will be performed. Testing will start January, 1981, and continue through December, 1982. The following paragraphs outline the program recommended by Boeing for the collector subsystem. The program is broken into 4 basic tasks, to be performed in parallel. These are; scanning of reflectors, alignment checks, weathering tests, and maintenance. Figure 10.3-1 provides a tabulation of the proposed task items as well as a schedule.

10.3.1 Reflector Scans

It is recommended that approximately 5% or 80 heliostats, selected throughout the field and representative of the field, be scanned on a monthly basis. This will provide a data file of optical and thermal performance change as a function of time and field location. Optimum receiver coordinates may be established knowing image signatures and centroids. In addition, it will assist in the establishing need for heliostat cleaning.

10.3.2 Alignment Checks

Alignment checks on 5% of the heliostat field (likely the same 80 heliostats as in 10.3.1 above) are recommended. These should be taken monthly for the first 3 months, then quarterly for the remainder of the program. These checks will provide experience with the alignment process, establish frequency of alignment checks, and give alignment updates to the control system.

10.3.3 Environmental Tests

Environmental effects will be monitored on 6 instrumented heliostats. They will be located in the field such that maximum and minimum wind effects will be experienced. Also, consideration should be given to their positioning relative to temperature extremes (north/south field - near/far field). All six heliostats will be instrumented for wind induced vibration and deflection, temperature of components, and inside/outside relative humidity.

Data lines provided by the drive and control assembly will be used to transmit data signals to the data acquisition system. It is assumed that weather station with wind velocity and direction, relative humidity, solar insolation, and hail monitoring instruments will be located at the pilot plant site. The instrumentation on these 6 heliostats should be monitored continuously with data pickups on a periodic basis.

10.3.4 Maintenance

Experience gained from the two-year test program will provide data for the development of a plant maintenance schedule. Analyses and experience from research experiments have provided preliminary maintenance, replacement and repair data. Figure 10.3-1 tabulates those maintenance items identified at this time.

Research experiment data suggests cleaning of enclosures will be required at less than 6 month intervals in summer, and possibly longer than 6 month intervals in winter. This is known to be variable depending upon weather conditions. Cleaning of reflectors is planned only when an enclosure is replaced. Replacement of enclosures, reflectors and blowers was based upon a 0.5%/year failure rate, or about 15 each over the 2-year period. Periodic checks on the backup power system for the enclosure blowers must be performed.

	1st YEAR												2nd YEAR											
	1	2	3	4	5	6	7	8	9	10	11	12	1	2	3	4	5	6	7	8	9	10	11	12
● REFLECTOR SCANS (80 HELIOSTATS)	□	□	□	□	□	□	□	□	□	□	□	□	□	□	□	□	□	□	□	□	□	□	□	□
● IMAGE SIGNATURE																								
● CENTROID																								
● INTEGRATED FLUX																								
● EFFICIENCY																								
● ALIGNMENT CHECKS	□	□	□						□			□	□									□		□
● ESTABLISH OUT-OF-ALIGNMENT FREQUENCY																								
● UPDATE ALIGNMENT																								
● ENVIRONMENTAL TESTS (6 UNITS) (DATA PICKUP)			□			□				□		□				□					□		□	
● ENCLOSURE DEFLECTION (WIND)																								
● MEMBRANE VIBRATION (WIND)																								
● TEMPERATURE/TIME																								
● HUMIDITY/TIME, CONDENSATE																								
● HAILSTONE MONITOR																								
● MAINTENANCE																								
● ENCLOSURE CLEANING				□						□												□		□
● REFLECTOR CLEANING	← CLEAN ONLY WITH ENCLOSURE REPLACEMENT →																							
● FILTER REPLACEMENT																								
● ENCLOSURE REPLACEMENT																								
● REFLECTOR REPLACEMENT																								
● BLOWER REPLACEMENT																								
● DRIVE & CONTROL MAINTENANCE																								
● ENCLOSURE/REFLECTOR REPAIR																								
● POWER-FAIL SIMULATION TESTS																								

Figure 10.3-1. Two-Year Test Program

11.0 REFERENCES

- 3.1-1 Preliminary Requirements Specification for Collector Subsystem - Central Receiver Solar Thermal Power System, Boeing Document D277-10002-1, prepared under ERDA Contract E-76-C-03-1111. Revised August 1977.
- 3.3.2.3-1 American National Standards Institute, Inc., "American National Building Code Requirements for Minimum Design Loads in Buildings and Other Structure," ANSI A58.1-1972. American National Standards Institute, Inc., 1430 Broadway, New York, N.Y. 10018
- 3.3.2.3-2 Telegram, AC Skinrood, Sandia Laboratories, Livermore, Ca., to W. I. Ratcheson, The Boeing Company, Seattle, Wash., Dec. 1976
- 3.3.2.3-3 Collector Subsystem Preliminary Design Baseline Report, Central Receiver Solar Thermal Power System, Prepared by Boeing Engineering and Construction, November 24, 1975, Boeing Document D277-10003-1
- 3.3.2.3-4 Journal of the Structural Division Proceedings of the ASCE, "New Distributions of Extreme Winds in the United States." H.C.S. Thom, July, 1968
- 3.3.2.3-5 Design Manual for Spherical Air Supported Radomes (Revised)," W. W. Bird and M. Kamrass, Cornell Aeronautical Laboratory Report No. UB-909-D-2, Rome Air Development Center Contract No. AF30(602)-976
- 3.3.2.3-6 Uniform Building Code, International Conference of Building Officials, Whittier, California, 1976 Edition
- 3.3.2.3-7 Collector Subsystem Quarterly Technical Progress Report, Central Receiver Solar Thermal Power System, Prepared by Boeing Engineering and Construction, Jan. 1977
- 3.3.2.3-8 Collector Subsystem Detailed Design Report, Central Receiver Solar Thermal Power System, Prepared by Boeing Engineering and Construction
- 3.3.2.3-9 Determination of Mechanical Properties of Polymer Film Materials, Final Report No. KD 75-9. The Singer Company, Kearfott Division, Little Falls, N. J., April 1975
- 3.3.2.3-10 Personal Conversation with Mr. Frank Edlin, Arizona State University (formerly of DuPont) August 4, 1976
- 3.3.3-1 Berning, P.H., Hass, G., and R.P. Madden, J. Opt. Soc. Am., Vol. 50, No. 6, June 1960, p. 586.
- 3.3.3.3-1 Collector Subsystem Preliminary Design Baseline Report, Central Receiver Solar Thermal Power System, Published by Boeing Engineering & Construction, November 24, 1975
- 3.3.3.3-2 Design Response Spectra for Seismic Design of Nuclear Power Plants, Regulatory Guide 1.60, U. S. Nuclear Regulatory Commission, Dec., 1973
- 3.3.3.3-3 Strong-Motion Earthquake Accelerograms; Digitized and Plotted Data; California Institute of Technology, Pasadena, California, September, 1971
- 3.3.3.3-4 Heliostat Array Simulation Computer Model Users Guide, Boeing Document D277-10004-1.

11.0 REFERENCES

(Continued)

- 3.3.7-1 Lightning Protection, J. L. Marshall, John Wiley & Sons, New York, 1973
- 3.3.7-2 "Electrical Protection Guide for Land-Based Facilities", Joslyn Electronic Systems, Santa Barbara Research Park.
- 3.3.7-3 "A Ground-Lightning Environment for Engineering Usage", by N. Cianos and E.T. Pierce, Technical Report 1, SRI Project 1834, Stanford Research Institute, Menlo Park, California.
- 9.0 Preliminary System Safety Design Criteria for the Central Receiver Solar Thermal Power System. Prepared under ERDA Contract EY-76-C-03-1110, Revised Feb., 1977.

12.0 BIBLIOGRAPHY

1. Central Receiver Solar Thermal Power System, Collector Subsystem, Program Plan, July 23, 1975, Boeing Document D277-10000-1. Revised June 1977.
2. Preliminary Requirements Specification for Collector Subsystem - Central Receiver Solar Thermal Power System, August 8, 1975, Boeing Document D277-10002-1. Revised August 1977.
3. Central Receiver Solar Thermal Power System, Collector Subsystem, Preliminary Design Baseline Report, November 24, 1975, Boeing Document D277-10003-1.
4. Central Receiver Solar Thermal Power System, Collector Subsystem, Research Experiments Conceptual Design Report, November 24, 1975, Boeing Document D277-10004-1.
5. Central Receiver Solar Thermal Power System, Collector Subsystem, Research Experiments Detail Design Report, February 24, 1976, Boeing Document D277-10022-1.
6. Central Receiver Solar Thermal Power System, Collector Subsystem, Quarterly Technical Progress Report, December 31, 1975, Boeing Document D277-10014-1.
7. Central Receiver Solar Thermal Power System, Collector Subsystem, Research Experiments, Quarterly Technical Progress Report, April 20, 1976, Boeing Document D277-10025-1.
8. Central Receiver Solar Thermal Power System, Collector Subsystem, Quarterly Technical Progress Report, July 20, 1976, Boeing Document D277-10028-1
9. Central Receiver Solar Thermal Power System, Collector Subsystem, Annual Technical Progress Report, November 1976, Boeing Document D277-10032-1

12.0 BIBLIOGRAPHY

(continued)

10. Central Receiver Solar Thermal Power System, Collector Subsystem, Quarterly Technical Progress Report, January 20, 1977, Boeing Document D277-10039-1.
11. Central Receiver Solar Thermal Power System, Collector Subsystem, Pilot Plant Preliminary Design Report, April 29, 1977, Boeing Document D277-10038-1.
12. Central Receiver Solar Thermal Power System, Collector Subsystem, Quarterly Technical Progress Report, April 29, 1977, Boeing Document D277-10042-1.
13. Central Receiver Solar Thermal Power System, Collector Subsystem, Final Report, August 15, 1977, Boeing Document D277-10047-1.